

University of St Andrews



Full metadata for this thesis is available in
St Andrews Research Repository
at:

<http://research-repository.st-andrews.ac.uk/>

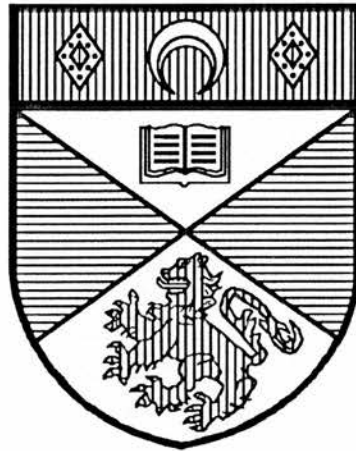
This thesis is protected by original copyright

**SYNTHESIS, CHARACTERISATION
AND STUDIES INVOLVING
POLY AND COPOLY(α,ω -ALKYLDIYNES)**

by

JOHN.C.KENNEDY, B.Sc

Thesis presented for the degree of
DOCTOR OF PHILOSOPHY



University of St Andrews

April 1992



Declaration

I John Charles Kennedy hereby certify that this thesis has been composed by myself, that it is a record of my own work, and that it has not been accepted in partial or complete fulfilment of any other degree of professional qualification.

Signed

Date ..16th April 1992.....

I was admitted to the Faculty of Science of the University of St. Andrews under Ordinance General No. 12 on October 1st 1988 and as a candidate for the degree of Ph.D. on October 1st 1989.

Signed

Date ..16th April 1992.....

I hereby certify that the candidate has fulfilled the conditions of the Resolution and Regulations appropriate to the Degree of Ph.D.

Signed

Date ..16th April 1992.....

In submitting this thesis to the University of St. Andrews I understand that I am giving permission for it to be made available for use in accordance with the regulations of the University Library for the time being in force, subject to any copyright vested in the work not being affected thereby. I also understand that the title and abstract will be published, and that a copy of the work may be made and supplied to any bona fide library or research worker.

Acknowledgements

I am greatly indebted to Professor J.R.MacCallum (Vice-Principal of the University of St. Andrews) for his supervision during the course of this research. I am also much obliged to Dr D.H.MacKerron (I.C.I. Chemicals and Polymers, Wilton in Teesside) for specialist advice and encouragement in areas of the research project. I am also indebted to S.E.R.C and I.C.I Chemicals and Polymers (Wilton in Teesside) for the C.A.S.E award.

My thanks are due to members of staff in the Department of Chemistry of the University of St. Andrews especially Dr J.A.Crayston, Dr S.Seth, Mr J.Smith for their help with areas of the research project.

My thanks also go to all past and present colleagues in the Chemistry Department(a special mention to Andrew, Glen and Neil), to all the friends I've met in St Andrews over the past 3 years and everybody I've had the pleasure to play a round of golf with!

Thanks also go to Mrs Alison Aiton for the typing of this thesis, Mr Jim Bews for help with the Mac and John Morrison for help with the Chem Draw package in the Mac.

Special thanks go to Colleen for her love, support and encouragement while finishing this thesis.

Finally, I wish to thank my parents for all the backing, understanding and support they have given to me throughout the many years of my education.

Lecture Courses

The following is a statement of the courses attended during the period of research ; New Synthetic Methods Using Silicon and Phosphorus (3 lectures), Dr R.K.Mackie ; Heterogeneous Catalysis (4 lectures), Dr J.A.Crayston and K.D.M.Harris ; Industrial Chemistry (4 lectures), Professor F.D.Gunstone and Dr C.Glidewell ; Pharmaceutical Chemistry (4 lectures), Dr R.A.Aitken and Dr A.R.Butler ; Photochemistry (4 lectures), Dr J.A.Crayston ; Cyclic Voltammetry in Organic and Inorganic Chemistry (4 lectures), Dr J.A.Crayston ; Semiconductor Growth Technology (3 lectures), Professor D.J.Cole-Hamilton ; Chemical Carcinogenesis (3 lectures), Dr C Thomson ; and Aspects of Materials Chemistry (3 lectures), Dr J.A.Crayston.

TABLE OF CONTENTS

TITLE PAGE	i
DECLARATION	ii
ACKNOWLEDGEMENTS	iii
LECTURE COURSES	iv
TABLE OF CONTENTS	v
ABSTRACT	x
CHAPTER 1 : INTRODUCTION	
1.1 Foreword	1
1.2 Solid-state diacetylene polymerisation	2
1.3 General behaviour and previous work on poly(α,ω -alkyldiynes)	9
1.4 Aims of the project	23
TABLES	26
FIGURES	28
CHAPTER 2 : SYNTHESSES AND ATTEMPTED SYNTHESSES OF α,ω -DIYNE MONOMERS	
2.1 Introduction	54
2.2 Syntheses of α,ω -diyne monomers - a discussion of methods used in their syntheses and results achieved	55
2.3 Experimental Section	70
2.3.1 Instrumentation and General techniques	70
2.3.2 Syntheses of monomers	72
2.3.2.1 α,ω -alkyldiyne monomers	72
2.3.3.2 trans-4-octene-1,7-diyne	75
2.3.2.3 1,4-diethynylbenzene	77
2.3.2.4 1,4-di-(4-ethynylphenyl)-2-butene	80
2.3.2.5 4,4'-diethynylbiphenyl	82

2.3.2.6 1,4-di-2-propynylbenzene	85
2.3.2.7 4,4'-bis(di-2-propynyl)-1,1'-biphenyl	85
FIGURES	87
CHAPTER 3 : SYNTHESSES OF POLY(α , ω -ALKYLDIYNES) AND COPOLY(α , ω -ALKYLDIYNES)	
3.1 Introduction	88
3.2 Oxidative (Glaser) Coupling - A Review	89
3.2.1 General features and mechanism	89
3.2.2 Methods for oxidative coupling	92
3.3 Criteria for Choosing the Two Oxidative Coupling Routes	94
3.3.1 Polymerisation using cupric salt - pyridine system - Eglinton polymerisation	95
3.3.2 Polymerisation using catalytic Glaser coupling(I) - a basis to establishing polymerisation route A	97
3.3.3 Polymerisation using catalytic Glaser coupling(II) - a basis to establishing polymerisation route B	102
3.4 Syntheses of poly(α , ω -alkyldiynes) and copoly(α , ω -alkyldiynes)	106
3.4.1 Syntheses of polymers - Route A	106
3.4.2 Syntheses of polymers - Route B	107
3.4.3 Polymers characteristics	108
TABLES	110

CHAPTER 4 : MOLAR MASS CHARACTERISATION OF
POLY(α,ω -ALKYLDIYNES) AND
COPOLY(α,ω -ALKYLDIYNES)

4.1 Introduction	112
4.2 Techniques used for molar mass characterisation of poly(α,ω -alkyldiynes) and copoly(α,ω -alkyldiynes)	114
4.2.1 Gel permeation chromatography (GPC)	115
4.2.2 End group analysis (EGA) by $^1\text{Hnmr}$ spectroscopy	116
4.3 Experimental section	117
4.3.1 Gel permeation chromatography (GPC)	117
4.3.2 End group analysis (EGA) by $^1\text{Hnmr}$ spectroscopy	119
4.4 Results and Discussion	127
4.4.1 Molar mass characterisation of polymers synthesised by route A	127
4.4.2 Molar mass characterisation of polymers synthesised by route B	131
4.4.3 Cyclisation of α,ω -alkyldiynes	138
4.4.3.1 Previous oxidative coupling work on α,ω -alkyldiynes which cyclise	138
4.4.3.2 Oxidative coupling work on α,ω -alkyldiynes investigated in this study	139
4.4.4 Mechanism of oxidative coupling of polymerisation routes A and B	143
TABLES	148
FIGURES	159

CHAPTER 5 : THERMAL BEHAVIOUR OF A SERIES	
OF A SERIES OF POLY(α,ω -ALKYLDIYNES)	
5.1 Introduction	179
5.2 Experimental details	180
5.3 Results and Discussion	182
5.3.1 Thermal analysis of poly(1,9-decadiyne) (P19D)	182
5.3.2 Thermal analysis of poly(1,10-undecadiyne) (P110U)	188
5.3.2.1 Annealing and quenching studies on P110U	189
5.3.2.2 Comparison of thermal behaviour of poly(1,10-undecadiyne)(P110U) with poly(1,8-nonadiyne)(P18N)	190
5.3.2.3 Thermal analysis of Cross-polymerised poly(1,10-undecadiyne)(XP110U)	192
5.3.3 Thermal analysis of poly(1,11-dodecadiyne) (P111D)	196
5.3.4 Thermal analysis of poly(1,7-octadiyne)(P17O)	196
5.4 Conclusions	197
TABLES	199
FIGURES	202

CHAPTER 6 : GENERAL BEHAVIOUR OF	
POLY(α , ω -ALKYLDIYNES)	
AND COPOLY(α , ω -ALKYLDIYNES)	
6.1 Introduction	226
6.2 Experimental details	228
6.3 Results and Discussion	233
6.3.1 Kinetics of photochemical cross-polymerisation by UV irradiation	233
6.3.1.1 Reaction kinetics involved in the photochemical cross-polymerisation reaction at $\lambda = 650$ nm for the poly(α , ω -alkyldiynes)	237
6.3.2 Studies involving a 50:50 copolymer of poly(1,9-decadiyne):poly(1,10-undecadiyne)	240
6.3.2.1 UV and solubility studies	240
6.3.2.2 Thermal analysis of the copolymer	240
6.3.3 Conductivity and resonance Raman spectroscopic studies on cross-polymerised poly(1,9-decadiyne) and poly(1,11-dodecadiyne)	244
6.3.4 Characterisation of the product from the polymerisation of 1,7-octadiyne	247
6.4 Conclusions and Recommendations	249
TABLES	251
FIGURES	256
BIBLIOGRAPHY	273

ABSTRACT

Poly(α,ω -alkyldiynes) are a class of compounds containing a diacetylene repeat unit in their chains. These polymers can undergo solid-state polymerisation upon UV irradiation and thermal annealing. A 1,4-addition reaction takes place within the crystalline segments of the poly(α,ω -alkyldiyne) chains to form a cross-polymerised network. This resulting network contains polydiacetylene chains, causing the structure to be highly coloured.

A series of poly(α,ω -alkyldiynes) and copoly(α,ω -alkyldiynes) were synthesised by catalytic Glaser coupling reactions. Two routes were investigated and developed. These routes were chosen in anticipation that high molar mass, linear and polydisperse polymers would be achieved. GPC curves revealed that this was possible for the majority of polymers synthesised by the first route. However a wide range of molar masses were obtained by the second route with a significant low molar mass tail present in almost all GPC curves. It was proposed that the low molar mass tail was a consequence of cyclic structures. From these results and observations a mechanism for the polymerisation of the α,ω -alkyldiynes was proposed.

Extensive studies on the thermal properties of poly(1,9-decadiyne) and poly(1,10-undecadiyne) were carried out by DSC. Substantial melt history effects were present for both polymers in the melt crystallised form. DSC was also used to estimate the degree of conversion to the cross-polymerised form for poly(1,10-undecadiyne).

The kinetics of the photochemical cross-polymerisation reaction were studied for the poly(α,ω -alkyldiynes) by visible spectroscopy for the first five minutes of UV exposure. The poly(α,ω -alkyldiynes) studied obeyed first-order kinetics. UV and DSC studies were performed

on a 50:50 copolymer powder and film of 1,9-decadiyne and 1,10-undecadiyne. It was shown that the copolymer powder had crystalline segments present and that the 1,4-addition reaction occurred photochemically and thermally but at a much slower rate than for the corresponding homopolymers.

To my family and friends

CHAPTER 1

INTRODUCTION

1.1 Foreword

Diacetylene compounds were first synthesised in the nineteenth century, around 1869, by Glaser.¹ Some of these were found to show colour changes on storage or on exposure to light but this is accompanied by no apparent change in their crystal structure or chemical composition. However it was not until 100 years later that Gerhard Wegner ² in 1969 demonstrated that this colour change was due to polymerisation of the diacetylene monomer in the crystalline solid state. It was this work which initiated the recent renewal of interest in polydiacetylenes. Much of the interest arises from the fact that macroscopic single crystals of some diacetylene monomers can polymerise in the solid state to give nearly perfect, extended chain polydiacetylene single crystals. These polydiacetylene single crystals also exhibit a fully conjugated and planar backbone in the crystalline solid state. This sparked interest for many early workers since these single crystals enabled one to study the inherent properties of a conjugated polymer chain without the complications of the irregular morphologies normally found in polymer systems.³ As a consequence of the anisotropic nature of these polydiacetylene single crystals interesting electrical and optical properties were expected. These expectations initiated much of the early work on polydiacetylenes.

Since Wegner's discovery in 1969, most of the work on polydiacetylenes has concentrated on understanding the nature of the solid-state polymerisation process. The following section will outline some of the fundamental aspects of the solid-state polymerisation reaction as a brief introduction for those not familiar with the solid-state polymerisation of diacetylenes. For a more thorough review of

the mechanism and kinetics of the diacetylene polymerisation the reader is referred to a number of reviews.³⁻⁹

The subject of this thesis is a relatively new class of diacetylene compounds i.e. poly(α,ω -alkyldiynes) and copoly(α,ω -alkyldiynes). The last two sections of the chapter will discuss previous work carried out on poly(α,ω -alkyldiynes) and present a brief summary of the aims of the present work.

1.2 Solid-state diacetylene polymerisation

The solid-state diacetylene polymerisation is a 1,4-addition reaction involving the triple bonds of the monomer, leading to a fully conjugated all-trans polymer chain (see figure 1.1). The reaction is typically initiated by UV light, x-rays, gamma rays, thermal annealing, or strain (depending upon the particular monomer under study) and the resultant polymer is always highly coloured due to the conjugated backbone structure.

In figure 1.1 two structures have been proposed for the conjugated backbone structure i.e. the acetylenic form and the butatrienic form. Data from structure analyses and spectroscopic studies performed on many polydiacetylenes indicate that the acetylenic form is preferred. (However in most cases a resonance hybrid of the two forms is observed).

This solid-state diacetylene polymerisation is an example of a topochemical solid-state polymerisation.³⁻⁹ A topochemical process is one in which the reaction path is defined by the arrangement of the

molecules within the unit cell.³ The topochemical polymerisation proceeds with a "direct transition from the monomer molecules to polymer chains without destruction of the crystalline lattice and without formation of non-crystalline intermediates".² In this sense a topochemical polymerisation can be viewed as a specific type of phase transition.

In an ideal topochemical reaction, the centres of the reacting molecules remain fixed and the reaction occurs via small rotations about the fixed positions.⁸ The preferred reaction path will be the one which requires the minimum displacement of the monomer molecules. This concept is referred to as the principle of least motion.¹⁰ The principle of least motion states that "those elementary reactions will be favoured that involve the least change in atomic position and electronic configuration".¹⁰

Therefore from the above discussion it would appear that there exists a maximum allowable distance between reactive centres in the monomer which, if exceeded, would prevent the reaction from occurring. Significant effort has been directed toward identification of the structural parameters which govern the diacetylene polymerisation. The arrangement of neighbouring molecules in the lattice absolutely necessary for polymerisation was derived in mathematical terms by Baughman⁴ and is based on X-ray crystallographical evidence. As depicted in figure 1.2 polymerisation is described as translational direction invariant motion of the structural units. Spacing of the reactive rod-like triple bonds along the growth direction is defined by the translational period d , along the lattice vector a and the angle γ , between rod direction and a .

Consequently, the distance S_1 between adjacent triple-bond systems is defined by $S_1 = d_1 \sin \gamma$.^{4, 5} Experience demonstrates that S_1 has to be smaller than 0.40 nm with the lowest limit at $S_1 = 0.34$ nm for polymerisation (the lower limit being twice the van der Waals radius for sp hybridised carbon atoms). Thus γ_1 in reactive arrangements is of the order of 45° or in other words in such structures carbon 4 of one molecule is very close to carbon 1' of the next molecule of the same stack. The parameters S_1 , γ_1 and d_1 are changed to S_2 , γ_2 and d_2 on polymerisation. High conversion to highly perfect polymer crystals is reached only when $(d_2 - d_1)$ is very small or preferably zero. Obviously, it would be favourable if d_1 was close to the polydiacetylene repeat distance of 4.91 \AA as this would minimise the motion needed for reaction.^{5, 8} Bloor has suggested that the most critical parameter for reaction is the distance that separates the two reactive carbon atoms i.e. carbon 4 and carbon 1' of the adjacent molecule. For most reactive diacetylenes this distance $D < 4.0 \text{ \AA}$.³

The above approach provides a basis for understanding the relationship between molecular arrangement and reactivity in diacetylene molecules. However quantitative predictions are not yet possible. Quantitative predictions will be successful only when the ability to predict the packing properties of organic molecules becomes more sophisticated. The problem is demonstrated by the fact that different crystal modifications of the same monomer can show different reactivities.^{4, 5, 8}

From the above discussion it is clear that the reactivity of a particular monomer is dictated by the molecular packing in the crystal.

X-ray diffraction data on various diacetylene monomers, emphasising the way in which crystal structure affects solid state reactivity has been summarised by Enkelmann.⁸ His work shows that overall packing of the diacetylene monomer is often dominated by the packing of the side groups. For this reason it is important that the side groups allow packing of the diacetylene units such that they are close enough in one direction to allow the reaction to occur preferentially along that direction.³ Side groups that contain aromatic rings generally show favourable packing (if the rings are separated from the diacetylene unit by a methylene spacer group), as do compounds which have diacetylene units as part of a ring system. Also diacetylenes with hydrogen-bonding side groups have been found to be generally reactive. Of course, any substituent which prevents the approach of neighbouring monomer units to be less than about 4Å will be unfavourable for reaction.⁵ It is possible for unsymmetrical monomers to be reactive provided the packing is appropriate.^{8, 9}

Although the packing behaviour of the substituents is crucial in determining reactivity, the chemical nature of the substituents has virtually no effect upon reactivity. Mesomeric or inductive effects of substituent groups have not yet been observed to affect polymerisation.

Topochemical polymerisations may proceed as homogeneous or heterogeneous reactions ^{8,9,11} schematically shown in figure 1.3a and b and these two reaction modes generally lead to products with different physical characteristics. In a heterogeneous topochemical process, the reaction is initiated at defect sites or at surfaces of the monomer phase, and proceeds with nucleation of the product phase (figure 1.3a). ^{8,9} A heterogeneous reaction will occur when the strain caused by lattice

mismatch between the monomer and polymer is concentrated at the interface between them. ^{3,11} If the polymerisation is heterogeneous, fibrillation of the monomer crystal eventually occurs.

Conversely, in a homogeneous topochemical process the polymer is formed as a solid solution of extended chain molecules which grow from points distributed at random throughout the parent crystal (figure 1.3b). The lattice strain created during the reaction is more evenly distributed throughout the monomer crystal lattice than for a heterogeneous reaction.³ In ideal cases a solid solution exists over the entire conversion range, and the monomer single crystal can be converted into a nearly perfect polymer single crystal.^{8, 12}

Baughman demonstrated that for some diacetylene monomers, a one-phase polymerisation might be ensured by choosing reaction conditions so that the kinetics of the polymerisation are fast compared to the kinetics of phase separation.⁴ For some diacetylene monomers the mode of initiation can determine whether the reaction will lead to a one-phase product. For these diacetylene monomers, irradiation can increase the rate of polymerisation and can lead to one-phase polymerisation, whereas thermal initiation for the same diacetylene monomer could lead to a phase separated product.^{3, 4}

Homogeneous topochemical reactions do not occur for many compounds but most diacetylene compounds can polymerise via a homogeneous process. ^{3-6,8,9,12} Therefore most polydiacetylenes can be obtained in the form of macroscopic single crystals. However, there are some exceptions to this rule. As mentioned above, the mode of initiation can determine whether the reaction will proceed

homogeneously or heterogeneously. For 2,4-hexadiynediol **13**, 1,6-di(-N-carbazolyl)-2,4-hexadiyne **8**, and N,N'-diacetyl-m,m'-diaminodiphenyldiacetylene **5**, the radiation-induced reaction proceeds homogeneously, whereas the thermally-induced reaction proceeds heterogeneously. Radiation polymerisation of 2,4-hexadiyne-1,6-diol-bis(phenylurethane) **11** proceeds homogeneously at the start of the reaction, but then converts to a heterogeneous process later on in the reaction.

Reaction kinetics in diacetylene polymerisations is a topic which has also been studied thoroughly. Many diacetylene compounds show autocatalytic behaviour.^{3,9,12,14,17} The most thoroughly investigated diacetylene compound is 2,4-hexadiyne-1,6-diol bis (p-toluenesulphonate) (PTS). The polymerisation process in PTS is particularly interesting because of the dramatic "autocatalytic effect" observed in the polymer conversion versus time curve obtained using monomer extraction techniques. Figure 1.4a shows the conversion as a function of time for the thermally induced polymerisation of PTS. Autocatalytic reactions as in figure 1.4a show the same general features. First, there is a slow increase in the conversion, referred to as the induction period. Following the induction period is the autocatalytic region, where there is a dramatic increase in conversion over a very short time period. Finally there is another region over which the conversion usually approaches 100%.¹⁴ The autocatalytic region for thermally induced reactions is normally more pronounced than that for photoinduced reactions ¹⁴ (eg as shown in figure 1.4b for PTS).

The solid-state reaction kinetics in single-phase polymerisations was studied by Baughman.¹² The kinetics were evaluated for the

monomer PTS using different approximations for the effect of structural changes at intermediate conversions. Conversion curves were calculated for monomer phases which undergo large dimensional changes in the reaction direction (crystal strain approximation) and for monomer phases which were essentially dimensionally invariant during reaction (nearest neighbour approach). Baughman's theory gives excellent agreement with the observed autocatalytic kinetics of thermally induced polymerisations. The autocatalytic effect is attributed to a strain-dependent rate of chain initiation and propagation. The theory predicts a more pronounced autocatalytic effect as lattice mismatch is increased.¹² The weaker autocatalytic effect for γ -ray induced polymerisation suggest that radiation-induced chain initiation is relatively insensitive to crystal strain.¹²

Later work on the kinetics of several other diacetylene monomers produced results which contradicted the conclusion that crystal strain is the most important factor governing diacetylene polymerisation kinetics³, even though Baughman's theory gives excellent quantitative agreement with the observed kinetics for PTS. Work on the energetics of the polymerisation reaction as well as the kinetics by Kollmar and Sixl¹⁴ has strengthened the work by Baughman. The theoretical results of Kollmar and Sixl agree well with experimental results for the monomer PTS, but further tests of the theory will be required before its validity can be assessed.

Other work concentrating on the energetics of the diacetylene polymerisation have also been published.^{15,16,18,19} The energetic changes that occur during the diacetylene polymerisation are shown in figure 1.5. Calorimetric studies of the thermal polymerisation process

have shown the activation energy for reaction is $\sim 1\text{eV}$. ^{16,19} After the biradical dimer intermediate has formed ^{19,20} the reaction has two options : it can either return to the monomer ground state or begin chain propagation. For every propagation step $\sim 1.6\text{eV}$ is released. ^{16,19}

In the photoinitiated reaction, the activation barrier is overcome by creating a monomer excited state which can then react with a monomer ground state to form the biradical dimer intermediate. The propagation is then continued as in the thermal polymerisation process. Chance and co-workers ^{18,19} have outlined the photopolymerisation process in detail for one particular monomer system, 4BCMUs, $\text{RC}\equiv\text{C}-\text{C}\equiv\text{CR}$, where R is $(\text{CH}_2)_4\text{OCONHCH}_2\text{COO}(\text{n-C}_4\text{H}_9)$. BCMU stands for [(butoxycarbonyl)methyl] urethane.

1.3 General behaviour and previous work on poly(α,ω -alkyldiynes)

The previous section of work discussed the solid state polymerisation of conventional low molar mass diacetylene compounds. The work involved in this research concerns another class of diacetylene compounds. This class of compounds are referred to as poly(α,ω -alkyldiynes) and copoly(α,ω -alkyldiynes). These polymers comprise of linear chains and have the following general structure:



or as in a copolymer; eg



Much work has already been carried out on the poly(α,ω -alkyldiynes) poly(1,8-nonadiyne) and poly(1,11-dodecadiyne) ²¹⁻³¹,

however other polymers and copolymers in this homologous series where $n = 4$ to 8 have not been investigated as thoroughly.

The rest of this section will now discuss previous work on poly(α,ω -alkyldiynes) and their general behaviour.

In 1981 Day and Lando synthesised poly(1,8-nonadiyne), poly(1,9-decadiyne) and poly(1,11-dodecadiyne) by an oxidative coupling route.²² Upon exposure to ultraviolet (UV) or γ -rays (or by thermal annealing or with high pressure) the poly(1,8-nonadiyne) and poly(1,11-dodecadiyne) turned deep blue in colour at the surface. However poly(1,9-decadiyne) did not turn deep blue in colour, (suggesting an unfavourable packing relation between diynes in the crystal structure preventing systematic diacetylene polymerisation). The deep blue colour is a consequence of the crystalline regions of these materials cross-polymerising via the usual diacetylene 1,4-addition reaction to yield a regular two dimensional network ²² (see figure 1.6 for poly(1,11-dodecadiyne)). The two dimensional structures for poly(1,8-nonadiyne) and poly(1,11-dodecadiyne) were examined by x-ray diffraction and preliminary structures were proposed.²²

The electrical conductivity of the cross-polymerised poly(1,11-dodecadiyne) was investigated ²² because it was anticipated that these polymers could be doped to high conductivities as the two dimensional network which formed after irradiation contained conjugated chains. The idea would be very attractive since the polymers are soluble and fusible and thus could be easily processed unlike conventional "conducting" polymers. After processing, the polymer could be cross-polymerised and doped. Initial experiments on cross-polymerised

poly(1,11-dodecadiyne) revealed the cross-polymerised material was in fact an insulator. Iodine doping raised the conductivity by some 2.5 orders of magnitude but the doped material was still a poor conductor.

Knol and co-workers doped a cross-polymerised material of poly(1,8-nonadiyne) and measured a specific conductivity of 10^{-6} S/cm.²⁶ Although this conductivity reading is more encouraging than that of Day and Lando's it is still many orders of magnitude smaller than that of other doped polymers having a conjugated backbone.

The molecular mechanism of cross-polymerisation in poly(1,11-dodecadiyne) was determined by a comparative analysis of the polymer structure to that of the cross-polymerised product.²³ Electron diffraction patterns were obtained from the polymer and cross-polymerised crystals of poly(1,11-dodecadiyne). Figure 1.7 and 1.8 show the ac and bc projections of both the polymer and cross-polymerised product. Table 1.1 compares the unit cell dimensions obtained before and after cross-polymerisation.

As shown in figures 1.7 and 1.8 the diacetylene backbone lies along the c-direction. This is because the neighbouring polymer chains are only $\sim 4\text{\AA}$ apart along the c-axis, whereas the chains in every other direction have a separation of at least 7\AA . The polymer molecules need only a slight rotation and translation along the c-axis to polymerise in accordance with the principle of least motion. The c-axis has a repeat distance of 9.92\AA , about double the diacetylene repeat distance (see Table 1.1). This doubling occurs because there are two diacetylene repeats in the unit cell along the c-axis.²³

A structural analysis was also performed on poly(1,8-nonadiyne). The molecular mechanism of cross-polymerisation was again deduced by a comparative analysis of the polymer structure to that of the cross-polymerised product.²⁴ Electron diffraction patterns were obtained from the polymer and cross-polymerised crystals of poly(1,8-nonadiyne). Figure 1.9 shows the scheme for the cross-polymerisation reaction of poly(1,8-nonadiyne). Figures 1.10 and 1.11 show the ac and bc projections of the crystal structure of both poly(1,8-nonadiyne) and its cross-polymerised product. Table 1.2 compares the unit cell dimensions before and after cross-polymerisation.

The diacetylene polymerisation takes place along the c-axis as it did in poly(1,11-dodecadiyne), the nearest neighbour distance along the axis being about 5Å. After reaction the polydiacetylene backbone (found to be acetylenic) had a repeat of about 4.85Å (Table 1.2), this is almost identical to the repeat distance of polydiacetylene of 4.9Å. Initially, it was thought that the reaction could also take place along the diagonal. However, the angular separation between the diacetylene rods of the polymer chain at the centre and in corner of the unit cell is too large. Therefore for the reaction to take place, a large rotation is necessary. For the chains along the c-axis this is not a requirement. Thus the reaction proceeds along the c-direction.²⁴

The molecular mechanism of the cross-polymerisation reaction of poly(1,11-dodecadiyne) was studied through Magic Angle Spinning (MAS) Carbon-13 nmr.²⁵ While diffraction studies characterises fully the molecular structure in the crystalline regions, specifically it was desired to know if the reaction proceeded preferentially in one direction in the unit cell and whether any reaction occurred in the amorphous

regions. High resolution carbon-13 nmr spectra of solid poly(1,11-dodecadiyne) before and after γ -irradiation were reported. One of the main results of this study was that the polydiacetylene chains in cross-polymerised poly(1,11-dodecadiyne) were of the acetylenic form (in agreement with the electron diffraction work ²³). The amorphous regions of the polymer were probed to check for any evidence of cross-polymerisation. It was anticipated that there would be little, if any, cross-polymerisation taking place in the amorphous regions, due to the fact that crystallographic register is needed between reacting units for this type of reaction. The nmr analyses showed that the cross-polymerisation reaction indeed seemed to be restricted to the crystalline regions of the polymer.²⁵

The previous discussion on poly(α,ω -alkyldiynes) dealt mainly with understanding the molecular mechanism of cross-polymerisation by analysing unit cell changes which take place upon reaction.²³⁻²⁵ More recent investigations have looked at the structure-property relationships in poly(α,ω -alkyldiynes). The cross-polymerised poly(α,ω -alkyldiynes) are conjugated, therefore an important property is their optical behaviour. Also, since the optical properties of these polymers were to be studied, the poly(α,ω -alkyldiynes) synthesised had to be very pure. Butera synthesised very pure, white semi-crystalline poly(α,ω -alkyldiynes) using a Glaser coupling reaction ²⁹ (the polymerisation procedure was based upon that of White ³², but with some modifications to enable the production of very pure poly(α,ω -alkyldiynes)).²⁹ Recent studies concentrated upon understanding the optical properties of the poly(α,ω -alkyldiynes) as a function of conversion to the cross-polymerised product.^{27,28,30,31} What will now be discussed is studies involving UV-visible spectroscopy and

resonance Raman spectroscopy carried out by Butera and workers, ^{30,31} which have helped in understanding the nature of the cross-polymerisation reaction ³⁰ and the unique thermochromic and solvatochromic transitions ³¹ which have been observed in poly(α,ω -alkyldiynes).

Figure 1.12 (a) (b) and (c) show visible spectra for poly(1,6-heptadiyne), poly(1,8-nonadiyne) and poly(1,11-dodecadiyne) films respectively.³⁰ The spectral features of all three cross-polymerised polymers are similar at low conversions. All three systems show two absorption maxima occurring near 575 and 620 nm. Also, with increasing UV exposure there is a continual broadening and blue shifting of the absorption envelope. This is more pronounced for cross-polymerised samples of poly(1,8-nonadiyne) and poly(1,11-dodecadiyne) than for cross-polymerised poly(1,6-heptadiyne) indicating that poly(1,6-heptadiyne) is considerably less photoreactive than poly(1,8-nonadiyne) and poly(1,11-dodecadiyne).

One likely factor contributing to the broadening and blue shifting of the spectrum with increasing UV exposure is UV-induced degradation of the polydiacetylene chains, which has been observed in polydiacetylene solutions ³³⁻³⁵ and could also reasonably be expected to occur in solid polydiacetylenes. ³⁶ Upon UV-induced degradation an array of shorter conjugation lengths is produced from chains that originally had long conjugation lengths, thus having an obvious effect to the broadening and blue shifting of the spectra.

Results from a sequence of visible spectra obtained from a thermally cross-polymerised poly(1,8-nonadiyne) film support this

suggestion ³⁰ (see figure 1.13). Spectra were taken on a solution cast poly(1,8-nonadiyne) film that was stored in the dark at $\sim 20^{\circ}\text{C}$ at various time intervals.

The main differences between the thermally cross-polymerised poly(1,8-nonadiyne) (figure 1.13) and the UV-initiated cross-polymerised poly(1,8-nonadiyne) (figure 1.12a) are;

(1) In the thermally cross-polymerised sample there is no decrease in the intensity of the high wavelength absorption at 620 nm, although there is some blue-shifting of this band. In the UV-initiated sample the 620 nm band starts to decrease after about 5 mins of UV exposure.

(2) In the thermally cross-polymerised sample there is a relative lack of absorption around 400 nm, compared to the UV-initiated sample.

(3) In the thermally cross-polymerised sample the intensity of absorbance at 575 nm does not seem to level off as it does for the UV-initiated sample.

These observations are all consistent with the suggestion that UV-induced chain degradation occurs in the UV-irradiated sample. In the thermally cross-polymerised sample, no chain degradation occurs, so an increase in intensity of the absorption maxima is observed at longer reaction times.

Another process that could possibly contribute to the observed broadening and blue shifting is accumulation of lattice strain imposed upon the growing polydiacetylene chains by the crystallite size

distribution and crystallite defect density of the distribution of the sample, thus causing a distribution of conjugation lengths.³⁷

Resonance Raman spectroscopy with various incident wavelengths was used to study the behaviour of the various conjugation lengths that comprise poly(1,8-nonadiyne).³⁰ Figure 1.14 shows the resonance Raman spectra of poly(1,8-nonadiyne) films exposed to UV light for 6 minutes using 6328Å and 5145Å incident wavelengths. These spectra have the same general features of resonance Raman spectra of conventional polydiacetylenes. Table 1.3 shows the comparison of observed resonance Raman frequencies using these two incident wavelengths for 6 minutes of UV exposure. The observed frequencies from the spectrum obtained by using incident wavelength of 5145Å are all higher than the corresponding frequencies obtained by using incident wavelength of 6328Å. This clearly indicates that the breadth of the bands observed in the visible spectrum of cross-polymerised poly(1,8-nonadiyne) is caused by the presence of a distribution of conjugation lengths in the sample. When an incident wavelength of 5145Å is used shorter conjugation lengths (of the order of nine to ten repeat units) were probed, whereas when an incident wavelength of 6328Å is used polydiacetylene chains with nearly infinite conjugation lengths were photoselected.³⁰

Figure 1.15 shows the C=C stretching region, recorded by using an incident wavelength of 5145Å for cross-polymerised poly(1,8-nonadiyne) after various UV exposure times.³⁰ At low UV exposure times, the C=C stretching band has only one maximum (1480 cm⁻¹) but has a broad high-frequency tail. At higher exposure times the high frequency tail becomes more prominent and a shoulder appears at 1515

cm^{-1} . This change in the double bond stretching region appears to be due to a population effect, as the UV exposure time is increased there is an increase in short conjugation lengths, as demonstrated by the increased absorption at short wavelengths and blue shifting in the visible spectrum. These shorter conjugation lengths give rise to the high frequency band. This behaviour is reminiscent of resonance Raman spectra of blue polydiacetylene solutions.³⁸

Figure 1.16 shows the C=C stretching region for four different cross-polymerised poly(1,8-nonadiyne) samples each exposed to 6 minutes UV irradiation.³⁰ It is observed that at long incident wavelengths there is only one $\nu(\text{C}=\text{C})$ band (i.e. incident wavelengths of 6328Å and 5145Å respectively) but when short incident wavelengths (i.e. incident wavelengths of 4965Å and 4880Å) are used two bands appear.³⁸

Figure 1.17 shows resonance Raman spectra of poly(1,6-heptadiyne), poly(1,8-nonadiyne) and poly(1,11-dodecadiyne) all exposed to UV light for 3 minutes. The incident wavelength of 6328Å was chosen. From figure 1.17 and Table 1.4 by comparative studies it was proven that the low frequency modes ($1000\text{--}1400\text{cm}^{-1}$) of cross-polymerised poly(1,8-nonadiyne) has a substantial contribution from side group motions. These studies also provide experimental justification of assumptions used by Lewis and Batchelder³⁹ to calculate the normal modes of polydiacetylene chains.

Other resonance Raman studies involved comparison of the resonance Raman intensity behaviour of the 720 and 1211 cm^{-1} bands with that of $\nu(\text{C}=\text{C})$ and $\nu(\text{C}\equiv\text{C})$ bands of cross-polymerised poly(1,8-

nonadiyne) with incident wavelength of 6328Å.³⁰ The plot in figure 1.18 indicates that structural changes take place in the aliphatic side chains after about 1 minute of UV-exposure. Butera and workers proposed that this change could be related to a phase change from the polymer crystal structure to the cross-polymerised crystal structure.³⁰

Butera and workers also observed chromic transitions in poly(α,ω -alkyldiynes) that had been cross-polymerised by exposure to UV light.^{28,31} Cross-polymerised poly(1,8-nonadiyne) can undergo chromic transitions that are surprisingly similar to those of conventional polydiacetylenes. ^{34,37,40-47} A solvatochromic transition can be induced by exposing the cross-polymerised materials to liquids that are good solvents for the virgin polymer. Similarly, a thermochromic transition can be induced by exposing the cross-polymerised material to temperatures greater than the melting point of the crystalline polymer. These transitions occur despite the fact that the cross-polymerised material is insoluble and infusible. This chromic behaviour is dependent upon the degree of conversion ; as conversion is increased less chromic change is observed. ³¹

Visible spectra showing the thermochromic and solvatochromic changes of several poly(1,8-nonadiyne) films with different UV exposure times are shown in figures 1.19 and 1.20 respectively. The changes that take place in the visible spectra of cross-polymerised poly(1,8-nonadiyne) are fundamentally similar for both thermal and solvent treatment. For samples given 30 seconds of UV exposure, a dramatic blue shift and broadening of the visible spectrum results, similar to that observed for the spectrum of a polydiacetylene in a good solvent. The absorption maxima at 620 and 575 nm have disappeared,

and the new maximum is at about 450 nm. As conversion is increased, there is less overall blue shifting of the spectrum. After about 17-25 minutes of UV exposure for thermally treated samples and 10-25 minutes for solvent treated samples the visible spectra before and after are almost identical in character.³¹

Comparison of figures 1.19 and 1.20 show that the spectral changes that take place after thermal and solvent treatment are very similar. The main difference is that there is more blue shifting of the spectra of the thermally treated samples. This is demonstrated in figure 1.21. In this figure, the peak shift after thermal or solvent treatment is plotted as a function of UV exposure time. For UV exposure, the thermochromic transition shows a greater shift than the solvatochromic transitions.³¹

The blue shift of over 150 nm for poly(1,8-nonadiyne) after heat or solvent treatment (shown in figures 1.19 and 1.20) for samples with 30s UV exposure indicates the average conjugation length of the polydiacetylene chains is reduced to about five or six repeat units.³¹ This is about the same conjugation length as found for polydiacetylenes dissolved in a good solvent or in the melt. ^{34,41,43} This would indicate a large degree of conformational disorder involving rotations about the polydiacetylene single bonds within the matrix of the cross-polymerised poly(1,8-nonadiyne).

In order to achieve this kind of long-range disorder, the cross-polymerised structure at low conversions must consist of isolated polydiacetylene chains within a poly(1,8-nonadiyne) matrix. This is demonstrated in figure 1.22. When the poly(1,8-nonadiyne) is exposed

to heat or solvent the long segments of polymer chains that separate the isolated polydiacetylene chains will "melt" or "solubilise". As they disorder these polymer segments will force the polydiacetylene chains to disorder causing a large decrease in the average conjugation length giving rise to the blue shift observed in the visible spectrum. Therefore, the non cross-polymerised segments of poly(1,8-nonadiyne) act like "solubilising side groups" found in soluble polydiacetylenes, in that these poly(1,8-nonadiyne) segments are responsible for the induced conformational disorder of the polydiacetylene chains. ^{41,42,48,49} At low conversions of cross-polymerisation considerable disorder takes place as the network structure is "loose". At high conversions of cross-polymerisation much less disorder takes place as the network structure is "filled in".³¹

On the basis of the visible spectroscopy evidence it was concluded that chromic transitions of cross-polymerised poly(1,8-nonadiyne) were order-disorder type processes.³¹

Wide angle X-ray diffractometer patterns shown in figure 1.23 support this order-disorder mechanism as a decrease in the amount of crystallinity is observed for thermally treated cross-polymerised poly(1,8-nonadiyne) samples.³¹

Resonance Raman spectra were also recorded at an incident wavelength of 6328Å for thermally treated cross-polymerised poly(1,8-nonadiyne) samples (see figure 1.24). The two main features of these spectra are the C=C stretching band and the C≡C stretching band, occurring at 1464 and 2107cm⁻¹, respectively, before thermal treatment.³¹ The other bands in the spectra are due to coupled modes

between the polydiacetylene backbone and the aliphatic spacers.³⁹ The resonance Raman spectrum from the sample with 30s UV exposure shows an almost complete loss of intensity after thermal treatment. This is expected on the basis of the drastic blue shift observed in the visible spectrum after thermal treatment (see figure 1.19). As the UV exposure is increased the resonance Raman spectra obtained after thermal treatment more closely resemble the spectra obtained before thermal treatment.

The observed intensity behaviour of $\nu(\text{C}=\text{C})$ and $\nu(\text{C}\equiv\text{C})$ are summarised in figure 1.25, where the intensity after thermal treatment (I_T) divided by the intensity before thermal treatment (I_I) is plotted as a function of UV exposure time. Figure 1.25 shows the I_T/I_I for both $\nu(\text{C}=\text{C})$ and $\nu(\text{C}\equiv\text{C})$ increase sharply at short UV exposure times and then reach a plateau after about 3–6 min of UV exposure. This is in contrast to the visible spectroscopic results which show that overall, the reaction continues well past 6 minutes of UV exposure.³¹ The difference stems from the fact that resonance Raman spectroscopy preferentially probes specific regions of conjugation length within the sample, whereas visible spectroscopy gives more general information.

Chromic behaviour was also observed for poly(1,6-heptadiyne) and poly(1,11-dodecadiyne). Although a detailed investigation of the chromic transitions of these polymers was not made the preliminary observations suggest that the chromic response is a general feature of the cross polymerised poly(α,ω -alkyldiynes).³¹

Butera and workers also studied the thermal behaviour of the poly(1,8-nonadiyne) using differential scanning calorimetry (DSC) in an

attempt to characterise the solid-state cross-polymerisation reaction.²⁹ Results from thermal analysis of the virgin polymer indicated that little, if any, thermally induced cross-polymerisation occurred during the heating scans.

Thermal analysis of poly(1,8-nonadiyne) that has been melt crystallised in the DSC shows a substantial melt history effect (see figure 1.26). When a poly(1,8-nonadiyne) sample is melted and then immediately cooled through its glass transition temperature (T_g) an exotherm is observed in the following heating scan at 335K (62°C), together with a T_g at 277K (4°C) and a melting endotherm at 363K (90°C). The exotherm at 335K (62°C) was due to crystallisation and not thermal cross-polymerisation as shown by Butera and workers.²⁹ These experiments in figure 1.26 show that as the poly(1,8-nonadiyne) is held at 430K (157°C) for longer periods of time, the subsequent heating scan shows less endothermic and exothermic area. After 25 minutes at 430K (157°C), the subsequent heating scan shows no evidence of crystallinity.²⁹

It was also shown that thermal analysis of cross-polymerised poly(1,8-nonadiyne) can yield semiquantative values on the degree of cross-polymerisation. Figure 1.27 shows DSC thermograms of solution cast poly(1,8-nonadiyne) films which were exposed to UV light for the indicated amount of time before heating in the DSC. Heats of fusion data were obtained for all these samples and a method used to calculate the degree of polymerisation from these values was carried out. The method was based on the fact that the cross-polymerised portions of the sample will be infusible, so the endothermic area decreases as the UV dose of the sample increases. The degree of conversion was plotted

against UV exposure time (minutes) as in figure 1.28, the apparent maximum degree of conversion in the crystalline regions of poly(1,8-nonadiyne) was found to be 78%.²⁹ Although the degree of conversion obtained for samples with long UV exposure times was probably overestimated by Butera's method, thermal analysis is one of the only methods with which an estimate of the degree of conversion can be made and is a convenient way to make relative comparisons of the conversion.²⁹

Preliminary studies of the T_g behaviour of thermally treated cross-polymerised poly(1,8-nonadiyne) samples, as shown in figure 1.29, show that it may be possible to estimate the degree of cross-polymerisation by monitoring changes in T_g breadth and position as a function of UV exposure.²⁹ However, more detailed studies of the T_g behaviour will be needed before estimates of the degree of conversion can be made using T_g data.

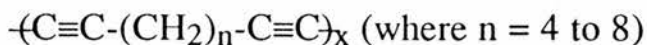
1.4 Aims of this project

The original goal of this project was to synthesise linear, high molar mass polymers and copolymers of the type $\text{-(C}\equiv\text{C(-X)-C}\equiv\text{C)}_n$ (where X can either be an alkyl group of the series (CH₂)₄ through to (CH₂)₈ or a substituted aromatic group which would lead to the synthesis of a novel α,ω -substituted aromatic diyne polymer) fully characterise these polymers, with the anticipation that high tensile modulus films could be fabricated.

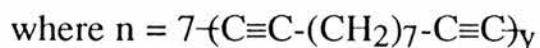
α,ω -alkyldiyne monomers of the type $\text{HC}\equiv\text{C-(CH}_2)_n\text{-C}\equiv\text{CH}$ (where $n = 4$ to 8) were successfully synthesised. However, novel α,ω -

substituted aromatic diyne monomers proved to be not trivial in their syntheses and no success was achieved. Therefore research in that area of work was abandoned.

The project was then reviewed so that only poly(α,ω -alkyldiynes) and copoly(α,ω -alkyldiynes) of the type below were synthesised;



or as in a copolymer; eg



Two Glaser oxidative coupling routes were investigated and developed. In choosing these two systems, certain important factors had to be considered;

- (1) A system that promoted high molar mass polymer — for film fabrication purposes.
- (2) A system which allowed isolation of a clean product — for latter characterisation.
- (3) A system which would not promote cyclisation — the two systems chosen involved using high concentrations since α,ω -alkyldiynes are susceptible to cyclisation under high dilution conditions.⁵⁰

Another goal of the polymerisation work was to study a range of polymers molar mass characteristics with the aim of achieving a fuller understanding of the mechanism of the polymerisation reaction.

This was achieved by using gel permeation chromatography (GPC) together with $^1\text{Hnmr}$ end group analysis (EGA) giving values for

number average molar mass (M_n) which could be compared with each other. Information from the shapes of GPC curves and M_n values provided a fuller understanding of the polymerisation reaction.

Another aim of this study was to carry out extensive thermal characterisation for the poly(α,ω -alkyldiynes) poly(1,9-decadiyne) and poly(1,10-undecadiyne) by DSC. A full study for the thermal characterisation of the virgin polymer poly(1,10-undecadiyne) and its cross-polymerised product is included in Chapter 5.

Other aims in this project involved studying the photochemical cross-polymerisation reaction of the poly(α,ω -alkyldiynes) and the UV and thermal behaviour of a 50:50 copoly(α,ω -alkyldiyne) of 1,9-decadiyne and 1,10-undecadiyne. This was performed to see if its behaviour was similar to that of the corresponding homopolymers. Visible spectra of the poly(1,9-decadiyne), poly(1,10-undecadiyne) and poly(1,11-dodecadiyne) are included. Plots involving absorbance at 650 nm for increasing UV exposure time (minutes) are included and the reaction order is determined. UV and DSC studies on a 50:50 copolymer powder and film of 1,9-decadiyne and 1,10-undecadiyne are performed. Conductivity and resonance Raman spectroscopy studies are also carried out on cross-polymerised films of poly(1,9-decadiyne) and poly(1,11-dodecadiyne).

Cell Parameters	Polymer	Cross-polymerised product
a,Å	13.25	9.17
b,Å	14.15 (chain axis)	12.25 (hydrocarbon chain axis)
c,Å	7.63	9.92 (diacetylene chain axis)
β ,deg	118.50	123.50

Table 1.1.
Comparison of the Unit Cell Dimensions for poly(1,11-dodecadiyne)
and its Cross-polymerised product.(from ref 23)

Cell Parameters	Polymer	Cross-polymerised product
a,Å	7.88	9.30
b,Å	21.00 (chain axis)	17.5 (hydrocarbon chain axis)
c,Å	5.67	4.85 (diacetylene chain axis)
β ,deg	90.8	101.71
volume(Å ³)	938.18	772.90

Table 1.2.
Comparison of the Unit Cell Dimensions for poly(1,8-nonadiyne)
and its Cross-polymerised product.(from ref 24)

obsd freq, cm ⁻¹		
$\lambda_0 = 6328 \text{ \AA}$	$\lambda_0 = 5145 \text{ \AA}$	band assignmts
2101	2111	$\nu(\text{C}\equiv\text{C})$
1464	1483	$\nu(\text{C}=\text{C})$
1362		
1339	1374 (br)	
1262	1281	
1211	1238	
1087	1104	
720	741	

Table 1.3. Comparison of Observed Resonance Raman Frequencies Using Incident Wavelengths of 6328Å and 5145Å for cross-polymerised poly(1,8-nonadiyne) (6min UV exposure).(from ref 30)

obsd freq, cm ⁻¹			
XP16H(A)	XP18N (B)	XP111D(C)	band assignmts
2100	2101	2099	$\nu(\text{C}\equiv\text{C})$
1460	1464	1464	$\nu(\text{C}=\text{C})$
1374	1362	1352	
1341	1339	1328	
1285	1262	1241	
(weak)		1274	
1221	1211	1209	$\nu(\text{C}-\text{C})$
1071	1087	1107	
726	720	714	

Table 1.4. Observed Resonance Raman Frequencies for cross-polymerised (A) poly(1,6-heptadiyne).(B) poly(1,8-nonadiyne) and (C) poly(1,11-dodecadiyne) Obtained by Using Incident Wavelength = 6328Å(from ref 30)

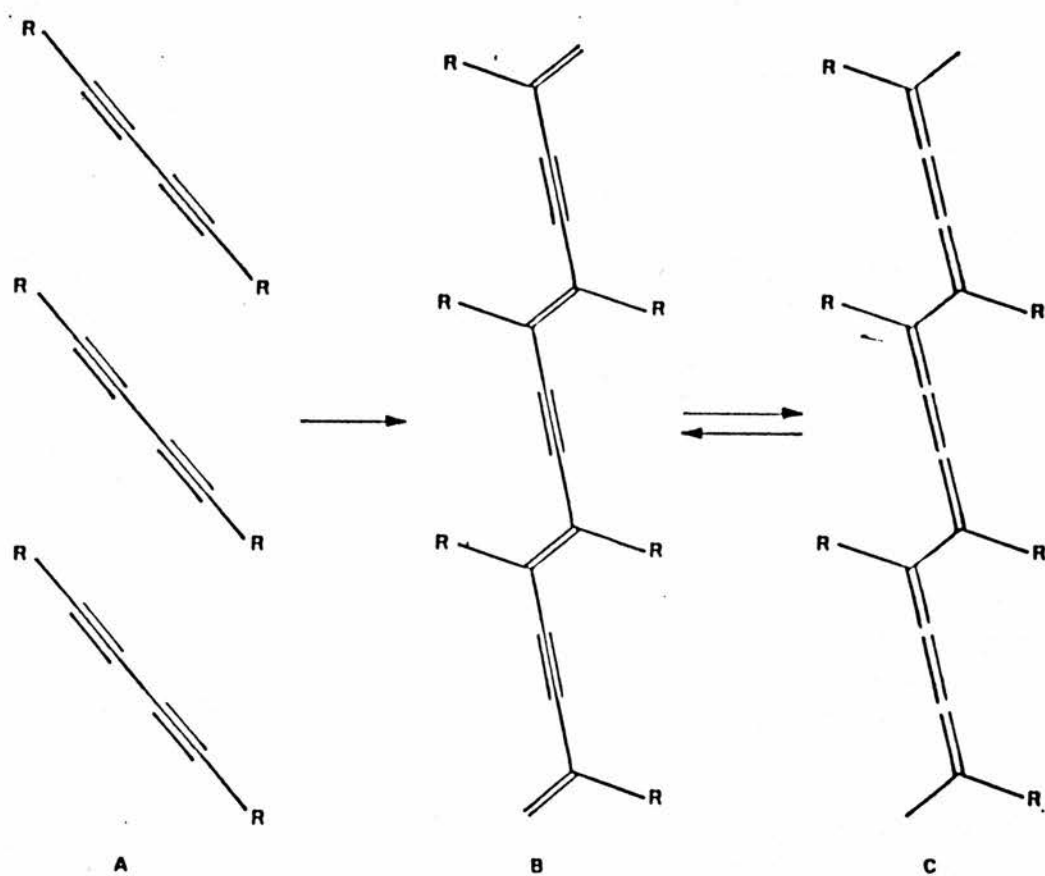


Figure 1.1. Schematic representation of the diacetylene polymerisation process.
 (A = monomer, B = acetylenic polymer, C = butatrienic polymer).
 (from ref 4)

Translational direction invariant motion

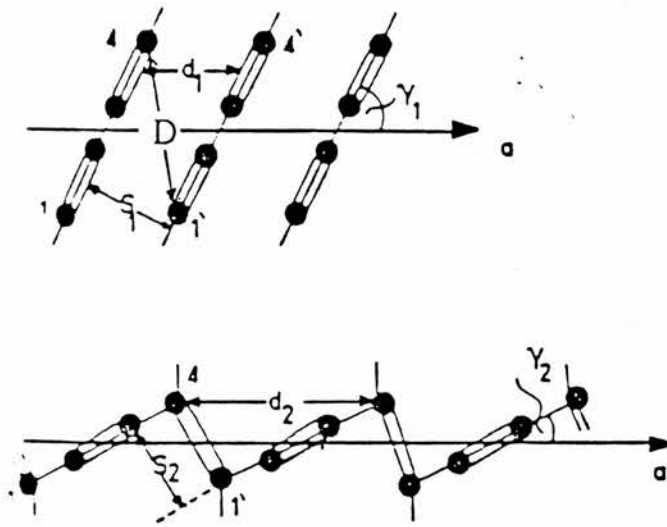


Figure 1.2. Explanation of topochemistry of diacetylene polymerisation according to ref 4 applying the least motion principle. (from ref 5)

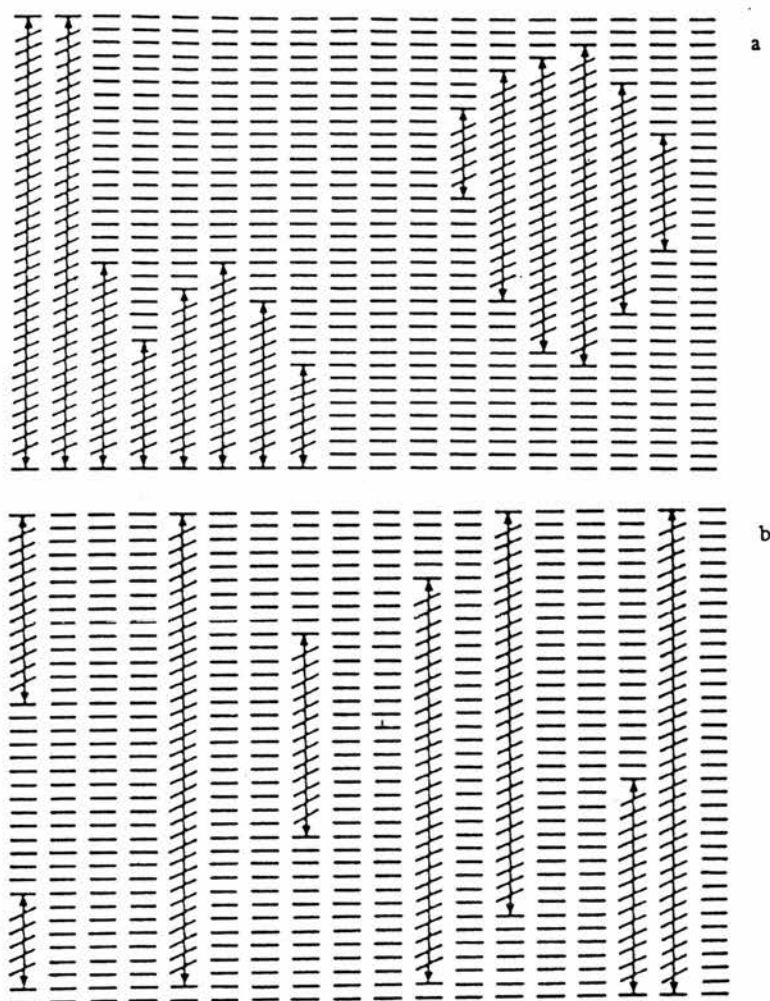


Figure 1.3. Mechanism of phase change in the course of a topochemical polymerisation a) heterogeneous b) homogeneous reaction. (from ref 5)

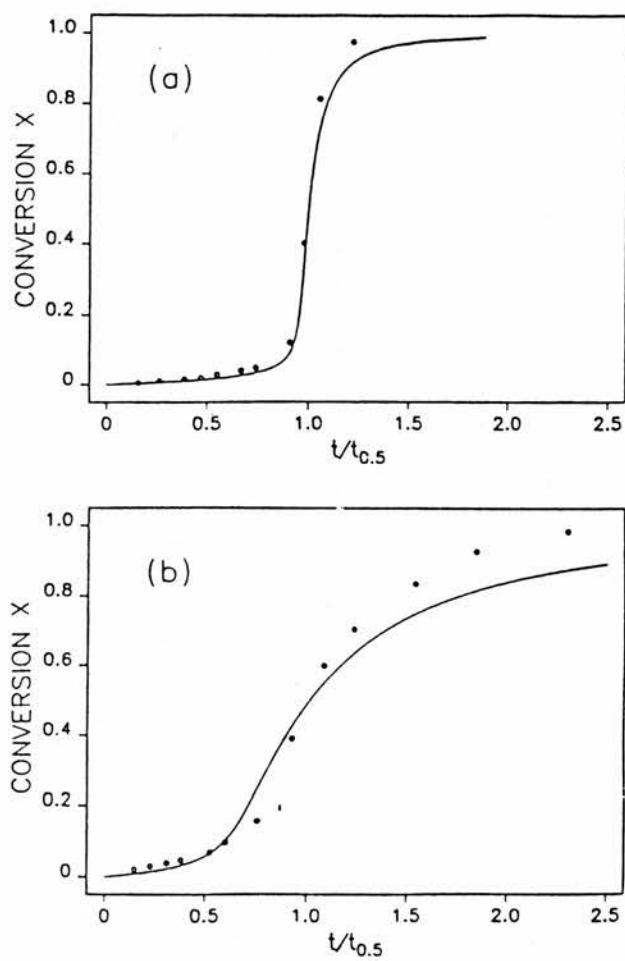


Figure 1.4. Conversion as a function of time for
a) thermally induced

b) photo induced polymerisation of PTS

The time scale is normalised with respect to the time of half conversion.
(from ref 14)

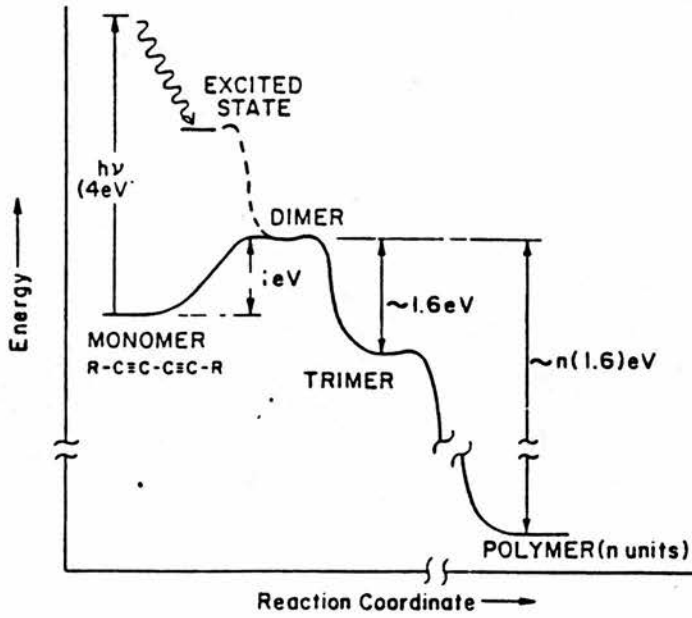


Figure 1.5. Reaction diagram for diacetylene polymerisation. (from ref 16)

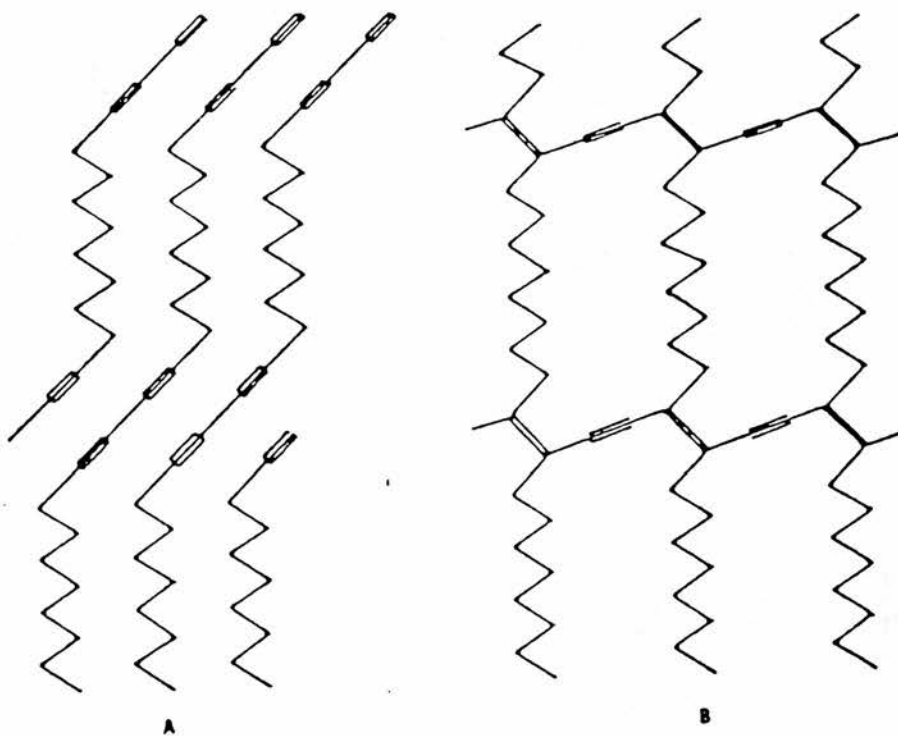


Figure 1.6. Cross-polymerisation reaction scheme for poly(1,11-dodecadiyne).
(A = polymer, B = cross-polymerised product).
H atoms omitted for clarity. (from ref 23)

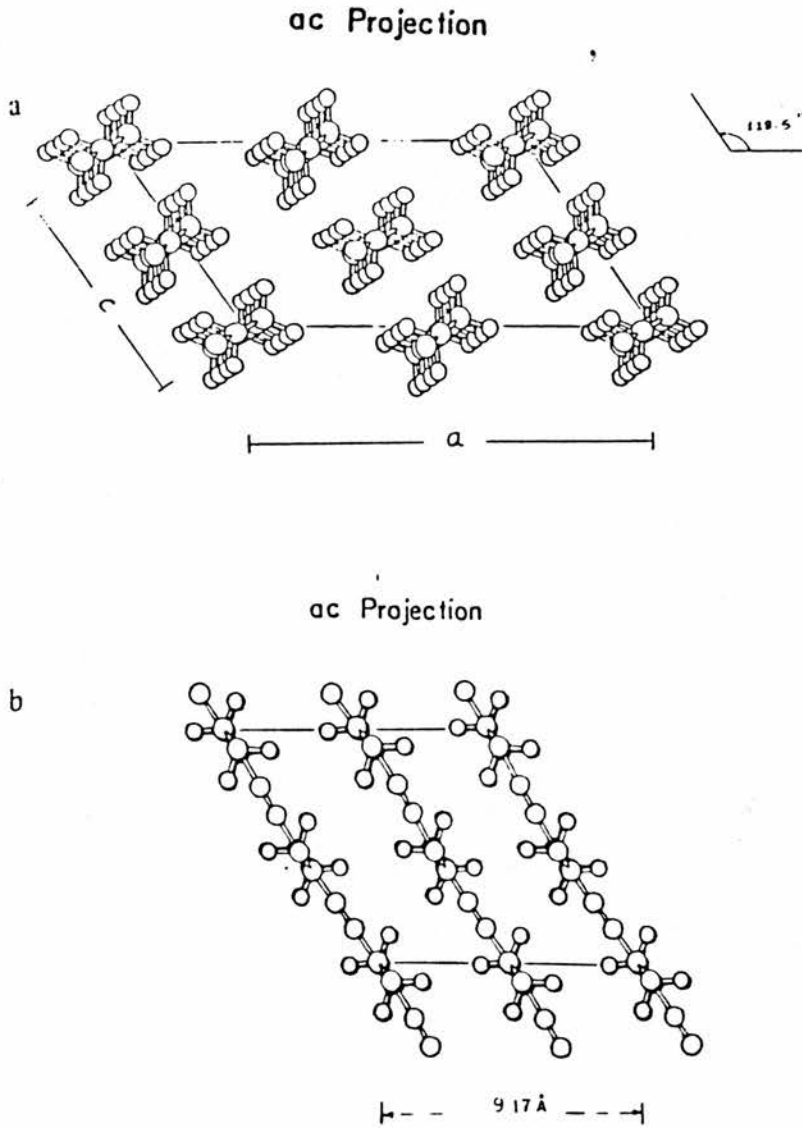


Figure 1.7. ac projections of (a) poly(1,11-dodecadiyne) (b) cross-polymerised poly(1,11-dodecadiyne). (from ref 23)

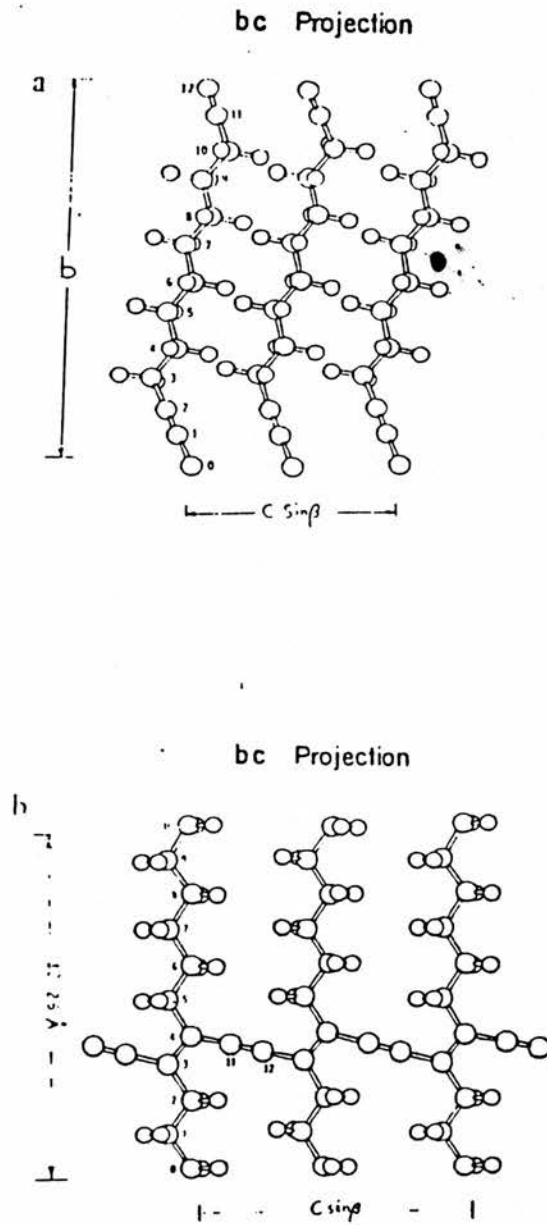


Figure 1.8.bc projections of(a) poly(1,11-dodecadiyne)(b) cross-polymerised poly(1,11-dodecadiyne).(from ref 23)

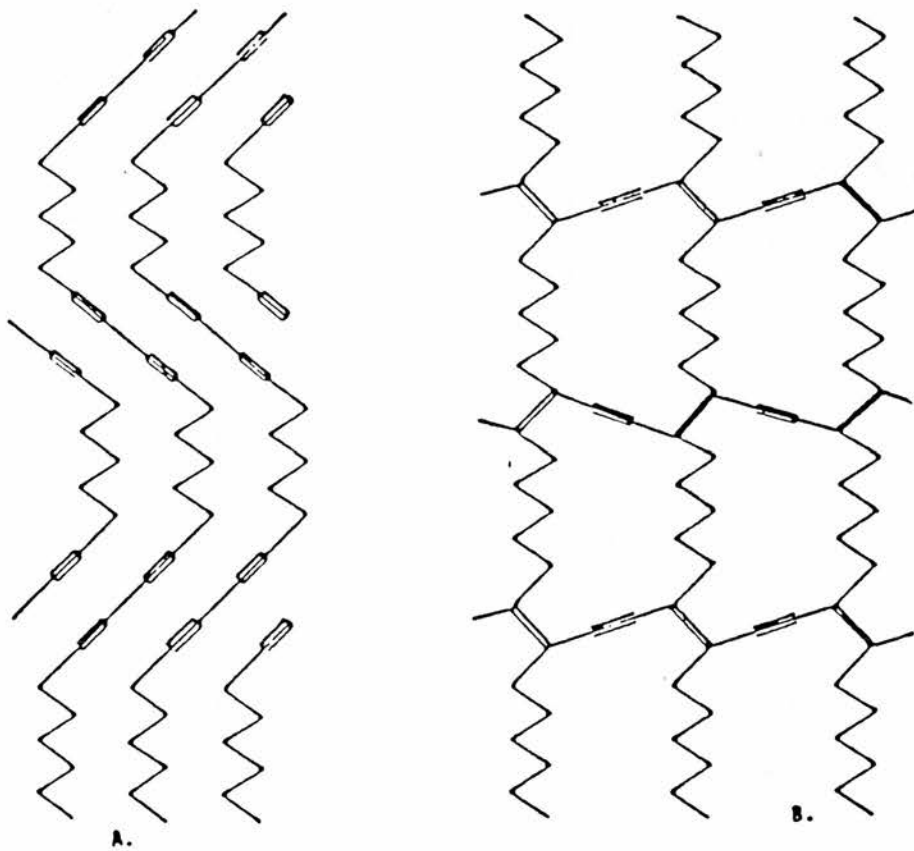
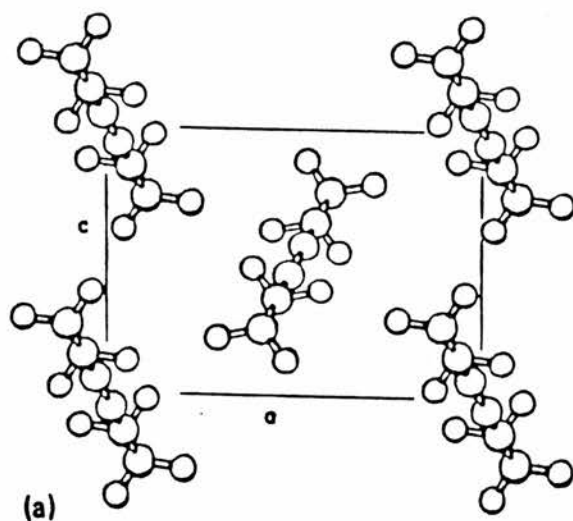


Figure 1.9. Cross-polymerisation reaction scheme for poly(1,8-nonadiyne).
(A = polymer, B = cross-polymerised product).
H atoms omitted for clarity. (from ref 24)

ac Projection



ac Projection

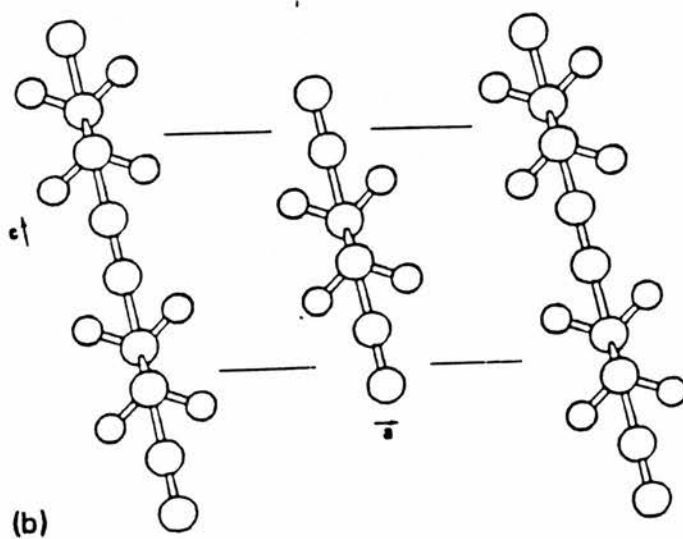
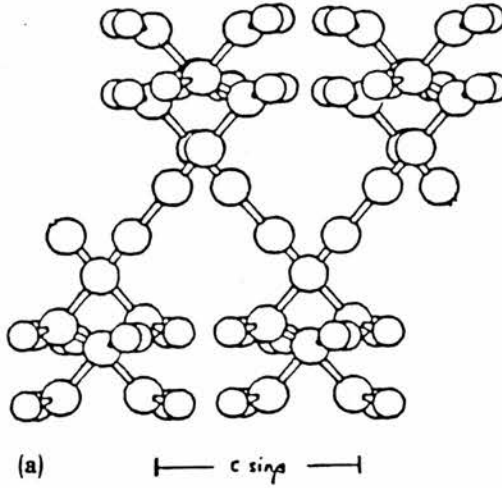


Figure 1.10.ac projections of(a) poly(1,8-nonadiyne)(b) cross-polymerised poly(1,8-nonadiyne). (from ref 24)

bc Projection



bc Projection

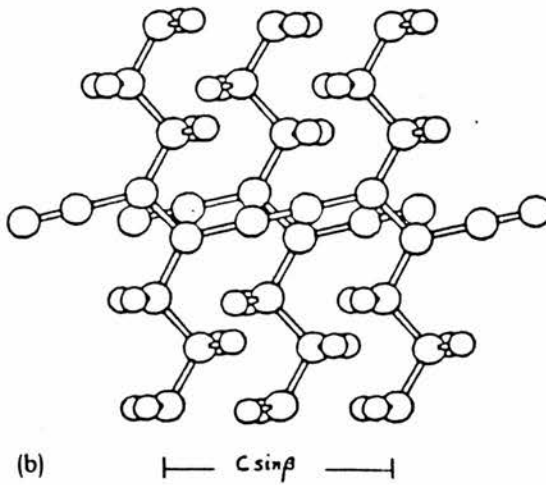


Figure 1.11.bc projections of (a) poly(1,8-nonadiyne) (b) cross-polymerised poly(1,8-nonadiyne). (from ref 24)

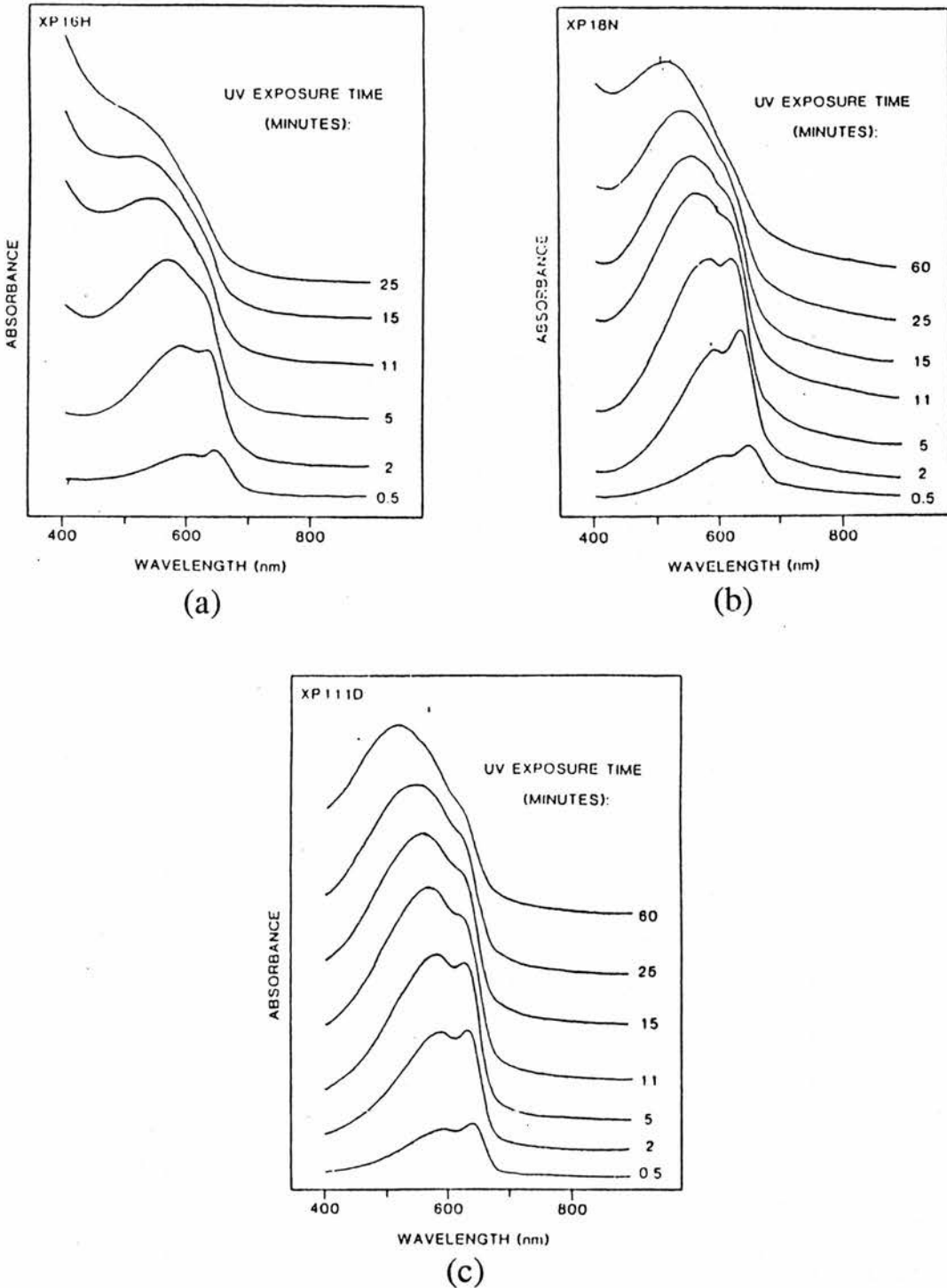


Figure 1.12. Visible absorption spectra of (a) poly(1,6-heptadiyne), (b) poly(1,8-nonadiyne) and (c) poly(1,11-dodecadiyne) films recorded after various UV exposure times. All spectra were corrected for scattering and arbitrarily offset. (from ref 30)

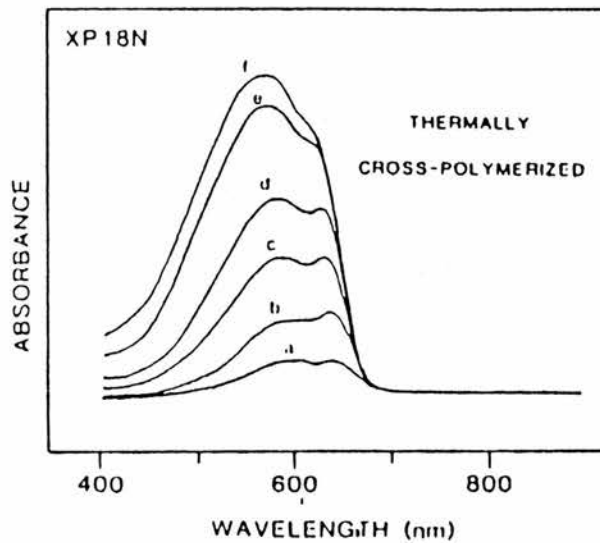


Figure 1.13. Visible absorption spectra of (a) poly(1,8-nonadiyne) film thermally polymerised in the dark at 20 for the following amount of time (a) 10 days (b) 15 days (c) 20 days (d) 25 days (e) 35 days and (f) 45 days. All spectra were corrected for scattering. (from ref 30)

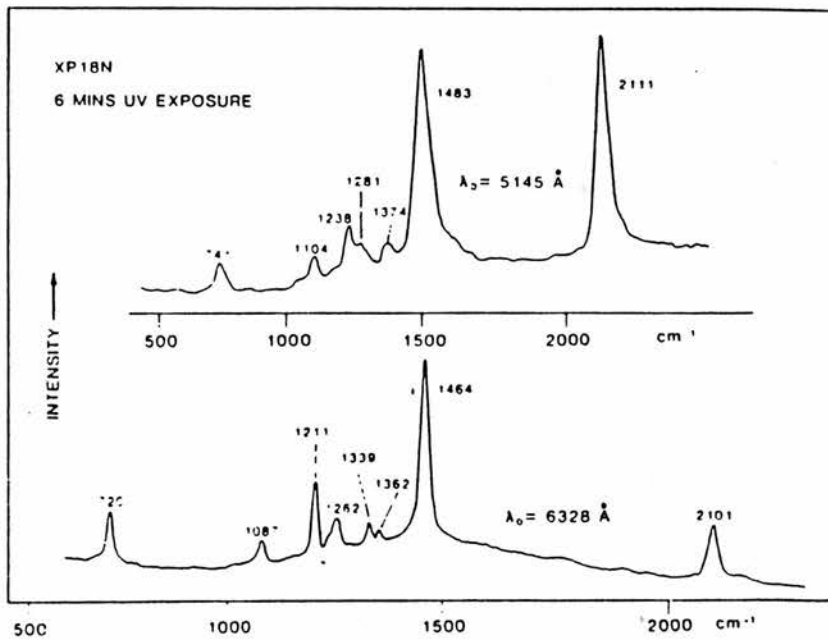


Figure 1.14. Resonance Raman spectra of poly(1,8-nonadiyne) films exposed to UV light for 6 minutes. Spectra were obtained by using 6328 Å and 5145 Å incident wavelengths. (from ref 30)

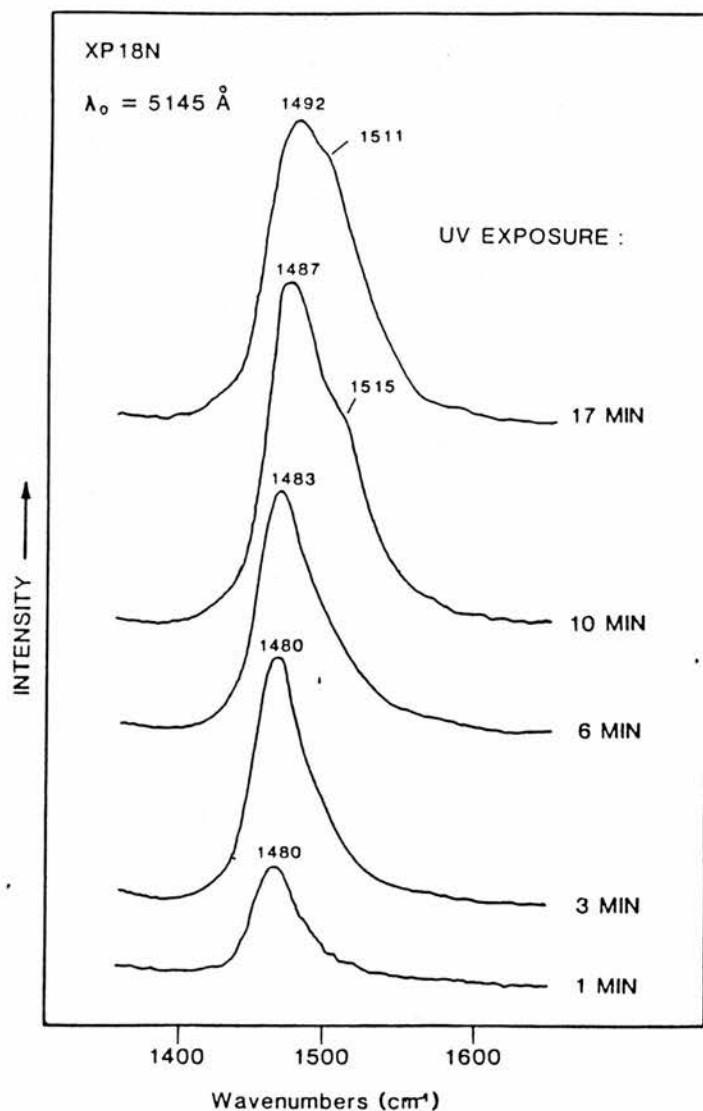


Figure 1.15. Resonance Raman spectra of poly(1,8-nonadiyne) films exposed to UV light for the indicated amount of time. Spectra were obtained by using 5145 \AA incident wavelength. (A different sample was used for each spectrum). The spectra were arbitrarily offset for clarity. (from ref 30)

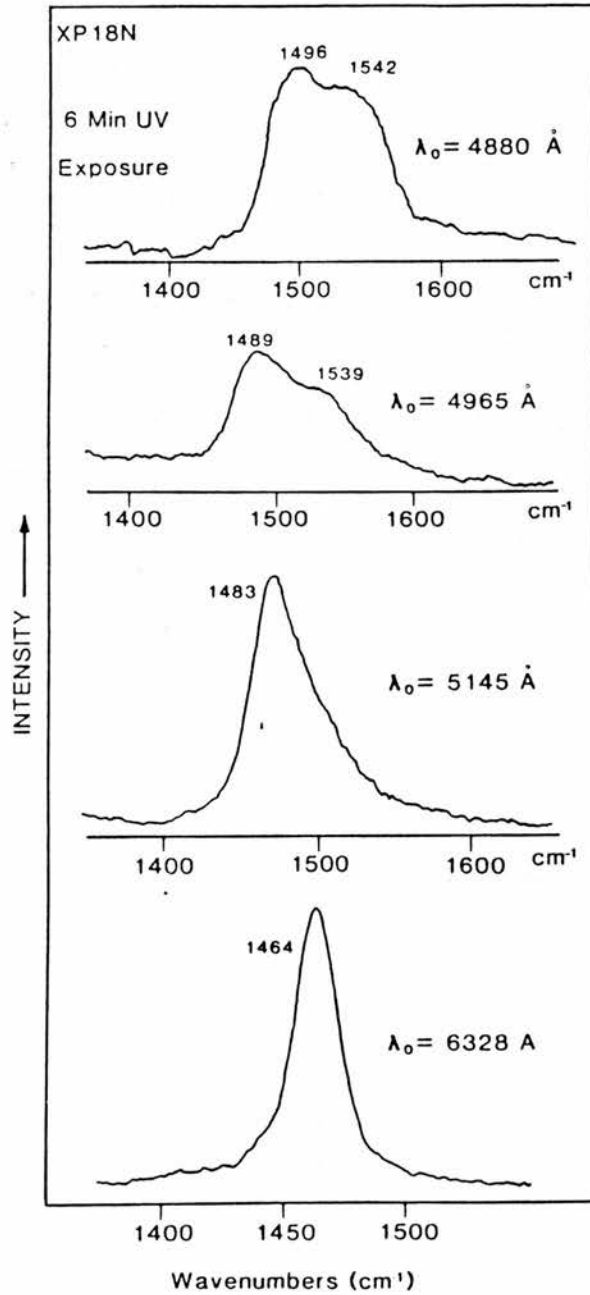


Figure 1.16. Resonance Raman spectra of the $\nu(\text{C}=\text{C})$ region for poly(1,8-nonadiyne) films exposed to UV light for 6 minutes. Spectra were obtained by using 6328, 5145, 4965, and 4880 Å incident wavelengths. (from ref 30)

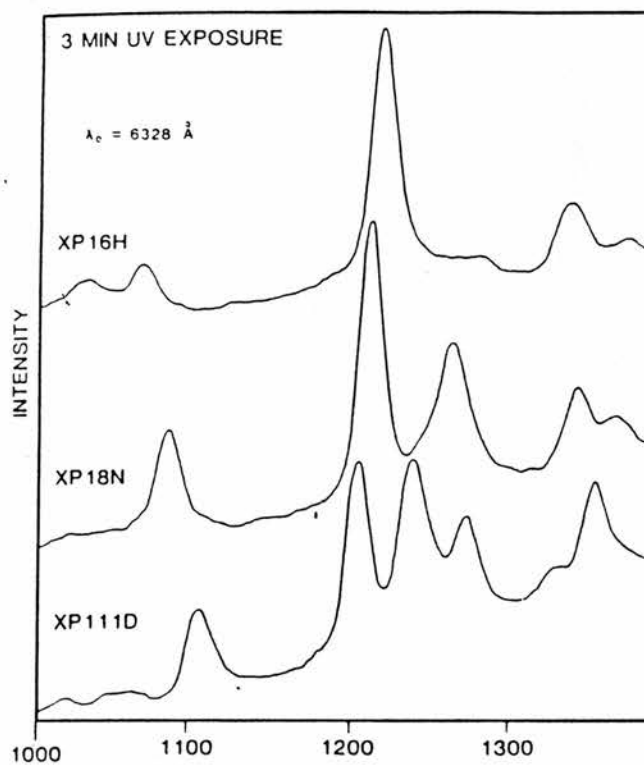


Figure 1.17. Resonance Raman spectra of (a) poly(1,6-heptadiyne), (b) poly(1,8-nonadiyne) and (c) poly(1,11-dodecadiyne) all exposed to UV light for 3 minutes. Spectra were arbitrarily offset for clarity. (from ref 30)

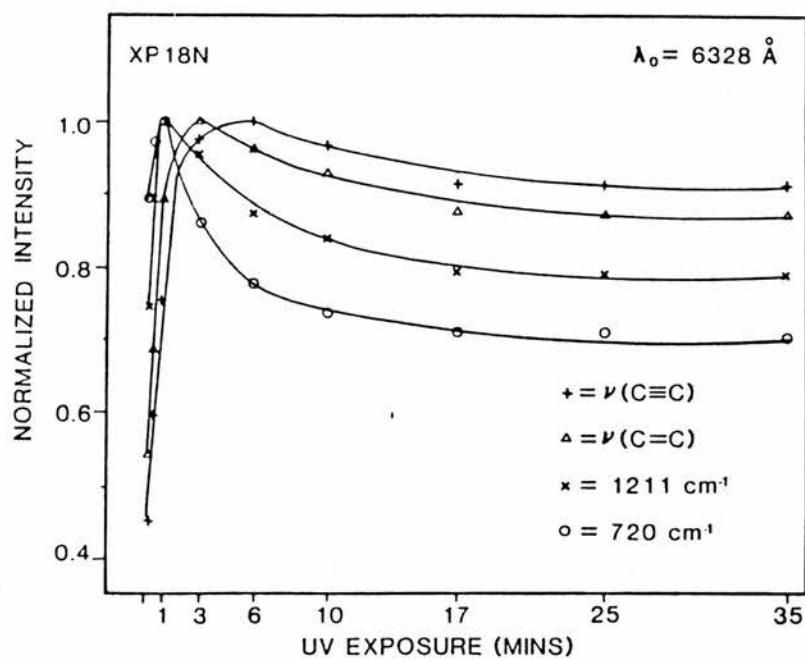


Figure 1.18. Normalised intensity of $\nu(\text{C}\equiv\text{C})$ (+), $\nu(\text{C}=\text{C})$ (Δ), the 1211 cm^{-1} band (x) and the 720 cm^{-1} (o) as a function of UV exposure time ($IW = 6328 \text{ \AA}$). (from ref 30)

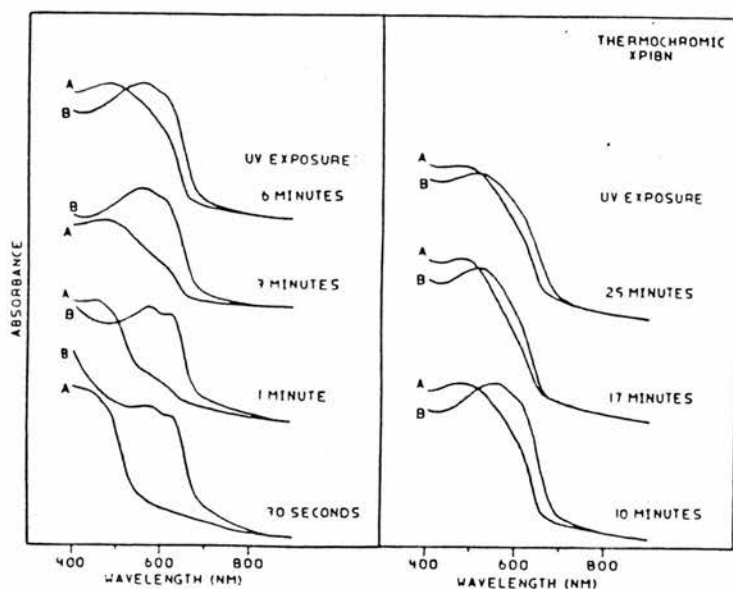


Figure 1.19. Visible spectra of cross-polymerised poly(1,8-nonadiyne) films. Spectra labelled (A) were recorded after the samples were heated to 115°C for 4 min and then returned to room temperature. Spectra labelled (B) were recorded before thermal treatment. Sets of spectra have been arbitrarily offset for clarity. (from ref 31)

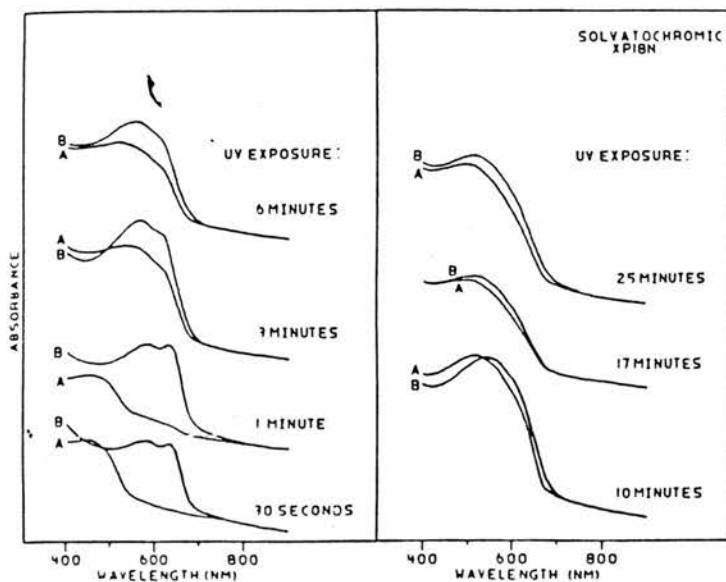


Figure 1.20. Visible spectra of cross-polymerised poly(1,8-nonadiyne) films. Spectra labelled (A) were recorded after the samples were soaked in methylene chloride for 5 min and then dried. Spectra labelled (B) were recorded before solvent treatment. Sets of spectra have been arbitrarily offset for clarity. (from ref 31)

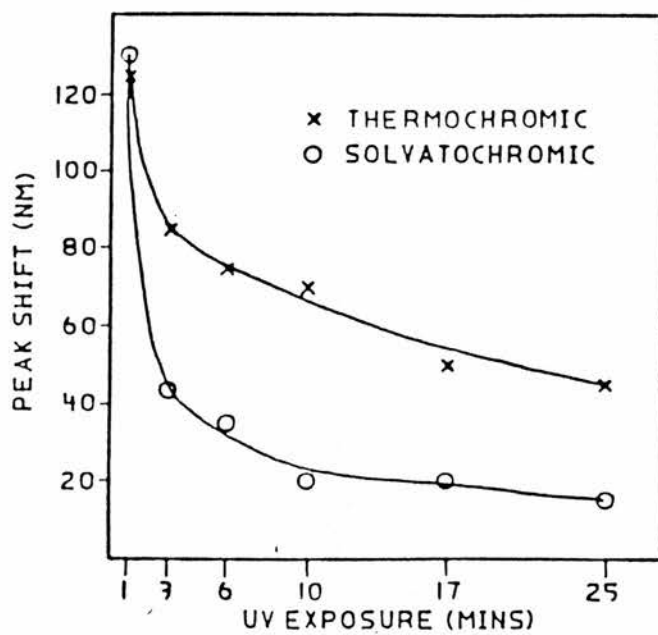


Figure 1.21. Change in absorbance maximum position for cross-polymerised poly(1,8-nonadiyne) after thermal and solvent treatment, as a function of UV exposure time. (from ref 31)

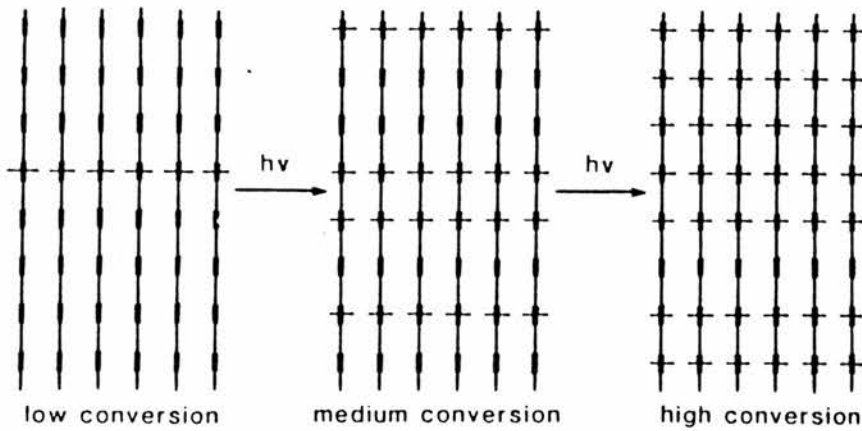


Figure 1.22. Scheme for the progressive development of the network structure in poly(1,8-nonadiyne). The vertical lines represent the polymer chains, and the dashed horizontal lines represent the polydiacetylene chains formed upon cross-polymerisation. (from ref 31)

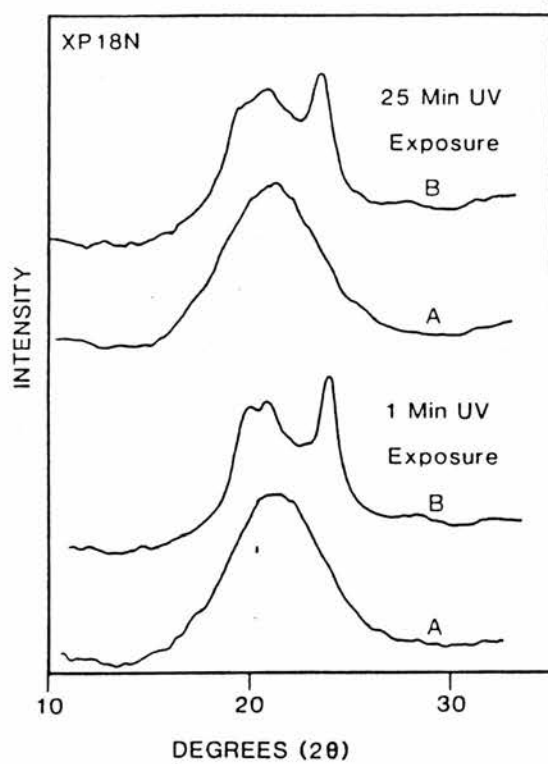


Figure 1.23. Wide-angle X-ray diffractometer patterns of cross-polymerised poly(1,8-nonadiyne): (A) after heating to 120° C for 2 minutes and then returning to room temperature; (B) before thermal treatment.
(from ref 31)

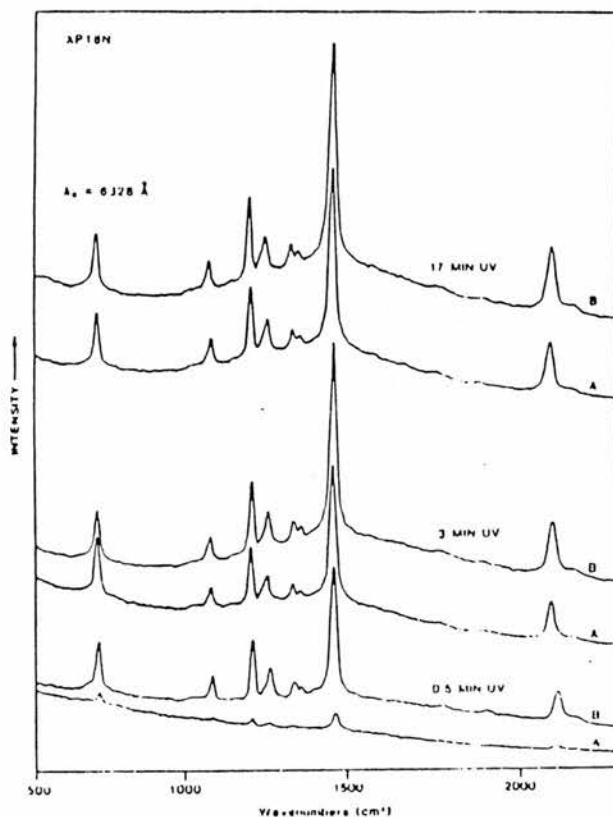


Figure 1.24. Resonance Raman spectra of cross-polymerised poly(1,8-nonadiyne) after various UV exposure times: (A) after heating to 120°C for 5 minutes and then returning to room temperature; (B) before thermal treatment. Incident wavelength = 6328 \AA . Sets of spectra were arbitrarily offset for clarity. (from ref 31)

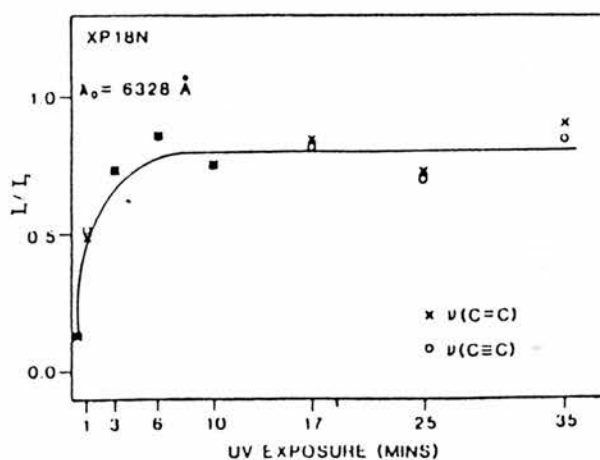


Figure 1.25. Fractional decrease in resonance Raman intensity for cross-polymerised poly(1,8-nonadiyne) after thermal treatment, as a function of UV exposure. I_T refers to the intensity after thermal treatment; I_1 refers to the intensity before thermal treatment. (from ref 31)

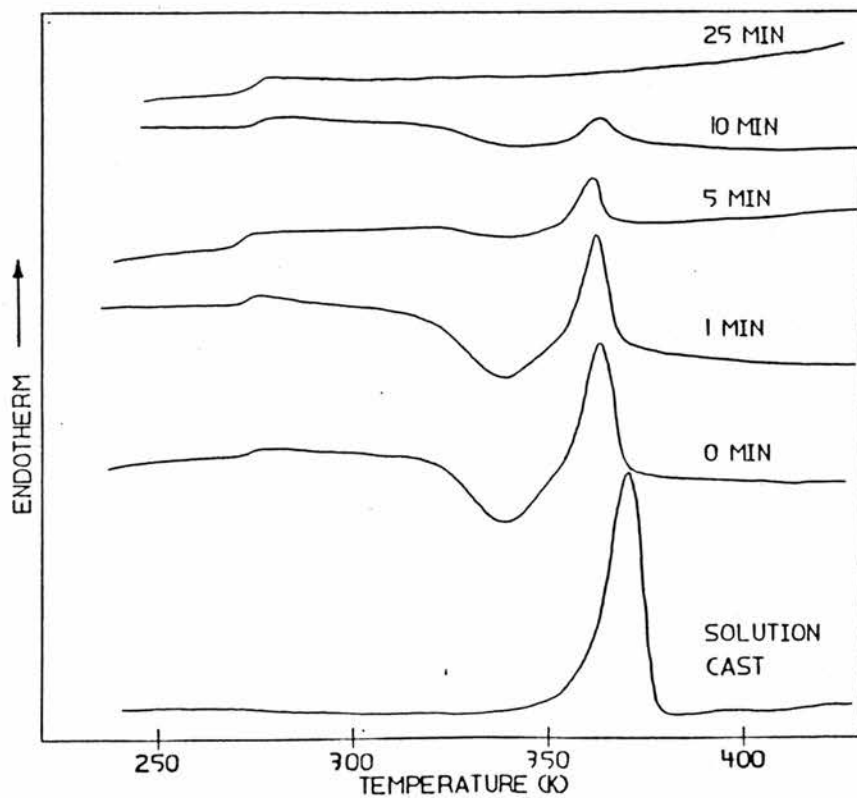


Figure 1.26. DSC thermograms of solution cast poly(1,8-nonadiyne) films which were heated from 220K (-53°C) to 430K (157°C), annealed at 430K for the indicated amount of time, and quenched to 220K. A thermogram from a solution cast film is shown for reference (all heating rates 20°C/min). (from ref 29)

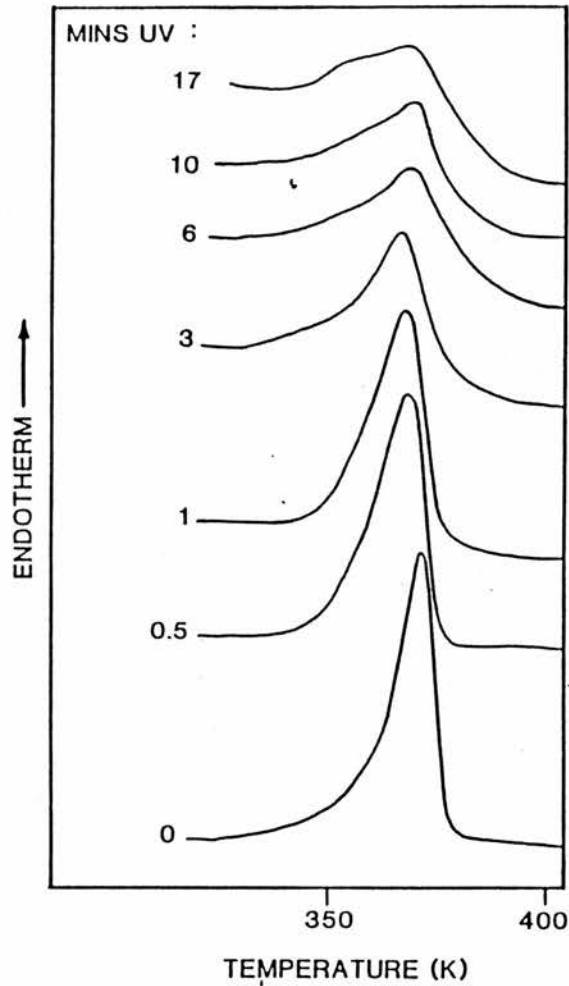


Figure 1.27. DSC thermograms of solution cast poly(1,8-nonadiyne) films which were exposed to UV irradiation for the indicated amount of time before heating in the DSC (heating rate 20°C/min). (from ref 29)

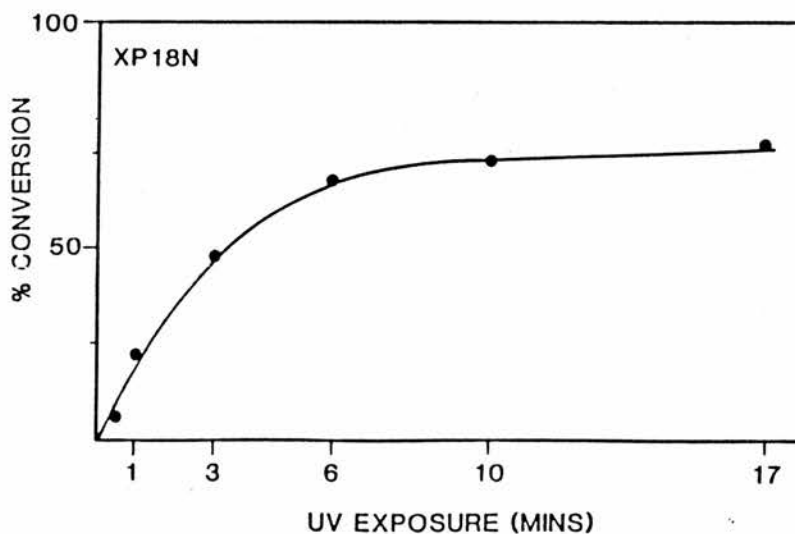


Figure 1.28. Percentage conversion to cross-polymerised form in the crystalline regions as a function of UV exposure for poly(1,8-nonadiyne). (from ref 29)

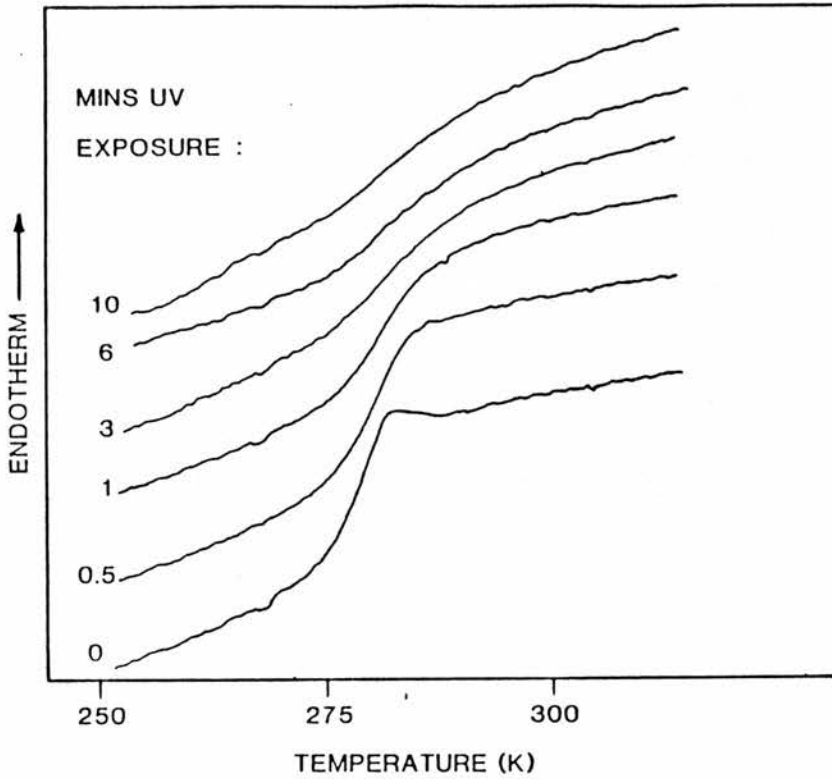


Figure 1.29. DSC thermograms for poly(1,8-nonadiyne) films which were exposed to UV irradiation for the indicated amount of time then heated from 230K (-43°C) to 430K (157°C), and quenched to 250K (-23°C) (heating rate 20°C/min). (from ref 29)

CHAPTER 2

SYNTHESES AND ATTEMPTED SYNTHESES OF α,ω -DIYNE MONOMERS

2.1 Introduction

The purpose of the work in this chapter is to synthesise α,ω -alkyldiyne monomers of the type $\text{HC}\equiv\text{C}-(\text{CH}_2)_n-\text{C}\equiv\text{CH}$ ($n=4$ to 8) and novel α,ω -aromaticdiyne monomers for their use in the oxidative polymerisation reaction (see Chapter 3). The synthesis of two other terminal diyne compounds trans-4-octene-1,7-diyne and 1,4-diethynylbenzene, which do not fall into either of the above two categories, are also carried out.

No oxidative polymerisation work is intended for the monomers trans-4-octene-1,7-diyne and 1,4-diethynylbenzene but both are included in this chapter because routes to their syntheses are relevant in the syntheses of the novel α,ω -aromaticdiyne monomers. The synthesis of trans-4-octene-1,7-diyne involves a copper catalysed reaction of an ethynylgrignard reagent with a dibromocompound. Attempts at synthesising novel α,ω -aromaticdiyne monomers also involve copper catalysed reactions of ethynylgrignard reagents with dibromocompounds or in some instances diiodocompounds. In this study the synthesis of 1,4-diethynylbenzene involves FVP of its corresponding phosphorus diylide. Attempts at synthesising the corresponding phosphorus diylide for FVP to give the novel α,ω -aromaticdiyne monomer 1,4-di-2-propynylbenzene are also carried out.

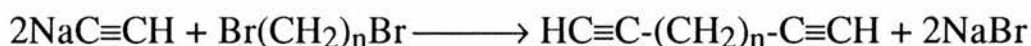
Before experimental details are reported the literature methods adopted in the syntheses of the α,ω -alkyldiynes, trans-4-octene-1,7-diyne and 1,4-diethynylbenzene will be discussed together with my results. Also, selected methods for the attempted syntheses of the novel

α,ω -aromatic diyne monomers will be discussed in conjunction with my results and findings .

2.2 Syntheses of α,ω -diyne monomers - a discussion of methods used in their syntheses and results achieved

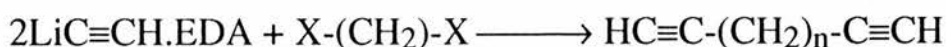
For the syntheses of α,ω -alkyldiyne monomers of the series $\text{HC}\equiv\text{C}-(\text{CH}_2)_n-\text{C}\equiv\text{CH}$ (where $n=4$ to 8) several methods can be employed but in essence only two methods need be used in their syntheses. Both involve action of alkali metal acetylides on α,ω -dihaloalkanes.

A Action of sodium acetylide on α,ω -dibromoalkanes in liquid ammonia,



The reaction was carried out by Lespiau and Journand ⁵¹ in 1929 when monomers 1,6-heptadiyne and 1,8-nonadiyne were synthesised. Since then several workers have synthesised α,ω -alkyldiynes by this method. Yields of up to 80% are obtained using this method. ^{50,52,53,54}

B Action of Lithium acetylenide-ethylenediamine complex on α,ω -dihaloalkanes in Dimethylsulphoxide



+ 2LiX

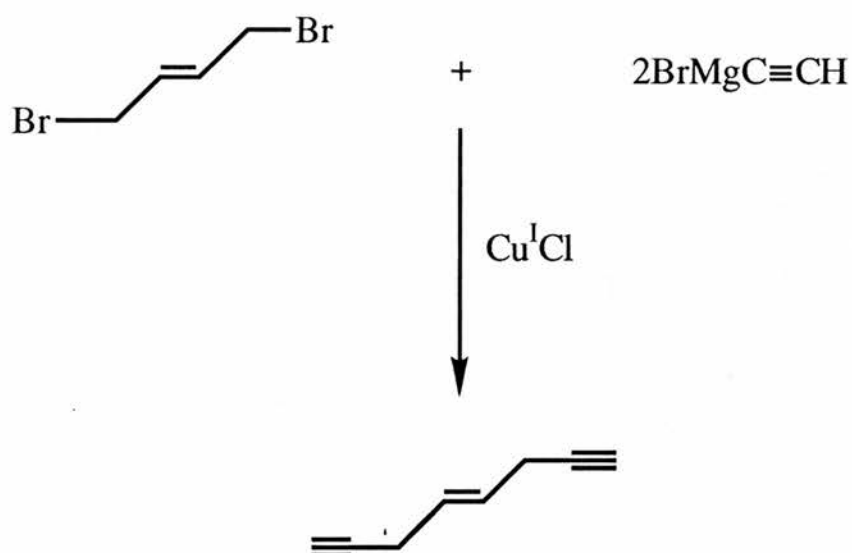
X=Cl, Br

The reaction was first carried out by Smith and Beumel ⁵⁵, in 1974 when monomers 1,7-octadiyne, 1,8-nonadiyne and 1,9-decadiyne were synthesised. They found that the α,ω -dibromoalkanes were more reactive than the α,ω -dichloroalkanes and they required lower addition temperatures, shorter reaction times and in general higher yields were obtained. The monomer, 1,9-decadiyne was obtained in 72% yield from 1,6-dichlorohexane but forcing conditions were required to remove all of the dichlorohexane. The purity of α,ω -alkyldiynes as initially isolated were 95–99% from the α,ω -dibromoalkanes, and 45–84% from the α,ω -dichloroalkanes with contaminants consisting of starting dihalide and ω -halo- α -alkyne.

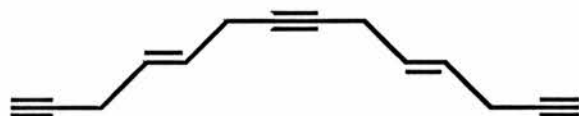
In 1990 Butera and workers ³⁰ synthesised 1,11-dodecadiyne from 1,8-dibromooctane and Lithium acetylenide-ethylenediamine complex (LiAc-EDA) by following Smith's work with some minor modifications.

Method A was selected in favour of method B for the synthesis of α,ω -alkyldiynes, yields ranging from 65–71% were obtained using this method. In Method B in order to obtain good yields an argon atmosphere and rigorously dry conditions must be employed. (Dimethylsulphoxide must be dried with calcium hydride and filtered before use).

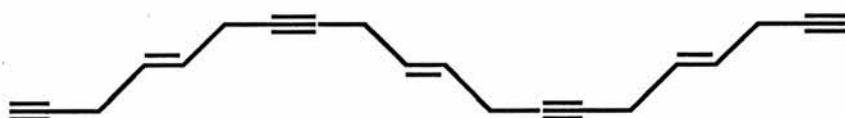
For the synthesis of trans-4-octene-1,7-diyne one method was employed. This was the literature method adopted by Gaoni and workers ⁵⁶ which involved condensation between trans-1,4-dibromo-2-butene and an excess of 2 molar equivalents of ethynylmagnesium bromide in the presence of cuprous chloride. Trans-4-octene-1,7-diyne was obtained in 25% yield.



Although trans-4-octene-1,7-diyne was the major product from the reaction Gaoni and workers ⁵⁶ isolated two additional substances;



(I) trans, trans-4,10-tetradecadiene-1,7,13-triyne

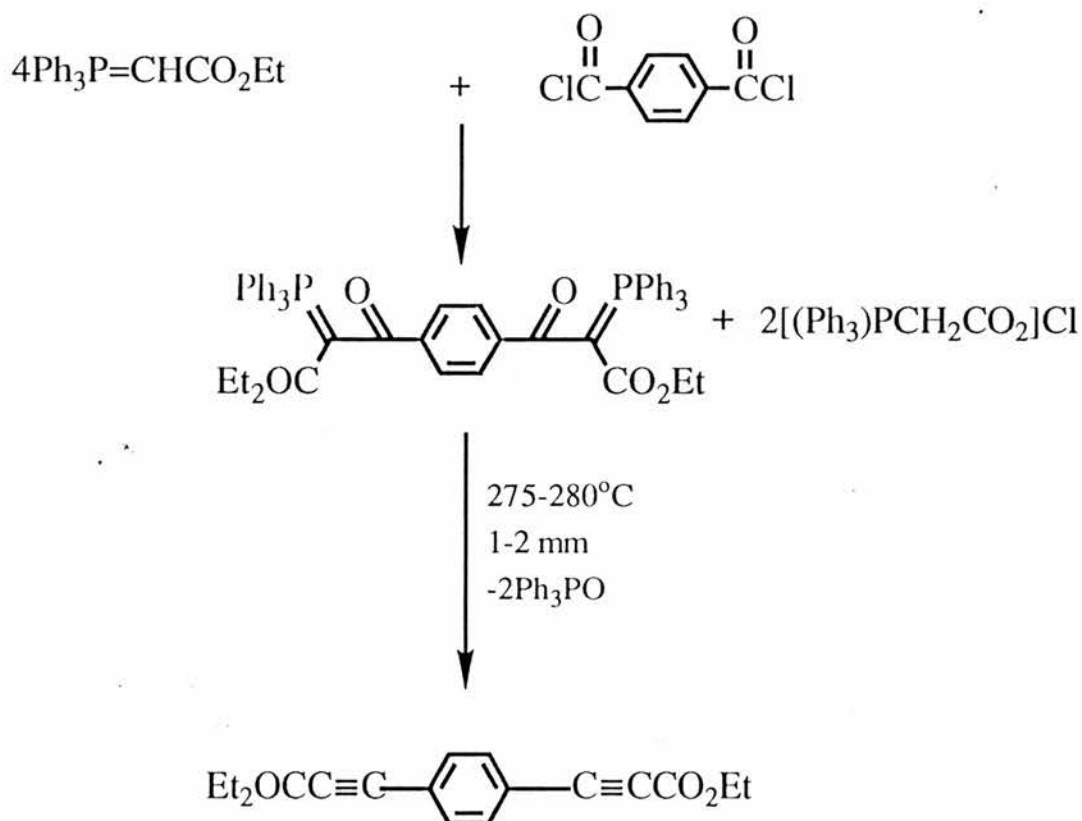


(II) all-trans-4,10,16-eicosatriene-1,7,13,19-tetrayne

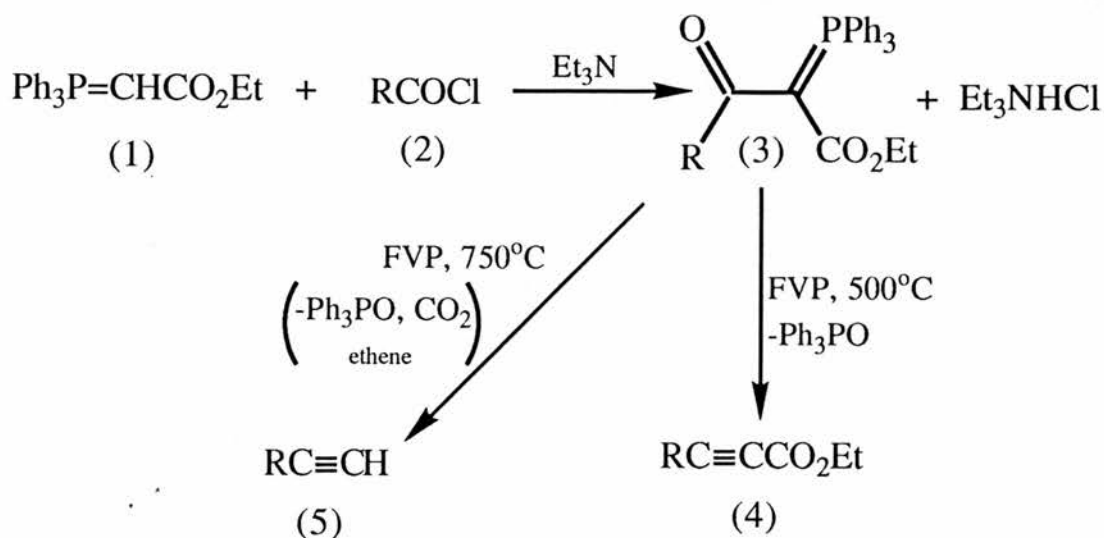
In this present work trans-4-octene-1,7-diyne was synthesised according to the literature method mentioned above and obtained in 18% yield.

For the synthesis of 1,4-diethynylbenzene flash vacuum pyrolysis (FVP) of the corresponding Phosphorus diylide was performed. A discussion of the previous work carried out in this area on diacetylenic compounds is included, before the actual route for obtaining 1,4-diethynylbenzene is shown.

In 1975 Henry obtained 1,4-di-(ethoxycarbonylmethylene triphenylphosphorane)benzene from 4 equivalents of ethoxycarbonylmethylenetriphenylphosphorane and terephthaloyl chloride in dry benzene at 25°C.⁵⁷ After recrystallisation of this compound from dry xylene pyrolysis at a pressure of 1–2 mm in a Wood's metal bath at 275–280°C yielded, 1,4-di-(carboethoxyethynyl)benzene. The following steps (essentially an extension of the method of Gough and Trippett⁵⁸) were involved. See reaction scheme overleaf.



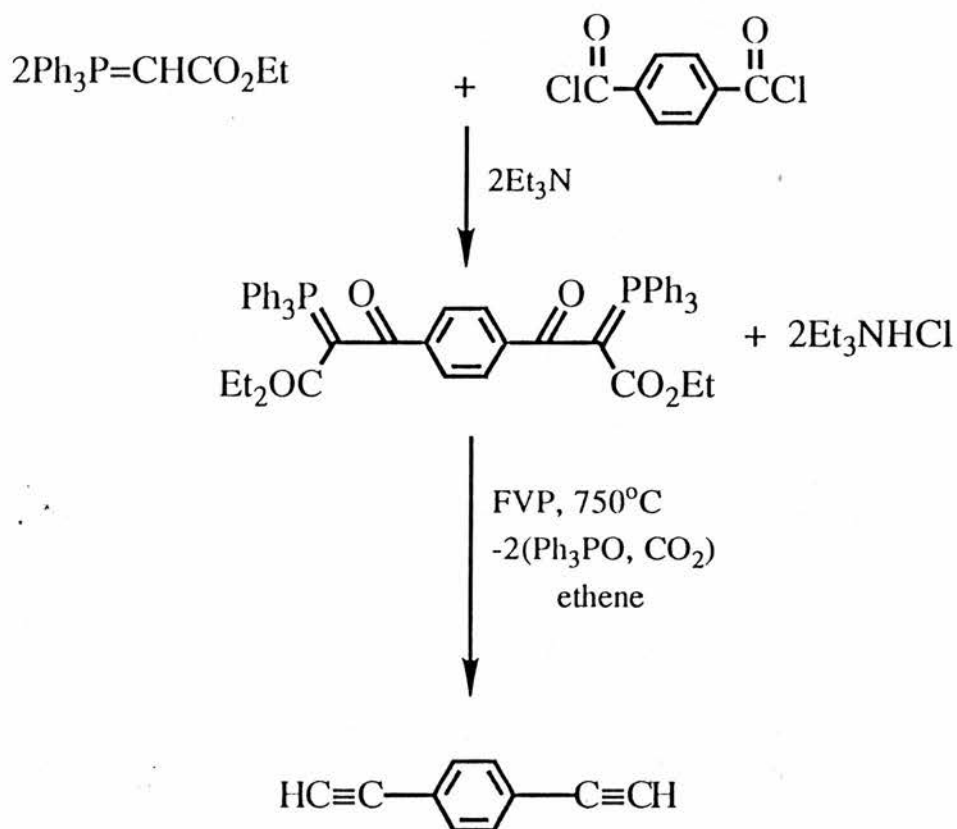
In 1990 Aitken ⁵⁹ reported a procedure which used one equivalent of ethoxycarbonylmethylenetriphenylphosphorane (1) with acid chlorides (2) to give ylides (3). The conventional pyrolysis of the methoxycarbonyl analogues of (3) have been known to be an efficient source of acetylenic esters. ⁵⁸ While it has been found that FVP of (3) at 500°C gives acetylenic esters (4) in good yield ⁶⁰, it was observed that upon simply raising the furnace temperature to 750°C, the extrusion of Ph₃PO is accompanied by loss of the ethoxycarbonyl group (presumably as ethene and CO₂) to give terminal alkynes (5). See reaction scheme overleaf.



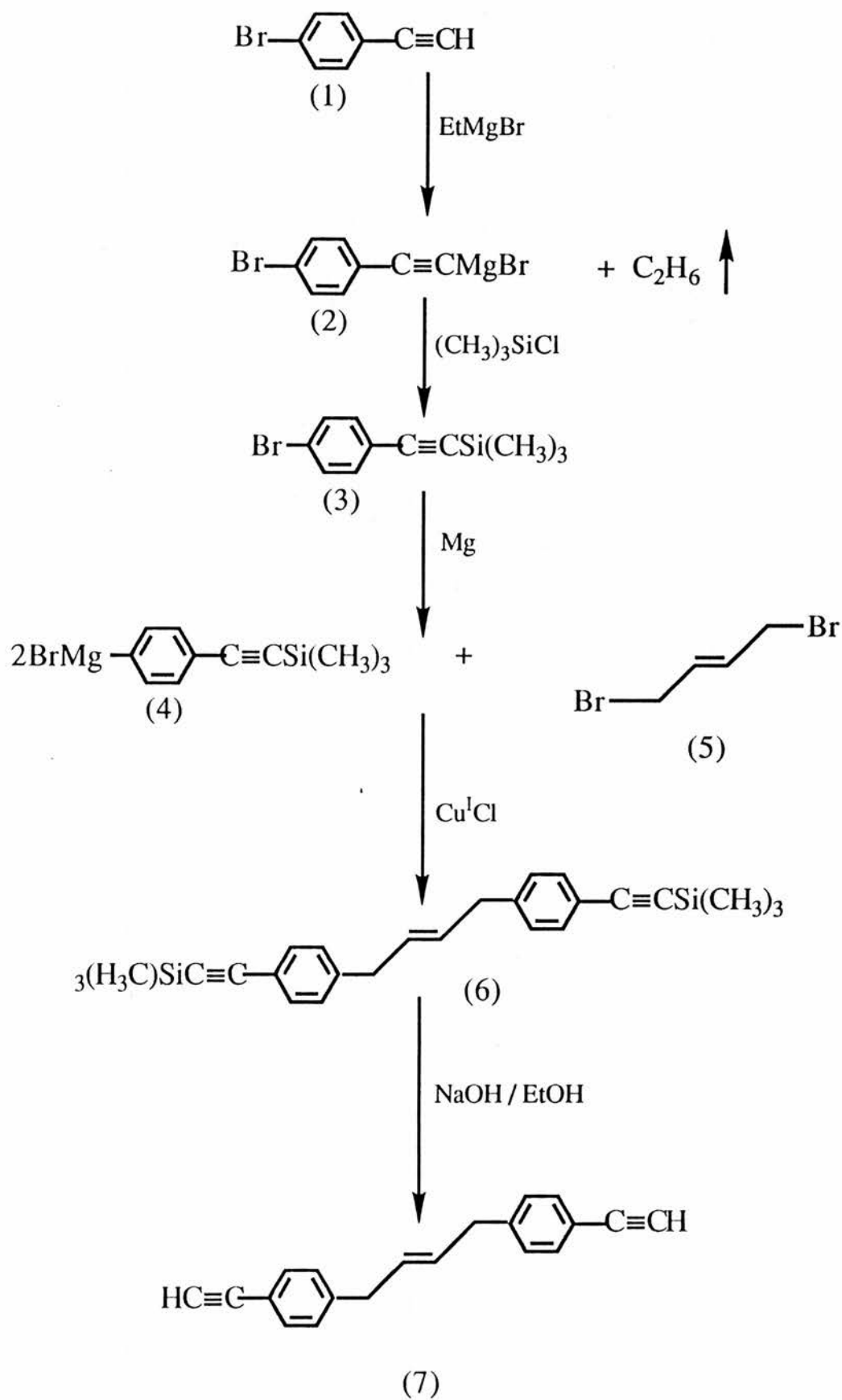
The route involved for obtaining 1,4-diethynylbenzene required reacting two equivalents of ethoxycarbonylmethylene triphenylphosphorane with terephthaloyl chloride to give 1,4-di-(ethoxycarbonylmethylenetriphenylphosphorane)benzene. FVP at 750°C of the diylide was performed with the extrusion of Ph₃PO accompanied by the loss of two ethoxycarbonyl groups. 1,4-diethynylbenzene* was successfully obtained in 77% yield from FVP of 1,4-di-(ethoxycarbonylmethylenetriphenylphosphorane)benzene. See reaction scheme overleaf.

* Note: The mass spectrum of 1,4-di-(ethoxycarbonylmethylenetriphenyl phosphorane)benzene is included. It mimics the fragmentation pattern which will occur on FVP of this compound - see **fig 2.1** page 87.

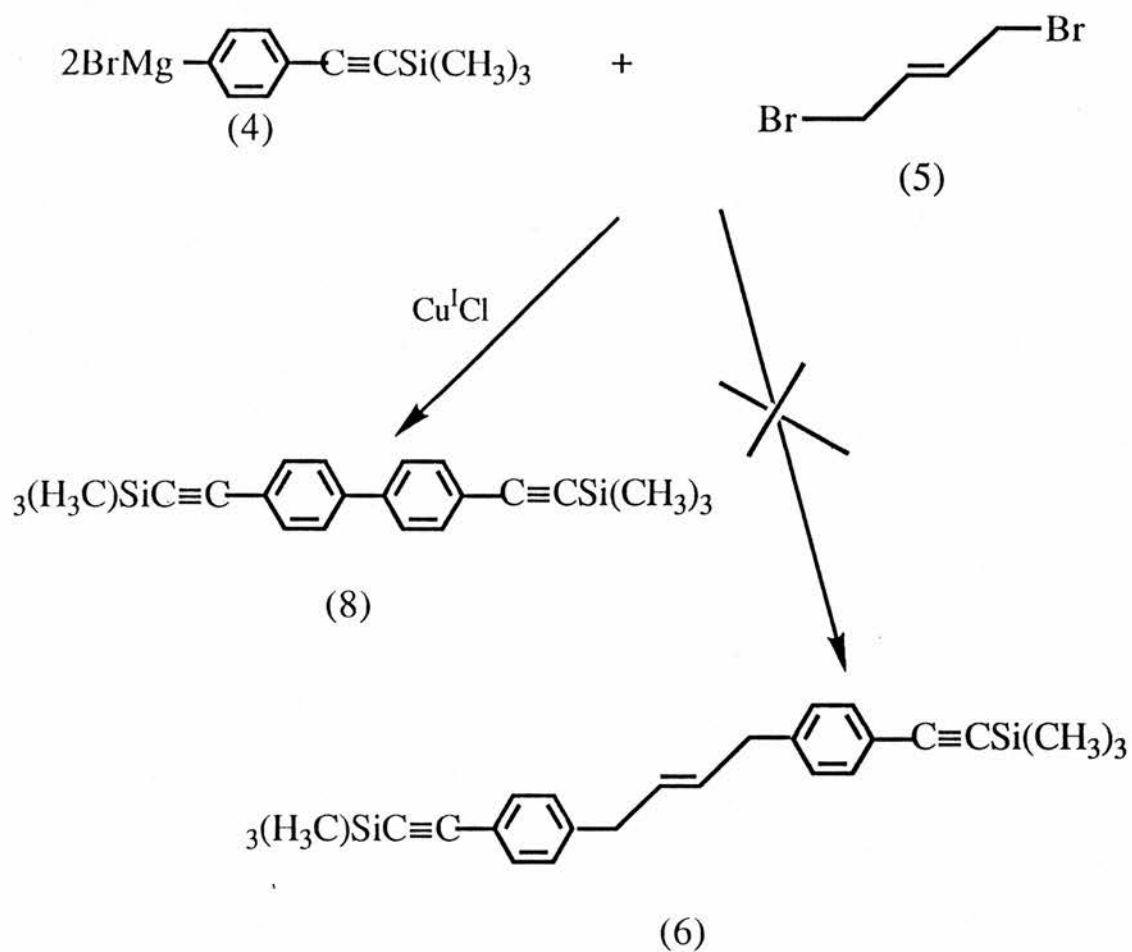
61



For the attempted synthesis of the novel compound 1,4-di-(4-ethynylphenyl)-2-butene the reaction scheme overleaf was proposed .



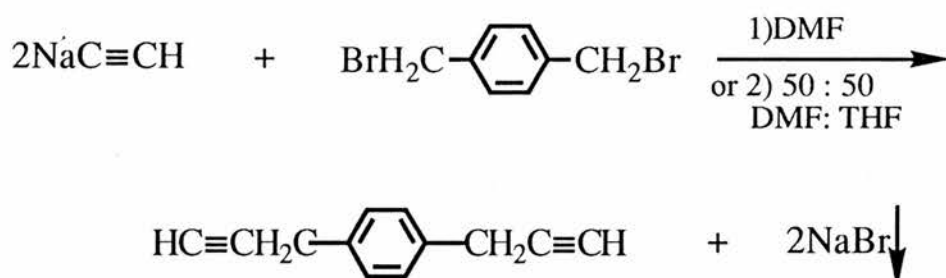
p-Bromophenylacetylene (1) was successfully synthesised by carefully following a literature method of Dufraisse and Dequesnes. ⁶¹ It was necessary to protect the terminal ethynyl group in the Grignard reactions required for the synthesis of 1,4-di-(4-ethynylphenyl)-2-butene(7). Eaborn and workers ⁶² found that a trimethylsilyl group can be used to protect a terminal ethynyl group in Grignard reactions and since the trimethylsilyl group can very easily be removed by dilute alkali such protection facilitates many syntheses. The literature work carried out by Eaborn ⁶³ was successfully repeated. p-Bromophenylethynylmagnesiumbromide(2) was prepared by reacting p-bromophenylacetylene (1) and ethylmagnesiumbromide. (2) was then treated with chlorotrimethylsilane to give (p-bromophenylethynyl)-trimethylsilane(3). (3) was then brought into contact with magnesium turnings to give p-(magnesiumbromidephenylethynyl)trimethylsilane (4). An excess of 2 molar equivalents of (4) was reacted with 1 molar equivalent of trans-1,4-dibromo-2-butene (5) in the presence of cuprous chloride with the hope of isolating 1,4-di-(4-2 trimethylsilylethynylphenyl)-2-butene (6). The reaction product from (4) and (5) was characterised. Characterisation by infrared spectroscopy, ¹Hnmr spectroscopy and mass spectroscopy revealed (6) did not form (see 2.3.2.4). 4,4'-di-(4-2 trimethylsilylethynyl)biphenyl (8) was synthesised as opposed to 1,4-di-(4-2 trimethylsilylethynylphenyl)-2-butene (6) showing that (4) favours self coupling. See reaction scheme overleaf.



Attempts to isolate 4,4'-diethynylbiphenyl from (8) were unsuccessful. Characterisation of the product by $^1\text{Hnmr}$ revealed a mixture of products which were difficult to separate (see 2.3.2.5).

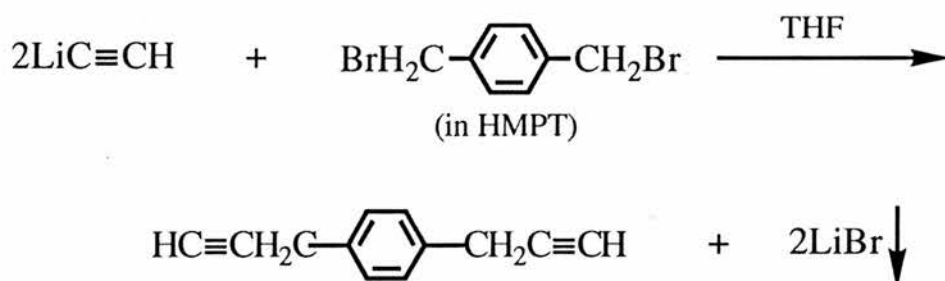
Four methods were employed in the attempted synthesis of the novel compound 1,4-di-2-propynylbenzene:

A Action of sodium acetylide on 1,4-bis(bromomethyl)benzene in 1) N,N'-dimethylformamide (DMF) solvent or 2) 50:50 N,N'-dimethylformamide (DMF):tetrahydrofuran (THF) solvent mixture.



Literature methods similar to those of 1) Kenny ⁶⁴ and 2) Kracht ⁶⁵ were employed in the attempted synthesis of 1,4-di-2-propynylbenzene. In both systems 1) and 2) 1,4-bis(bromomethyl)benzene was recovered in almost quantitative yield.

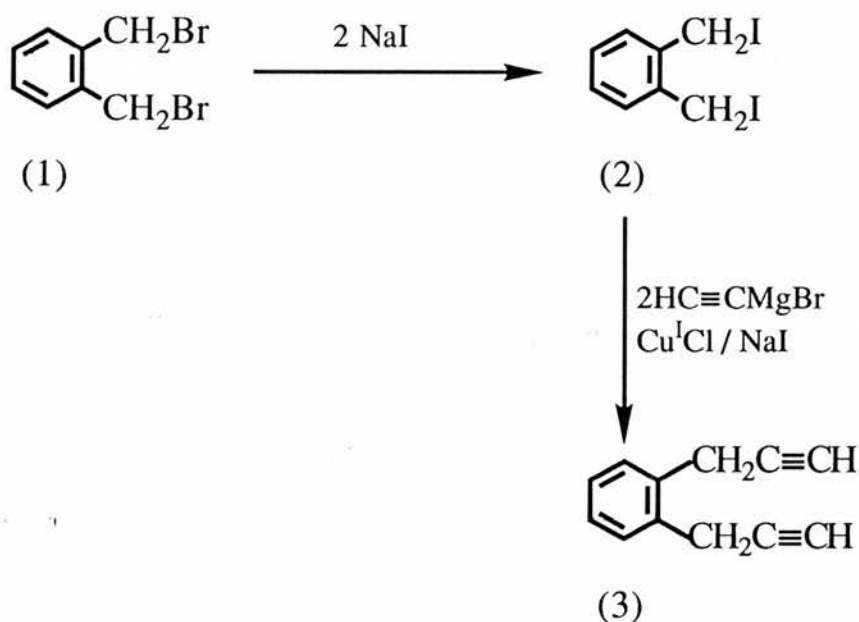
B Addition of 1,4-bis(bromomethyl)benzene in hexamethylphosphorictriamide (HMPT) to lithium acetylide in tetrahydrofuran.



The literature method of Beckmann ⁶⁶ was employed in the attempted synthesis of 1,4-di-2-propynylbenzene. 1,4-bis(bromomethyl)benzene was recovered in almost quantitative yield.

C Action of ethynylmagnesiumbromide on 1,4-bis-(iodomethyl)benzene in tetrahydrofuran.

In 1973 Bowes ⁶⁷ isolated the 1,2 (ortho) analogue of di-2-propynylbenzene (3) using the following reaction scheme ;



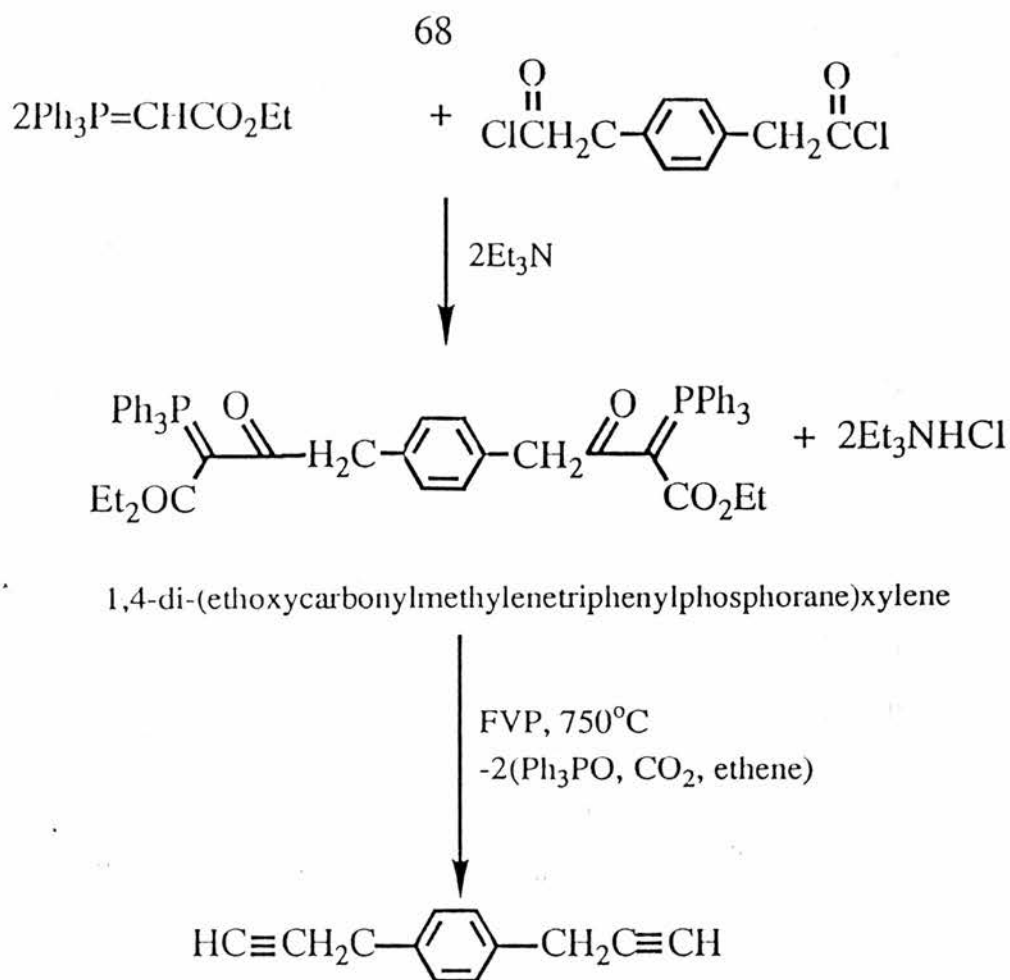
Initially, Bowes attempted to synthesise (3) by the copper-catalysed reaction of ethynylmagnesium bromide with 1,2-bis(bromomethyl)benzene (1) but was unsuccessful; mostly starting material was recovered. This was unexpected since the copper catalysed reaction between allylic bromides and acetylenic Grignard compounds has been carried out successfully in the past. Bowes then decided to synthesise the more reactive diiodide (2) and react this with ethynylmagnesium bromide as it would stand a greater chance of success. (2) was simply synthesised by reaction of the dibromide (1) with sodium iodide in acetone solution. ⁶⁸ In model studies Bowes found that when benzyliodide was reacted with ethynyl magnesium

bromide in the presence of copper (I) chloride, the products included some benzyl bromide, the result of an exchange reaction. The reaction was suppressed by the addition of sodium iodide to the reaction mixture, with consequent improvement in the yield of propargylbenzene. 1,2-di-2-propynylbenzene (3) was synthesised in 34% yield by the overnight reaction of 1,2-bis(iodomethyl)benzene with an excess of 2 molar equivalents of ethynylmagnesium bromide in THF, in the presence of copper (I) chloride and sodium iodide.

Attempts at isolating 1,4-di-2-propynylbenzene using the method described above were unsuccessful. No conversion to the 1,4-di-2-propynylbenzene was achieved. However, instead of recovering the starting material 1,4-bis(iodomethylbenzene), 1,4-bis(bromomethylbenzene) was recovered. This was confirmed by the melting point of the recovered material. Therefore it was assumed that because the reaction was unsuccessful, an exchange reaction occurred to give the material 1,4-bis(bromomethylbenzene) as the product.

D Attempted preparation of the intermediate 1,4-di-(ethoxycarbonylmethylenetriphenylphosphorane)xylene for flash vacuum pyrolysis (FVP) to give 1,4-di-2-propynylbenzene.

The reaction scheme overleaf was proposed for obtaining 1,4-di-2-propynylbenzene. (Note: The theory was identical for 1,4-diethynylbenzene see 2.3.2.3)

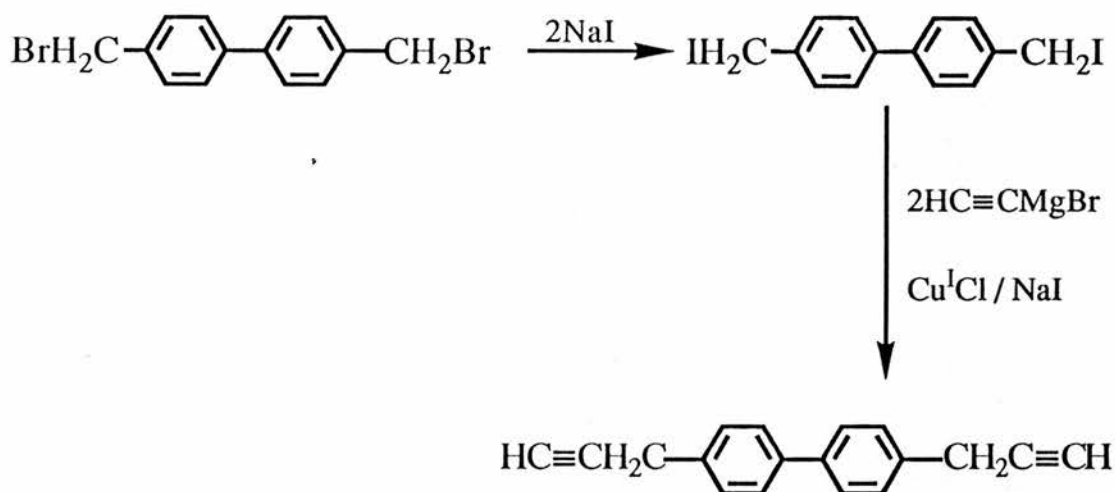


³¹Pnmr and ¹³Cnmr spectroscopy were used in the characterisation of the reaction product between ethoxymethylenetriphenylphosphorane and 1,4-bis-(carbonylchloridemethyl)benzene. A mixture of products were revealed i.e. 1) ethoxymethylenetriphenylphosphorane (starting material) 2) triphenylphosphineoxide and 3) 1,4-di-(ethoxycarbonylmethylenetriphenylphosphorane)xylene (the required product).

This method was abandoned because isolation of the required product was not possible.

One method was employed in the attempted synthesis of the novel compound 4,4'-bis(di-2-propynyl)-1,1'-biphenyl. This involved action of ethynylmagnesiumbromide on 4,4'-bis(iodomethyl)-1,1'-biphenyl in

tetrahydrofuran (procedure similar to method C for 1,4-di-2-propynylbenzene).



No conversion to 4,4'-bis(di-2-propynyl)-1,1'-biphenyl was achieved. Again, in this instance 4,4'-bis(bromomethyl)-1,1'-biphenyl was recovered instead of 4,4'-bis(iodomethyl)-1,1'-biphenyl. This was confirmed by the melting point of the recovered material. Therefore it was assumed that because the reaction was unsuccessful, an exchange reaction occurred to give the material 4,4'-bis(bromomethyl)-1,1'-biphenyl.

2.3 Experimental Section

2.3.1 Instrumentation and General Techniques

1. NMR Spectroscopy

a) ^1H NMR.

Routine spectra were obtained at 60 MHz on a Varian EM-360 spectrometer. High resolution spectra were obtained at 300 MHz on a Brüker AM-300 spectrometer.

b) ^{13}C NMR.

All spectra were obtained at 75 MHz on a Brüker AM-300 spectrometer.

c) ^{31}P NMR.

Spectra were obtained at 32 MHz on a Varian CFT-20 spectrometer.

Most spectra were obtained on solutions in deuteriochloroform, except where mentioned otherwise. Chemical shifts (δ) are expressed in parts per million to high frequency of tetramethylsilane for ^1H and ^{13}C and to high frequency of phosphoric acid for ^{31}P .

2. Infra-red Spectroscopy

Spectra were obtained on a Perkin-Elmer 1420 ratio recording spectrophotometer. Spectra were recorded for liquids as thin films and solids as nujol mulls between sodium chloride plates.

3. Ultraviolet/visible Absorption Spectroscopy

Ultraviolet/visible absorption spectra were recorded on a Perkin-Elmer Lambda 5 UV-visible spectrophotometer over the range 200-300 nm in spectroscopic grade methylene chloride, spectroscopic grade ethanol and spectroscopic grade isooctane.

4. Mass Spectrometry

Mass spectra were obtained on a Finnigan Incos 50 mass spectrometer.

5. Melting Points

Melting points were determined using an Electrothermal melting point apparatus and are uncorrected.

Drying and Purification of Solvents

Commercially available solvents were used without further purification unless otherwise indicated. Dry dichloromethane was prepared by storing over molecular sieves. Dry ether and dry toluene

were prepared by storing over sodium wire. Extra dry tetrahydrofuran was prepared by drying with sodium wire and then distilling from potassium benzophenone ketyl. Dry N,N'-dimethylformamide was prepared by heating under reflux with calcium hydride under a nitrogen atmosphere for 2 h then distilling onto molecular sieves.

7. Flash Vacuum Pyrolysis (FVP)

This was carried out using a conventional system with a horizontal 30 x 2.5 cm silica tube heated to a temperature of 750°C by a Carbolite Eurotherm Tube Furnace MTF-12/38A. The temperature was measured by a Pt/Pt -13% Rh thermocouple situated at the centre of the furnace and the whole system was maintained at a pressure of 10^{-2} - 10^{-3} mm Hg by an Edwards Model E2M5 high capacity rotary oil pump, the pressure being measured on a Pirani gauge. After pyrolysis the product(s) were dissolved out of the trap in deuteriochloroform and analysed directly by NMR. Yields were estimated by adding a known amount of dichloromethane to the solution and comparing the NMR signals.

2.3.2 Syntheses of monomers

2.3.2.1 α,ω -alkyldiyne monomers

- a) 1,7-octadiyne $(\text{HC} \equiv \text{C} - (\text{CH}_2)_4 - \text{C} \equiv \text{CH})$
- b) 1,8-nonadiyne $(\text{HC} \equiv \text{C} - (\text{CH}_2)_5 - \text{C} \equiv \text{CH})$
- c) 1,9-decadiyne $(\text{HC} \equiv \text{C} - (\text{CH}_2)_6 - \text{C} \equiv \text{CH})$
- d) 1,10-undecadiyne $(\text{HC} \equiv \text{C} - (\text{CH}_2)_7 - \text{C} \equiv \text{CH})$
- e) 1,11-dodecadiyne $(\text{HC} \equiv \text{C} - (\text{CH}_2)_8 - \text{C} \equiv \text{CH})$

Preparation of (1) Sodium amide and (2) Sodium acetylide used in the synthesis of the α,ω -alkyldiyne monomers

(1) Preparation of Sodium amide.

Into a 2 litre three-necked round-bottomed flask were placed 700-800 ml of liquid ammonia. Very small pieces (5-10 mm³) of sodium were introduced until a blue colour persisted (0.1g of sodium was sufficient). Subsequently a catalytic quantity (~0.1g) of powdered ferric nitrate was dissolved in the ammonia. Immediately after a uniformly brown solution had been obtained 15g (0.65 mole) of sodium was introduced portionwise into the flask (pieces of approx 0.5 g sodium). The sodium was completely converted to sodamide within an hour (the sodamide is a grey suspension). The mirror of sodium which was still present in the necks of the flask was removed by very vigorous stirring. After the stirring was discontinued, the sodamide suspension settled out.

(2) Preparation of Sodium acetylide.

To a suspension of ~0.6 mole of sodamide in approximately 600 ml of liquid ammonia was added 0.5 g of triphenylmethane. After 2-5 min a pinkish colour had developed [(C₆H₅)₃C⁻]. Acetylene gas (freed from acetone) was passed quickly through the suspension, which became increasingly thinner. Introduction of acetylene was stopped when the pink colour had completely disappeared indicating a slight excess of gas. The experiment could be terminated within 15 min if the acetylene flow was sufficiently rapid.

General procedure for Synthesis of α,ω -alkyldiyne monomers.

To a vigorously stirred solution of ~0.6 mole of sodium acetylide in approximately 500 ml of liquid ammonia was added 0.12 mole of the dibromoalkane over a period of 15 min. During the addition, a slow stream of acetylene gas was passed through the flask. Stirring was continued for 2 more hours, after which 8 g of solid NH_4Cl were added in 1 g portions during 15 min. The ammonia was allowed to evaporate. To the residue were successively added 300 ml of water and 60 ml of pentane. The organic layer was separated, dried over MgSO_4 , and filtered. Evaporation of the pentane from the filtrate under vacuum left an orange coloured liquid which was distilled *in vacuo*;

Compound a 1,7-octadiyne (8.9g,69%),bp40°C(14mm) lit **54** bp37°C(10mm),infra red bands $\nu(\text{cm}^{-1})$; 3300 (s), 2120 (m) (terminal acetylene), 2800-2900 (s) and 1430-1470 (s) (aliphatic); $^1\text{Hnmr}$ spectrum (CDCl_3), δH 2.2 (m, 4H, methylene protons attached to acetylenic groups), 1.98 (t, 2H, acetylenic protons) and 1.5 (s, 4H methylene protons); ultraviolet, λ max in dichloromethane = 242 nm.

Compound b 1,8-nonadiyne (9.4 g, 65%), bp57°C (15mm) lit **54** bp52°C (10 mm), infra red bands (as **Compound a**); $^1\text{Hnmr}$ spectrum (CDCl_3), δH 2.2 (m, 4H, methylene protons attached to acetylenic groups), 1.98 (t, 2H, acetylenic protons) and 1.5 (s, 6H methylene protons); ultraviolet, λ max in dichloromethane = 242 nm.

Compound c 1,9-decadiyne (10.9 g, 68%), bp 76°C(15mm) lit **54** bp 70°C(10 mm), infra red bands (as **Compound a**); $^1\text{Hnmr}$

spectrum (CDCl_3), δH 2.15 (m, 4H, methylene protons attached to acetylenic groups), 1.94 (t, 2H, acetylenic protons) and 1.5 (s, 8H methylene protons); ultraviolet, λ max in dichloromethane = 242 nm.

Compound d 1,10-undecadiyne (12.6 g, 71%), bp 87°C (15mm) lit ⁵³ bp $93^\circ\text{-}94^\circ\text{C}$ (20 mm), infra red bands (as **Compound a**); $^1\text{Hnmr}$ spectrum (CDCl_3), δH 2.15 (m, 4H, methylene protons attached to acetylenic groups), 1.94 (t, 2H, acetylenic protons) and 1.35 (m, 10H methylene protons); ultraviolet, λ max in dichloromethane = 241 nm.

Compound e 1,11-dodecadiyne (13.6g,70%), bp 105°C (15mm) lit ⁵³ bp 104°C (15mm), infra red bands (as **Compound a**); $^1\text{Hnmr}$ spectrum (CDCl_3), δH 2.15 (m, 4H, methylene protons attached to acetylenic groups), 1.94 (t, 2H, acetylenic protons) and 1.35 (m, 12H methylene protons); ultraviolet, λ max in dichloromethane = 241 nm.

2.3.2.2 trans-4-octene-1,7-diyne

Cuprous chloride (0.4 g) was added to a solution of ethynylmagnesium bromide (800 ml, 0.5 M solⁿ, 0.4 mol) in tetrahydrofuran. This was followed by addition of a solution of trans - 1,4-dibromo-2-butene (32 g, 0.15 mol) in tetrahydrofuran (60 ml) over a period of 15 min with stirring (no appreciable exothermic reaction occurred). The mixture was stirred for a further 30 min and more cuprous chloride (0.2 g) was then added. The stirred mixture was heated slowly during 1 hr in a water bath to an internal temperature of $55\text{-}66^\circ\text{C}$, when an exothermic reaction occurred and external heating

was stopped. The internal temperature began to fall after ca 30 min. The mixture was then heated at 55-60°C for a further 1.5 hr and stirred overnight at room temperature. Ether and ice-water were added and the aqueous layer was re-extracted with ether. The combined organic layers were washed with water and saturated sodium chloride solution and were then dried and evaporated under reduced pressure. Distillation of the residue through a short column gave two fractions corresponding to the compound **trans-4-octene-1,7-diyne**.*

Fraction	Bp.°C.(mm),	Weight, g
1	55-60 (21)	2.5
2	62-64 (21)	1.5

The combined fractions 1 and 2 on low-temperature crystallisation from an equal volume of pentane yielded **trans-4-octene-1,7-diyne** (2.8 g, 18%) as large plates: bp 55-57°C (23 mm) lit ⁵⁶ bp 59-60°C (25 mm); infra red bands ν (cm⁻¹) (CHCl₃) at 3250 (s), 2100 (m) (terminal acetylene) and 960 (s) (trans double bond; ¹Hnmr spectrum (CDCl₃), δ H 5.72 (m, 2H, olefinic protons attached), 2.92 (m, 4H, methylene protons) and 1.91 (m, 2H acetylenic protons); no absorption in the ultraviolet (isooctane).

* Although **trans-4-octene-1,7-diyne** was the major product from the Grignard reaction, less volatile hydrocarbons were also formed which were isolated by Y.Gaoni and workers.⁵⁶

2.3.2.3 1,4-diethynylbenzene

1) Preparation of ethoxycarbonylmethylenetriphenylphosphonium-bromide.

Ethylbromoacetate (16.70g,100mmol) and triphenylphosphine (26.2g, 100 mmol) in 200 ml of toluene were heated under reflux for 3 h. The resulting precipitate was filtered off, washed with ether and dried giving 96.5 g (96%) of ethoxycarbonylmethylenetriphenylphosphoniumbromide as a white powder mp 157°C (lit ⁶⁹ 158°C).

2) Preparation of Ethoxycarbonylmethylenetriphenylphosphorane.

Sodium hydroxide (6g,0.15 mol) in water(3,000 ml) was added to a solution of ethoxycarbonylmethylenetriphenylphosphoniumbromide (64.4 g, 0,15 mol). A milky white precipitate formed which was extracted into a small quantity of dichloromethane. The dichloromethane layer was washed several times with water to remove any excess alkali and then dried over MgSO₄ and filtered. Evaporation of solvent from the filtrate under vacuum gave an oily residue which solidified on cooling. Recrystallisation from petroleum spirit 60-80°C/ethylacetate (4/1 vol/vol) gave needle type crystals (37.8 g, 72%), mp 115-117°C, 127-129°C (lit ⁷⁰ 116-117°C, 129-130°C).

3) Preparation of 1,4-di-(ethoxycarbonylmethylenetriphenylphosphorane)benzene

Ethoxycarbonylmethylenetriphenylphosphorane (3.43 g, 0.0197 mol) and triethylamine (2 g, 0.0197 mol) were dissolved in the minimum amount of dry toluene (50 ml) and stirred at room temperature, while terephthaloyl chloride (1 g, 9.65 mmol) in dry toluene (10 ml) was added slowly. The mixture was stirred at room temp overnight and then poured into water and the organic product extracted into dichloromethane. The dichloromethane layer was washed with water, dried over MgSO_4 and filtered. Evaporation of solvent from the filtrate under vacuum gave a yellow solid which was washed with ether and dried under vacuum. Recrystallisation from dry xylene gave white needle type crystals (2.60 g, 33%), mp 251-252°C (lit ⁵⁷ mp 252-253°C); $\delta\text{P} + 18.79$; δH 7.6 (m, 4H, aromatic protons from benzene ring), 3.7 (q, 4H, methylene protons), 0.6 (t, 6H, methyl protons); δC 192.90 (d, keto C), 167.63 (d, ester C), 144.00 (d, disubstituted benzene C), 13.34 (d), 131.72 (d), 128.54 (d), 127.53 (s), 126.34 (d) (aromatic C's), 68.92 (d, ylide C, $J_{\text{P-C}} 112.2$ Hz), 58.57 (s, methylene C), 13.80 (s, methyl C). m/z . 277 ($\text{Ph}_3\text{P}=\text{O}$), 270 [(M^+)-(2 $\text{Ph}_3\text{P}=\text{O}$)], 225, 198, 153 and 126; Characteristic M.S. breakdown; i.e. [(M^+)-(2 $\text{Ph}_3\text{P}=\text{O}$)], [(M^+)-(2 $\text{Ph}_3\text{P}=\text{O}+\text{OC}_2\text{H}_5$)], [(M^+)-(2 $\text{Ph}_3\text{P}=\text{O}+\text{CO}_2\text{C}_2\text{H}_4$)], [(M^+)-(2 $\text{Ph}_3\text{P}=\text{O}+\text{CO}_2\text{C}_2\text{H}_4+\text{OC}_2\text{H}_5$)] and [(M^+)-(2 $\text{Ph}_3\text{P}=\text{O}+2\text{CO}_2\text{C}_2\text{H}_4$)] see figure 2.1 page 87 (for fragmentation process)

4) Flash vacuum pyrolysis of 1,4-di-(ethoxycarbonylmethylene-triphenylphosphorane)benzene.

FVP of the title compound (2g, 750°C, 2.2×10^{-2} mmHg, inlet 200–240°C) gave a yellow solid at the cold trap. The solid in the cold trap was dissolved out with the minimum amount of CDCl_3 and its ^1H nmr and ^{13}C nmr obtained. (Yield = 0.23 g, 77%); δ_{H} 7.5 (s, 4H, aromatic protons), 3.1 (s, 2H, acetylenic protons); δ_{C} 132.01 (aromatic carbons), 122.58 (aromatic carbons on positions 1 and 4 on ring), 83.04 (quaternary acetylenic carbon), 79.11 (acetylenic carbon attached to H); ultraviolet λ max in ethanol = 289 nm.

From the above data it shows that FVP was successful and 1,4-diethynylbenzene was obtained.

2.3.2.4 1,4-di-(4-ethynylphenyl)-2-butene

1) Preparation of p-bromophenylacetylene

This was synthesised according to the literature procedure of Dufraisse and Dequesnes. ⁶¹

The product was recrystallised from ethanol (8g, 48%) mp = 64–65°C (lit ⁶¹ mp 65°C)

2) Preparation of (p-Bromophenylethynyl)trimethylsilane.

p-Bromophenylethynylmagnesiumbromide was prepared from p-bromophenylacetylene (5.8g, 0.032 mole) and ethylmagnesiumbromide (0.032 mole) in absolute tetrahydrofuran (ca. 50 ml) and was treated with chlorotrimethylsilane (3.46, 0.032 mole), (cf. ref ⁶³). Addition of saturated aqueous ammonium chloride followed by separation, drying (Na₂SO₄) and fractionation of the tetrahydrofuran layer gave material, bp 74–75°C/0.3 mm, which solidified in the receiver. Crystallisation from methanol afforded (p-Bromophenylethynyl)trimethylsilane (7.0g, 86%), mp 62°C (lit ⁶² mp 62°C).

3) Attempted preparation of 1,4-di-(4-(2-trimethylsilylethynyl)phenyl)-2-butene (cf ref ⁵⁶)

(p-Bromophenylethynyl)trimethylsilane (5.1g, 0.02 mole) was brought into reaction with magnesium turnings (0.5 g, 0.021 g-atom) by boiling in absolute tetrahydrofuran (30 ml) for 2 hr. The Grignard reagent so prepared was filtered and to this solution was added dropwise

a solution of trans-1,4-dibromo-2-butene (1.71g, 8 mmol) in 15 ml of absolute tetrahydrofuran over a period of 15 min. The reaction mixture was stirred under a N₂ purge. A catalytic quantity of Cu(I)Cl (0.25g) was added. An exothermic reaction occurred and external cooling was applied to the reaction. The reaction was then heated at 55–60°C for a further 1.5 hr and stirred overnight at room temperature under a nitrogen purge. Addition of saturated aqueous ammonium chloride was followed by extraction of the organic product into dichloromethane. The dichloromethane layer was washed with water and saturated sodium chloride solution, dried over MgSO₄, filtered and the solvent removed under vacuum to leave a pale yellow solid. The product was filtered and then dried under vacuum; Yield 3.10g, (Theoretical Quantitative Yield of 1,4-di-(4-2 trimethylsilylethynylphenyl)-2-butene = 3.20g); infra red bands ν (cm⁻¹) 3030 (w) (aromatic C-H str), 2850–3000 (m) (alkane C-H str), 2160 (m) (terminal acetylene), 1500 (s) (alkane (CH₃)₃-Si-), 1390–1400 (characteristic m/s doublet) alkane (CH₃)₃-Si-, 860, 825 (s) (p-disubstituted benzene).

Note: No characteristic trans (-HC = CH-) frequency present at 1700 cm⁻¹ or 960 cm⁻¹

¹Hnmr spectrum (CDCl₃), δ _H 7.25 (m, 8H, aromatic protons), 0.3 (s, 19H, methyl protons).

In the mass spectrum the molecular ion [M⁺] peak at m/z 346 corresponds to the compound 4,4'-di-(4-2 trimethylsilylethynyl)-biphenyl.

From the above characterisation 4,4'-di-(4-2 trimethylsilylethynyl)biphenyl was synthesised as opposed to 1,4-di-(4-2 trimethylsilylethynylphenyl)-2-butene.

2.3.2.5 4,4'-diethynylbiphenyl (see 2.3.2.4.)

4,4'-di (4-2 trimethylsilylethynyl)biphenyl (1.55g, 4.48 mmol) and aqueous methanolic (95%) 0.1M alkali (50 ml) were heated with stirring for 2 hr. The mixture was added to an equal volume of water and extracted with ether. The aqueous solution was then acidified with dilute sulphuric acid (2N), to leave a yellow coloured solution. The solution was extracted into ether, dried over MgSO_4 and filtered. Evaporation of the solvent from the filtrate under vacuum gave an oily residue. Attempted crystallisation from ethanol gave an oily product which was characterised by $^1\text{Hnmr}$ and gave a mixture of products which were difficult to separate.

2.3.2.6 1,4-di-2-propynylbenzene

Several methods were employed in the attempted synthesis of 1,4-di-2-propynylbenzene;

1)Preparation of sodium acetylide via liquid ammonia route, followed by evaporation of liquid ammonia solvent with replacement by another solvent or solvent pair. Then addition of 1 molar equivalent of 1,4-bis(bromomethyl)benzene in the respective solvent or solvent pair, to an excess of 2 molar equivalent of sodium acetylide.

The systems chosen were (a) N,N'-Dimethylformamide at 70°C for 3 hrs.⁶⁴

(b) N,N'-Dimethylformamide/Tetrahydrofuran – 50/50 mixture at 60°C for 3 hrs.⁶⁵

In the two systems chosen (a) and (b) 1,4-bis(bromomethyl)benzene was recovered in almost quantitative yield. No conversion to 1,4-di-2-propynylbenzene was achieved.

2)(Cf ref ⁶⁶)

Preparation of monolithium acetylide from n-butyllithium and acetylene gas in absolute tetrahydrofuran at 0°C. Then addition of 1 molar equivalent of 1,4-bis(bromomethyl)benzene in absolute hexamethylphosphorictriamide to an excess of 2 molar equivalents of monolithium acetylide in absolute tetrahydrofuran, ensuring the reaction temperature did not exceed 15°C during the addition. The reaction mixture was left stirring for a further 1 hr. 1,4-bis(bromomethyl)benzene was recovered in almost quantitative yield. No conversion to 1,4-di-2-propynylbenzene was achieved.

3)* (Cf ref 67).

An excess of 2 molar equivalents of ethynylmagnesium bromide was prepared from ethylmagnesiumbromide and acetylene gas in absolute tetrahydrofuran. A catalytic quantity of copper (I) chloride and sodium iodide were then added to this solution. After five minutes stirring 1 molar equivalent of 1,4-bis(iodomethyl)benzene (m.pt. 170°C) (prepared by a literature method 68) in absolute tetrahydrofuran was added over ten minutes. The reaction was stirred overnight. The following day more copper (I) chloride was added, and the reaction mixture was heated at 55°C for 4 hours, with stirring. The mixture was then allowed to cool. After work up characterisation by ¹Hnmr spectroscopy and the compounds melting point (~145°C) revealed that starting material 1,4-bis(bromomethyl)benzene was recovered from the reaction and no conversion to 1,4-di-2-propynylbenzene was achieved.

4) Attempted preparation 1,4-di-(ethoxycarbonylmethylenetriphenylphosphorane)xylene for Flash Vacuum Pyrolysis to give 1,4-di-2-propynylbenzene

Addition of 1 molar equivalent of 1,4-di-(carbonylchloridemethyl)benzene in dry toluene to 2 molar equivalents of ethoxycarbonylmethylenetriphenylphosphorane in dry toluene containing 2 molar equivalents of triethylamine yielded three peaks by ³¹Pnmr;

* In the PhD thesis of C M Bowes, University College, London, 1974 pages 114–15 it was reported that 1,2-di-2-propynylbenzene was synthesised using the same procedure as 3) obtaining a yield of 34%.

$\delta_p = 28.67$ ppm -triphenylphosphineoxide

$\delta_p = 17.24$ ppm -ethoxycarbonylmethylenetriphenylphosphorane

$\delta_p = 17.10$ ppm -1,4-di-(ethoxycarbonylmethylene-
triphenylphosphorane)benzene

^{13}C nmr spectroscopy also revealed a mixture of starting material, $\text{Ph}_3\text{P}=\text{O}$ and the desired product.

1,4-di-(ethoxycarbonylmethylenetriphenylphosphorane)xylene was difficult to isolate so this technique was abandoned.

2.3.2.7 4,4'-bis(di-2-propynyl)-1,1'-biphenyl

Method 3) used in 2.3.2.6 was employed for 4,4'-bis (di-2-propynyl)-1,1'-biphenyl.

An excess of 2 molar equivalents of ethynylmagnesium bromide was prepared from ethylmagnesiumbromide and acetylene gas in absolute tetrahydrofuran. A catalytic quantity of copper (I) chloride and sodium iodide were then added to this solution. After five minutes stirring 1 molar equivalent of 4,4'-bis (iodomethyl)-1,1'-biphenyl(m.pt.195°C) (prepared by a literature method ⁶⁸), in absolute tetrahydrofuran was added over ten minutes. The reaction was stirred overnight. The following day more copper (I) chloride was added and the reaction mixture was heated at 55°C for 4 hrs, with stirring. The mixture was then allowed to cool. After work up characterisation by ^1H nmr spectroscopy and the compounds melting point (~170°C) revealed that starting material 4,4'-bis (bromomethyl)-1,1'-biphenyl

was recovered from the reaction and no conversion to 4,4'-bis (di-2-propynyl)-1,1'-biphenyl was achieved.

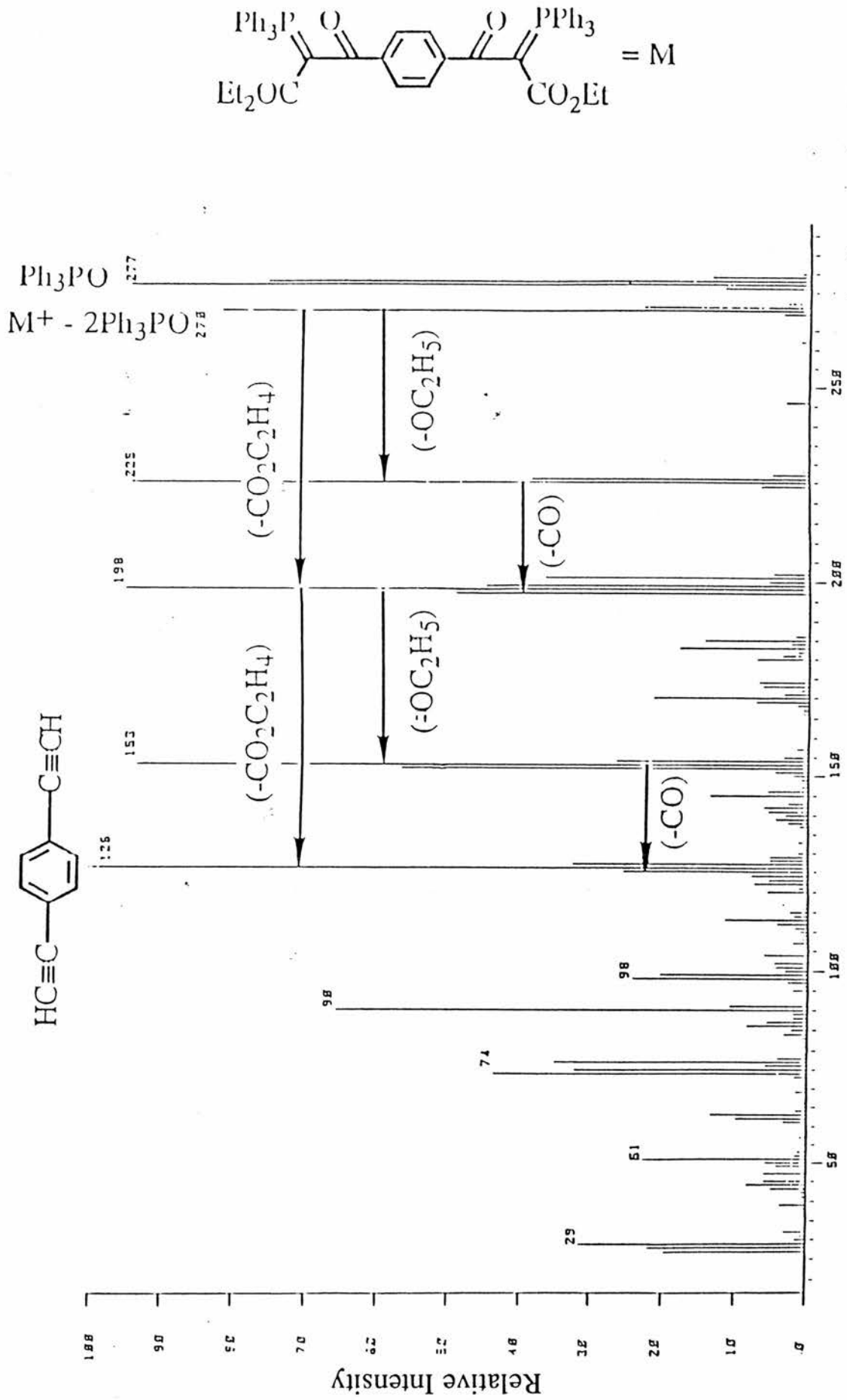


Figure 2.1. Mass spectrum of 1,4-di-(ethoxycarbonylmethylene)-

triphenylphosphorane)benzene - arrows are shown to illustrate the fragmentation process.

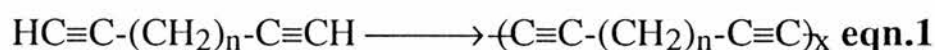
CHAPTER 3

SYNTHESES OF POLY(α,ω -ALKYLDIYNES)

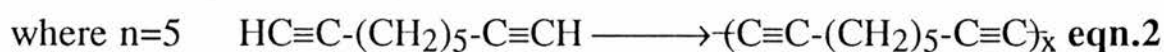
AND COPOLY(α,ω -ALKYLDIYNES)

3.1 Introduction

The materials which are investigated in this study are polymers and copolymers of the α,ω -alkyldiyne series, $\text{HC}\equiv\text{C}-(\text{CH}_2)_n-\text{C}\equiv\text{CH}$ ($n=4$ to 8). These polymers are synthesised from α,ω -alkyldiynes using an oxidative coupling reaction.



or as in a copolymer; eg

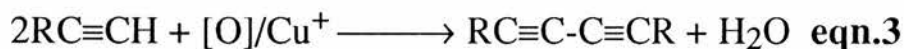


The purpose of the work in this chapter is to describe how I arrived at the two oxidative coupling polymerisation routes chosen for my study. Before outlining the actual polymerisation procedures I adopted, it is necessary to review the background work. The review will include some of the general features and mechanism of the oxidative coupling reaction, also it will discuss a variety of methods which can be used to perform the oxidative coupling reaction. The next section of the chapter will discuss a criteria for choosing the two oxidative coupling routes. Finally, the actual synthetic procedures used for producing the polymers are outlined.

3.2 Oxidative (Glaser) Coupling — A Review

3.2.1 General features and mechanism

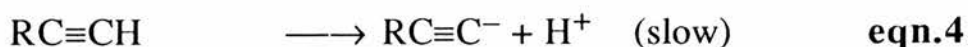
The oxidative coupling of acetylenes was first performed in 1869, by Glaser ¹, who obtained diphenyldiacetylene by atmospheric oxidation of copper phenylacetylide in aqueous ammonia solution. Since then, oxidative coupling of copper derivatives of monosubstituted acetylenes (the Glaser reaction) has been widely used for the preparation of various disubstituted diacetylenes.



Typical Glaser Oxidative Coupling method.

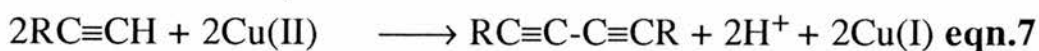
The Glaser oxidative coupling method is used primarily to couple terminal alkynes to form symmetrical molecules containing a diacetylene functional group.^{71,72} The mechanism of oxidative coupling is not fully understood but some workers have postulated more certain details which will be discussed below.

The coupling reaction is performed by mixing the terminal alkyne with a copper salt and an amine ligand in a suitable solvent. Copper compounds effectively catalyse the reaction.⁷³ Both copper (I) and copper (II) salts promote the coupling reaction but in fact only copper (II) is the actual oxidant, as shown in the following mechanism.

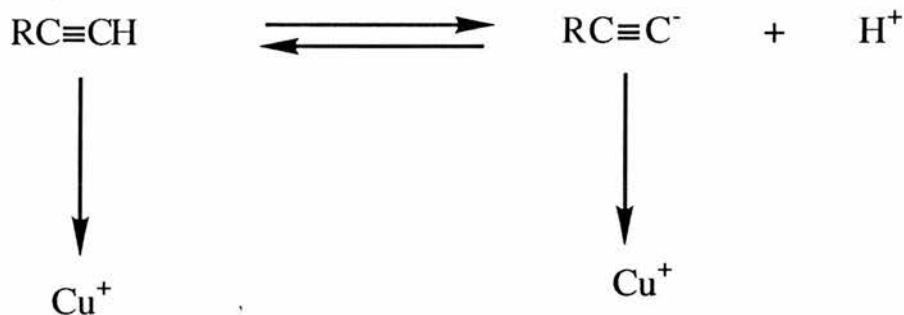




The copper (I) will then oxidise back to copper (II) ^{50,71-74}



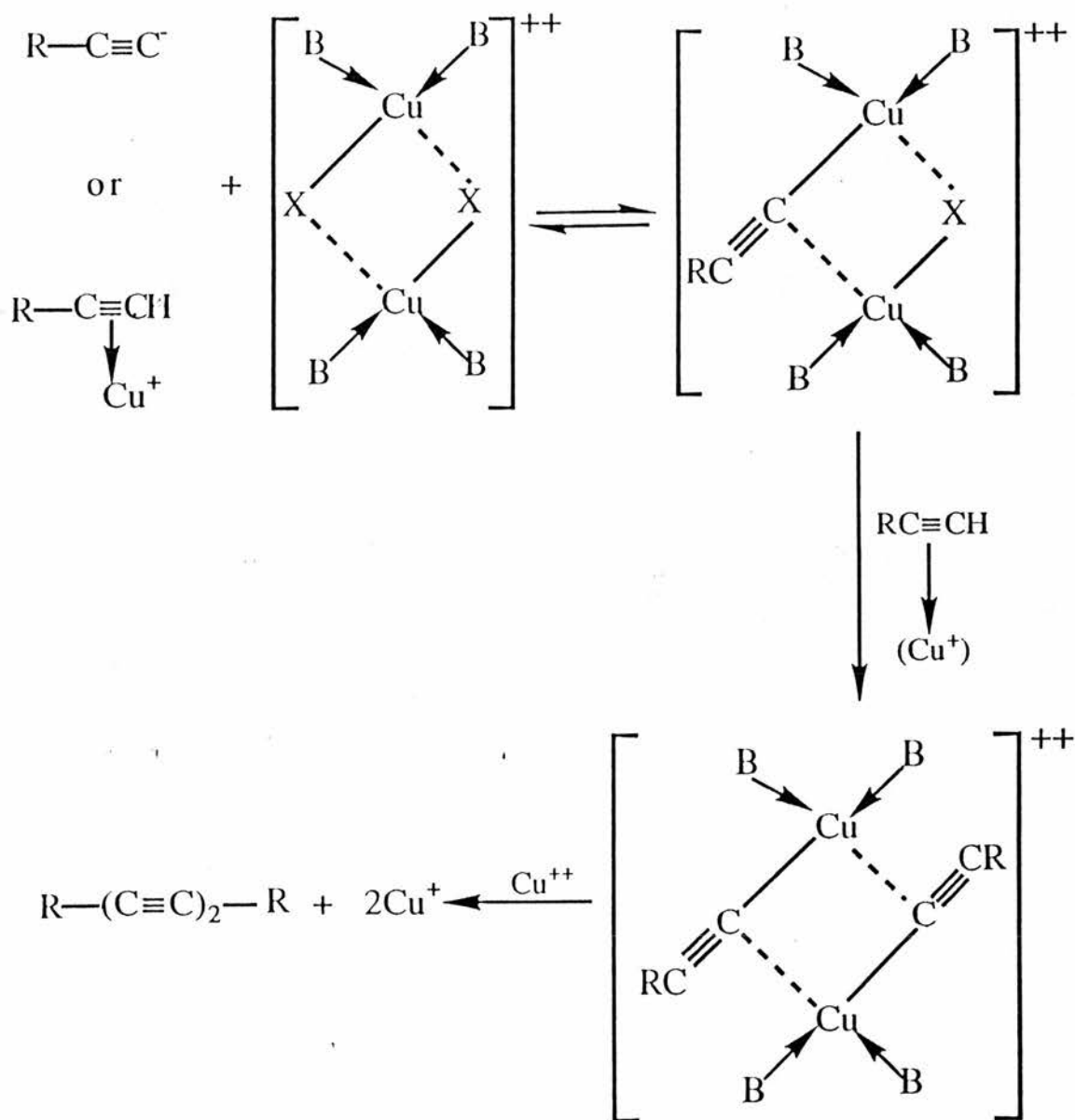
There is some element of doubt about **eqn 4**, ^{72,73,75} but the following points have been accepted. Under acidic conditions the reaction rate increases with cuprous ion concentration. It has been suggested that this behaviour is due to the formation of a copper (I) acetylene type complex and this complex accelerates the dissociation step. (**eqn 4**)



In an alkaline system, the anion can form without the copper (I) acetylene pi-complex and, therefore, the reaction rate will be dependent on the acidity of the acetylenic hydrogen, therefore the greater the acidity the faster the rate. ^{50,73}

Because the reaction is second order with respect to the concentration of the alkyne, the reaction complex must incorporate two

alkyne molecules. In order to explain this rate dependence the following mechanism was suggested. ^{72,73}



X-ray diffraction ⁸¹ has confirmed the bridged dimeric structure for the catalyst complex and is consistent with detailed mechanistic studies. ^{21,72,73,75,81}

3.2.2 Methods for oxidative coupling

There are essentially four methods which have been used to accomplish oxidative coupling of terminal alkynes:

- 1) **Glaser's original coupling reaction**
- 2) **Modified Glaser coupling**
- 3) **Eglinton method (cupric salt-pyridine system)**
- 4) **Hay's catalytic Glaser coupling**

The four methods will be outlined below and the following section will discuss each one of them individually as a potential method for polymerisation route by oxidative coupling.

1) **Glaser's original coupling reaction** — This reaction was carried out by first adding the terminal alkyne to an ammoniacal solution of copper (I) chloride, isolating the precipitated cuprous derivative then oxidising the derivative to produce the diacetylenic product.^{73,75}

2) **Modified Glaser coupling** — A generally better method still called the Glaser reaction, is to mix the alkyne with aqueous cuprous chloride-ammonium chloride solution in an atmosphere of air or oxygen. This is more advantageous than the original coupling reaction as the cuprous derivative which is frequently too insoluble to couple well does not have to be isolated. However, a disadvantage of this coupling is that it proceeds slowly when catalytic amounts of copper (I) salt are used. An excess in the order of 3 moles of copper (I) salt per

mole of the terminal alkyne is needed to make the reaction proceed rapidly.⁷⁵

3) **Eglinton method (cupric salt-pyridine system)**— Coupling by cupric salts in pyridine is an important variation of Glaser's original coupling reaction. It was first developed in 1956 by Eglinton and Galbraith.⁵⁰ The coupling reaction utilises copper (II) salts in a pyridine reaction medium.^{72,76} In this procedure the alkyne is mixed with a solution of copper (II) acetate in pyridine (or a pyridine/methanol mixture). Cuprous salt is present in large enough concentration to start the reaction:



eqn.9

Pyridine neutralises the HX formed. In addition, pyridine complexes with the copper salts and is a powerful solvent for most of the reactants and products. With catalytic amounts of cupric salts, the reactions are very slow, but with excess cupric salt, they are fast. When the copper (II) salt is added in excess, it is not necessary to use oxygen to regenerate copper (II) from the copper (I) formed during the course of the reaction. This is one of the best laboratory procedures, and probably is the most satisfactory route for producing unsaturated macrocycles. Eglinton and Galbraith found that under high dilution conditions, cyclic conjugated diynes could be formed from α,ω -diynes.⁵⁰ Depending upon reaction conditions it is possible to obtain compounds ranging from cyclic 'monomers' to large macrocycles with more than 50 units.^{50,75,77} Coupling aliphatic alkynes using this

method is generally slow. Compounds which have a more acidic acetylene hydrogen, eg $\text{PhC}\equiv\text{CH}$, are more suitable using this method.

4) **Hay's catalytic Glaser coupling** — In 1960 Hay ⁷⁸ reported another significant improvement in Glaser coupling reaction. Certain cuprous salt-amine complexes can be used in catalytic amounts to effect rapid Glaser coupling. Pyridine is able to serve as both ligand and solvent:

Hay ⁷⁴ found later that his cuprous chloride-tertiary amines (such as pyridine) couple aliphatic alkyne compounds slowly. He was able to prepare much more active catalysts by using bidentate tertiary amines, such as N,N,N',N'-tetramethylethylenediamine (TMEDA). The complexes are more soluble in organic solvents and thus are doubly advantageous.

Hay did a comparative study of three catalyst systems: (1) Copper (II) acetate-pyridine, (2) copper (I) chloride-pyridine, and (3) copper (I) chloride-TMEDA. He found that system (3) had by far the fastest reaction rate.⁷⁴ The rates of system (1) and (2) were very similar to each other due to the fact that the copper (I) of system (2) will be rapidly oxidised to copper (II).

3.3 Criteria for Choosing the Two Oxidative Coupling Routes

In choosing the two oxidative coupling routes for my study, certain important factors had to be considered. First, it was necessary

to choose a reaction system that will promote high molar mass polymer i.e. a reaction system which would allow the polymer formed to stay in solution long enough for high molar mass to be achieved. Second, it was important to choose a route to allow isolation of a clean product as utilisation of these polymers in later work requires the polymers to be pure to give meaningful results. In all oxidative coupling procedures highly coloured copper complexes are used, therefore this aim is not easy to achieve as is the case in other polymerisation routes. Finally, since α,ω -alkyldiynes are susceptible to cyclisation under high dilution conditions oxidative coupling routes employing high concentration conditions were investigated with the hope of isolating predominantly linear structures.

In the following sections previous literature work on the oxidative coupling of α,ω -alkyldiyne monomers and other terminal diynes will be discussed in view of these three factors mentioned above and polymerisation by the two routes will be established.

3.3.1 Polymerisation using cupric salt-pyridine system - Eglinton polymerisation

On paper, the Eglinton polymerisation is the simplest oxidative coupling reaction to carry out as it does not require oxygen to be supplied at any time during the course of the reaction. Day and Lando²² synthesised α,ω -alkyldiyne polymers 1,8 nonadiyne, 1,9-decadiyne and 1,11-dodecadiyne using a large excess of cupric chloride dissolved in an equivolume solution of ethanol and pyridine. In all three cases polymers were obtained which were typically light brown in colour and rubbery in nature possibly due to acetylene trimerisation or crosslinking

through the diacetylene group. It was necessary to promote polymerisation by using high temperatures $\sim 75^{\circ}\text{C}$ initially, and even higher temperatures during the final stages of the reaction.

This work was repeated on several occasions with no success in obtaining high molar mass polymer even on increasing the temperature of the reaction for polymerisation. Solution cast films from a dilute solution of methylene chloride were poor, possessing little mechanical strength, indicating low molar mass polymer. Also on each occasion a brown, rubbery type material was obtained even after rigorous work up and purification. It was impossible to remove the brown colour, this brown colour being caused by degradation, but also it may be possible that there is residual copper complex remaining in the polymer, as such a large excess of copper salt is present in the coupling reaction, therefore purification is extremely difficult.

Other difficulties using the Eglinton polymerisation route are:

- 1) Ethanol/pyridine is a poor solvent for the polymers and thus when the polymer chain is growing, the higher molar mass species tend to precipitate out of solution, hence high molar mass is not easy to achieve.
- 2) Using the Eglinton polymerisation method means that there may be a tendency for the polymers to cyclise — although cyclisation is more likely to occur under high dilution conditions/low monomer concentrations. ⁵⁰ Nevertheless, this technique is the most likely to promote this occurrence.

In this study it was decided to abandon the Eglinton polymerisation due to the low molar mass polymers obtained and the difficulties encountered in purification of these polymers. An alternative route would be to follow the catalytic Glaser coupling first carried out by Hay ⁷⁸ and workers in 1960. All Glaser coupling reactions use very low concentrations of copper salt therefore purification of the final product is much easier than the Eglinton system.

The next section of work describes how the first route (**Route A**) was chosen as an oxidative coupling polymerisation route for my studies.

3.3.2 Polymerisation using catalytic Glaser coupling (I) - a basis to establishing polymerisation Route A

In 1960 Hay ⁷⁸ used a copper (I) chloride-pyridine system (2g Cu(I)Cl, 250ml pyridine) for the polymerisation of m- and p-diethynylbenzene(s). Poly(m-diethynylbenzene) had a molar mass of at least 7,000 (this was determined by infrared analysis of end groups) ($\equiv\text{CH}$ stretching, 3290 cm^{-1}) and the polymer was light yellow in colour. Poly(p-diethynylbenzene) gave a bright yellow product that was completely insoluble in all solvents and decomposed rapidly at about 100°C . Pyridine was functioning as a solvent and a ligand.

In section 3.2.2 it was outlined that Hay in 1962 did a comparative study of the reaction rate of ligands in the oxidative polymerisation reaction. He found that TMEDA (a tertiary amine bidentate ligand) used in a catalytic amount with copper (I) chloride

caused a marked increase in the rate of reaction. ⁷⁴ (The reaction system consisted of 1g (0.01 mole) $\text{Cu}(\text{I})\text{Cl}$, 1.2g (0.01 mole) TMEDA, 135 ml acetone and 0.02 mole of terminal monoalkyne). In a later study by Hay ⁷⁹ in 1967 he polymerised the α,ω -alkyldiynes 1,6-heptadiyne, 1,7-octadiyne and 1,8-nonadiyne (the reaction system consisted of 2g (0.02 mole) $\text{Cu}(\text{I})\text{Cl}$, 7g (0.058 mole) TMEDA, 135ml pyridine and 0.05 mole of α,ω -alkyldiyn monomer). Number average molar masses were low as high catalyst concentrations had been employed to achieve rapid polymerisation rates in order to carry out as high an extent of reaction as possible before the polymer precipitated out of the solution.

In 1970, Hay utilised the reaction of copper (I) chloride with TMEDA to polymerise a variety of diacetylene polymers based upon bispropargyl ethers of bisphenols ⁸⁰ (the following reaction system was employed 2g (0.02 mole) $\text{Cu}(\text{I})\text{Cl}$, 4g (0.033 mole) TMEDA, 120 ml pyridine in 380ml nitrobenzene — to this was added 50g, 0.165 mole of bisphenol-A-dipropargyl ether in 100ml nitrobenzene). Number average molar masses of up to 18,000 were obtained by osmometry. These polymers were ultraviolet light sensitive and would crosslink on exposure to this source.

In 1971, White ³² modified Hay's system in an attempt to synthesise higher molar mass polymers. Several methods were explored to provide a polymerisation system in which the polymer remained soluble for the duration of the reaction. A variety of solvents were examined. 1,2-dichlorobenzene was a successful solvent for the polymers he was attempting to synthesise.

Previously Hay ^{74,78-80} had employed high catalyst concentrations to achieve rapid polymerisation rates before the polymer had the chance to precipitate out of solution. With precipitation no longer a problem, catalyst concentrations could be considerably lower with low copper salt concentrations making purification easier (the reaction system employed by White was 0.150g(0.0015 mole) Cu^(I)Cl, 0.23ml (0.0015 mole) TMEDA, 1.7ml pyridine in 48ml 1,2-dichlorobenzene — to this was added 0.0396 mole terminal diyne in 10ml 1,2-dichlorobenzene). White ³² synthesised several homopolymers and copolymers of *m*- and *p*-diethynylbenzenes, bisphenol-A-dipropargyl ether, and poly(α,ω -alkyldiynes) 1,5-hexadiyne, 1,6-heptadiyne, 1,7-octadiyne and 1,8-nonadiyne.

White's system is the most advantageous system for an oxidative coupling route so far as;

(a) It allows the polymer formed to stay in solution long enough for high molar mass to be achieved (reaction temp of 60°C was employed for the α,ω -alkyldiyne polymerisation).

(b) Isolation of a clean product will be easier in this system as a small amount of copper salt is used, making the product from this reaction much easier to purify than any other route.

(c) α,ω -alkyldiynes synthesised by this route are unlikely to cyclise on polymerisation because of high monomer concentrations employed.⁵⁰

In 1989, Butera and workers ^{29,30} synthesised poly(α,ω -alkyldiynes) using a polymerisation procedure based upon that of White with some modifications. The differences between White's procedure and the reaction used by Butera were;

1)**Purification step** — In Butera's procedure the product was reprecipitated three times instead of only once by White so as to increase purity.

2)**Polymerisation delay time** — In Butera's procedure after the α,ω -alkyldiyne monomer was added in 1,2-dichlorobenzene solvent to the stirring mixture the reaction was allowed to proceed overnight at room temperature (with continuous oxygen flow) to form a milky green suspension. Then the temperature of the flask was increased to 60°C and left to polymerise for 4 hours. In White's procedure he did not have this overnight polymerisation delay time the flask contents were polymerised immediately.

Butera synthesised ^{29,30} three α,ω -alkyldiyne polymers using this route. Molar mass averages were obtained for all three polymers using gel permeation chromatography (GPC). The polymers synthesised and their molar masses are listed below;

poly(α,ω -alkyldiyne)	Mn	Mw	polydispersity (PDI)=(Mw/Mn)
poly(1,6-heptadiyne)	14300	30000	2.1
poly(1,8-nonadiyne)	17500	33500	1.9
poly(1,11-dodecadiyne)	18800	38500	2.05

All three polymers were soluble in methylene chloride, chloroform, tetrahydrofuran and 1,2-dichlorobenzene at room temperature.

Butera's system had the added advantage over White's system because:

(a) Repeated reprecipitation leads to isolation of a purer product.

(b) The polymerisation delay time has better control over the polydispersity of the poly(α,ω -alkyldiynes) formed. GPC traces of the poly(α,ω -alkyldiynes) gave almost ideal polydisperse curves (theoretically polydispersity being 2). With almost ideal polydispersity at high molar masses it will be very unlikely that cyclic structures **50** will have formed and the polymer will comprise of a distribution of linear molar masses (**Note**: all molar masses reported were with respect to a polystyrene standard).

The previous discussion clearly indicates that the route chosen by Butera **29,30** (essentially a modified procedure of White's) to synthesise poly(α,ω -alkyldiynes) fulfils the criteria for choosing an oxidative coupling route for the purpose of this study. In the present study this route was chosen for polymerisation and copolymerisation of a series of α,ω -alkyldiynes and will be referred to as **Route A**. Temperature was varied in the polymerisation reaction from 60-80°C in an attempt to maximise the molar mass. Time was also increased by an hour from the polymerisation time adopted by Butera.**29,30** The concentration of the reagents were not optimised for **Route A** as polymer precipitation became a major problem.

3.3.3 Polymerisation using catalytic Glaser coupling (II) - a basis to establishing Polymerisation Route B

In 1975 Kevelam ²¹ and workers carried out a study of influence of concentrations of catalyst, monomer, water, ligand and oxygen on the rate of oxidative polymerisation of 1,8-nonadiyne at 26°C in the presence of homogenous catalysts derived from cuprous chloride (copper (I) chloride) and tertiary amines (pyridine, TMEDA and triethylamine (TEA)). From his results the following conclusions were made:

1) Reaction is nearly first order in Cu_2Cl_2 initially up to the solubility limit of the active catalyst.

2) Reaction is second to first order in 1,8-nonadiyne (monomer) for low to medium conversions.

3) The reaction rate decreases with increasing water content.

4) The reaction rate is enhanced by increasing ligand concentration and increasing basicity of the ligand: TEA > TMEDA > pyridine.

The reaction system chosen for the polymerisation work consisted of 0.25g (1.28×10^{-3} mole) Cu_2Cl_2 , 0.64 mole of TMEDA or TEA, 80ml pyridine and 0.0216 mole of 1,8-nonadiyne. A 50:1 molar ratio of ligand to catalyst was used. (Note in White and Butera's ^{29,30,32} work a 1:1 molar ratio of TMEDA to $\text{Cu}^{(I)}\text{Cl}$ was used). The polymers synthesised by this route resulted in low molar mass, eg M_n (number average) values of about 2,500 were obtained. Only when low oxygen pressures were used M_n values of up to 6,000 were obtained. M_n

values were measured by vapour pressure osmometry in chloroform or benzene at 37°C.

There are several reasons why the molar mass of the poly(1,8-nonadiyne) synthesised by Kevelam is low;

1) Polymerisation temperature — At a temperature of 26°C the chain growth will be terminated because the polymer will start to precipitate from the reaction mixture.

2) Solvent — Although pyridine has been a chosen solvent for oxidative polymerisation reactions in the past ⁷⁸ 1,2 -dichlorobenzene is a far superior solvent as the polymer will remain soluble for the duration of the reaction.

3) Cyclic oligomers — may be formed by oxidative coupling by an intramolecular oxidative coupling of two acetylenic end groups. The system used by Kevelam is dilute (as previously mentioned there is a tendency for the polymers to cyclise under high dilution conditions ⁵⁰).

4) Retardation of oxidative coupling by water, which strongly affects chain growth by a step-mechanism in the final stages of the reaction.

5) Concentration — using a more concentrated system will promote higher molar mass. An improvement in the polymerisation procedure of Kevelam's was reported by Knol ²⁶ and workers in 1984. Initially Knol followed the same procedure adopted by Kevelam, but two important factors were changed in the polymerisation.

1) Solvent — Pyridine solvent was replaced by 1,2-dichlorobenzene.

2) Molecular sieve was added to the reaction mixture in order to remove the water generated during the polymerisation.

The modified procedure doubled the molar mass. M_n values of 5,000 were achieved (measured by vapour pressure osmometry). Further improvements were made by Knol. When the polymerisation was carried out at 65°C without changing the other reaction conditions the polymer remained in solution and its M_n was increased to 15,900 (measured in a chloroform solution at 27°C with a Knauer membrane osmometer). Knol also found that the molar mass could be increased further up to values of about 20,000 by optimising the concentration of the reagents. The reaction system employed was 0.0125g (1.26 mmol) $\text{Cu}^{\text{I}} \text{Cl}$, 0.77g (6.62 mmol) TMEDA, 13.75ml of 1,2-dichlorobenzene, 0.2g (1.67 mmol) of 1,8-nonadiyne and 2.5g of molecular sieve (**Note:** A 50:1 molar ratio of TMEDA to $\text{Cu}^{\text{I}} \text{Cl}$ was used).

Knol claimed molar masses, measured by membrane osmometry, were as high as 20,000. However, with the exclusion of molar mass distribution curves by gel permeation chromatography (GPC) it is not possible to predict whether cyclic or oligomeric structures have formed from the polymerisation reaction.

For the purpose of this study Knol's route was selected as the second route (**Route B**) for polymerisation and copolymerisation of a series of α,ω -alkyldiynes. It is of particular interest to study the molar mass distribution of these polymers by GPC to give an indication whether polydisperse linear polymers can be synthesised using Knol's route.

Three factors were varied in the polymerisation reaction in an attempt to maximise the molar mass further;

(a)time

(b) temperature

(c) concentration — in all reactions a more concentrated system was used to further eliminate the possibility of cyclic species forming.

The essential differences between **Route A** and **Route B** are:

- (1) Polymerisation delay time
- (2) Ratio of copper (I) chloride:TMEDA
- (3) Solvent system.

(1) Polymerisation delay time — In **Route A** a polymerisation delay time was included in the syntheses of the polymers whereas in **Route B** this was excluded and the flask contents were polymerised immediately.

(2) Copper (I) chloride:TMEDA — In **Route A** the copper (I) chloride:TMEDA ratio is 1:1 whereas in **Route B** the copper (I) chloride:TMEDA ratio is 1:50.

(3) Solvent system — In **Route A** 1,2-dichlorobenzene: pyridine solvent system is used whereas in **Route B** 1,2-dichlorobenzene solvent is used exclusively.

3.4 Syntheses of poly(α,ω -alkyldiynes) and copoly(α,ω -alkyldiynes)

Materials The monomers 1,7-octadiyne, 1,8-nonadiyne, 1,9-decadiyne, 1,10-undecadiyne and 1,11-dodecadiyne synthesised as in Chapter 2 were distilled prior to use. All other reagents and solvents (Aldrich, high purity) were generally used without drying.

3.4.1 Syntheses of Polymers — Route A

To a 50ml wide-mouthed Erlenmeyer flask, equipped with a magnetic stirrer, an oxygen inlet tube, and a thermometer 20ml 1,2-dichlorobenzene, 0.71 ml(8.8 mmole) pyridine, 0.096ml(0.625 mmole) TMEDA and 0.0625g(0.625 mmole) copper (I) chloride were added, producing a light green solution. Oxygen was then bubbled through the stirring solution for 40 minutes (the solution turned dark green shortly after oxygen flow was started). A solution of 0.0165 mole of the chosen α,ω -alkyldiyne monomer(s) in 4ml of 1,2-dichlorobenzene was then slowly added to the stirring reaction mixture. The reaction was allowed to proceed overnight (with continuous oxygen flow), after which time, in most cases, a milky green suspension was formed. The flask was then placed in an oil bath at temperatures ranging from 70-90°C. Upon placing the flask into the oil bath the reaction mixture turned clear and was dark green in colour. The reaction was allowed to polymerise at the desired temperature for 5hrs (an hour more than the polymerisation time adopted by Butera ^{29,30}). After this time, the flask was removed from the oil bath and allowed to cool (with stirring) for 15 minutes. The mixture was then added dropwise to a stirred solution of 5ml concentrated HCl in 250ml methanol. The resultant precipitate

was allowed to stir for 15 min in the methanol/HCl mixture. The precipitate was then dried over a büchner funnel (with aspiration) and subsequently dissolved in 100 ml of methylene chloride. The polymer was reprecipitated four times, twice in methanol/HCl and twice in pure methanol to obtain a white product. The polymer was dried over a büchner funnel (with aspiration) then under vacuum at room temperature and its yield recorded. The polymer was then dissolved in methylene chloride, the solution was filtered using 'Hyflo-supercel' filtering agent to give a clear solution. The polymer was stored in methylene chloride as a 1% weight/volume solution* (A small quantity of this purified polymer was evaporated, dried under vacuum and then dissolved in deuteriochloroform for $^1\text{Hnmr}$ -End group analysis(EGA) studies).

3.4.2 Syntheses of polymers — Route B

To a 25ml wide-mouthed Erlenmeyer flask, stirred in an oil bath (temperatures ranging from 70–90°C) equipped with a magnetic stirrer, an oxygen inlet tube, and a thermometer were added 10ml 1,2-dichlorobenzene, 3.8 ml (25 mmole) TMEDA and 1g of molecular sieve A4 drying agent. Once the desired temperature of the solution was reached, 0.05g (0.5 mmole) of copper (I) chloride was added. Oxygen was then bubbled through the stirring solution for 40 minutes (the solution turned dark green shortly after oxygen flow was started). A solution of 7.45 mmol of the chosen α,ω -alkyldiyne(s) in 5ml of 1,2-dichlorobenzene was added to the stirring reaction mixture. The

* The polymer was filtered to remove any low molar mass species which may affect the polydispersity of the polymers. The polymers were stored in dilute solution for two reasons a) they were light sensitive in the solid state b) to cast films from the solution.

reaction mixture was left to polymerise at the desired temperature for the chosen length of time. After then, the flask was removed from the oil bath and allowed to cool (with stirring for 15 min).

Note: The remainder of this procedure is the same as **Route A** - the only difference being the quantities of acid and solvents used in the work up. In Route B 2ml concentrated HCl, 100ml methanol and 50ml of methylene chloride were used.

3.4.3 Polymers characteristics; Polymerisation conditions for a range of polymers together with their yields and solubility characteristics were tabulated (see Table 3.1 and 3.2).

For the polymers synthesised by **Route A** all polymers, except for poly(1,7-octadiyne), were very soluble in chloroform, methylene chloride and tetrahydrofuran at room temperature. 1,2-dichlorobenzene and 1,2-dichloroethane will also dissolve the polymers, but not as readily as the above solvents. Poly(1,7-octadiyne) was insoluble in a range of solvents at room temperatures and elevated temperatures. However, it was sparingly soluble in 1,2-dichlorobenzene at elevated temperatures.

For the polymers synthesised by **Route B** all polymers, except for poly(1,11-dodecadiyne), were very soluble in chloroform, methylene chloride and tetrahydrofuran at room temperature. 1,2-dichlorobenzene and 1,2-dichloroethane will also dissolve the polymers, but not as readily as the above solvents. Poly(1,11-dodecadiyne) was very soluble in chloroform and methylene chloride at room temperature, but

insoluble in tetrahydrofuran at room temperature and only sparingly soluble in 1,2-dichlorobenzene at room temperature.

It was noted that the polymers stored in methylene chloride solution synthesised from **Route B** were darker in colour (i.e. orange/light brown) than those synthesised from **Route A** (which were clear to light yellow in colour).

In the following chapter the molar mass of the polymers synthesised by both **Route A** and **Route B**, are presented in detail.

At the end of Chapter 4(4.4.4) a summary is included for the polymers synthesised by both polymerisation routes A and B and a mechanism is proposed for the oxidative coupling reaction which has been described in this chapter.

Polymer	Temperature of polymerisation	Time of polymerisation	Yield(%)	Solubility Characteristics
A1) poly(1,7-octadiyne)	65°C	5 hours	87	* - see footnote
A2) poly(1,8-nonadiyne)	65°C	5 hours	91	** -see footnote
A3) poly(1,9-decadiyne)	60°C	5 hours	93	**
A4) poly(1,9-decadiyne)	80°C	5 hours	89	**
A5) poly(1,9-decadiyne)	65°C	5 hours	91	**
A6) 50:50 poly(1,8-non):poly(1,9-dec)	65°C	5 hours	87	**
A7) poly(1,10-undecadiyne)	65°C	5 hours	88	**
A8) 50:50 poly(1,9-dec):poly(1,10-undec)	65°C	5 hours	90	**
A 9) poly(1,11-dodecadiyne)	65°C	5 hours	85	**

(N.B. Every reaction has an overnight polymerisation delay time at room temperature) * insoluble in a range of solvents at room temperature and elevated temperatures. Sparingly soluble in 1,2-dichlorobenzene at elevated temperatures. ** Very soluble in a range of solvents at room temperature-chloroform, methylene chloride and tetrahydrofuran. Soluble in 1,2-dichlorobenzene and 1,2-dichloroethane at room temperature.

Table 3.1 Polymers synthesised by route A

Polymer	Temperature of polymerisation	Time of polymerisation	Yield(%)	Solubility Characteristics
B1) poly(1,8-nonadi- yne)	60°C	6 hours	84	*- see footnote
B2) poly(1,8-nonadi- yne)	60°C	8 hours	89	*
B3) poly(1,9-decadi- yne)	80°C	6 hours	86	*
B4) poly(1,9-decadi- yne)	80°C	10 hours	85	*
B5) poly(1,9-decadi- yne)	40°C	15 hours	89	*
B6) poly(1,9-decadi- yne)	60°C	15 hours	91	*
B7) poly(1,9-decadi- yne)	80°C	15 hours	90	*
B8) poly(1,11-dode- cadiyne)	80°C	8 hours	83	** - see footnote
B9) 50:50 poly(1,9- dec):poly(1,10-undec)	60°C	8 hours	88	*
B10) 80:20 poly(1,9- dec):poly(1,11-dodec)	60°C	8 hours	85	*

* Very soluble in chloroform, methylenechloride and tetrahydrofuran at room temperature, soluble in 1,2-dichlorobenzene and 1,2-dichloroethane at room temperature. ** Very soluble in chloroform, methylenechloride, insoluble in tetrahydrofuran at room temperature. Only sparingly soluble in 1,2-dichlorobenzene at room temperature.

Table 3.2 Polymers synthesised by route B

CHAPTER 4

MOLAR MASS CHARACTERISATION OF POLY(α,ω -ALKYLDIYNES) AND COPOLY(α,ω -ALKYLDIYNES)

4.1 Introduction

The purpose of the work described in this chapter is to study the molar mass characteristics of polymers synthesised by polymerisation routes A and B (with the exclusion of polymer A1 poly(1,7-octadiyne) as a consequence of its insolubility) in the previous chapter. Two techniques are involved.

- (1) Gel permeation chromatography (GPC)
- (2) End group analysis (EGA) by ^1H nmr spectroscopy

The first section of this chapter outlines previous techniques which are employed in the molar mass characterisation of the poly(α,ω -alkyldiynes) (i.e. osmometry and GPC). This is followed by a brief summary of the two techniques employed in this study for molar mass characterisation of the poly(α,ω -alkyldiynes) and copoly(α,ω -alkyldiynes).

The next section of this chapter outlines the instrumentation involved in the GPC and the end group analysis (EGA) by ^1H nmr spectroscopy. GPC curves are included for all polymers synthesised by polymerisation routes A and B. Values for M_n (number average molar mass), M_w (weight average molar mass) and PDI (Polydispersity = M_w/M_n) are quoted. One GPC curve from polymerisation route A and the majority of GPC curves from polymerisation route B had a significant low molar mass tail present. It was proposed that the low molar mass tail was not only a consequence of linear oligomeric structures but also low molar mass cyclic structures formed during the polymerisation. The values obtained by the computer were considerably

lower than anticipated due to the presence of the low molar mass tail. Curve idealisation calculations are performed manually to give M_n values which only included the Gaussian shape high molar mass segment. ^1H nmr spectra together with expansions are included for the polymers which showed a Gaussian distribution of high molar masses i.e. the majority of polymers from polymerisation route A. M_n values by EGA are included for all polymers synthesised by polymerisation routes A and B. M_n values obtained by EGA on the polymers which had a low molar mass tail in their corresponding GPC curves will in theory give a higher M_n value than anticipated if the low molar mass tail is a consequence of cyclics. Therefore the M_n value obtained by the EGA calculation was reduced accordingly to account for the higher molar mass segment only.

Also in this chapter the consequence of the low molar mass tail with reference to the cyclisation of α,ω -alkyldiynes is discussed. Finally the mechanism of oxidative coupling of polymerisation routes A and B is discussed.

4.2 Techniques used for molar mass characterisation of poly(α,ω -alkyldiynes) and copoly(α,ω -alkyldiynes)

Introduction

Previously two techniques have been used in the molar mass characterisation of poly(α,ω -alkyldiynes). These are shown in Table 4.1 (page 148).

1) Osmometry

Both Kevelam **21** and Knol **26** used vapour pressure osmometry for the molar mass characterisation of poly(1,8-nonadiyne). For higher molar mass polymers synthesised by Knol number average molar masses (M_n) were determined exclusively by membrane osmometry.

2) Gel permeation chromatography (GPC)

Butera **31** used GPC for the molar mass characterisation of three poly (α,ω -alkyldiynes); poly(1,6-heptadiyne), poly(1,8-nonadiyne) and poly(1,11-dodecadiyne). M_n values as high as 20,000 and M_w values of as high as 40,000 were obtained. Polydispersity (M_w/M_n) values were almost ideal, i.e. ~ 2 for the polymers that he studied. (A Perkin Elmer 10C chromatograph, employing a UV detector and an LC column, was used with THF as the solvent at 40°C; the molar masses reported were with respect to polystyrene standards).

In the present study GPC was used for the molar mass characterisation of all polymers synthesised by routes A and B (with the exclusion of polymer A1 poly(1,7-octadiyne) as a consequence of its insolubility). End group analysis (EGA) by ^1H nmr spectroscopy was used for all polymers synthesised by both routes A and B as a means of comparison with the GPC results.

4.2.1 Gel permeation chromatography (GPC)

GPC separates the polymer samples into fractions according to their sizes by means of a sieving action. This is achieved using a non-ionic stationary phase of packed spheres (often crosslinked polystyrene beads) whose pore size distribution can be controlled.

The polymers in the present study are characterised best by this technique, i.e. instead of assigning the polymers molar mass by a single molar mass the polymers are characterised by a molar mass distribution and the associated molar mass averages. The typical distributions, shown in figure 4.1 (page 159) can be described by a number of averages.⁸²

$$M_n = \frac{\sum N_i M_i}{\sum N_i} = \text{number average molar mass}$$

$$M_w = \frac{\sum N_i M_i^2}{\sum N_i M_i} = \text{weight average molar mass}$$

$$M_z = \frac{\sum N_i M_i^3}{\sum N_i M_i^2} = \text{Z average molar mass}$$

The breadth of distribution can often be gauged by establishing the polydispersity index $(PDI)=(M_w/M_n)$. Ideally, polydispersity should be equal to 2 for a normal distribution of molar masses (i.e. a Gaussian shape curve).

In the present study GPC was performed on all polymers synthesised by routes A and B and their molar mass distribution curves are included. (Molar masses are reported with respect to polystyrene standards).

4.2.2 End group analysis (EGA) by $^1\text{Hnmr}$ spectroscopy

End group analysis (EGA) is limited to linear polymers and estimates the number average molar mass (M_n).

The sensitivity of this method decreases rapidly as the chain length increases and the number of end groups drops. Therefore, a practical upper limit will restrict what molar mass values can be measured.

EGA assigns an absolute M_n value for the polymer molar mass, unlike GPC which assigns an M_n value for the polymers molar mass relative to polystyrene standards.

In the present study EGA was performed on all polymers synthesised by polymerisation routes A and B. $^1\text{Hnmr}$ spectra together with expansions are included for the polymers which showed a Gaussian distribution of high molar masses, i.e. the majority of polymers from

polymerisation route A. M_n values by EGA are included for all polymers synthesised by polymerisation routes A and B.

4.3 Experimental section

Instrumentation involved in GPC and end group analysis(EGA) by $^1\text{Hnmr}$ spectroscopy is discussed in this section of the work. Also included is a sample curve idealisation calculation in 4.3.1 and a sample EGA calculation in 4.3.2.

4.3.1 Gel permeation chromatography (GPC)

The GPC analyses were carried out at ICI Wilton, Materials Centre, Middlesbrough, Cleveland by using a MC/GPC/3 series chromatograph (equipped with a Shodex 'mixed gel column' capable of wide molar mass range resolution), using a refractive index detector and chloroform as solvent (1 ml/min @ 24°C). All molar masses are reported with respect to polystyrene standards.

Results from molar mass measurements are reported in Tables 4.2 and 4.3(pages 149-153) for polymerisation routes A and B respectively, and GPC molar mass distribution in curves for both polymerisation routes are shown in figures 4.4 to 4.21(pages 161-169) inclusively.

One GPC curve from polymerisation route A and the majority of GPC curves from polymerisation route B had a significant low molar mass tail present. A Gaussian shape distribution of molar masses was not achieved as in figure 4.1(page 159). Therefore these molar mass

distributions curves were idealised to represent a Gaussian shape at high molar masses by outlining a curve inside the authentic GPC molar mass distribution curve, i.e. eliminating the low molar mass tail. Hence the following calculations for (a) Number average molar mass (M_n) and (b) Weight average molar mass (M_w) were performed;

(a) Number average molar mass (M_n)

$$M_n = \frac{\sum N_i M_i}{\sum N_i} = \frac{\sum W_i}{\sum W_i / M_i}$$

(b) Weight average molar mass (M_w)

$$M_w = \frac{\sum N_i M_i^2}{\sum N_i M_i} = \frac{\sum W_i M_i}{\sum W_i}$$

M_i = molar mass

N_i = number of molecules with molar mass M_i

W_i = the mass of a fraction with the molar mass M_i i.e. $W_i = N_i M_i$

A typical example of this calculation will now be shown below. (It is for the polymer poly(1,8-nonadiyne) synthesised by polymerisation route B — shown in figure 4.2(page 160)).

Before curve idealisation is performed the polymer has an $M_n = 8,460$ and $M_w = 48,100$ giving an overall polydispersity of 5.7.

For this polymer the GPC curve was idealised and the data was manipulated in the following manner;

$$M_n = \frac{\sum W_i}{\sum W_i/M_i}$$

$$(\sum W_i = 0.41+1.05+1.69+1.92+1.42+0.78+0.3+0.15 = 7.72)$$

$$\begin{aligned} (\sum W_i/M_i &= 0.41/10^{3.75}+1.05/10^{4.0}+1.69/10^{4.25}+1.92/10^{4.5}+ \\ &1.42/10^{4.75}+0.78/10^{5.0}+0.3/10^{5.25}+0.15/10^{5.5}) \\ &= 3.68 \times 10^{-4} \end{aligned}$$

$$M_n = \frac{7.72}{3.68 \times 10^{-4}} = 20,978$$

$$M_w = \frac{\sum W_i M_i}{\sum W_i}$$

$$\begin{aligned} (\sum W_i M_i &= 0.41 (10^{3.75})+1.05(10^{4.0})+ \dots \text{etc} \\ &= 362209.66 \end{aligned}$$

$$M_w = \frac{362209.66}{7.72} = 46,918$$

$$\text{Polydispersity Index (PDI)} = \frac{M_w}{M_n} = \frac{46918}{20978} = 2.24$$

Similar calculations were performed on the remainder of the polymers which had the low molar mass tail present and are reported in Tables 4.2 and 4.3 for polymerisation routes A and B respectively.

Note: These M_n values only give an estimate of what the molar mass averages would be if a Gaussian distribution of linear molar masses were achieved from the polymerisation reaction.

4.3.2 End group analysis (EGA) by $^1\text{Hnmr}$ spectroscopy

EGA calculations were performed on all polymers synthesised by polymerisation routes A and B. $^1\text{Hnmr}$ spectra together with expansions

are shown in figures 4.22 to 4.30(pages 170-178) inclusively. These are polymers whose GPC curves were Gaussian in shape and molar masses high enough to assume linear structures were synthesised. Mn values obtained by EGA are reported in Tables 4.4 and 4.5(pages 154-158) for polymerisation routes A and B respectively.

All $^1\text{Hnmr}$ spectra were recorded at 300 MHz on a Brüker AM-300 spectrometer.

A typical EGA calculation for the polymer poly(1,10-undecadiyne) is included for polymer A7 synthesised by polymerisation route A. The polydispersity (PDI) of the polymer is almost ideal (i.e. $M_w/M_n=2.09$) and Mn value is high enough to assume a distribution of linear molar masses.

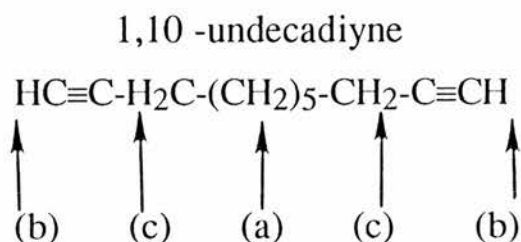
(1) $^1\text{Hnmr}$ spectrum of the monomer 1,10-undecadiyne (see figure 4.22 on page170).

This spectrum reveals three peaks;

(a) $\delta\text{H}=1.35$ ppm (multiplet) — represents ten methylene protons in the middle of the monomer chain.

(b) $\delta\text{H}=1.94$ ppm (triplet) — represents two terminal alkyne protons at either end of the monomer chain.

(c) $\delta\text{H}=2.15$ ppm (multiplet) — represents four methylene protons attached to the two terminal alkyne groups.



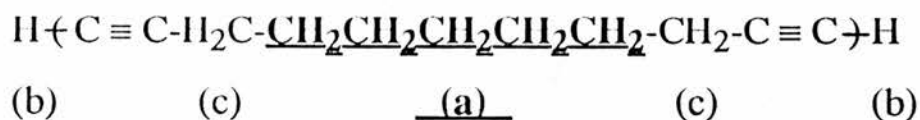
When the monomer is oxidatively polymerised to give a linear structure the signal for the two terminal alkyne end groups (b) at $\delta_{\text{H}} = 1.94$ ppm decreases in intensity with respect to the two signals (a) and (c) for the methylene protons in the polymer chain. As the molar mass of the polymer increases the signal (b) decreases in intensity even further. Therefore at high molar masses the signal (b) is broad and indistinguishable with respect to signals (a) and (c) in the $^1\text{Hnmr}$ spectrum.

(2) $^1\text{Hnmr}$ spectrum of poly(1,10-undecadiyne) — see figure 4.23(page171). In the $^1\text{Hnmr}$ spectrum of poly(1,10-undecadiyne) the triplet signal for the two terminal alkyne groups is barely recognisable, therefore integration of the signal is not possible. In order to obtain a number average molar mass (M_n) of this polymer expansion of this peak with respect to either signal (a) or signal (c) is necessary. In all end group analysis calculations signal (b) was expanded with respect to signal (a).

(3) EGA calculation for linear poly(1,10-undecadiyne)

First of all it was necessary to expand the triplet peak (b) for the two terminal alkyne protons by a factor of 8 with respect to the multiplet peak (a) for the $(\text{CH}_2)_5$ protons (which occur along the main chain of the linear polymer) so the areas of both peaks can be compared (this is shown in figure 4.24 on page172).

To obtain a value for M_n the areas of the peaks were simply cut out, weighed and the following series of arithmetical calculations were performed;



mass of the multiplet peak (a) for $(\text{CH}_2)_5$ protons = 0.1625g

mass of the triplet peak (b) for two terminal alkyne protons = 0.0020g.

There are ten protons which occur along the main chain of the linear polymer and two terminal alkyne protons at either end of the polymer chain.

In order to obtain a value for the number of repeat units (n) in the polymer chain, the mass of the multiplet peak (a) for the $(\text{CH}_2)_5$ protons must be divided by 5, i.e.

mass of $-\text{CH}_2-$ in main chain of linear polymer = $0.1625\text{g}/5 = 0.03304\text{g}$

and the mass of the triplet peak (b) for the terminal alkynes must be divided by 8, i.e.

mass of $\text{HC}\equiv\text{C}\sim\text{C}\equiv\text{CH} = 0.0020\text{g}/8 = 2.5\times 10^{-4}\text{g}$ at either ends of linear polymer chain.

Then the number of repeat units can be obtained by the following expression overleaf;

Number of repeat units

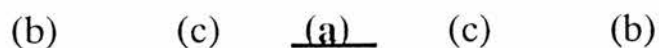
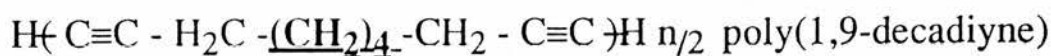
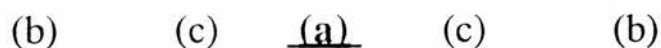
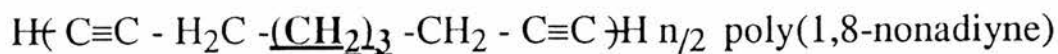
$$n = \frac{\text{mass of } -\text{CH}_2\text{-in the main chain of the linear polymer}}{\text{mass of } \text{HC}\equiv\text{C} \sim\sim\sim \text{C}\equiv\text{CH} \text{ at either ends of the linear polymer chain}}$$

The number of repeat units n , is then multiplied by the relative molar mass (r.m.m.) of the repeat unit for the monomer 1,10-undecadiyne giving the number average molar mass of the polymer, poly(1,10-undecadiyne).

$$\begin{aligned} M_n &= n \times \text{r.m.m. (1,10-undecadiyne)} \\ &= 132.16 \times 148 \\ &= \underline{19,600} \end{aligned}$$

The calculation is similar for a copolymer but some modifications are included.

eg a 50:50 copolymer of 1,8-nonadiyne:1,9-decadiyne. The assumption is being made that there is exactly 50% of n for each polymer, i.e;



Therefore, the mass of the multiplet peak (a) will be a 50% mixture of $(\text{CH}_2)_3$'s and $(\text{CH}_2)_4$'s, i.e. an equivalent of seven protons occurring along the main chain of the linear polymer.

In order to obtain a value for the number of repeat units (n) in the polymer chain the mass of the multiplet peak (**a**) must be divided by 3.5 to give the 'mass of $-\text{CH}_2-$ in main chain of linear polymer.'

The M_n value is obtained by $n \times \text{r.m.m.}$. Therefore the r.m.m. consists of 50% r.m.m. of 1,8-nonadiyne and 50% r.m.m. of 1,9-decadiyne.

$$M_n = n \times \left(\frac{120+134}{2} \right)$$

Similar calculations were performed for a range of polymers synthesised by both polymerisation routes A and B.

M_n values obtained by EGA on the polymers which had a low molar mass tail in their corresponding GPC curves will in theory have a higher M_n value than anticipated if the low molar mass tail is a consequence of cyclics. (If cyclics are present in the low molar mass region an exaggerated value for M_n will be obtained as the methylene protons from the main chain of the linear polymer and the methylene protons from the cyclics are compared with end group protons from the linear polymer exclusively). **Note:** No end group protons exist in cyclic structures.

Therefore the values obtained from the EGA calculation were reduced accordingly to account for the higher molar mass segment only.

An explanation of how this was carried out is now discussed. By considering figure 4.3(page 160), poly(1,8-nonadiyne) synthesised by

polymerisation route B, this polymer has an Mn value of 8,544 calculated by EGA. The low molar mass tail was idealised to represent a Gaussian shape by outlining a curve in the low molar mass region of the GPC curve.

To estimate the proportion of low molar mass tail the area of the low molar mass tail and the area of the whole GPC curve were weighed and the proportion of low molar mass tail was expressed as a decimal proportion of 1.

$$\text{proportion of low molar mass} = \frac{\text{mass of the low molar mass tail}}{\text{mass of the whole GPC curve}}$$

For this particular polymer in figure 4.3

$$\text{proportion of low molar mass} = \frac{0.0178\text{g}}{0.1363\text{g}} = 0.13$$

The original Mn value obtained by the EGA was 8,544. To obtain the new reduced Mn value, the original Mn value is multiplied by a factor of 0.87 i.e. (1 - 0.13).

Therefore the new reduced value to account for low molar mass cyclics is $8,544 \times 0.87 = 7,433$

Similar calculations were performed on the remainder of the polymers which had the low molar mass tail present and are reported in Tables 4.4 and 4.5 for polymerisation routes A and B respectively. **Note:** These Mn values give an estimate of what the values would be if the low molar mass tail comprised of predominantly cyclics. It was anticipated

that on performing these calculations that the corrected reduced Mn value for EGA (EGA(corr)) and the corrected Mn value after curve idealisation for GPC (GPC(corr)) could be linked by a consistent multiplication factor F;

$$F = \frac{\text{GPC(corr)}}{\text{EGA(corr)}} \quad (\text{see 4.4.1})$$

4.4 Results and Discussion

4.4.1 Molar mass characterisation of polymers synthesised by route A

GPC curves are shown in figures 4.4 to 4.11(pages 161-164) inclusively.

Mn, Mw and PDI values before and after curve idealisation are included in Table 4.2(pages 149-150)

¹Hnmr spectra together with expansions are shown in figures 4.22 to 4.30(pages 170-178) inclusively for the polymers whose corresponding GPC curves are Gaussian in shape at high molar masses.

Mn values by EGA before and after reduction to account for the low molar mass tail are included in Table 4.4(pages 154-155).

Note: Curve idealisation work and reduction to account for the low molar mass tail is performed on only the one polymer i.e. poly(1,8-nonadiyne) polymer A2.

In all cases from polymerisation route A, with the exception of one polymer, GPC curves are Gaussian in shape at high molar masses. The one exception to this being polymer A2 -poly(1,8-nonadiyne) polymerised for 5 hours @ 65°C.

Figure 4.4 shows a GPC curve which is atypically Gaussian in shape with a combination of low and high molar masses i.e. a large distribution of molar masses with PDI as high as 6.37 (see Table 4.2). The low molar mass tail is most likely a consequence of linear oligomeric structures with the possibility of low molar mass cyclic structures present also. With reference to Table 4.4 the M_n value obtained by GPC before curve idealisation is 5,890 whereas the M_n value obtained by EGA is as high as 15,000. This would strongly favour the argument for low molar mass cyclics as a high value for EGA suggests that the calculation overestimates the number of methylene protons contributing to the M_n value. When cyclic structures are present the calculations will involve methylene protons from the linear chains and also methylene protons from the cyclic structures. Therefore these methylene protons will be compared with the terminal protons from the linear chains exclusively as the cyclic structures do not possess end group protons. Hence an exaggerated M_n value will be obtained by EGA.

A curve idealisation calculation was performed on the GPC curve of this polymer and the M_n value of 5,890 was increased to 27,600 (see Table 4.2). Also an M_n reduction calculation for EGA on the GPC curve to account for the low molar mass tail was performed. The M_n value obtained by EGA of 15,000 was reduced to 12,000 (see Table 4.4).

These new corrected values for GPC and EGA for the above polymer and the GPC and EGA values for the remainder of the polymers were compared with each other (see Table 4.4). In all cases the M_n values by GPC(corr) were a factor greater than M_n values by

EGA(corr). M_n values obtained by EGA for all the polymers were absolute values whereas M_n values by GPC were calculated relative to polystyrene standards. As a means of comparison a multiplication factor, F , was calculated for all the polymers. This is shown below;

$$F = \frac{M_n \text{ by GPC (corr)}}{M_n \text{ by EGA (corr)}}$$

Values for F were in the range 1.13 to 2.76 (shown in Table 4.4)

Since errors were bound to arise in the EGA calculation an average value for the multiplication factor F was calculated from the eight values in Table 4.4. A value of 1.78 was obtained. Errors involved in the EGA work included;

(a) Judgement of where the baseline should be set for the multiplet peak of the methylene protons when it was cut out. Consistency was required.

(b) Also in some cases the triplet peak was poorly resolved. (The sensitivity of EGA decreases rapidly as the chain length increases because the number of end groups drops). Therefore cutting this peak out was difficult and required careful work with no guarantee of an accurate result for M_n .

However EGA does have an obvious advantage over GPC (when studying a distribution of linear molar masses exclusively) in that an absolute value is obtained by EGA, whereas in GPC a value relative to a polystyrene standard is obtained.

All polymerisations carried out by route A were of a duration of 5 hours. In route A initial polymerisation work was performed on

poly(1,9-decadiyne). Three different temperatures were investigated for polymerisation. Figures 4.5, 4.6 and 4.7 show GPC curves for poly(1,9-decadiyne) polymerised at temperatures of 60, 80 and 65°C with respective M_n values of 20,900, 19,600 and 29,300 being obtained by GPC (see Table 4.2). Since 65°C gave the highest M_n value this temperature was employed for the remainder of the polymerisation work in route A.

It was shown that all poly and copoly(α,ω -alkyldiynes) studied in route A, with the only exception being poly(1,8-nonadiyne), gave Gaussian shape curves at high molar masses by GPC.

As previously mentioned poly(1,8-nonadiyne) gave a combination of low and high molar masses in an atypical Gaussian shape curve by GPC, with a distinct low molar mass tail. The presence of the low molar mass tail will be discussed in section 4.4.3. An M_n value of 5,890 with PDI of 6.37 was obtained by GPC for poly(1,8-nonadiyne) (see Table 4.2). However Butera ³¹ synthesised poly(1,8-nonadiyne) using polymerisation conditions of 60°C for 4 hours and obtained an M_n value of 14,300 with PDI of 2.1 by GPC suggesting a Gaussian shape curve at high molar masses. Figure 4.11 shows a GPC curve for poly(1,11-dodecadiyne) synthesised at 65°C for 5 hours with an M_n value of 14,300 and PDI of 2.28 obtained by GPC (see Table 4.2). Butera ³¹ also synthesised poly(1,11-dodecadiyne) using polymerisation conditions of 60°C for 4 hours and obtained an M_n value of 18,800 with PDI of 2.05 by GPC. The molar mass characteristics obtained by Butera show that higher M_n values for both poly(1,8-nonadiyne) and

poly(1,11-dodecadiyne) can be achieved using lower temperatures and shorter polymerisation times.

Figures 4.8, 4.9 and 4.10 show GPC curves for a 50:50 copolymer of 1,8-nonadiyne:1,9-decadiyne, poly(1,10-undecadiyne) and a 50:50 copolymer of 1,9-decadiyne:1,10-undecadiyne all polymerised at 65°C for 5 hours. M_n values of 24,100, 28,300 and 28,300 were respectively obtained by GPC with PDI values being close to 2 in every case (see Table 4.2). The three polymers displayed a Gaussian distribution of high molar masses suggesting linear polymers had formed.

Note: In the copolymer of 1,8-nonadiyne with 1,9-decadiyne negligible quantities of low molar mass material was obtained (see figure 4.8) whereas in the homopolymer of 1,8-nonadiyne low molar mass material was markedly present (see figure 4.4).

4.4.2 Molar mass characterisation of polymers synthesised by route B

GPC curves are shown in figures 4.12 to 4.21(pages 165-169) inclusively.

M_n , M_w and PDI values before and after reduction to account for the low molar mass tail are included in Table 4.3(pages 151-153).

M_n values by EGA before and after reduction to account for the low molar mass tail are included in Table 4.5(pages 156-158).

In the majority of cases from polymerisation route B GPC curves are atypically Gaussian in shape with a combination of low and high molar masses.

As mentioned in section 3.3.3 three factors were varied in the polymerisation reaction in an attempt to maximise the molar mass (M_n).

- (a) time
- (b) temperature
- (c) concentration — in all polymerisation systems the concentration was increased.

Figures 4.12 and 4.13 show GPC curves for polymer B1-poly(1,8-nonadiyne) synthesised at 60°C for 6 hours and polymer B2-poly(1,8-nonadiyne) synthesised at 60°C for 8 hours respectively.

Both GPC curves are atypically Gaussian in shape with a large distribution of molar masses. The low molar mass tail is most likely a consequence of linear oligomeric structures with the possibility of low molar mass cyclic structures present also. Polymer B1 has an M_n value of 12,356 and PDI of 4.69 whereas polymer B2 has an M_n value of 8,460 and PDI of 5.69. After curve idealisation an M_n value of 23,788 was obtained for polymer B1 and an M_n value of 20,978 was obtained for polymer B2 with both PDI values being close to 2. From these GPC results it would appear that the shorter polymerisation time of 6 hours at 60°C produces higher molar mass poly(1,8-nonadiyne) (see Table 4.3).

M_n values obtained by EGA before reduction to account for the low molar mass tail are 12,320 for polymer B1 and 8,544 for polymer

B2. These values are very close to the values obtained by GPC before curve idealisation (i.e. polymer B1 $M_n = 12,356$ and polymer B2 $M_n = 8,460$). However after reduction to account for the low molar mass tail M_n values obtained by EGA for polymer B1 and B2 are 10,400 and 7,433 respectively. Therefore these EGA results confirm that the shorter polymerisation time of 6 hours at 60°C does produce higher molar mass poly(1,8-nonadiyne) (see Table 4.5).

Figures 4.14 and 4.15 show GPC curves for polymer B3-poly(1,9-decadiyne) synthesised at 80°C for 6 hours and polymer B4-poly(1,9-decadiyne) synthesised at 80°C for 10 hours respectively.

Again both GPC curves are atypically Gaussian in shape with a large distribution of molar masses. The low molar mass tail is most likely to be a consequence of linear oligomeric structures with the possibility of low molar mass cyclic structures present also. Polymer B3 has an M_n value of 9,621 and PDI of 4.22 whereas polymer B4 has an M_n value of 7,660 and PDI of 3.24. After curve idealisation an M_n value of 23,343 was obtained for polymer B3 and an M_n value of 11,708 was obtained for polymer B4 with both PDI values being close to 2. From these GPC results it would appear that the shorter polymerisation of 6 hours at 80°C produces higher molar mass poly(1,9-decadiyne) (see Table 4.3).

M_n values obtained by EGA before reduction to account for the low molar mass tail are 11,000 for polymer B3 and 10,006 for polymer B4. After reduction to account for the low molar mass tail M_n values obtained by EGA for polymer B3 and B4 are 9,735 and 9,590 respectively. These EGA results confirm that the shorter

polymerisation time of 6 hours at 80°C does produce higher molar mass poly(1,9-decadiyne) (see Table 4.5).

Figures 4.16, 4.17 and 4.18 show GPC curves for polymer B5, B6 and B7 i.e. poly (1,9-decadiyne) synthesised for 15 hours at 40°C, 60°C and 80°C respectively.

Figure 4.16 shows a GPC curve which is essentially Gaussian in shape, but a low molar mass tail is evident. Polymer B5 has an Mn value of 16,700 and PDI of 3.86. Figure 4.17 shows a GPC curve which is Gaussian in shape but at very low molar masses. Polymer B6 has an Mn value of 3,266 and PDI of 1.66 i.e. the polymer is comprised of mainly low molar mass material. Figure 4.18 shows a GPC curve which is atypically Gaussian in shape with a large distribution of molar masses and a low molar mass tail very evident. Polymer B7 has an Mn value of 9,379 and PDI of 3.88. Therefore curve idealisation work was performed on polymer B5 and B7 only. After curve idealisation an Mn value of 26,877 was obtained for polymer B5 and an Mn value of 13,596 was obtained for polymer B7 with both PDI values being close to 2. From the GPC results the following conclusions were made for poly(1,9-decadiyne) polymerised for 15 hours;

(a) Low polymerisation temperatures (40°C) — Produces high Mn values with a low percentage of low molar mass material.

(b) Intermediate polymerisation temperatures (60°C) — Produces very low Mn values with essentially low molar material evenly distributed.

(c) High polymerisation temperatures (80°C) — Produces intermediate Mn values with a broad distribution of molar masses.

The low M_n value of 3,266 obtained by GPC on polymer B6 gave a correspondingly very high M_n value of 17,563 by EGA (see Table 4.5). This strongly suggests that a high percentage of low molar mass cyclics were formed during the polymerisation.

M_n values obtained by EGA before reduction to account for the low molar mass tail are 13,788 for polymer B5 and 10,290 for polymer B7. After reduction to account for the low molar mass tail M_n values obtained by EGA for polymer B5 and B7 are 13,300 and 9,585 respectively. These EGA results confirm that for the polymerisation time of 15 hours the lower polymerisation temperature of 40°C does produce higher molar mass poly(1,9-decadiyne) (see Table 4.5).

Figure 4.19 shows a GPC curve for polymer B8-poly(1,11-dodecadiyne) synthesised at 80°C for 8 hours.

The GPC curve is atypically Gaussian in shape with a large distribution of molar masses and a very evident low molar mass tail. Polymer B8 has an M_n value of 6,988 with PDI of 3.60. After curve idealisation an M_n value of 17,985 was obtained with PDI close to 2 (see Table 4.3). M_n values obtained by EGA before and after reduction to account for the low molar mass tail are 12,418 and 11,027 respectively.

Figure 4.20 shows a GPC curve for polymer B9-50:50 copolymer of 1,9-decadiyne:1,10-undecadiyne synthesised at 60°C for 8 hours.

The GPC curve is Gaussian in shape at high molar masses, however there is a significant low molar mass tail. Polymer B9 has an

Mn value of 17,290 with PDI of 2.85. After curve idealisation an Mn value of 23,565 was obtained with PDI close to 2 (see Table 4.3). Mn values obtained by EGA before and after reduction to account for the low molar mass tail are 14,453 and 13,884 respectively.

Figure 4.21 shows a GPC curve for polymer B10–80:20 copolymer of 1,9-decadiyne:1,11-dodecadiyne synthesised at 60°C for 8 hours.

The GPC curve is Gaussian in shape at low to intermediate molar masses. Polymer B10 has an Mn value of 5,900 with PDI of 2.15. As with polymer B6 no curve idealisation work by GPC or Mn reduction work to account for the low molar mass tail by EGA could be carried out. The low Mn value of 5,900 obtained by GPC on polymer B10 gave a correspondingly very high Mn value of 10,043 by EGA (see Table 4.5) again strongly suggesting that a high percentage of low molar mass cyclics were formed during the polymerisation.

The new corrected values for GPC and EGA for all polymers from polymerisation route B were compared with each other as described in 4.4.1. In the majority of cases the Mn values by GPC(corr) were a factor greater than Mn values by EGA(corr). In only two cases were the Mn values by GPC(corr) less than Mn values by EGA (corr), hence the multiplication factor F less than 1. These were polymer B6 and B10 where a Gaussian distribution of low molar mass material was obtained by GPC. Therefore, as already mentioned, no curve idealisation work by GPC or Mn reduction work to account for the low molar mass tail by EGA could be carried out. For the purpose of this work F values from polymer B6 and B10 were excluded as they

were not meaningful. Values for F were in the range 1.22 to 2.82. Since errors were bound to arise in the EGA calculation (see 4.4.1) an average value for the multiplication factor F was calculated from the eight values in Table 4.5. A value of 1.94 was obtained.

Polymers synthesised by both polymerisation routes A and B produce similar material at high molar mass. This was evident after curve idealisation work was performed on the majority of polymers produced by polymerisation route B.

Upon fabricating films by solution casting from a 1% weight/volume solution of methylene chloride it was found that films of polymers synthesised by polymerisation route A were of superior strength to films of polymers that were synthesised by polymerisation route B.

The next section of this chapter discusses the consequence of the low molar mass tail with reference to the cyclisation of α,ω -alkyldiynes.

4.4.3 Cyclisation of α,ω -alkyldiynes

It was proposed that the low molar mass tail which is present in the GPC curve for poly(1,8-nonadiyne) from polymerisation route A (see figure 4.4) and the majority of GPC curves from polymerisation route B was not only a consequence of oligomeric linear type structures, but also low molar mass cyclic structures formed during the course of the polymerisation.

Cyclic structures are greatly favoured using homogeneous, non-aqueous mildly basic conditions.⁷⁵ The effect of dilution has not been properly evaluated although it is anticipated that the smaller the concentration of the α,ω -alkyldiyne the less tendency there will be to form linear oligomeric or polymeric structures.

4.4.3.1 Previous oxidative coupling work on α,ω -alkyldiynes which cyclise

(A) Using cupric acetate/pyridine system.

High dilution systems will yield increased proportions of the smaller cyclic hydrocarbons.⁵⁰ Concentrations of $\sim 0.0035 \text{ mol dm}^{-3}$ used for tetradeca-1,13-diyne ($\text{HC}\equiv\text{C}-(\text{CH}_2)_{10}-\text{C}\equiv\text{CH}$) yields cyclic monomer and dimer in 17% and 30% yield respectively. The yield being improved when the dilution is higher.

Moderate concentration systems yield increased proportions of the higher cyclic hydrocarbons.^{75,83} Concentrations of ~ 0.075 to 0.13 mol dm^{-3} were used for monomers of the series $\text{HC}\equiv\text{C}-(\text{CH}_2)_n-\text{C}\equiv\text{CH}$ (where $n=2$ to 6). On oxidative coupling cyclic trimers, tetramers, pentamers, hexamers and heptamers were formed.

(B) Using cuprous chloride ($\text{Cu}^{\text{I}}\text{Cl}$) and oxidant.^{77,84-86} High concentration systems yield predominantly linear dimers and tetramers but in some instances cyclic dimers were formed. Concentrations of ~ 0.7 to 1.25 mol dm^{-3} were used for monomers of the series $\text{HC}\equiv\text{C}-(\text{CH}_2)_n-\text{C}\equiv\text{CH}$ (where $n=2$ to 6). On oxidative coupling it was found that as well as linear dimers and tetramers being formed, cyclic dimers were formed in the case of 1,6-heptadiyne, 1,7-octadiyne and 1,8-nonadiyne, but not in the case of 1,5-hexadiyne and 1,9-decadiyne.

From the above observations it is evident that cyclisation can occur in both dilute and concentrated medium for (A). It can also occur in a highly concentrated medium for (B) with the α,ω -alkyldiyne monomers 1,6-heptadiyne, 1,7-octadiyne, and 1,8-nonadiyne.

4.4.3.2 Oxidative coupling work on α,ω -alkyldiynes investigated in this study

In this study polymerisation route A and B both involve cuprous chloride/TMEDA and an oxidant, therefore comparisons can be made with (B) in section 4.4.3.1

As a basis for polymerisation route A work was carried out with reference to Butera's system.³¹ In the original study by Butera the α,ω -alkyldiyne concentration employed was $0.665 \text{ mol dm}^{-3}$. There were no reports of a low molar mass tail in the GPC curves for poly(1,6-heptadiyne), poly(1,8-nonadiyne) and poly(1,11-dodecadiyne).

The same α,ω -alkyldiyne concentration of $0.665 \text{ mol dm}^{-3}$ was employed for polymerisation route A in this present study, with a low molar mass tail being evident in the GPC curve of poly(1,8-nonadiyne).

As a basis for polymerisation route B work was carried out with reference to Kevelam's ²¹ and Knol's ²⁶ systems. In the original study by Kevelam the 1,8-nonadiyne concentration employed was 0.27 mol dm^{-3} . This was modified by Knol as the 1,8-nonadiyne concentration was decreased to $0.102 \text{ mol dm}^{-3}$. In both Kevelam's and Knol's study no GPC was performed therefore no low molar mass tail could be observed.

In this study the α,ω -alkyldiyne concentration was increased to 0.4 mol dm^{-3} for polymerisation route B, with a low molar mass tail being evident for the majority of polymers in their GPC curve.

The two concentrations of $0.665 \text{ mol dm}^{-3}$ and 0.40 mol dm^{-3} employed for the α,ω -alkyldiynes in polymerisation route A and B respectively lie close to the values employed for the concentration of the α,ω -alkyldiynes for (B) in section 4.4.3.1 (i.e. 0.7 to 1.25 mol dm^{-3}).
77,84-86

Further reasoning which favours cyclic structures of α,ω -alkyldiynes contributing to the low molar mass tail include;

(a) Values of M_n by EGA which are very high compared with their corresponding M_n value by GPC as already discussed in section 4.4.1 and 4.4.2 (As cyclic structures do not possess end group protons hence M_n value by EGA will be exaggerated).

(b) In the GPC curves the low molar mass tail elution peak values are ~ 1200 which can correspond to cyclic pentamer, hexamer and heptamer as the elution values of the α,ω -alkyldiynes monomers are ~ 200 .

(c) Mildly basic conditions promote cyclisation. (In polymerisation route B, the coordinating ligand TMEDA is present in excess).

(d) Moderate concentrations employed with the cupric acetate/pyridine system (~ 0.075 to 0.13 mol dm^{-3}) produced higher cyclics i.e. trimers, tetramers, pentamers, hexamers and heptamers of the α,ω -alkyldiynes 1,6-heptadiyne, 1,7-octadiyne, 1,8-nonadiyne and 1,9-decadiyne.^{75,83}

Although in this study systems involved cuprous chloride/TMEDA and oxidant the concentrations employed were also moderate i.e. $0.665 \text{ mol dm}^{-3}$ and 0.4 mol dm^{-3} for polymerisation route A and B respectively. Therefore it was possible that higher cyclics as mentioned above may have formed.

However reasoning for not favouring the cyclic structures contributing to the low molar mass tail must also be considered and are as follows;

(a) High dilution conditions are more likely to favour the formation of cyclic structures.⁵⁰ In a highly dilute system there will be less tendency to form linear structures as the chains will be vastly separated, and cyclise.

(b) Since the polymers consist of a small $(\text{CH}_2)_n$ unit ($n=4$ to 8) then the distance between the ends of monomer is small favouring oligomerisation/polymerisation.

(c) In the present polymerisation study it is sterically more favourable for linear structures to form. ⁸⁷

(d) Trial mass spectrometry runs on polymers from both polymerisation route A and B did not isolate any cyclic species, therefore were not conclusive.

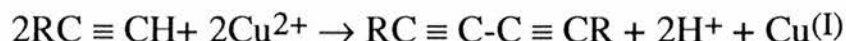
Although there is not any direct evidence to conclude that cyclic structures do or don't contribute to the low molar mass tail in the GPC curves, it can be argued that they are present on the basis of points (a) to (d) on pages 140-141.

Further examination of the low molar mass tail is required to fully establish whether or not cyclic structures were present. If time had permitted and the facilities were at hand a useful analytical tool would have been preparative GPC. An example of this technique was described by Dodgson and workers ⁸⁸ who separated broad fractions of cyclic and linear poly(dimethylsiloxanes).

4.4.4 Mechanism of oxidative coupling of polymerisation routes A and B

From chapter 3 (3.2) several points were concluded about the mechanism of the oxidative coupling reaction for terminal alkynes;

- (a) The cupric ion (copper II) is the actual oxidant **50,72,73**



the Cu(I) can then oxidise back to Cu(II) for further coupling.



(b) Under acidic conditions the reaction rate increases with increasing Cu(I) conc. **50,72,73**

(c) The greater the acidity of the terminal alkyne the faster the reaction rate. **50,73**

(d) The reaction is second order with respect to the concentration of the alkyne. **72,73**

(e) A bridged dimeric structure was isolated for the catalyst complex — confirmed by x-ray diffraction studies, and consistent with detailed mechanistic studies. **21,50,72,73,81**

The mechanism is straightforward for coupling of a monofunctional terminal alkyne to a diacetylene e.g. phenylacetylene oxidatively coupled by Hay.⁷⁴ However oxidative coupling of a difunctional terminal alkyne to a linear polymer is more complicated and needs further elaboration.

The next section summarises results and findings from previous oxidative polymerisation studies on poly(1,8-nonadiyne) by Kevelam and Knol, and this present study involving oxidative polymerisation

route A and B. A mechanism for the oxidative polymerisation of the α,ω -alkyldiynes is then proposed.

(1) Increasing the basicity of ligand i.e. TEA>TMEDA>py and ligand concentration increases the reaction rate.^{21,74}

(2) On increasing the polymerisation temperature from 26 to 65°C (i.e. Kevelam's and Knol's work) and decreasing the concentration of the α,ω -alkyldiyne a corresponding increase in reaction rate and molar mass were achieved.

(3) On increasing the polymerisation temperature from 60–80°C in route A an optimum polymerisation temperature of 65°C was established for poly(1,9-decadiyne) (M_n value of 29,300 was achieved).

(4) On increasing the polymerisation temperature from 40–80°C in route B for poly(1,9-decadiyne) the M_n values go through a minimum.

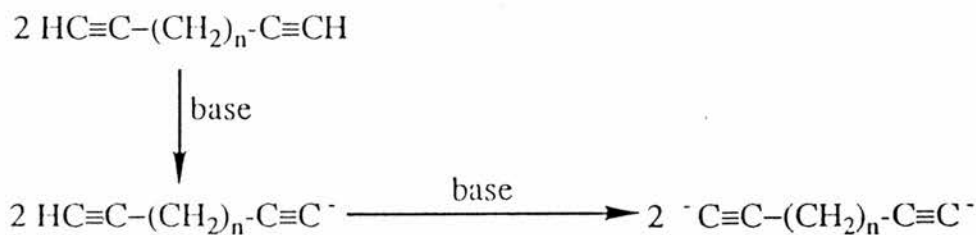
(5) On increasing the time for polymerisation for both monomers 1,8-nonadiyne and 1,9-decadiyne there is a corresponding decrease in molar mass (M_n).

As mentioned in chapter 3 (3.3.3) there were three main differences between polymerisation routes A and B ; 1) Polymerisation delay time 2) $\text{Cu}(\text{I})\text{Cl}:\text{TMEDA}$ ratio, and 3) Solvent system employed.

In polymerisation route A the $\text{Cu}(\text{I})\text{Cl}:\text{TMEDA}$ ratio is 1:1 with pyridine controlling the basicity of the reaction medium. In polymerisation route B the $\text{Cu}(\text{I})\text{Cl}:\text{TMEDA}$ ratio is 1:50 with no pyridine solvent present , therefore the excess TMEDA controls the basicity of the reaction medium. In route A the pyridine solvent is present in 13 molar equivalents greater than the $\text{Cu}(\text{I})\text{Cl}$ and TMEDA molar equivalents. In route B the TMEDA is in excess by 49 molar equivalents. Kevelam has shown that the reaction rate for oxidative

coupling increases with increasing ligand concentration and increased basicity of ligand. ²¹ Pyridine has a pK_b of 8.75 ⁸⁹ and TMEDA has a pK_b of 4.9. ⁹⁰ Therefore, since TMEDA is present in 3-4 times greater amount than pyridine and it is more basic than pyridine, the rate of oxidative coupling for polymerisation route B will be faster than for polymerisation route A. The solubility of the bridged dimeric catalytic complex decreases with increasing TMEDA concentration causing a maximum reaction rate. ²¹ Also, the more basic the ligand the more it will facilitate the entrance of the acetylenic end group in the bridged dimeric catalytic complex.

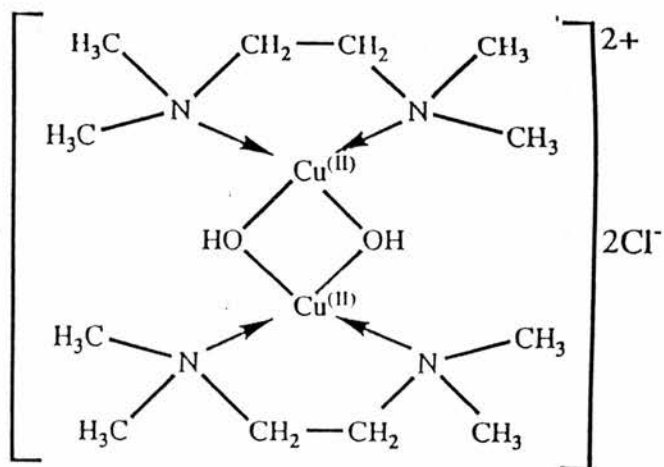
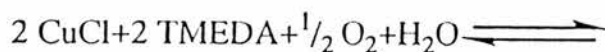
However, more importantly since there is a greater concentration of base in polymerisation route B it is conceivable that the two end group protons could be removed from an α,ω -alkyldiyne monomer, dimer, trimer, tetramer, pentamer, etc giving a doubly negatively charged terminal diacetylene, i.e for the case of the α,ω -alkyldiyne monomer;



When there is a high concentration of these doubly negatively charged terminal diacetylenes present there will be a high probability that two of these will coordinate like bidentate ligands to the bridged dimeric catalytic complex, then on intramolecular oxidative coupling a cyclised product will form. However, as the reaction proceeds to higher molar mass polymer then cyclisation will be less of a problem as linear polymerisation is more sterically favourable.⁸⁷

A mechanism for the polymerisation of the α,ω -alkyldiynes to give both linear and cyclic structures is shown overleaf.

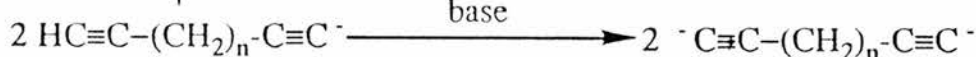
Mechanism



The above structure = [complex]



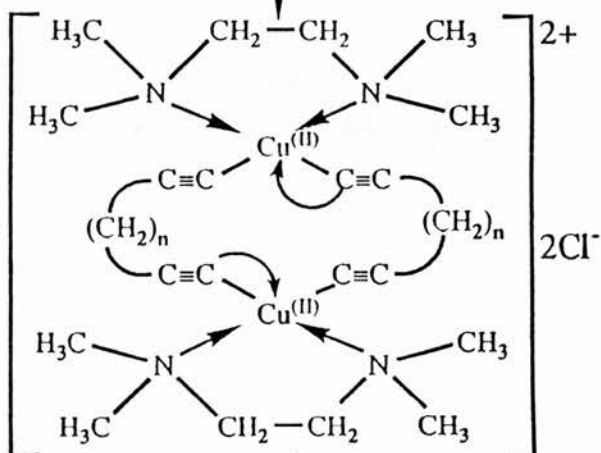
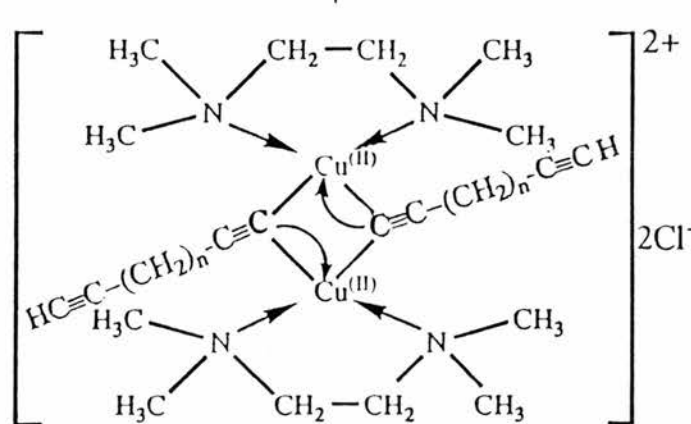
base



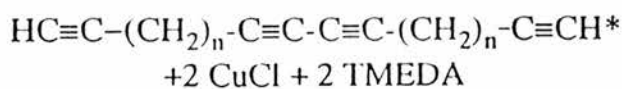
(The dianions act as bidentate ligands)

Linear route [complex]

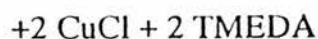
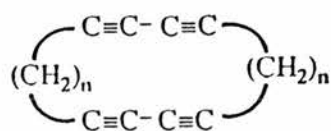
[complex] Cyclic route



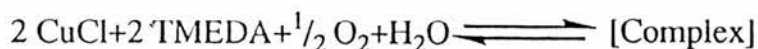
Intramolecular oxidative transfer occurs after electron transfer to the cupric ions



continued on p 147



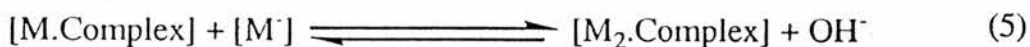
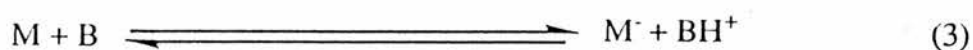
Then the catalytic complex reforms;



* This structure can continue to polymerise linearly or cyclise.

The above mechanism can also be explained for both linear and cyclic routes by the way of kinetic expressions.

Linear route



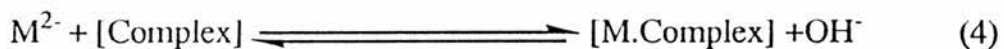
then the catalytic complex reforms i.e ;



and steps (3) to(6) repeat themselves.

Cyclic route

(1) and (2) as above



then the catalytic complex reforms as above.

L=ligand , M=monomer , B=base , D=dimer , CD=cyclic dimer

Polymer Chemist	poly(α,ω -alkyldiynes) synthesised	Technique used for Molar mass characterisation	Molar mass characteristics
Kevelam	poly(1,8-nonadiyne)	Vapour pressure osmometry measured in benzene or chloroform solution at 37°C	Mn values in the region of 2000 to 6000 were obtained
Knol	poly(1,8-nonadiyne)	1) Vapour pressure osmometry (as above) 2) Membrane osmometry measured in a chloroform solution at 27°C	1) Mn values of up to 5000 were obtained 2) Mn values in the region of 15,000 to 20,000 were obtained
Butera	poly(1,6-heptadiyne) poly(1,8-nonadiyne) poly(1,11-dodecadiyne)	Gel Permeation Chromatography in tetrahydrofuran at 40°C	Mn values of up to 20,000 Mn values of up to 40,000 Polydispersity almost ideal for all polymers (i.e., $M_w/M_n \approx 2$)

Table 4.1 Techniques used for molar mass characterisation of poly(α,ω -alkyldiynes)

polymer and conditions	Mn	Mw	PDI	After curve idealisation		
				Mn	Mw	PDI
A2)poly(1,8-nonadiyne)*	5,890	37,500	6.37	27,600	45,704	1.65
A3)poly(1,9-decadiyne)#	20,900	46,500	2.22	20,900	46,500	2.22
A4)poly(1,9-decadiyne) §	19,600	45,600	2.33	19,600	45,600	2.33
A5)poly(1,9-decadiyne)*	29,300	180,000	6.14	29,300	180,000	6.14
A6)50:50 poly(1,8-non):poly(1,9-dec)*	24,100	73,900	3.07	24,100	73,900	3.07
A7)poly(1,10-undecadiyne)*	28,300	59,200	2.09	28,300	59,200	2.09

Table 4.2 GPC molar mass characteristics of polymers produced by route A(continued.....)

polymer and conditions	Mn	Mw	PDI	After curve idealisation		
				Mn	Mw	PDI
A8)50:50 poly(1,9- dec):poly(1,- 10-undec)*	28,300	59,600	2.11	28,300	59,600	2.11
A9)poly (1,11-dode- cadiyne)*	14,100	32,100	2.28	14,100	32,100	2.28

N.B. Every reaction has an overnight polymerisation delay time at room temperature

* = 5 hrs @ 65°C, # = 5 hrs @ 60°C, § = 5 hrs @ 80°C

Table 4.2 GPC molar mass characteristics of polymers produced by route A

polymer and conditions	Mn	Mw	PDI	Mn After curve idealisation	Mw After curve idealisation	PDI
B1)poly(1,8-nonadiyne) 6 hrs @ 60°C	12,536	58,742	4.69	23,788	55,711	2.34
B2)poly(1,8-nonadiyne) 8 hrs @ 60°C	8,460	48,100	5.69	20,978	46,918	2.24
B3)poly(1,9-decadiyne) 6 hrs @ 80°C	9,621	40,604	4.22	23,343	44,236	1.90
B4)poly(1,9-decadiyne)10 hrs @ 80°C	7,660	24,802	3.24	11,708	26,719	2.28

Table 4.3 GPC molar mass characteristics of polymers synthesised by route B (continued.....)

polymer and conditions	Mn	Mw	PDI	Mn After curve idealisation	Mw	PDI
B5)poly(1,9-decadiyne)15 hrs @ 40°C	16,700	64,400	3.86	26,877	55,696	2.10
B6)poly(1,9-decadiyne)15 hrs @ 60°C	3,266	5,435	1.66	3,266	5,435	1.66
B7)poly(1,9-decadiyne)15 hrs @ 80°C	9,379	36,421	3.88	13,596	37,637	2.77
B8)poly(1,11-dodecadiyne) 8 hrs @ 80°C	6,998	25,160	3.60	17,985	28,786	1.60

Table 4.3 GPC molar mass characteristics of polymers synthesised by route B (continued.....)

polymer and conditions	Mn	Mw	PDI	Mn After curve idealisation	Mw After curve idealisation	PDI
B9)50:50 poly(1,9-dec) :poly(1,10- undec) 8 hrs @ 60°C	17,290	49,299	2.85	23,565	45,641	1.94
B10)80:20 poly(1,9-dec) :poly(1,11- dodec) 8 hrs @ 60°C	5,900	12,703	2.15	5,900	12,703	2.15

Table 4.3 GPC molar mass characteristics of polymers synthesised by route B

polymer and conditions	Mn by EGA	Mn by EGA (CORR)	Mn by GPC	Mn by GPC (CORR)	$F = \left(\frac{\text{Mn by GPC(CORR)}}{\text{Mn by EGA(CORR)}} \right)$
A2)poly(1,8-nonadiyne)*	15,000	12,000	5,890	27,600	2.30
A3)poly(1,9-decadiyne)#	13,625	13,625	20,900	20,900	1.54
A4)poly(1,9-decadiyne)§	12,380	12,380	19,600	19,600	1.58
A5)poly(1,9-decadiyne)*	10,520	10,520	29,300	29,300	2.79
A6)50:50 poly(1,8-non):poly(1,9-dec)*	15,757	15,757	24,100	24,100	1.53
A7)poly(1,10-undecadiyne)*	19,600	19,600	28,300	28,300	1.44

Table 4.4. Mn values by EGA before and after reduction to account for low the molar mass tail and Mn values by GPC before and after curve idealisation for polymers produced by route A(continued.....)

polymer and conditions	Mn by EGA	Mn by EGA (CORR)	Mn by GPC	Mn by GPC (CORR)	$F = \left(\frac{\text{Mn by GPC(CORR)}}{\text{Mn by EGA(CORR)}} \right)$
A8)50:50 poly(1,9-dec):poly(1,10-undec)*	14,362	14,362	28,300	28,300	1.97
A9)poly(1,11-dodeca-diyne)*	12,454	12,454	14,100	14,100	1.13

N.B Every reaction has an overnight polymerisation delay time at room temperature.

* = 5hrs @ 65°C, # = 5hrs @ 60°C, § = 5hrs @ 80°C

Table 4.4. Mn values by EGA before and after reduction to account for the low molar mass tail and Mn values by GPC before and after curve idealisation for polymers produced by route A

polymer and conditions	Mn by EGA	Mn by EGA (CORR)	Mn by GPC	Mn by GPC (CORR)	$\bar{P} = \left(\frac{M_n \text{ by GPC (CORR)}}{M_n \text{ by EGA (CORR)}} \right)$
B1)poly(1,8-nonadiyne)-6hrs@60°C	12,320	10,400	12,536	23,788	2.29
B2)poly(1,8-nonadiyne)-8hrs@60°C	8,544	7,433	8,460	20,978	2.82
B3)poly(1,9-decadiyne)-6hrs@80°C	11,000	9,735	9,621	23,343	2.40
B4)poly(1,9-decadiyne)-10hrs@80°C	10,006	9,590	7,660	11,708	1.22
B5)poly(1,9-decadiyne)-15hrs@40°C	13,788	13,300	16,700	26,877	2.02

Table 4.5 Mn values by EGA before and after reduction to account for the low molar mass tail and Mn values by GPC before and after curve idealisation for polymers produced by route B(continued.....)

polymer and conditions	Mn by EGA	Mn by EGA (CORR)	Mn by GPC	Mn by GPC (CORR)	$F = \left(\frac{M_n \text{ by GPC (CORR)}}{M_n \text{ by EGA (CORR)}} \right)$
B6)poly(1,9-decadiyne)-15hrs@60°C	17,563	17,563	3,266	3,266	0.19*
B7)poly(1,9-decadiyne)-15hrs@80°C	10,290	9,585	9,385	13,596	1.41
B8)poly(1,11-dodecadiyne)-8hrs@80°C	12,418	11,027	6,998	17,985	1.63
B9)50:50-poly(1,9-dec):poly-(1,10-undec)-8hrs@60°C	14,453	13,884	17,290	23,565	1.70

Table 4.5 Mn values by EGA before and after reduction to account for the low molar mass tail and Mn values by GPC before and after curve idealisation for polymers produced by route B(continued.....)

Polymer and conditions	Mn by EGA	Mn by EGA (CORR)	Mn by GPC	Mn by GPC (CORR)	$F = \left(\frac{\text{Mn by GPC(CORR)}}{\text{Mn by EGA(CORR)}} \right)$
B10)80:20 poly(1,9-dec):poly-(1,11-dodec)-8hrs@60°C	10,043	10,043	5,900	5,900	0.59*

*These two values for F were excluded in my study (see section 4.4.2)

Table 4.5 Mn values by E.G.A before and after reduction to account for the low molar mass tail and Mn values by GPC before and after curve idealisation for polymers produced by route B

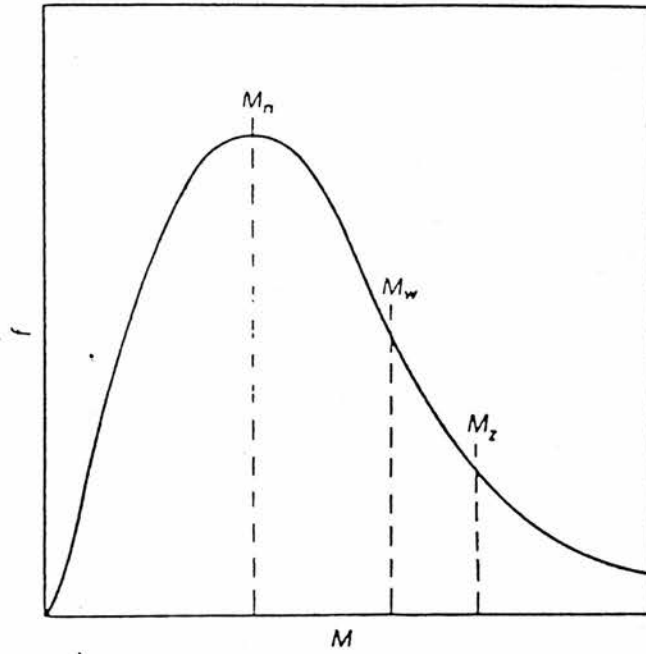


Figure 4.1 Typical distribution of molar masses for a synthetic polymer sample, where f is the fraction of polymer in each interval of M considered.

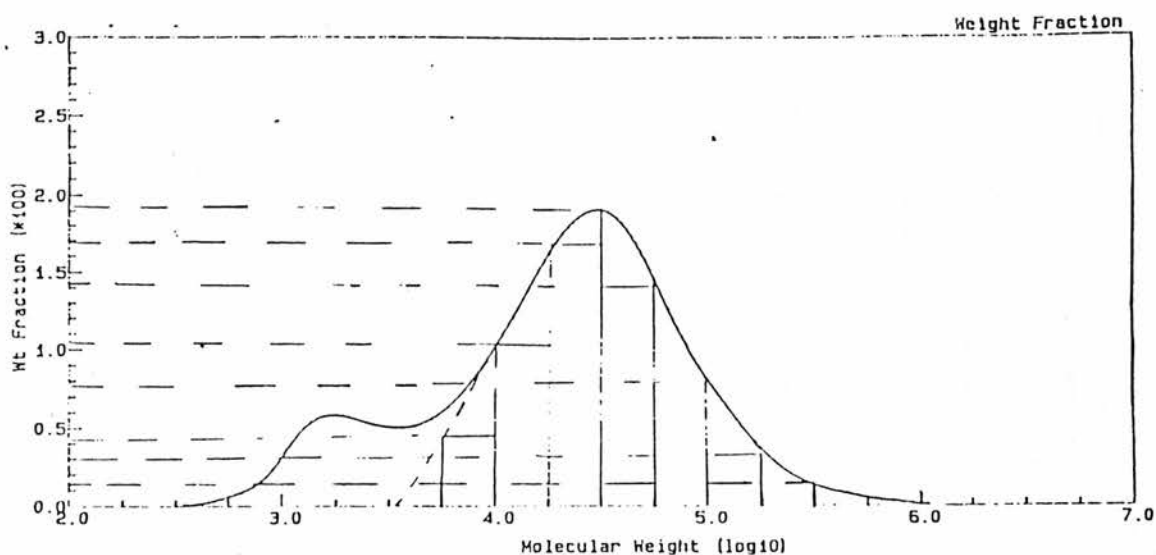


Figure 4.2 GPC curve of polymer B2-poly(1,8-nonadiyne) - synthesised by polymerisation route B for 8 hours @ 60°C - a corrected curve for curve idealisation work.

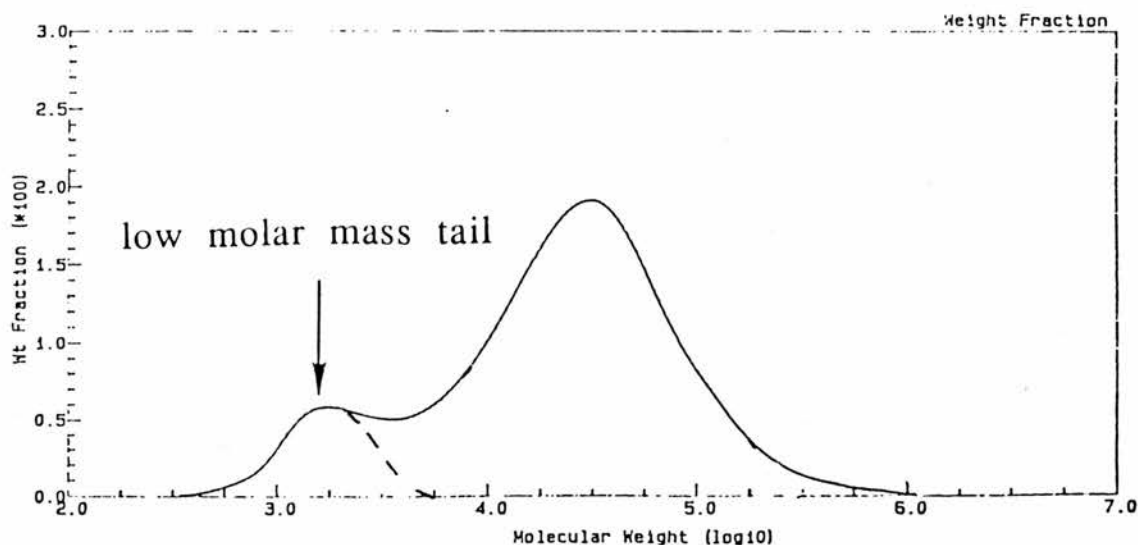


Figure 4.3 GPC curve of polymer B2-poly(1,8-nonadiyne) - synthesised by polymerisation route B for 8 hours @ 60°C - a corrected curve to account for the low molar mass tail in Mn reduction calculations for end group analysis(EGA).

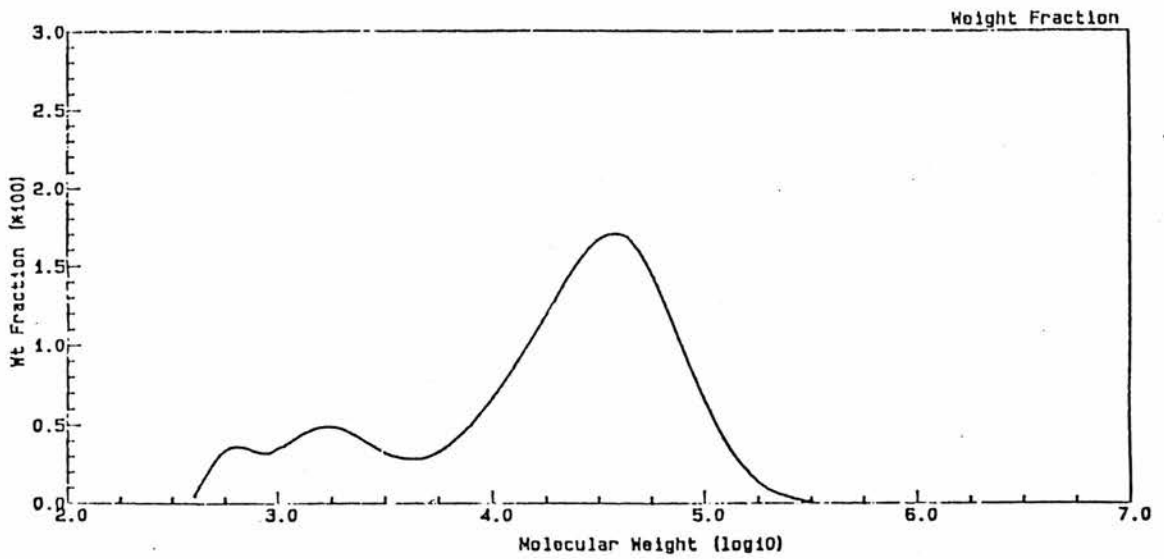


Figure 4.4 GPC curve of polymer A2-poly(1,8-nonadiyne) 5 hours @ 65°C.

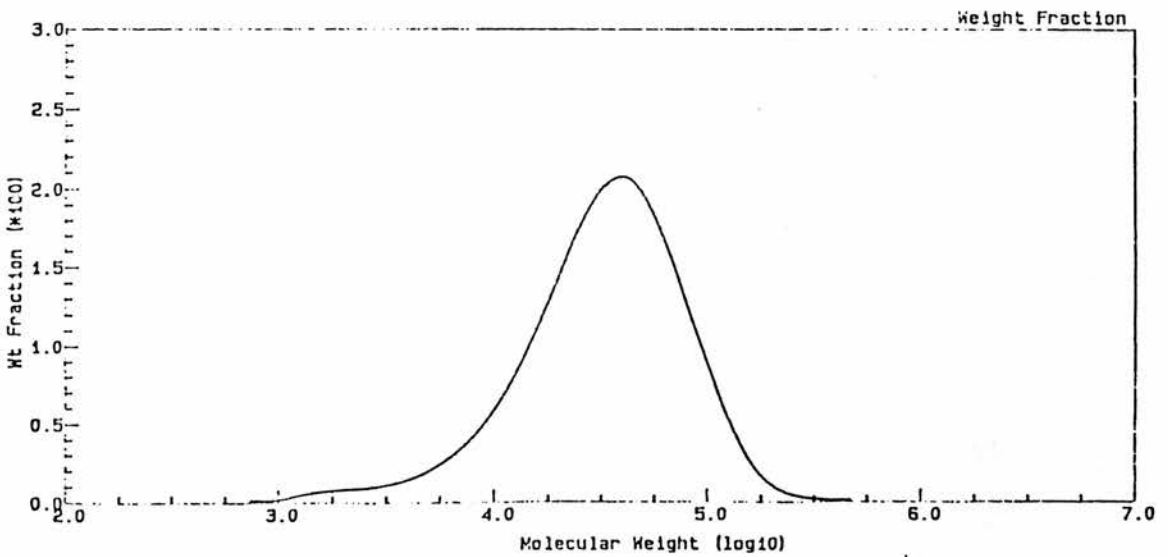


Figure 4.5 GPC curve of polymer A3-poly(1,9-decadiyne) 5 hours @ 60°C.

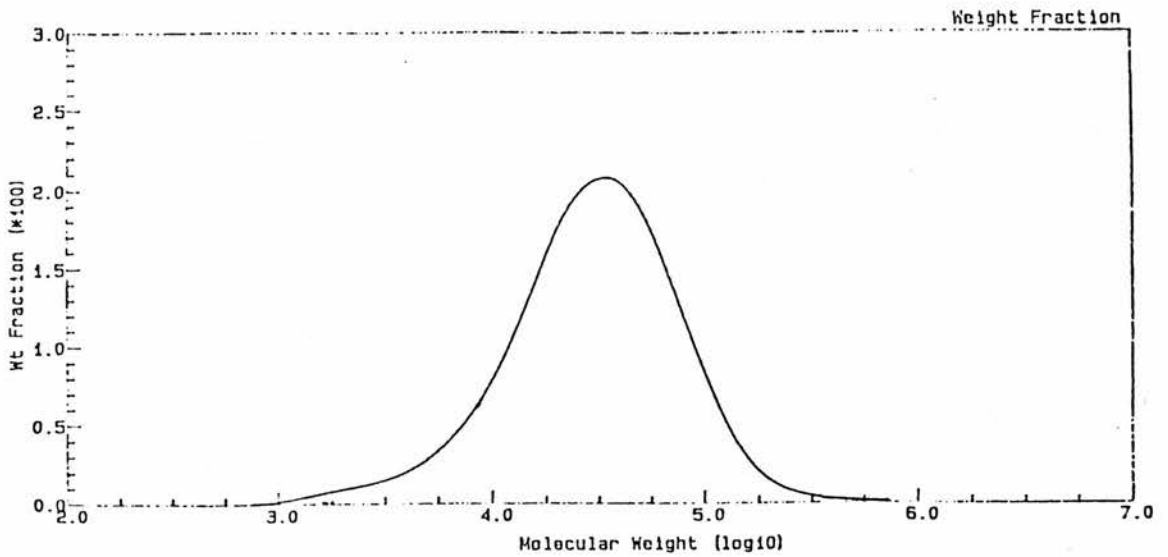


Figure 4.6 GPC curve of polymer A4-poly(1,9-decadiyne) 5 hours @ 80°C.

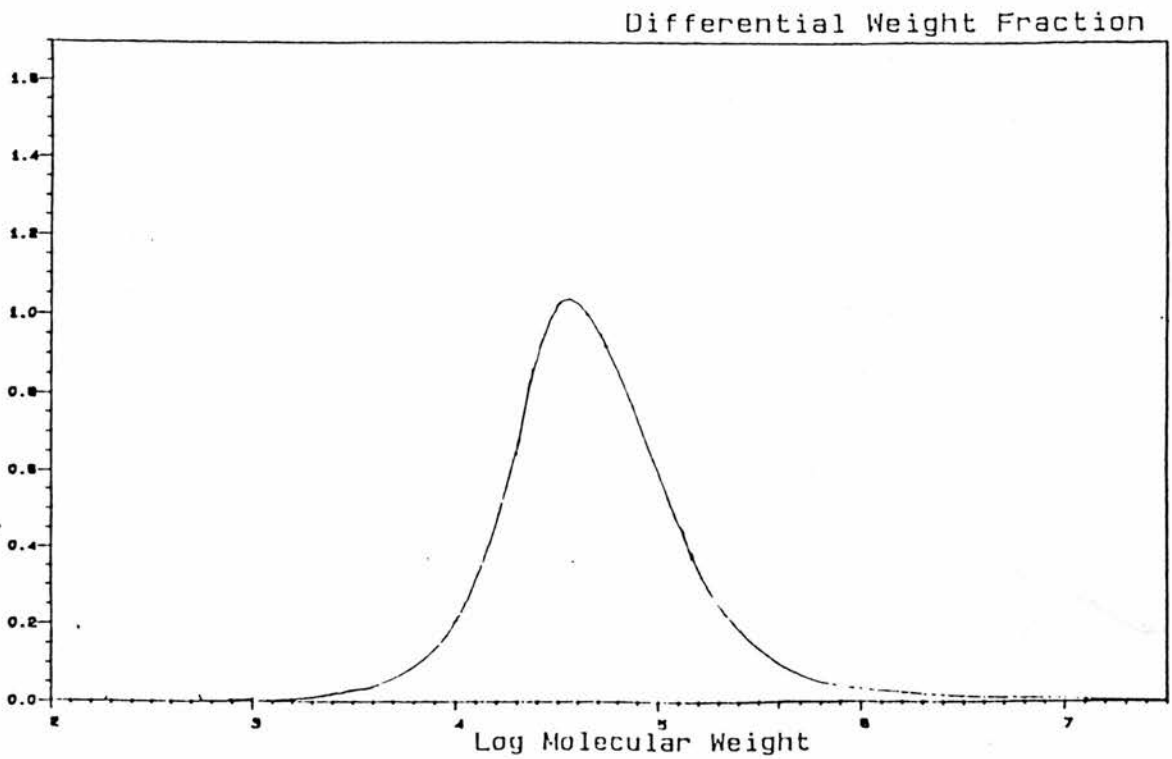


Figure 4.7 GPC curve of polymer A5-poly(1,9-decadiyne) 5 hours @ 65°C.

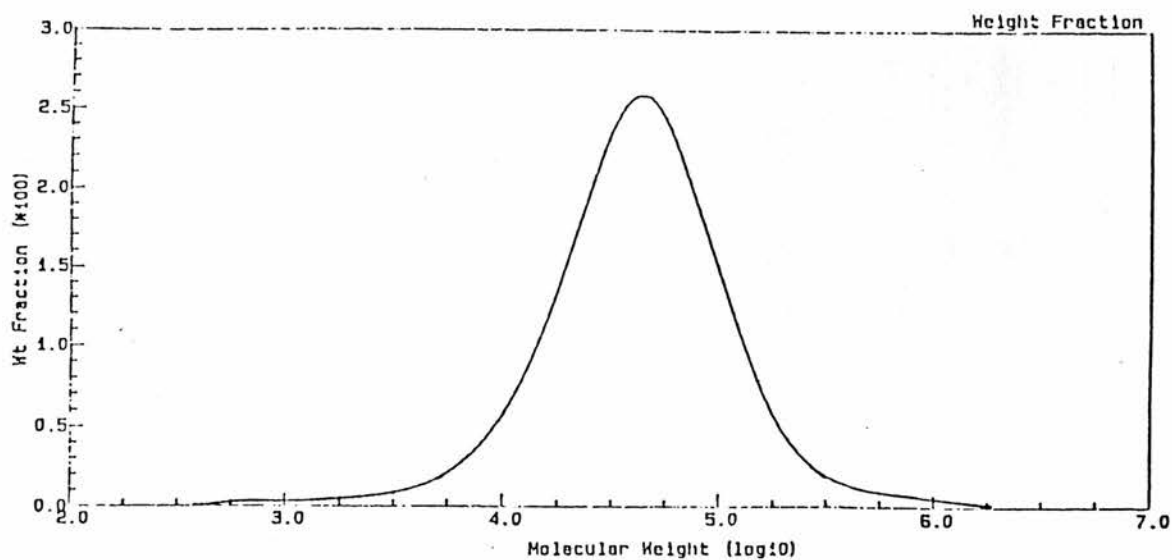


Figure 4.8 GPC curve of polymer A6 - 50:50 poly(1,8-non) : poly(1,9-dec) 5 hours @ 65°C.

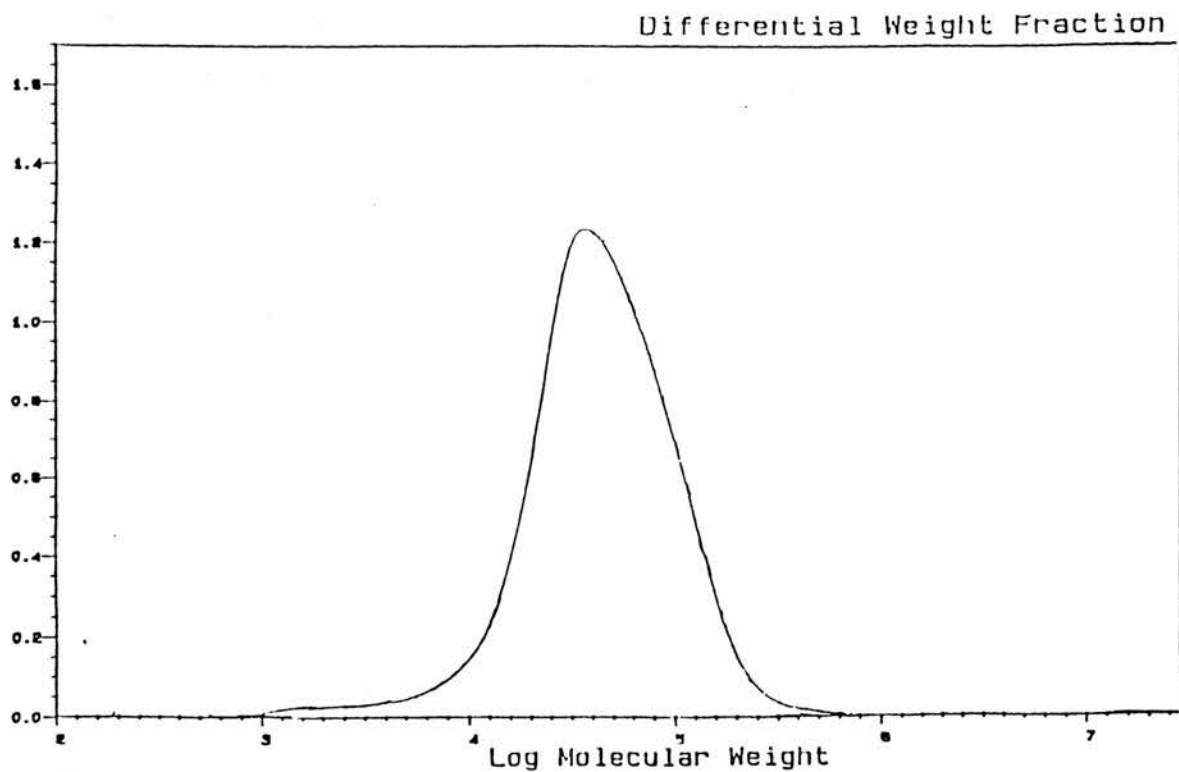


Figure 4.9 GPC curve of polymer A7-poly(1,10-undecadiyne) 5 hours @ 65°C.

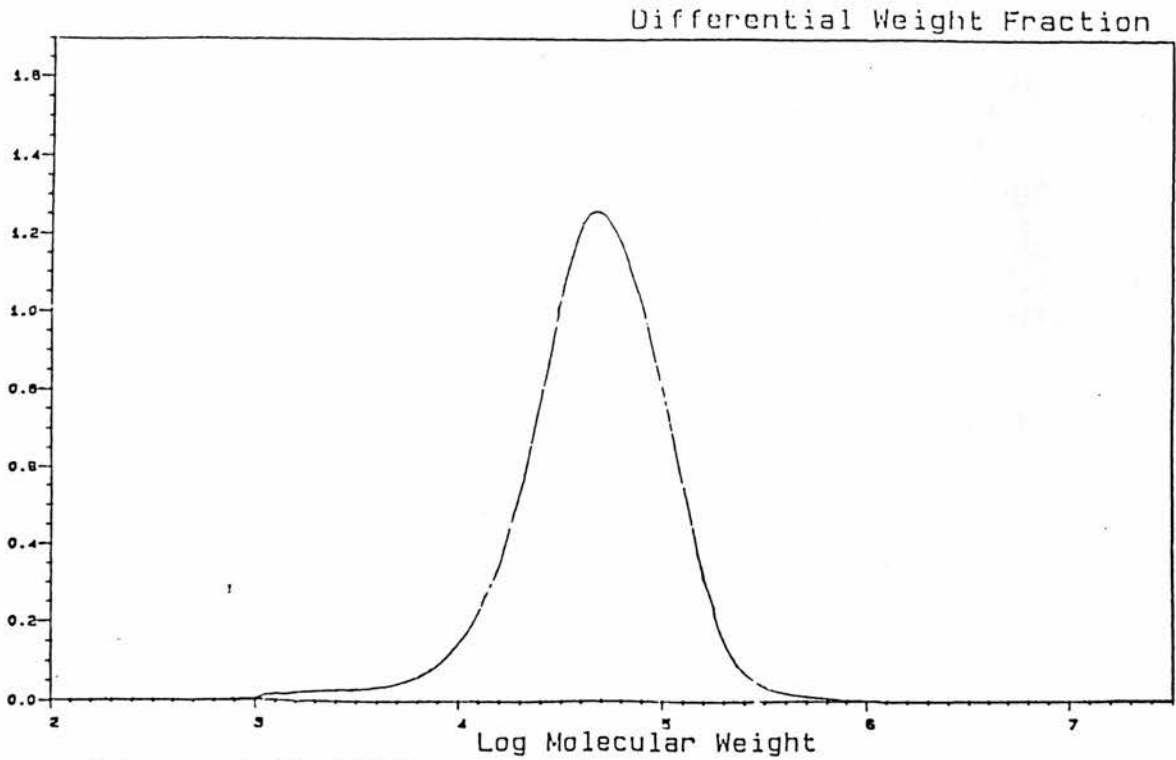


Figure 4.10 GPC curve of polymer A8 - 50:50 poly(1,9-dec):poly(1,10-undec) 5 hours @ 65°C.

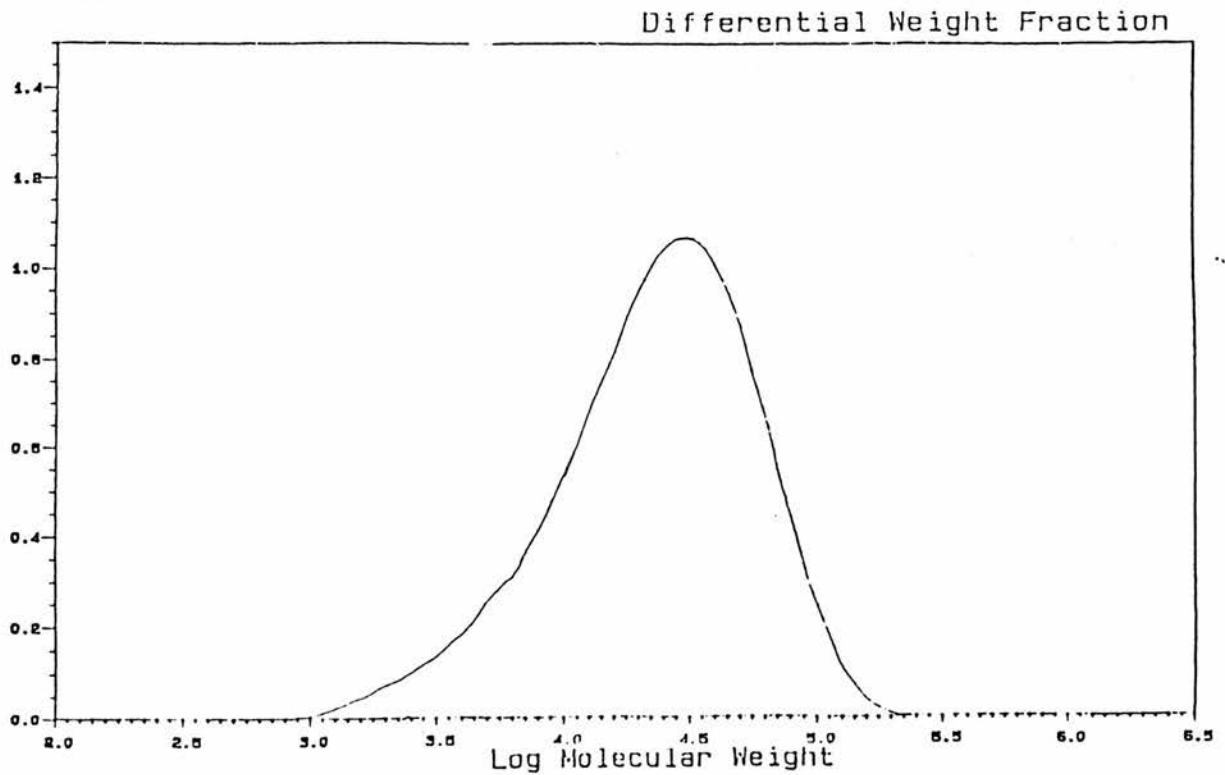


Figure 4.11 GPC curve of polymer A9-poly(1,11-dodecadiyne) 5 hours @ 65°C.

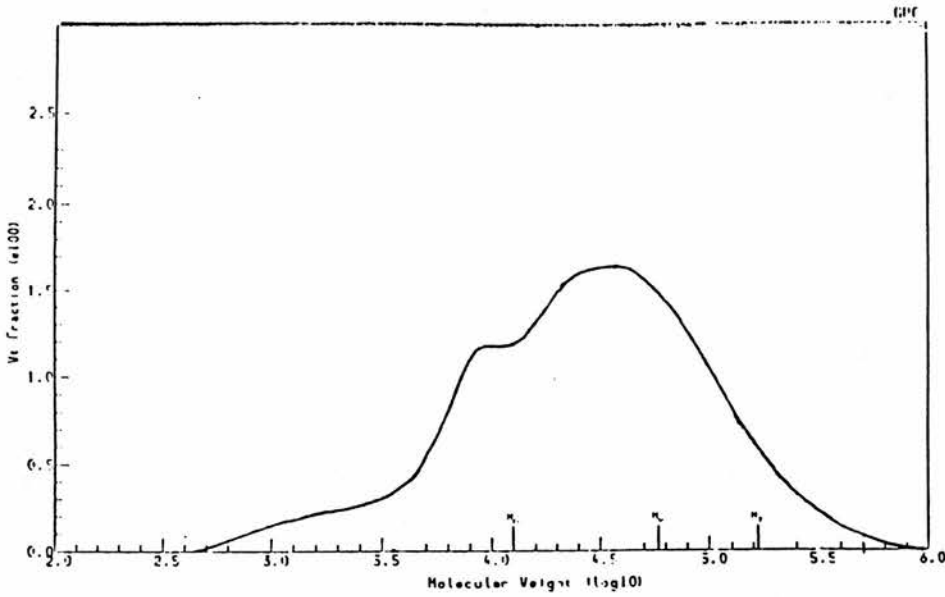


Figure 4.12 GPC curve of polymer B1-poly(1,8-nonadiyne) 6 hours @ 60°C.

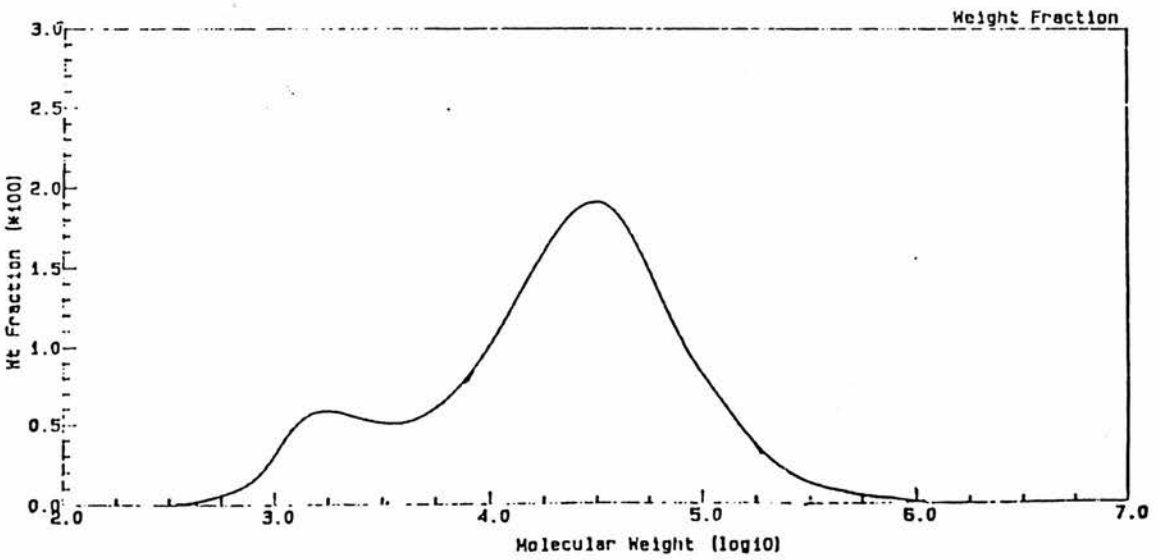


Figure 4.13 GPC curve of polymer B2-poly(1,8-nonadiyne) 8 hours @ 60°C.

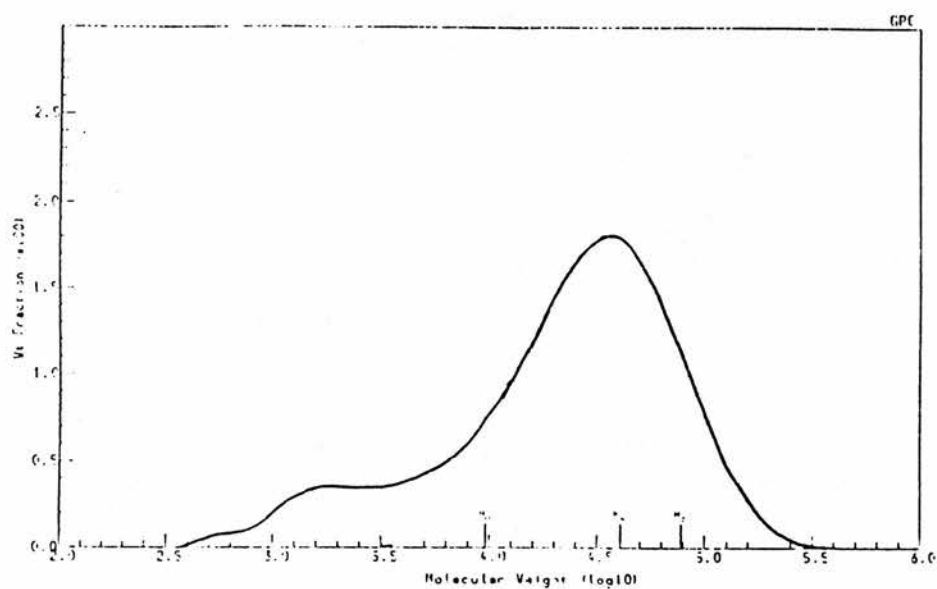


Figure 4.14 GPC curve of polymer B3-poly(1,9-decadiyne) 6 hours @ 80°C.

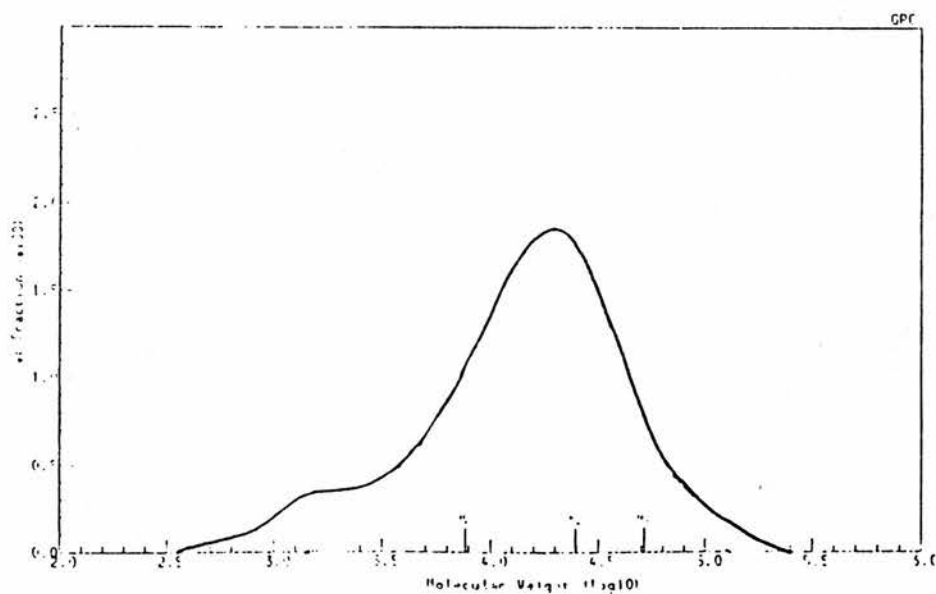


Figure 4.15 GPC curve of polymer B4-poly(1,9-decadiyne) 10 hours @ 80°C.

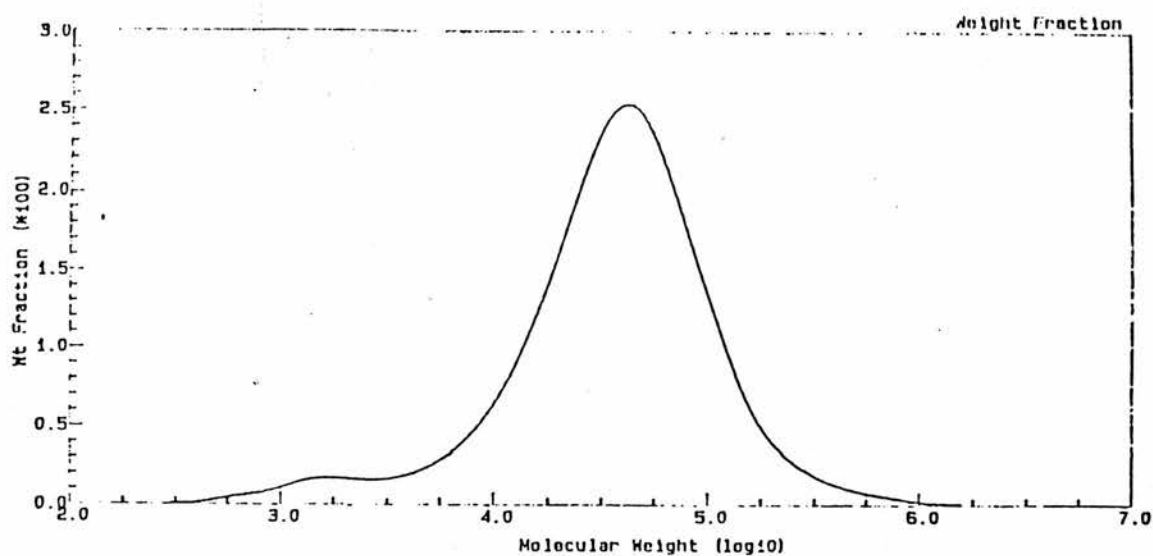


Figure 4.16 GPC curve of polymer B5-poly(1,9-decadiyne) 15 hours @ 40°C.

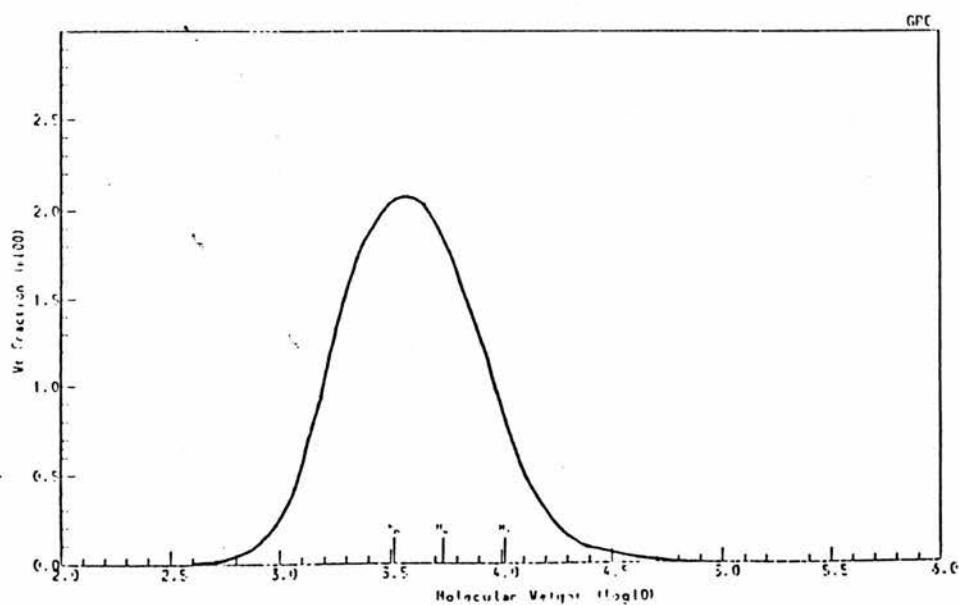


Figure 4.17 GPC curve of polymer B6-poly(1,9-decadiyne) 15 hours @ 60°C.

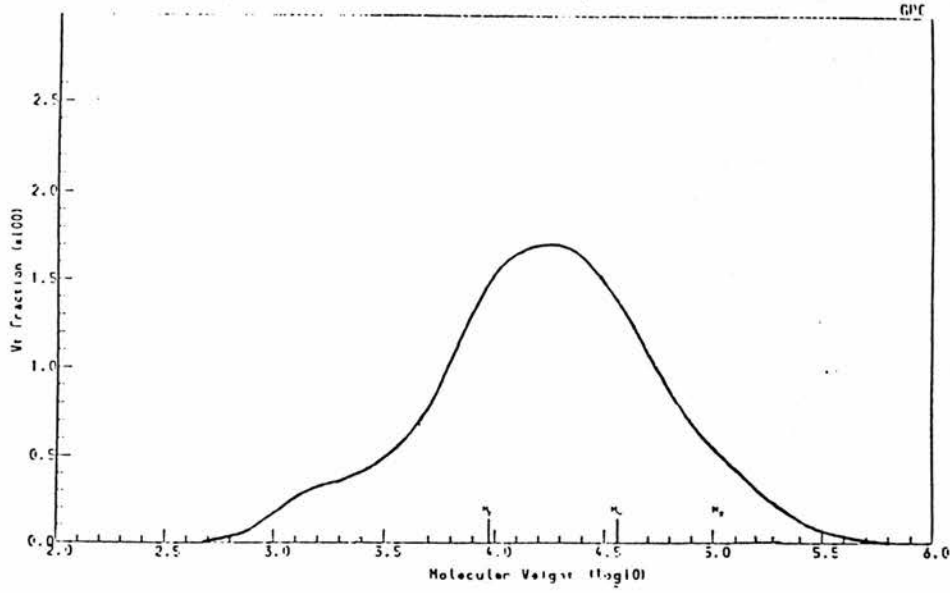


Figure 4.18 GPC curve of polymer B7-poly(1,9-decadiyne) 15 hours @ 80°C.

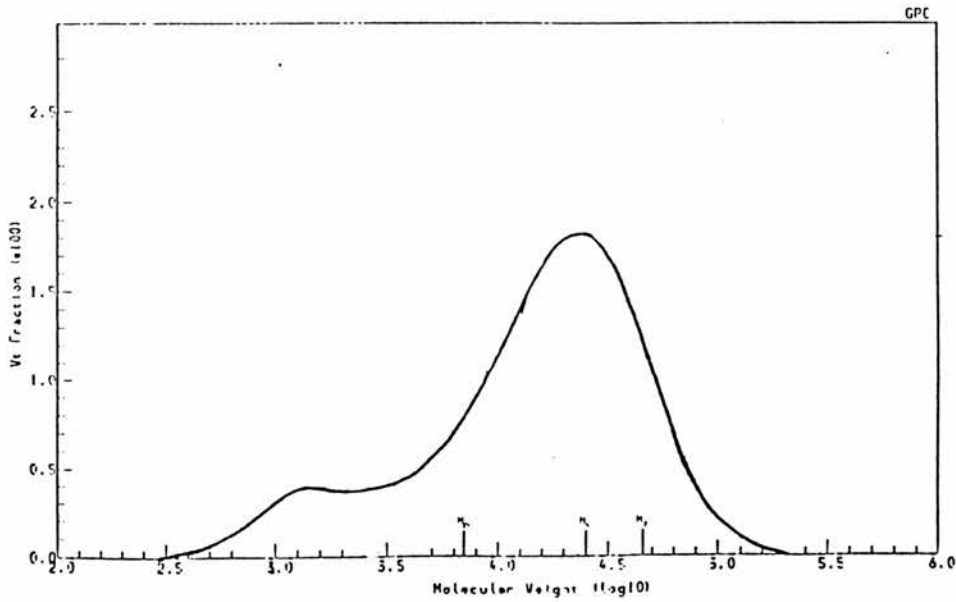


Figure 4.19 GPC curve of polymer B8-poly(1,11-dodecadiyne) 8 hours @ 60°C.

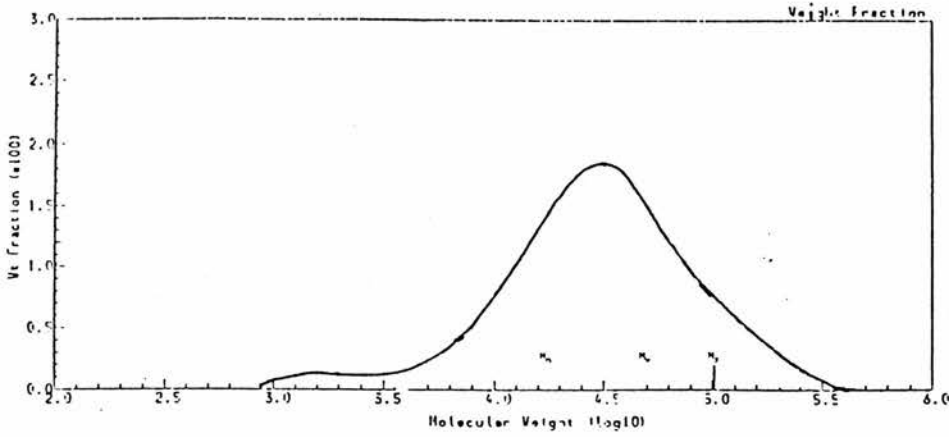


Figure 4.20 GPC curve of polymer B9-50:50 poly(1,9-dec):poly(1,10-undec) 8 hours @ 60°C.

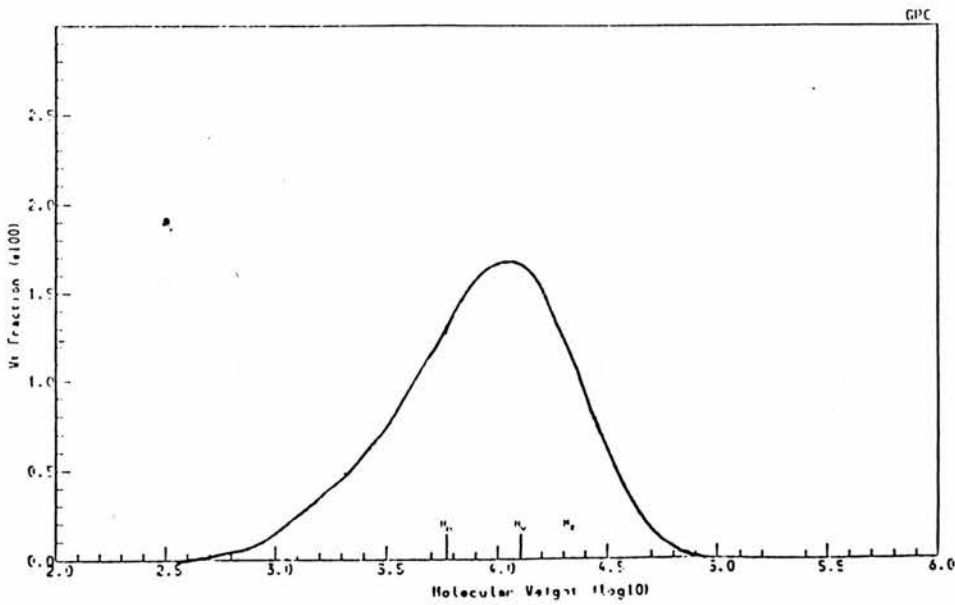


Figure 4.21 GPC curve of polymer B10-80:20 poly(1,9-dec):poly(1,11-dodec) 8 hours @ 60°C.

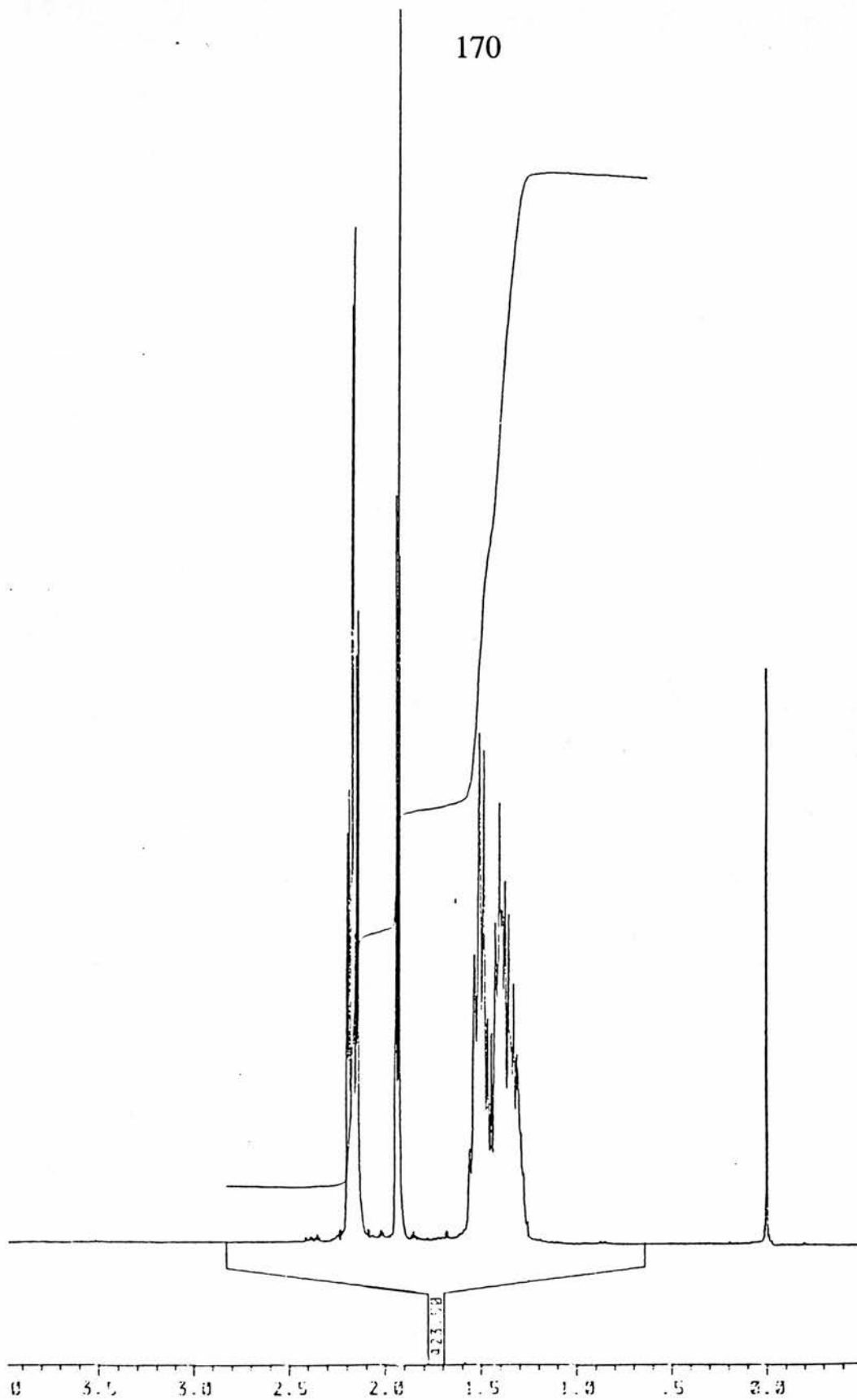


Figure 4.22 ^1H Nmr spectrum of 1,10-undecadiyne.

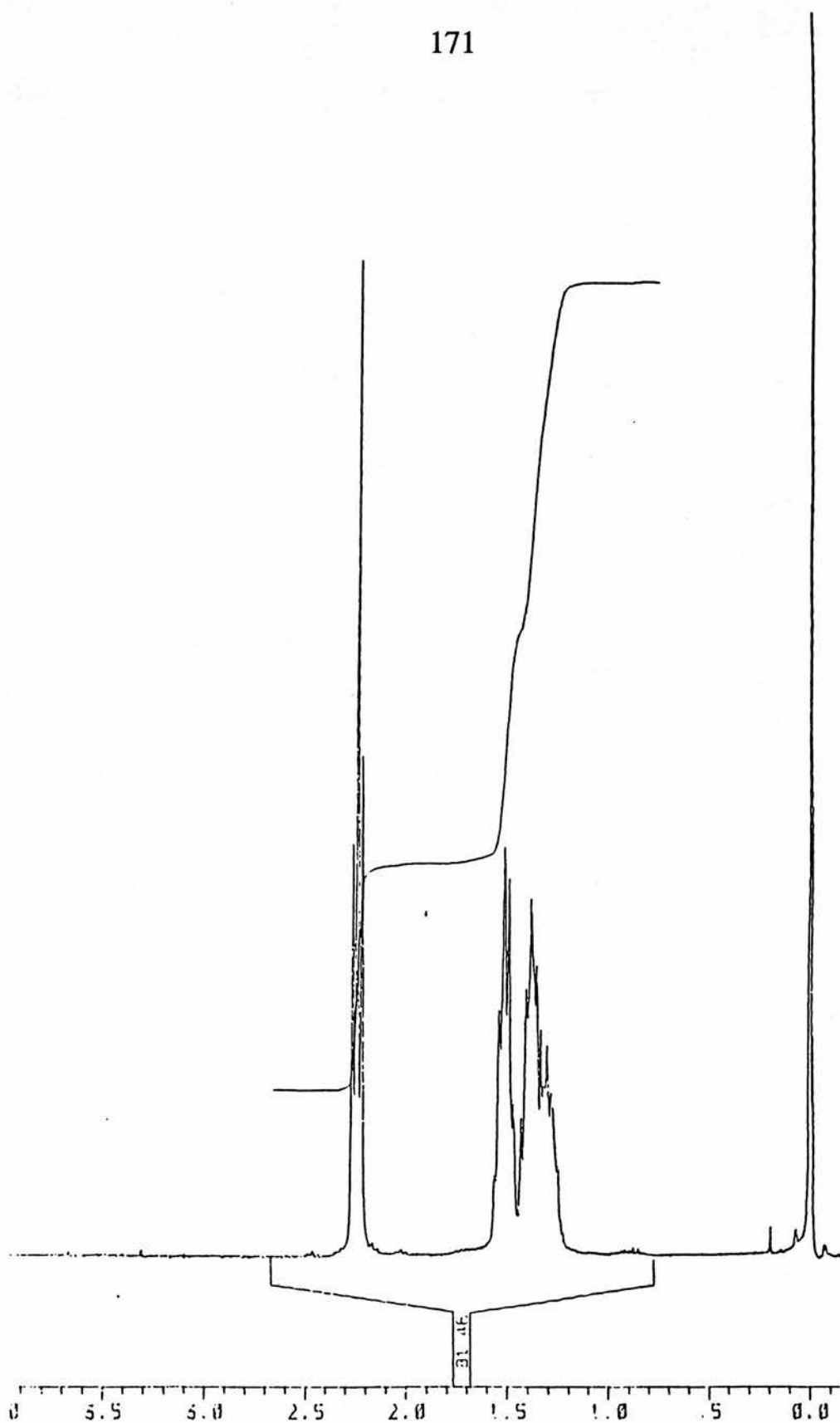


Figure 4.23 ^1H NMR spectrum of poly(1,10-undecadiyne).

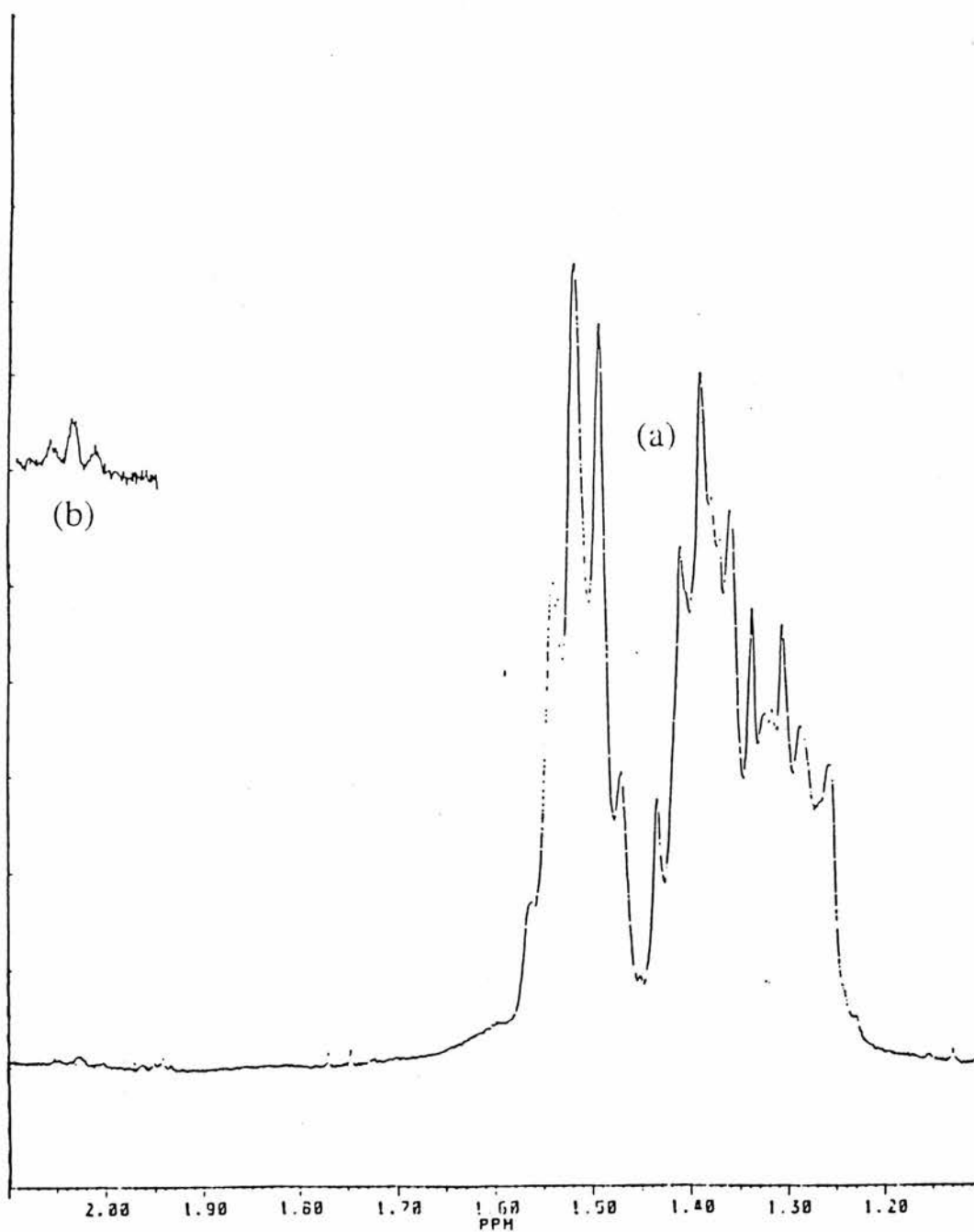


Figure 4.24 Expansion of triplet signal for two terminal alkyne groups (b) by a factor of 8 with respect to the $(\text{CH}_2)_5$ protons (a) which occur along the length of the linear polymer chain.

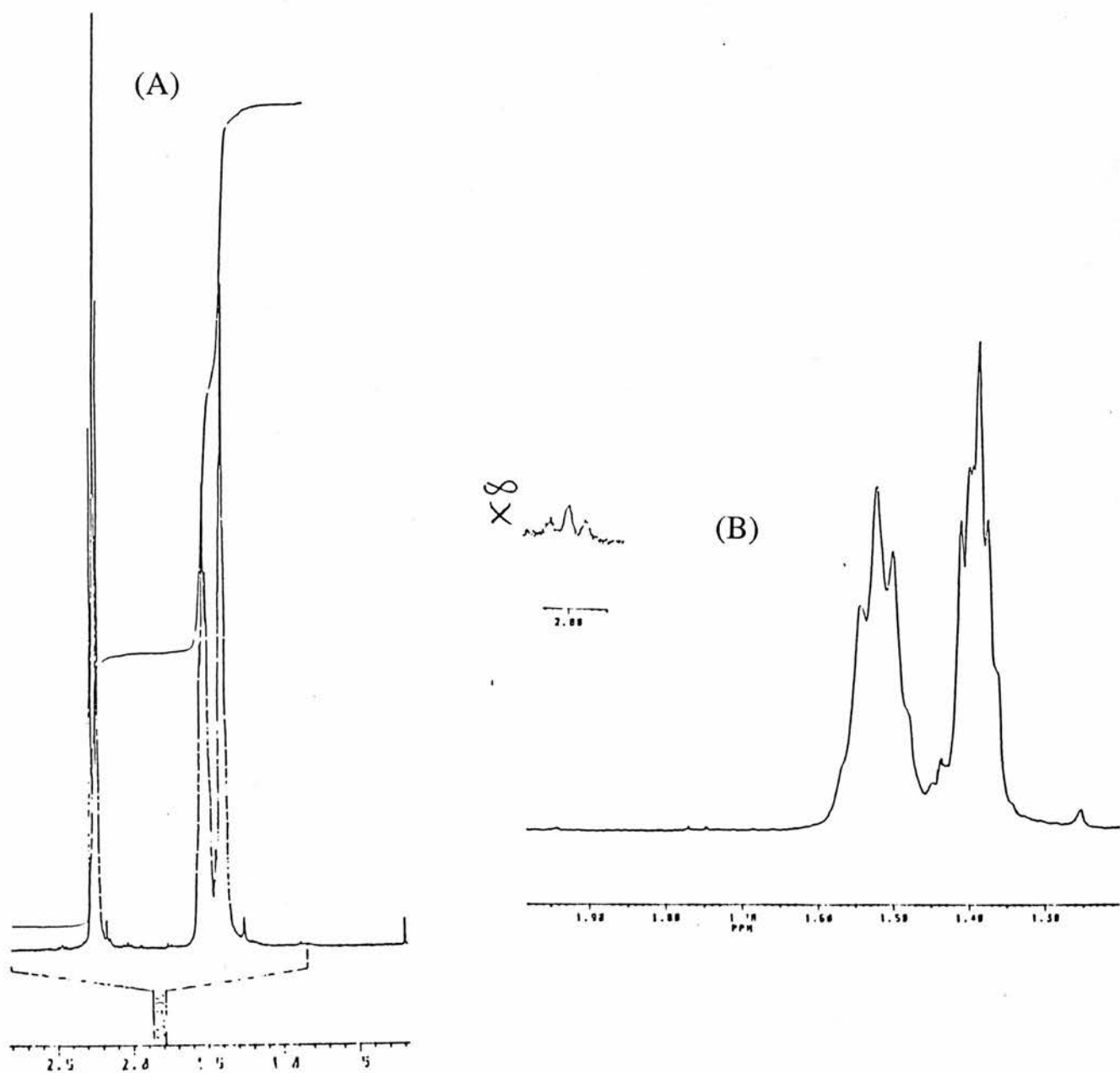


Figure 4.25 (A) ^1H nmr spectrum of polymer A3 - poly(1,9-decadiyne) 5 hours @ 60°C. (B) Expanded triplet signal for terminal alkyne at $\delta \sim 2.0\text{ppm}$ (by a factor of 8) with respect to the multiplet for the methylene protons at $\delta \sim 1.5\text{ppm}$ for the EGA calculation.

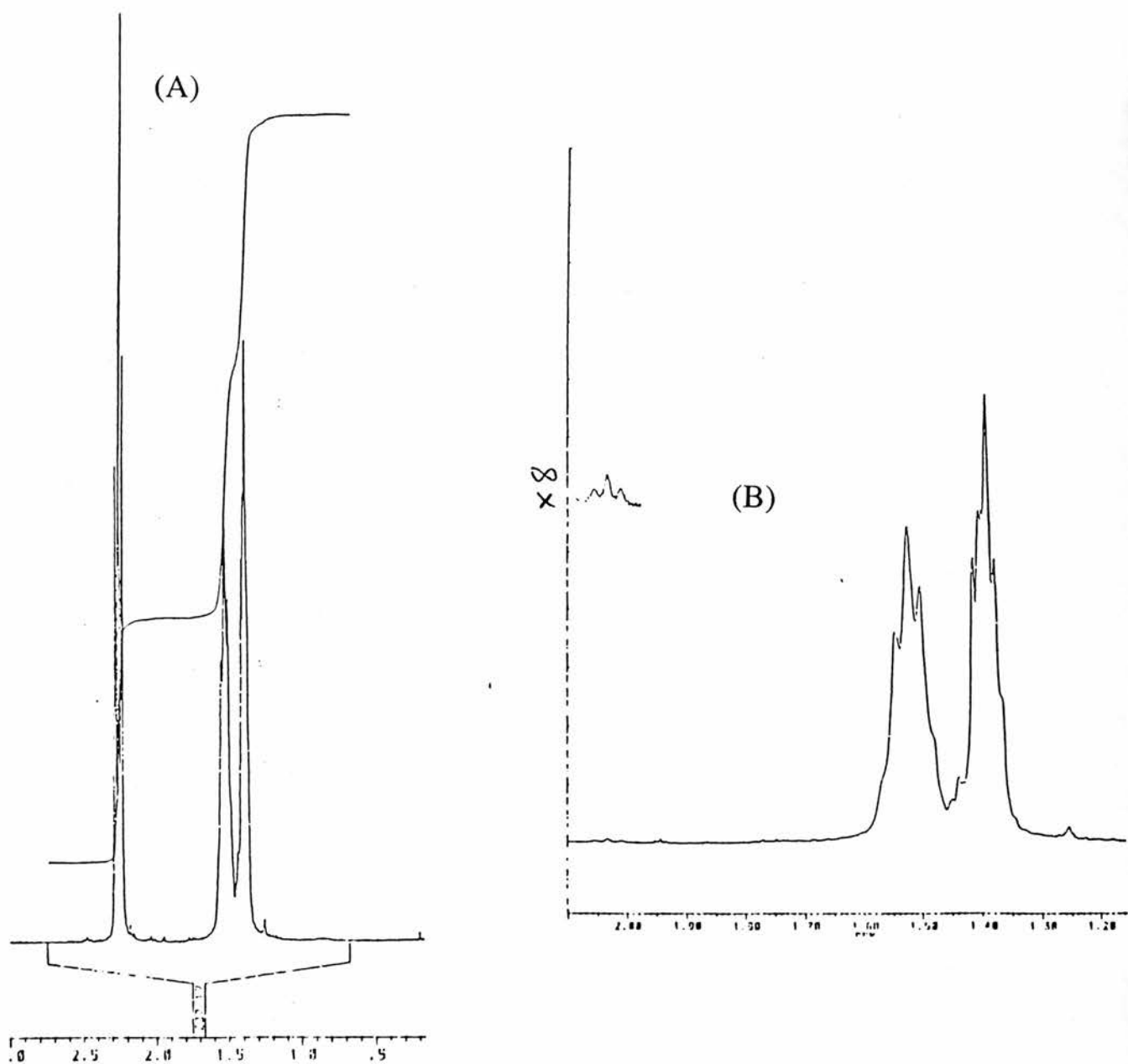


Figure 4.26 (A) ^1H Nmr spectrum of polymer A4 - poly(1,9-decadiyne) 5 hours @ 80°C . (B) Expanded triplet signal for terminal alkyne at $\delta \sim 2.0\text{ppm}$ (by a factor of 8) with respect to the multiplet for the methylene protons at $\delta \sim 1.5\text{ppm}$ for the EGA calculation.

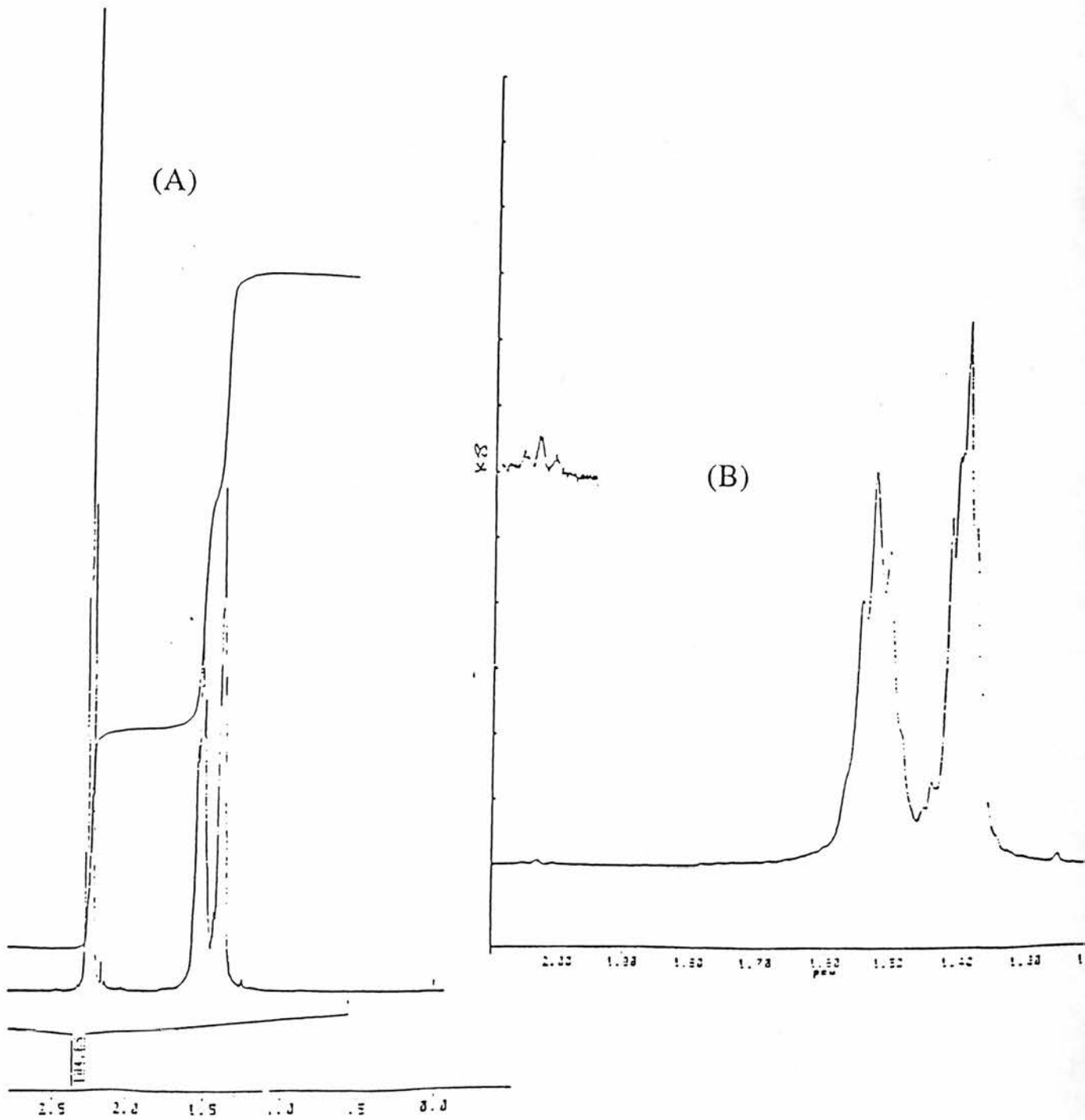


Figure 4.27 (A) ^1H Nmr spectrum of polymer A5 - poly(1,9-decadiyne) 5 hours @ 65°C .(B) Expanded triplet signal for terminal alkyne at $\delta \sim 2.0\text{ppm}$ (by a factor of 8) with respect to the multiplet for the methylene protons at $\delta \sim 1.5\text{ppm}$ for the EGA calculation.

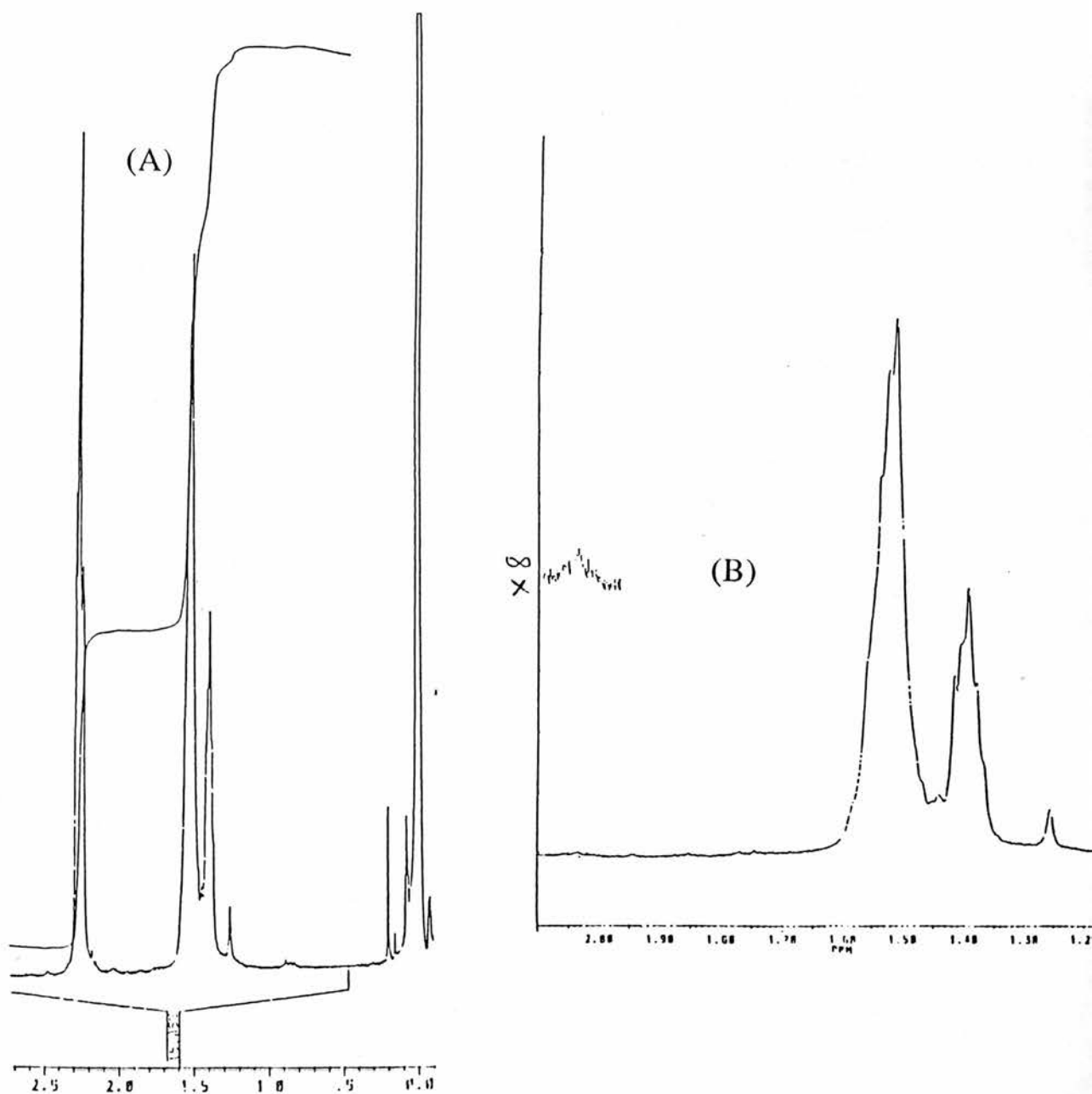


Figure 4.28 (A) ¹Hnmr spectrum of polymer A6 - 50:50 poly(1,8-non):poly(1,9-dec) 5 hours @ 65°C. Expanded triplet signal for terminal alkyne at $\delta \sim 2.0\text{ppm}$ (by a factor of 8) with respect to the multiplet for the methylene protons at $\delta \sim 1.5\text{ppm}$ for the EGA calculation.

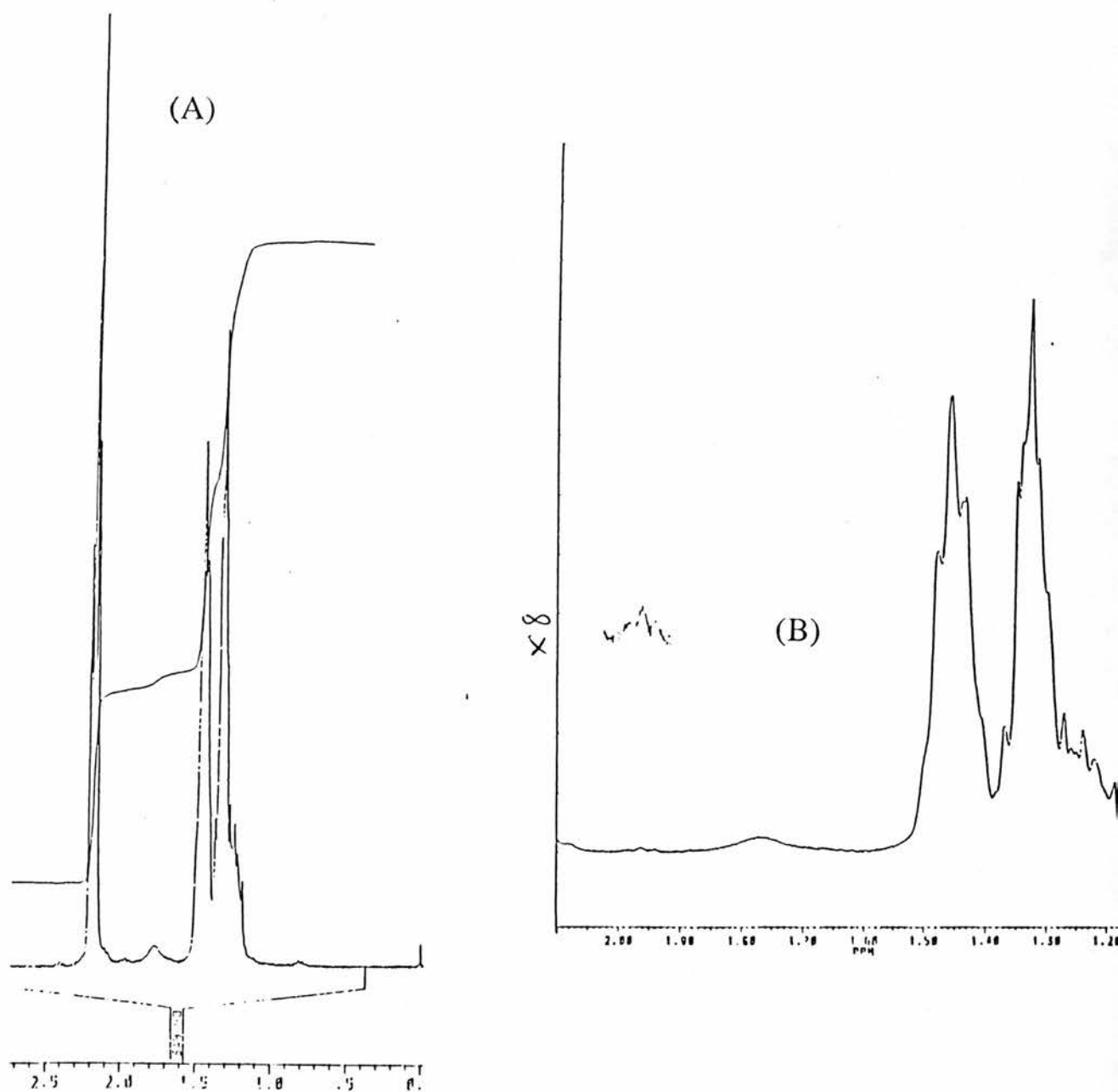


Figure 4.29 (A) ¹Hnmr spectrum of polymer A8 - 50:50 poly(1,9-dec):poly(1,10-undec) 5 hours @ 65°C.(B) Expanded triplet signal for terminal alkyne at $\delta \sim 2.0\text{ppm}$ (by a factor of 8) with respect to the multiplet for the methylene protons at $\delta \sim 1.5\text{ppm}$ for the EGA calculation.

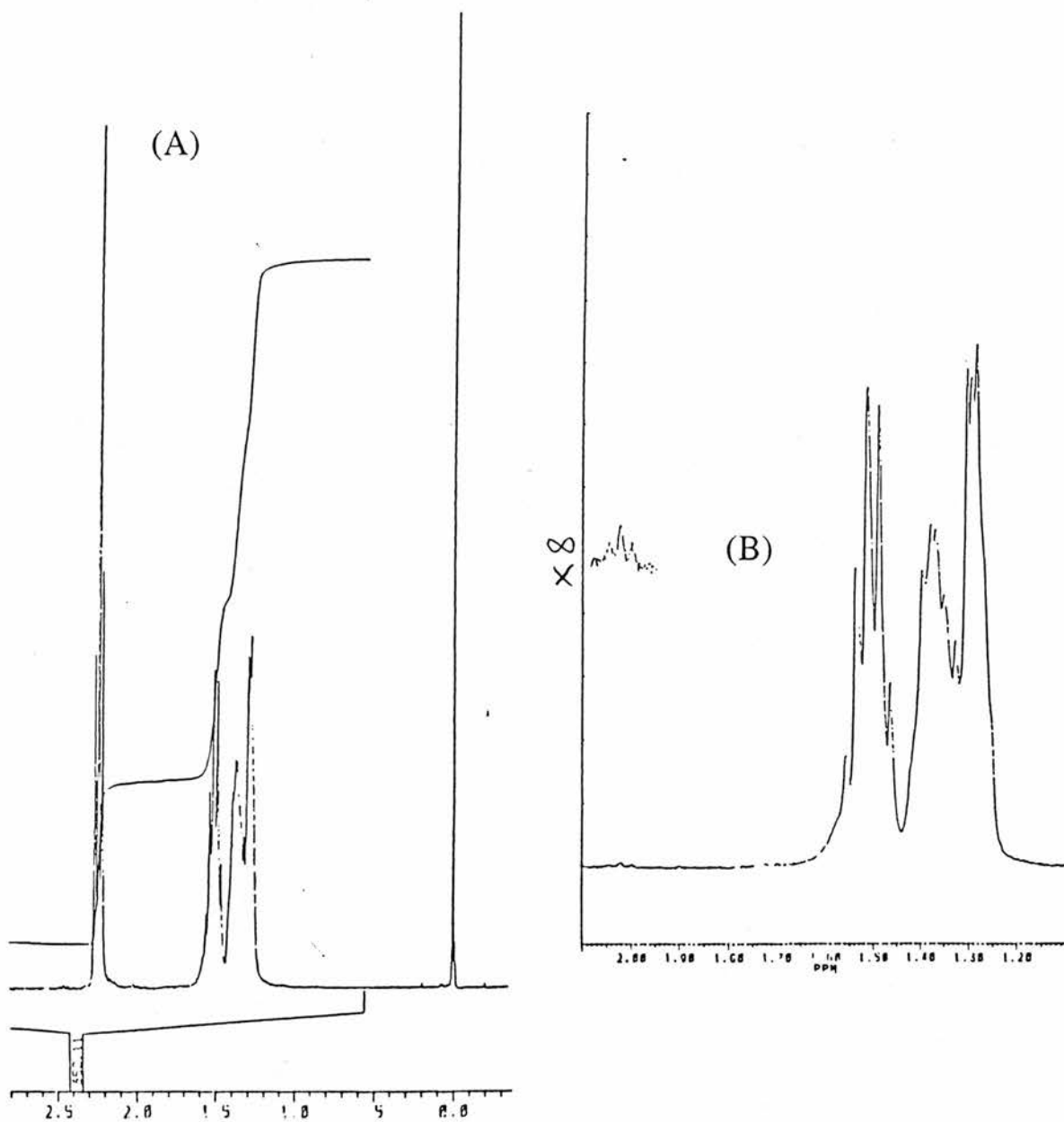


Figure 4.30 (A) ^1H Nmr spectrum of polymer A9 - poly(1,11-dodecadiyne) 5 hours @ 65°C . (B) Expanded triplet signal for terminal alkyne at $\delta \sim 2.0\text{ppm}$ (by a factor of 8) with respect to the multiplet for the methylene protons at $\delta \sim 1.5\text{ppm}$ for the EGA calculation.

CHAPTER 5

THERMAL BEHAVIOUR OF A SERIES OF POLY(α,ω -ALKYLDIYNES)

5.1 Introduction

The work described in this chapter concerns the thermal behaviour of a series of poly(α,ω -alkyldiynes); poly(1,7-octadiyne) (P17O), poly(1,9-decadiyne) (P19D), poly(1,10-undecadiyne) (P110U) and poly(1,11-dodecadiyne) (P111D).

The thermal behaviour of poly(1,8-nonadiyne) was studied previously by Butera and workers.²⁹

The main purpose of this study is to characterise these polymers. Particular attention is focused on the poly(α,ω -alkyldiynes) P19D and P110U with a comprehensive study of their thermal behaviour.

Other work in this chapter investigates the thermal behaviour of poly(1,10-undecadiyne) (P110U) both before and after various degrees of cross-polymerisation. This is performed with a view to determine if thermal analysis could be used to monitor the degree of conversion to the polydiacetylene. (Since the cross-polymerised material is a rigid network which should be infusible, the endotherm observed when cross-polymerised P110U is heated in the DSC should be proportional to the unreacted crystalline portion of the P110U). However in reality the situation is more complicated than described above, DSC can be used semi-quantitatively to monitor the degree of cross-polymerisation. The thermal properties of the cross-polymerised material are discussed in light of the behaviour of the pure P110U.

Poly(1,11-dodecadiyne) (P111D) and poly(1,7-octadiyne) (P17O) are also characterised.

5.2 Experimental details

Materials: synthesis of poly(1,7-octadiyne), poly(1,9-decadiyne), poly(1,10-undecadiyne) and poly(1,11-dodecadiyne).

Poly(1,7-octadiyne), poly(1,9-decadiyne), poly(1,10-undecadiyne) and poly(1,11-dodecadiyne) were polymerised using the procedure for polymerisation route A outlined in Chapter 3. All were polymerised for 5 hours at 65°C

Molar mass characteristics: Molar mass characteristics were determined by GPC in Chapter 4 for all polymers excluding poly(1,7-octadiyne).

	Mn	Mw	PDI
poly(1,9-decadiyne)	29,300	180,000	6.14
poly(1,10-undecadiyne)	28,300	59,200	2.09
poly(1,11-dodecadiyne)	14,100	32,100	2.28

Thermal Analysis:

Sample preparation — Poly(1,9-decadiyne), poly(1,10-undecadiyne) and poly(1,11-dodecadiyne) used for thermal analysis were thin films. The thin films were cast by placing 5ml of the respective polymer in methylene chloride solution onto a carefully cleaned 6cm diameter Petri dish. The dish was covered by a large beaker and the solvent slowly allowed to evaporate. This process was carried out on top of a levelled glass plate to ensure film uniformity. Also, the film casting procedure was always carried out in a dark

environment. Films were cast overnight and were loosened from the Petri dish by cooling with liquid nitrogen and secured onto a cardboard sheet to prevent buckling. The films were dried in a vacuum oven for 30–45 minutes prior to use. Drying time was kept to a minimum, so as to minimize the possibility of thermal cross-polymerisation.

Poly(1,7-octadiyne) used for thermal analysis was in the form of a yellow powder.

Cross polymerisation was effected by irradiating the poly(1,10-undecadiyne) films with UV light ($1600 \mu\text{W}/\text{cm}^2$ at 254 nm). Very thin films were used so UV light could penetrate the films at all conversions studied. The films were exposed to only yellow light or darkness prior to use.

Differential scanning calorimetry(DSC) — All DSC scans were performed on a Perkin-Elmer DSC7 equipped with a glove box and nitrogen purge. Samples were prepared using standard, crimped sample pans sealed under nitrogen. Transition temperatures have been corrected using indium and zinc standards. Peak maxima were used for determining melting temperatures (T_m) and crystallisation temperatures (T_c). Glass transition temperatures (T_g) were taken as the midpoint in the transition curve. Heating rates and cooling rates are specified in the text. Samples that are referred to as being 'quenched' were cooled at a programmed cooling rate of $200^\circ\text{C}/\text{min}$. (It should be noted that although $200^\circ\text{C}/\text{min}$ is the programmed cooling rate, the actual cooling rate is somewhat less since the DSC is not capable of temperature control at such high rates).

5.3 Results and Discussion

5.3.1 Thermal analysis of poly(1,9-decadiyne) (P19D)

The first experiment in this section consisted of thermally cycling a solution cast sample four times observing the melting and crystallisation behaviour of the polymer.

Figure 5.1 shows an example of a DSC heating scan from -40°C to 160°C ($10^{\circ}\text{C}/\text{min}$ scan rate) of a solution cast film of P19D. The scan reveals a double melting endotherm with the minor melting endothermic peak at 97°C and the major melting endothermic peak at 116°C . There is also evidence of a T_g at 36°C . This sample was then cooled at $10^{\circ}\text{C}/\text{min}$ to produce figure 5.2. This shows an exothermic peak at 82°C . On reheating from -40 to 160°C at $10^{\circ}\text{C}/\text{min}$ figure 5.1 scan A is produced. Compared to the first scan, scan A shows a decrease in endothermic area and decrease in the melting temperature of the major melting endothermic peak from 116°C to 111°C . Upon cooling the sample again to -40°C ($10^{\circ}\text{C}/\text{min}$ cooling rate) (figure 5.2 scan A) there is a decrease in exothermic area and a decrease in the exothermic peak from 82°C to 76°C . On subsequent heating at $10^{\circ}\text{C}/\text{min}$ (figure 5.1 scan B), there is a further decrease in the endothermic area and also T_m which falls from 111°C to 100°C . Upon further cooling to -40°C ($10^{\circ}\text{C}/\text{min}$ cooling rate) (figure 5.2 scan B) there is a further decrease in the exothermic peak from 76°C to 69°C .

This heating cycle was repeated twice to produce figures 5.1 scans C and D and the cooling cycle repeated once to produce figure 5.2 scan C. Repeated cycling causes a continuing decrease in the

endothermic and exothermic areas for figures 5.1 and 5.2 respectively and also slight decreases in peak values for both.

Table 5.1 lists the Heats of Fusion (ΔH_f in J/gram) and Heats of Crystallisation (ΔH_c in J/gram) for endothermic and exothermic peaks in figures 5.1 and 5.2 respectively.

The behaviour observed for P19D can be ascribed to the melting and crystallisation behaviour of the polymer which can be observed in a conventional polymer system. The cause of the double melting endotherm will be discussed later.

The decrease in exothermic and endothermic area which occurs upon increasing cycling can be explained by examining the effect of melt treatment on the subsequent crystallisation behaviour. This is studied in the following experiment.

The second experiment consisted of annealing the P19D samples for four different times at a temperature of 160°C. After annealing the samples were then quenched to -50°C and reheated at 10°C/min from -30°C to 160°C to produce scans A, B, C and D shown in figure 5.3 (a heating scan for a solution cast film is shown for reference). These experiments show that as the P19D is held at 160°C for longer periods of time, the subsequent heating scan shows less endothermic area and there is a decrease in the endothermic peak from 119°C to 84°C. After 30 mins at 160°C, the subsequent heating scan shows that crystallinity is present as T_m is still present. From the DSC scans on figure 5.3 it would appear possible that both minor and major melting peaks could

be individually isolated by annealing studies at 160°C. This will be discussed later.

Table 5.2 lists the Heats of Fusion (ΔH_f in J/gram) and endothermic melting peaks for the P19D samples.

The studies in the second experiment show that the amount of time the melt is held at 160°C can affect the subsequent crystallisation behaviour. Melt history effects similar to those described for P19D have been observed using optical microscopy and density methods for various other polymer systems.⁹¹⁻⁹⁵ In these polymer systems the temperature of the melt and the amount of time the melt is held at any particular temperature can prove critical in the crystallisation behaviour. The primary nucleation rate can be altered by the prior melt treatment thus explaining these effects. Therefore if the melt treatment is not too severe, the residual local order can remain in the melt and act as primary nucleation sites for crystallisation. Crystallisation temperature (T_c) is also critical for further crystallisation and this will influence the melt history. If T_c is low enough to be within the range where homogeneous nucleation is predominant, the previous melt conditions will not significantly effect the crystallisation process,^{92,94} since the number of nucleation sites carried from the melt will be small compared to the number of spontaneously formed nuclei, and because the nucleation rate will be high even without residual order carried down from the melt.⁹¹ If the crystallisation temperature is high (i.e. $T_m - T_c$ is small) the primary nucleation rate can be greatly influenced by the amount of residual order carried from the melt. In this case the primary nucleation rate decreases with more severe melt treatment (i.e. higher temperatures or

longer times in the melt).⁹³ The influence of melt treatment seems to be limited to the primary nucleation rate (the spherulitic growth rate has been shown to be unaffected).⁹⁴

The behaviour observed in the annealing studies for P19D (see figure 5.3) can be understood on the basis of the above discussion. The longer the P19D is held at 160°C, the less residual order will remain in the melt before cooling. The residual order will be 'frozen-in' when quenching from the melt. Therefore on reheating the P19D the sites of residual order will act as sites for primary nucleation. The amount of crystallisation will be inversely proportional to the amount of time the melt spends at 160°C. (There is no crystallisation peak present in the heating up scans but the melt transition temperature (endothermic peak) is still present indicating crystallinity). The most important observation is that even after a period of thirty minutes at 160°C there is still residual order left in the melt. Therefore in order to destroy residual order in the melt it is necessary to use higher temperatures for annealing and longer periods of time in the melt at higher temperatures. Thus any subsequent crystallisation will be prevented.

In an attempt to prevent subsequent crystallisation a P19D sample was annealed at 200°C for 1 hour. After annealing the sample was then quenched to -60°C and reheated at 10°C/min from -40°C to 160°C to produce figure 5.4(a). (Again a heating scan for a solution cast film is shown for reference, figure 5.4). Figure 5.4(a) shows no evidence of a crystalline melting point thus suggesting that residual order in the melt is destroyed after 1 hour at 200°C, and that this residual order in the melt is necessary to cause crystallisation during the next heating scan (at a heating rate of 10°C/min).

One aspect of interest of the P19D melting behaviour is the double melting endotherm which is observed on the heating scan of the freshly solution cast film in figures 5.1, 5.3 and 5.4 (these thermograms reveal a minor peak with peak values ranging from 97°C to 98°C and a major peak with peak values ranging from 116°C to 119°C). This type of behaviour is presumed to be due to one of two causes;

(1) The existence of two different crystal phases in the polymer sample, each having its own discrete melting temperature.

(2) Less perfect crystals formed together with more perfect crystals from the solution casting process. Recrystallisation of these less perfect crystals occurs during the DSC heating scan. ⁹⁶

To confirm that this double melting behaviour was not exclusive to this particular sample of P19D, another P19D sample was solution cast and its DSC scan run between 40°C to 160°C at 10°C/min. The P19D chosen was synthesised using polymerisation route A, with polymerisation conditions of 60°C for 5 hours. The molar mass characteristics of the polymer were as below;

$$M_n=20,900; M_w=46,500 \text{ and } PDI=2.22$$

Figure 5.5 reveals that the double melting endotherm is also present, with the onset of melting occurring at 88°C with the minor melting endothermic peak at 97°C, and the major melting endothermic peak at 115°C.

This double melting endotherm is characteristic of the melting behaviour of P19D for a solution cast film and that there are arguably two different crystal phases present.

A DSC scan was run on a P19D powder sample of the same polymer between 40°C and 160°C at 10°C/min revealing only one melting endotherm at 111°C (see figure 5.5(a)). This suggests that the double melting endotherm is characteristic of the solution casting process.

Earlier on in the discussion it was noted that from the annealing studies performed at 160°C on the P19D films (see figure 5.3, scans A and C) that it was possible to isolate both the minor and major melting endotherms by DSC. If the P19D sample is immediately quenched to -50°C from the melt at 160°C (Annealing time=0 minutes) then re-run at 10°C/min a single melting peak is obtained at 114°C which corresponds to the major melting peak at 116°C. If the P19D sample is annealed at 160°C for 20 minutes, quenched to -50°C and then re-run at 10°C/min a single melting peak is obtained at 94°C which corresponds to the minor melting peak at 97°C.

Attempts to duplicate this DSC work carried out by use of an air oven and liquid nitrogen coolant. Two methods were employed;

(1) Heating the P19D films slowly in an air oven up to a temperature of 160°C, annealing the samples for the appropriate time, then rapidly quenching the samples into liquid nitrogen.

(2) Heating the P19D films slowly in an air oven up to a temperature of 160°C, annealing the samples for the appropriate time, then switching the air oven off leaving the cooling fan on. (This method will be more likely to mimic the DSC conditions as samples quenched in the DSC instrument are cooled at a programmed rate of 200°C/min. However in practice the actual cooling rate is somewhat less since DSC is not capable of temperature control at such high rates).

Attempts to isolate the two melting structures proved to be unsuccessful when the above methods were employed. No evidence of an endothermic melting peak in either (1) or (2) was present when the samples were scanned between 40°C and 160°C at 10°C/min in the DSC. This suggests that the melt history of the P19D has been destroyed using these conditions in an air oven.

5.3.2 Thermal analysis of poly(1,10-undecadiyne) (P110U)

The first experiment in this section consisted of thermally cycling a solution cast sample three times observing melting and crystallisation behaviour of the polymer.

Figure 5.6 shows an example of a DSC heating scan from -50°C to 120°C (10°C/min scan rate) of a solution cast film of P110U. The scan reveals a melting endotherm at 73°C. This sample was then cooled at 10°C/min to -50°C and subsequently reheated at 10°C/min to produce figure 5.6 scan A. Compared to the first scan, scan A shows a decrease in endothermic area and a decrease in the melting temperature from 73°C to 57°C. In addition, a T_g at -16°C is observed in scan A, whereas it is not present in the original scan. There is also an exothermic peak at 31°C, this is the most significant difference as this exotherm is not present in the original scan.

Upon cooling the sample to -50°C (10°C/min cooling rate) and then heating again at 10°C/min to produce figure 5.6 scan B, there is a further decrease in the endothermic area with T_m staying constant at

57°C, and a decrease in exothermic area compared to scan A. T_g also stays constant at -16°C. However T_c increases to 37°C. This cooling and heating cycle was repeated once more to produce figure 5.6 scan C. Again there is a further decrease in endothermic area and exothermic area, with T_m and T_g staying constant at 57°C and -16°C respectively.

Table 5.3 lists the Heats of Fusion (ΔH_f in J/gram), Heats of Crystallisation (ΔH_c in J/gram) for endothermic and exothermic peaks respectively for figures 5.6.

The P110U polymer is markedly different from the P19D polymer as there is no evidence of crystallisation in the cooling down scans as no exotherms are recorded for P110U.

5.3.2.1 Annealing and quenching studies on P110U

The second experiment performed on P110U involved annealing the sample at a temperature of 120°C for fifteen minutes then quenching this sample to -70°C and reheating this sample at 10°C/min from -50°C to 120°C to produce figure 5.7 scan A (a heating scan for a solution cast film is shown for reference, figure 5.7).

The purpose of this experiment was to see if it was possible to prevent further crystallisation of the P110U sample i.e. destroy the samples melt history.

Figure 5.7 scan A shows that this was achieved by annealing at 120°C for a period of fifteen minutes followed by quenching to -70°C as there is negligible evidence of a crystalline

melting point on this reheating scan. However there is a glass transition temperature, T_g , at -15°C (see figure 5.7 scan A).

5.3.2.2 Comparison of thermal behaviour of poly(1,10-undecadiyne) P110U with poly(1,8-nonadiyne) P18N.

Similar thermal behaviour to P110U was observed for P18N. This was reported by Butera and workers.²⁹ Butera postulated that the exothermic peak observed in the heating scans during the thermal cycling work was a consequence of cross-polymerisation of the P18N. There are many examples in the literature of diacetylene materials which are thermally reactive.^{17,98,99} He claimed that with each heating scan more P18N would be cross-polymerised, therefore, be rendered infusible, hence the decrease in the heat of fusion as the sample is thermally cycled. Butera performed two experiments to help determine whether the observed exotherm was caused by cross-polymerisation, or by crystallisation. The first experiment involved heating a solution cast P18N film to the centre of the exotherm (62°C) on the DSC and then holding the film at this temperature for a period of 10 hours. However the isotherm obtained from the experiment showed no sign of exothermic response, therefore, no cross-polymerisation had taken place. (Examination of the sample after the 10 hour period revealed that some cross-polymerisation did occur as the sample had a slight blue colouration).

The second experiment consisted of thermally cycling a solution cast film of P18N three times between the temperatures of -53°C and 157°C (heating and cooling rates were $20^{\circ}\text{C}/\text{min}$). This was followed by annealing the sample at 62°C (centre of the exotherm) for

40 minutes then the sample was quenched to -53°C and again heated at $20^{\circ}\text{C}/\text{min}$ to 157°C . This DSC trace showed an increase in endothermic area when annealing at the exothermic temperature of 62°C . This increase in endothermic area was conclusive evidence that the exothermic peak at 62°C was a consequence of crystallisation and not cross-polymerisation. If cross-polymerisation had taken place the DSC trace would have shown less endothermic area because more of the P18N would be cross-polymerised and, therefore, infusible after the annealing treatment.

Similar isothermal studies and thermal cycling experiments were performed on P110U.

The isothermal studies involved holding a solution cast film of P110U for several hours at various temperatures on and above 31°C (the centre of the exothermic peak) i.e. below the melting point (T_m) of 73°C . In all cases no sign of exothermic response was noted. Visual examination revealed a very faint blue colouring of the P110U sample. Some diacetylene materials exhibit an autocatalytic polymerisation when isothermal studies are performed at the right temperature. **17,98** Therefore it was concluded that P110U does not show this autocatalytic reactivity. However P110U does slowly cross-polymerise in the dark at room temperature and higher temperatures up to 73°C (T_m). This reaction is very slow and takes hours before any cross-polymerisation can be detected visually.

The thermal cycling studies involved thermally cycling P110U three times between -50°C and 120°C (heating and cooling rates $10^{\circ}\text{C}/\text{min}$) then annealing the sample at 31°C (centre of the exotherm)

for ~1 hour followed by quenching the sample to -70°C then reheating the sample at -50°C to 120°C at $10^{\circ}\text{C}/\text{min}$. Again, as with P18N an increase in endothermic area was achieved which was conclusive evidence that the exothermic peak at 31°C was a consequence of crystallisation and not cross-polymerisation. If there were even minimal cross-polymerisation taking place during the heating scans recrystallisation would be significantly limited. ⁹⁹

The thermal behaviour of the cross-polymerised P110U will now be discussed.

5.3.2.3 Thermal Analysis of Cross-Polymerised poly(1,10-undecadiyne) XP110U

It is possible to monitor the cross-polymerisation reaction of P110U by performing thermal analysis studies on the cross-polymerised material at varying UV exposure times. This was shown by Butera and workers ²⁹ when the cross polymerisation of poly(1,8-nonadiyne) P18N was studied by thermal analysis.

Although the cross-polymerised poly(1,10-undecadiyne) XP110U is to a large extent infusible, this infusibility yields invaluable information about the degree of cross-polymerisation. In theory, the infusible segments will be the cross-polymerised P110U. Therefore, the observed heat of fusion in a sample of a given degree of cross-polymerisation will be a consequence of the crystalline material which has not yet undergone cross-polymerisation. As the heat of fusion decreases the degree of cross-polymerisation increases. By dividing the heat of fusion from a P110U sample with a given UV exposure time to

that of a pure P110U sample (both polymer samples from the same batch) of the same degree of crystallinity and then subtracting this value from 1, the degree of cross-polymerisation of P110U can be obtained.

$$[1 - (H_{f,t} / H_{f,0})] \times 100 = \% \text{ converted crystalline eqn (1)}$$

$H_{f,t}$ = heat of fusion from P110U sample exposed to UV for time t .

$H_{f,0}$ = heat of fusion from pure P110U polymer.

This value % converted crystalline corresponds to the degree of cross-polymerisation of the crystalline regions exclusively. However, the overall degree of conversion of the sample is obtained by multiplying the above value by the degree of crystallinity.

$$\begin{aligned} & \% \text{ converted crystalline} \times \% \text{ crystallinity} \\ & = \% \text{ converted sample eqn (2)} \end{aligned}$$

For this study % converted crystalline [eqn (1)] is the most significant value, so only this quantity will be dealt with.

Figures 5.8 (a)–(g) shows DSC traces of seven samples of P110U (identically prepared) which were given the indicated amount of UV exposure. As expected on increasing the amount of UV exposure the heat of fusion (J/gram) decreases, the endothermic melting peak becomes smaller and broader in area, and the peak value proceeds to lower temperatures. The heats of fusion from these melting traces were converted to % converted crystalline (degree of conversion) values for each respective sample. Figure 5.9 shows a plot of percentage conversion to XP110U against UV exposure time for the results obtained from the endotherms shown in figures 5.8 (a)–(g). This plot

in figure 5.9 shows that conversion starts to level-off to approximately 70% after 8 minutes of UV exposure. Chance and Patel ¹⁷ showed that this type of curve is common for UV initiated polymerisations.

There are several errors and assumptions which are introduced into this technique which question the validity of the DSC results.

(1) Errors are introduced every time a baseline is determined for the endothermic melting peaks, i.e. each time a heat of fusion is calculated an error is incurred.

(2) The assumption is being made that only unreacted segments of the P110U will contribute to the heat of fusion. This assumption does not hold true especially at low conversions as shown by Butera and workers ^{28,30} by UV-visible spectroscopic and resonance Raman studies. It was shown that there was some disordering of the polydiacetylene segment of the cross-polymerised structure. Therefore at low conversions the degree of conversion is probably underestimated.

(3) The assumption is being made that all unreacted portions of the P110U can contribute to the heat of fusion. However, this assumption may not hold true at higher cross-polymerisation conversions where it is very likely that there will be many short unreacted portions of P110U 'trapped' in the cross-polymerised material. Therefore these 'trapped' P110U segments can't disorder properly and hence a lowering of the heat of fusion will result, leading to an overestimation of the degree of conversion to the cross-polymerised product. The value of 76% obtained for XP110U after 20 mins of UV exposure (shown in figure 5.9) is probably an unrealistically high value.

(4) There are several reasons why UV initiated polymerisation of diacetylenes does not proceed to 100% conversion as opposed to gamma ray or thermally initiated polymerisations which can reach 100% conversion. **17,18,97**

(a) depth of penetration of UV light into the sample.

(b) quenching of the monomer excited state by previously formed polydiacetylene chains.

(c) degree of conversion is often below 50% even after long exposure times.

(d) Inhomogeneity of the cross-polymerisation — sample thickness is very large compared to the depth of the UV light. **18** This will be negligible in my study as thin films were purposely cast.

(5) There is a possibility that the cross-polymerisation reaction takes place in the paracrystalline regions of the P110U. Butera **30** has shown by UV-visible spectroscopic studies of P18N films, which were quenched to the amorphous state and then irradiated, that little or no reaction takes place in the amorphous regions. Also Lando and co-workers **25** have shown by solid-state ^{13}C nmr studies of poly(1,11-dodecadiyne) (P111D) that the cross-polymerisation reaction takes place in the crystalline regions of the polymer. However, this does not rule out the possibility that cross-polymerisation reaction does not take place in paracrystalline regions of P110U if they are present. This phenomenon has been suggested before when studies of diacetylene-block copolymers **100,101** were shown to cross-polymerise but having no evidence of crystallinity. Equation (2), i.e. % converted crystalline \times % crystallinity = % converted sample, implies that the cross-polymerisation reaction only takes place in the crystalline regions. Although it is difficult to imagine that paracrystallinity would be important in the cross-polymerisation of P110U as it is with the block

copolymers, **100,101** it must not be neglected completely. If cross-polymerisation takes place anywhere else other than the crystalline regions of the P110U, the % converted sample from eqn (2) will be smaller in value than the actual value.

5.3.3 Thermal analysis of poly(1,11-dodecadiyne)(P111D)

Figure 5.10 shows an example of a DSC heating scan from 45°C to 115°C (10°C/min scan rate) of a solution cast film of P111D. The scan reveals that the P111D has a melting endotherm at 91°C. No further thermal cycling, annealing or quenching studies were performed on this polymer.

5.3.4 Thermal analysis of poly(1,7-octadiyne)(P17O)

Figure 5.11 shows an example of a DSC heating scan from 45°C to 300°C (10°C/min scan rate) of a yellow powdered sample of P17O. The scan reveals that the P17O is infusible and there is a large exothermic degradation peak which commences at ~ 150°C. (Thermogravimetric analysis confirmed that degradation had taken place as there was a substantial weight loss recorded from a sample of P17O that was submitted).

5.4 Conclusions

Poly(1,9-decadiyne)(P19D) was thermally cycled revealing endothermic melting and exothermic crystallisation peaks on the heating up and cooling down scans respectively. On increased cycling a decrease in endothermic and exothermic (heats of fusion and heats of crystallisation respectively) and peak values were obtained. This melting and crystallisation behaviour of P19D would be observed in a conventional polymer system. P19D reveals a T_g at 36°C and reproducible twin melting from freshly cast films (a minor melting peak at $\sim 97^\circ\text{C}$ and a major melting peak at $\sim 116^\circ\text{C}$) arguably due to the presence of two different crystal phases in the P19D film. However a DSC scan run on a P19D powder sample revealed a single melting endotherm at 111°C , suggesting that the double melting endotherm is characteristic of the solution casting process (i.e. less perfect crystals formed together with more perfect crystals). Annealing studies by DSC on P19D films at 160°C for various times from 0 to 30 minutes followed by quenching to -50°C and then reheating the P19D samples revealed that both minor and major melting peaks could be isolated. Attempts to duplicate this DSC work and isolate the two melting peaks were performed using an air oven and liquid nitrogen as a coolant. This proved to be unsuccessful as there was no evidence of endothermic melting on subsequent examination by DSC.

Poly(1,10-undecadiyne) (P110U) was thermally cycled revealing melting on the heating up scans but no evidence of crystallisation on the cooling down scans. On the first reheating scan a decrease in endothermic area (heat of fusion) and the melting peak from 73°C to 57°C was obtained. Also a T_g was evident at -16°C and an exothermic

peak was present at 31°C. It was shown that this exotherm was due to crystallisation and not thermal cross-polymerisation of P110U. It was also shown that thermal analysis of XP110U can give an insight into the values of the degree of cross-polymerisation in a semi-quantitative manner. This method was based on the fact that the cross-polymerised portions of the P110U sample will be infusible, so the endothermic area (heat of fusion) decreases with increasing UV exposure time. There are several errors and assumptions which were made with the realisation that long UV exposure times will most likely overestimate the degree of conversion by this technique. However, thermal analysis was a good method for estimating the degree of conversion to the cross-polymerised product.

The melting endotherm for poly(1,11-dodecadiyne) (P111D) was observed at 91°C and also the decomposition exotherm for poly(1,7-octadiyne)(P17O) was observed commencing at ~150°C.

Scan no	ΔH_f (J/gram)	T_m (°C)
1st run	64.53	94(minor peak) 116(major peak)
A	30.60	111
B	25.06	106
C	20.69	100
D	19.55	97

Table 5.1(a) Heating Up Scans.

Scan no	ΔH_c (J/gram)	T_c (°C)
1st run	35.20	82
A	29.13	76
B	25.27	69
C	23.29	64

Table 5.1(b) Cooling Down Scans.

Table 5.1 Data for Thermal cycling of P19D.

Time held at 160°C	ΔH_f (J/gram)	T_m (°C)
0	33.01	114
10	30.33	111
20	22.80	94
30	18.26	84

Table 5.2 Data for Annealing of P19D at 160°C.

Scan no	ΔH_f (J/gram)	T_m (°C)	ΔH_c (J/gram)	T_c (°C)
1st run	66.69	73	–	–
A	11.61	57	4.46	31
B	3.47	57	2.31	37
C	1.04	57	–	–

Table 5.3 Data for Thermal cycling runs of P110U.

UV exposure time (mins)	ΔH_f (J/gram)	T_m ($^{\circ}$ C)
0	59.40	73
1	36.66	71
2	31.18	66
5	20.83	64
10	18.14	64
15	16.97	64
20	13.90	63

Table 5.4.Data for Thermal Analysis of Cross-polymerised P110U

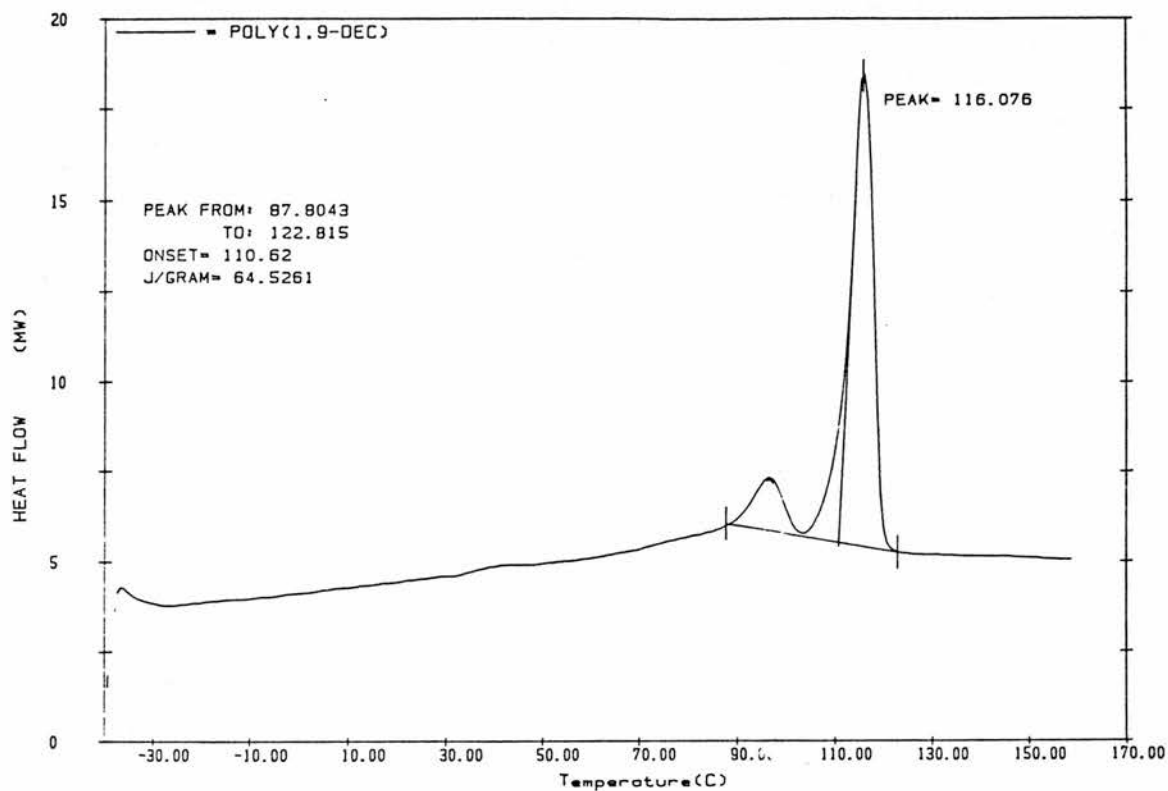


Figure 5.1 DSC thermogram of a solution cast film of P19D from -40°C to 160°C (at $10^{\circ}\text{C}/\text{min}$). 1st heating cycle. Original scan.

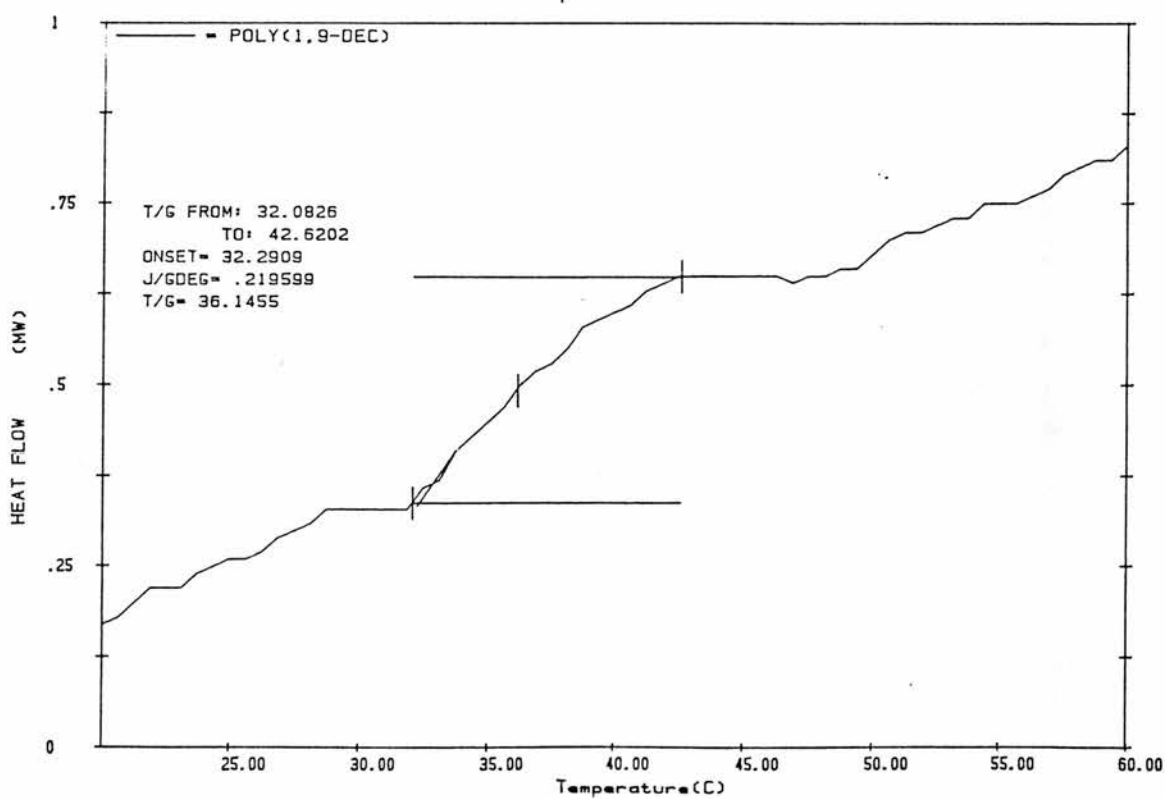


Figure 5.1 T_g calculation from the above thermogram.

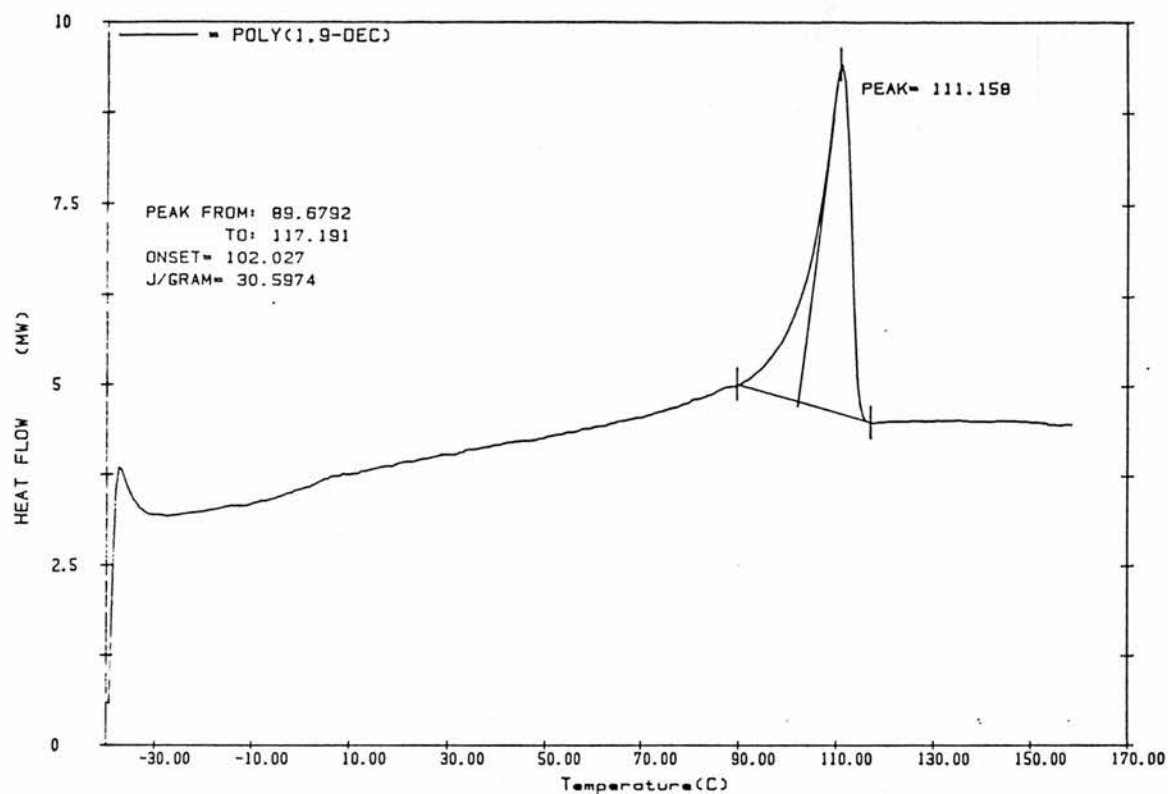


Figure 5.1 scan A DSC thermogram of P19D from -40°C to 160°C (at $10^{\circ}\text{C}/\text{min}$). 2nd heating cycle.

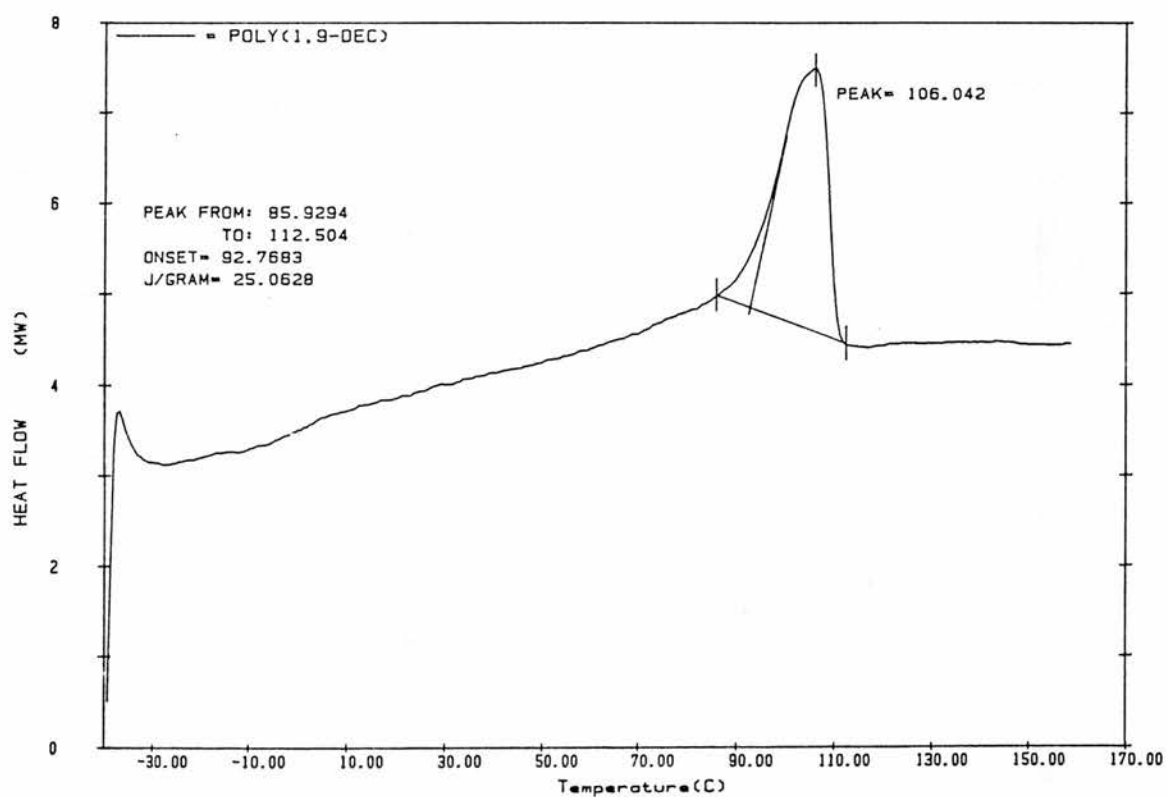


Figure 5.1 scan B DSC thermogram of P19D from -40°C to 160°C (at $10^{\circ}\text{C}/\text{min}$). 3rd heating cycle.

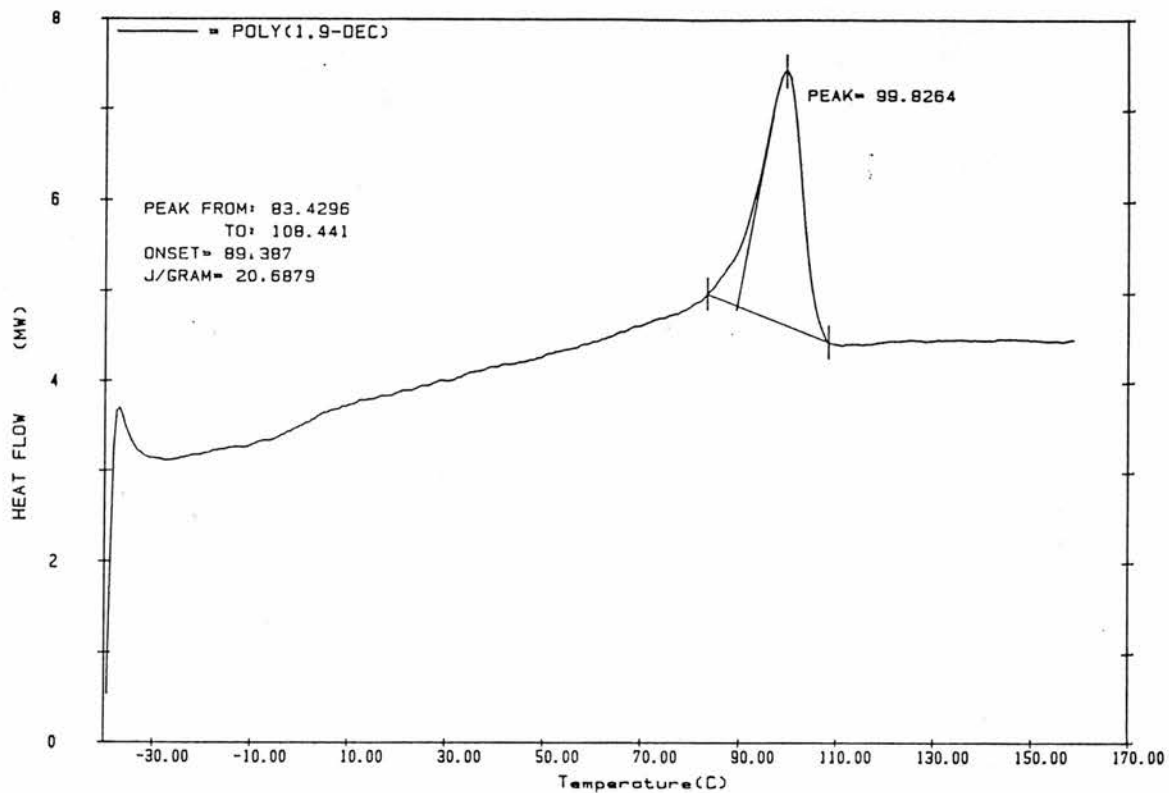


Figure 5.1 scan C DSC thermogram of P19D from -40°C to 160°C (at $10^{\circ}\text{C}/\text{min}$).4th heating cycle.

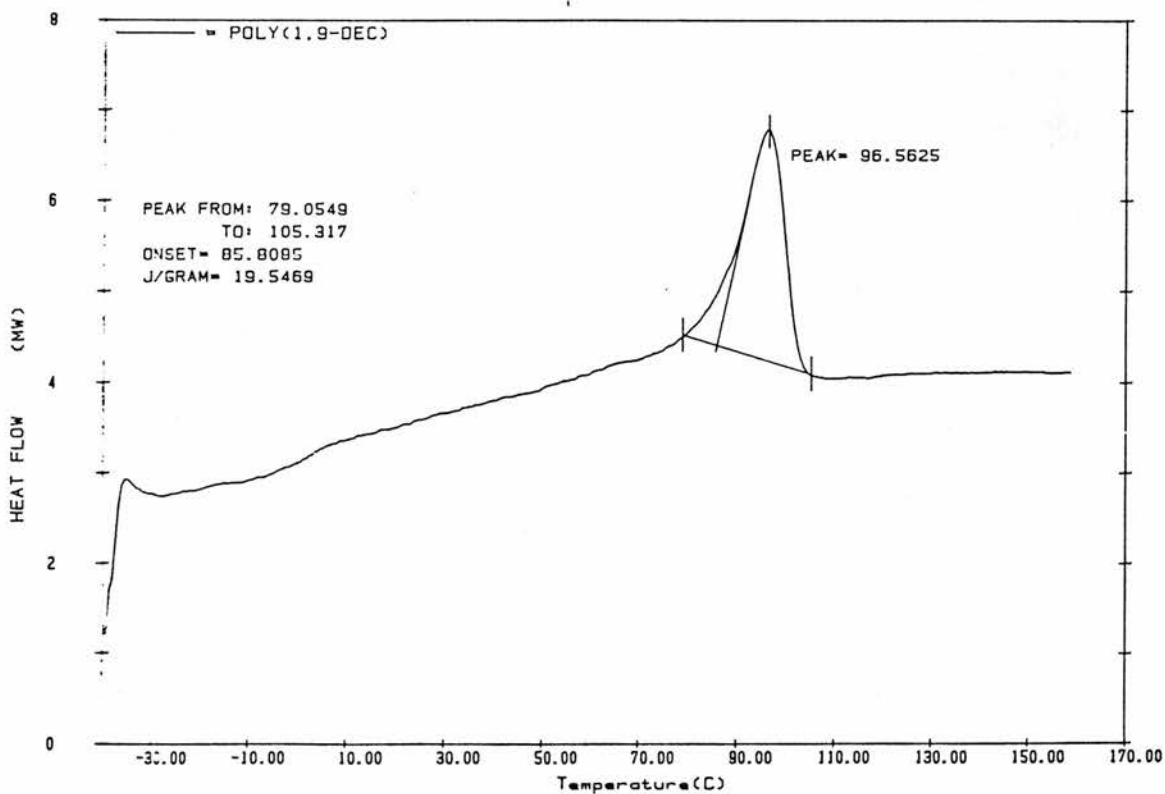


Figure 5.1 scan D DSC thermogram of P19D from -40°C to 160°C (at $10^{\circ}\text{C}/\text{min}$).5th heating cycle.

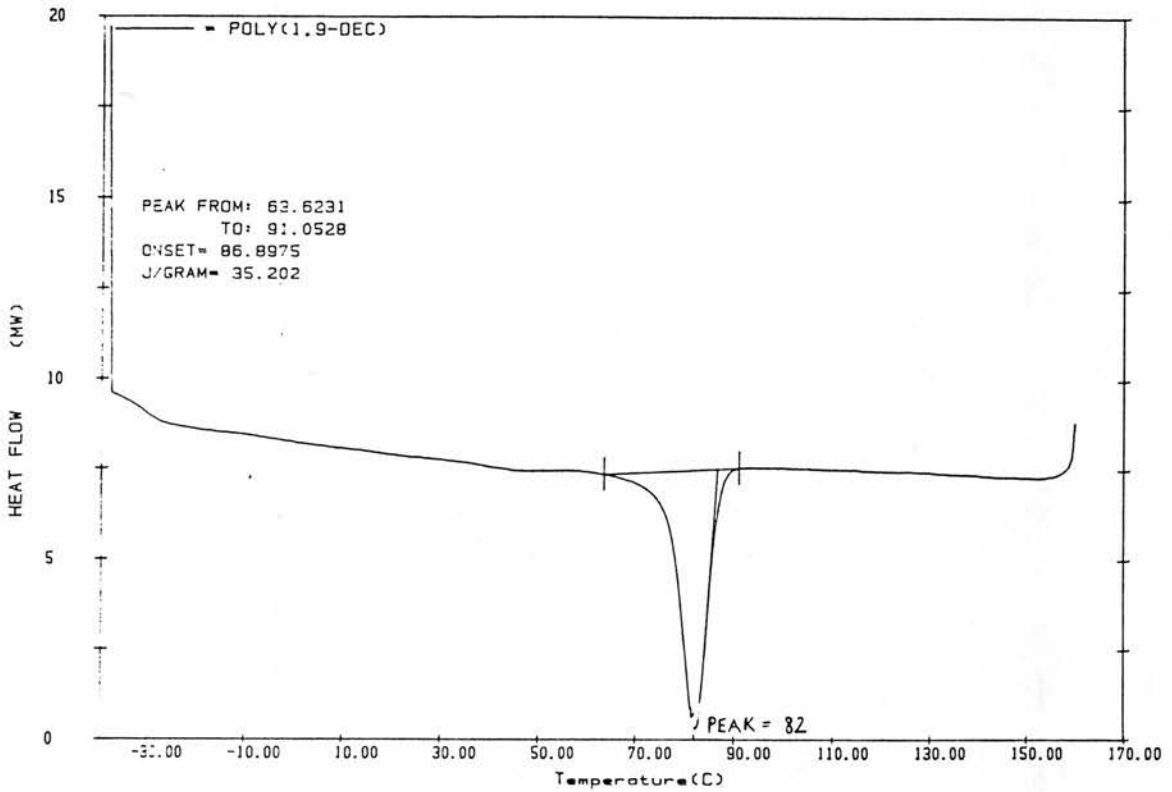


Figure 5.2 DSC thermogram of P19D from 160°C to -40°C (at 10°C/min) 1st cooling cycle.

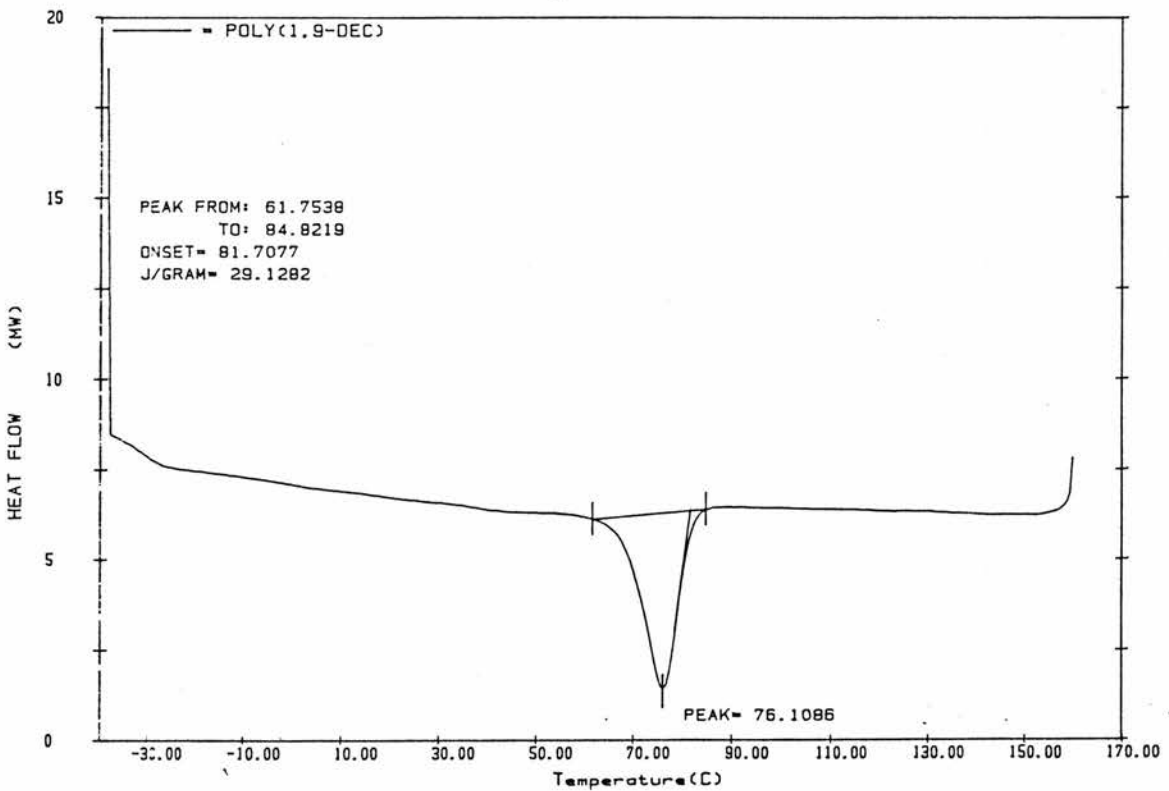


Figure 5.2 scan A DSC thermogram of P19D from 160°C to -40°C (at 10°C/min) 2nd cooling cycle.

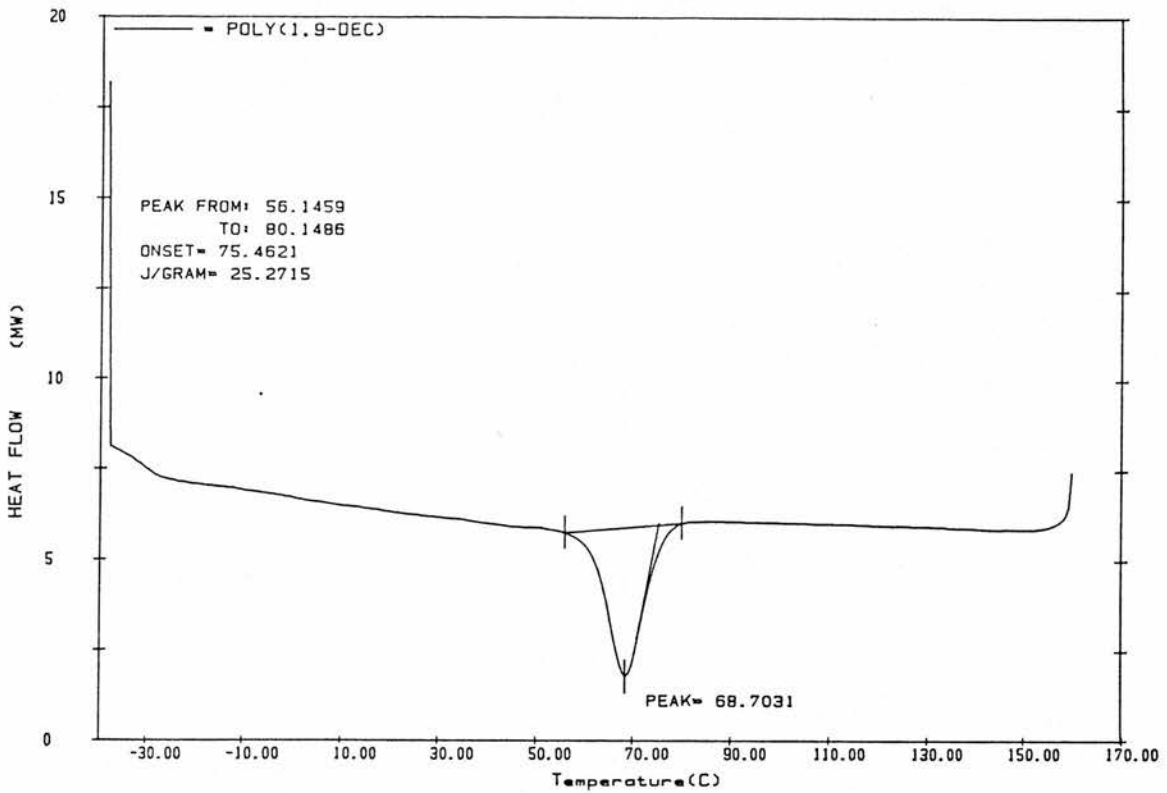


Figure 5.2 scan B DSC thermogram of P19D from 160°C to -40°C (at 10°C/min) 3rd cooling cycle.

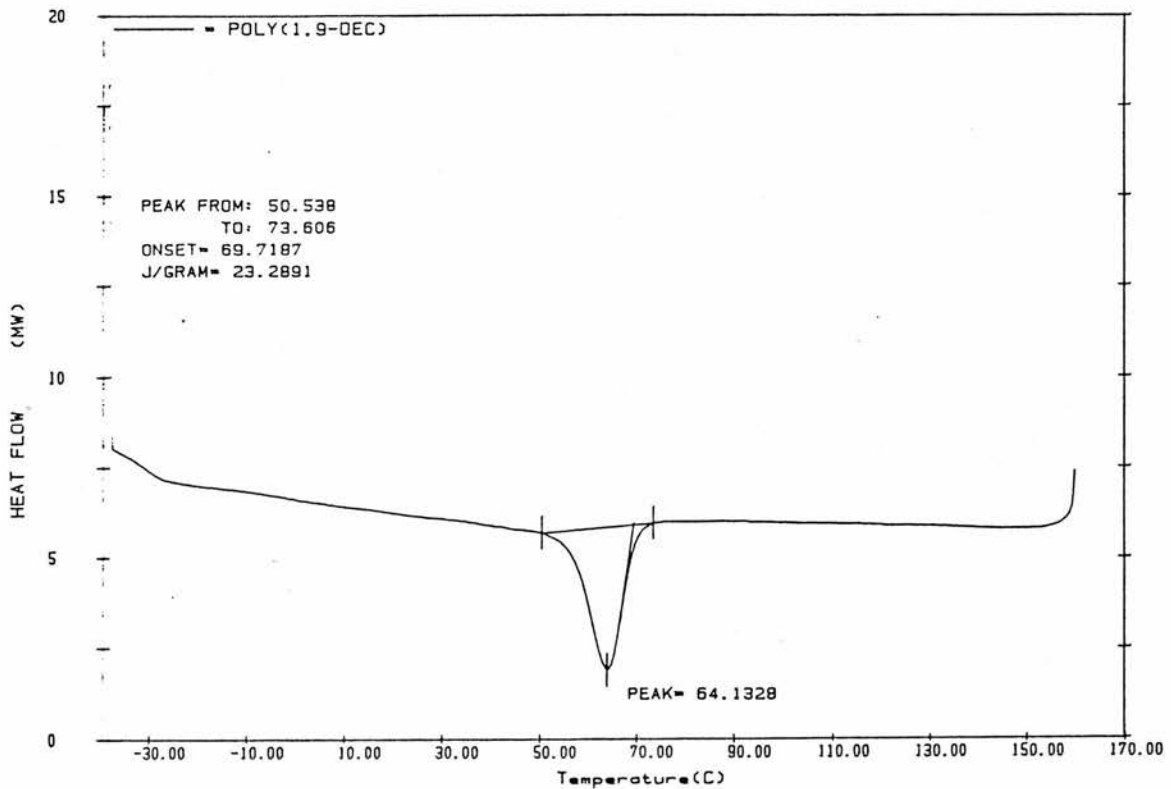


Figure 5.2 scan C DSC thermogram of P19D from 160°C to -40°C (at 10°C/min) 4th cooling cycle.

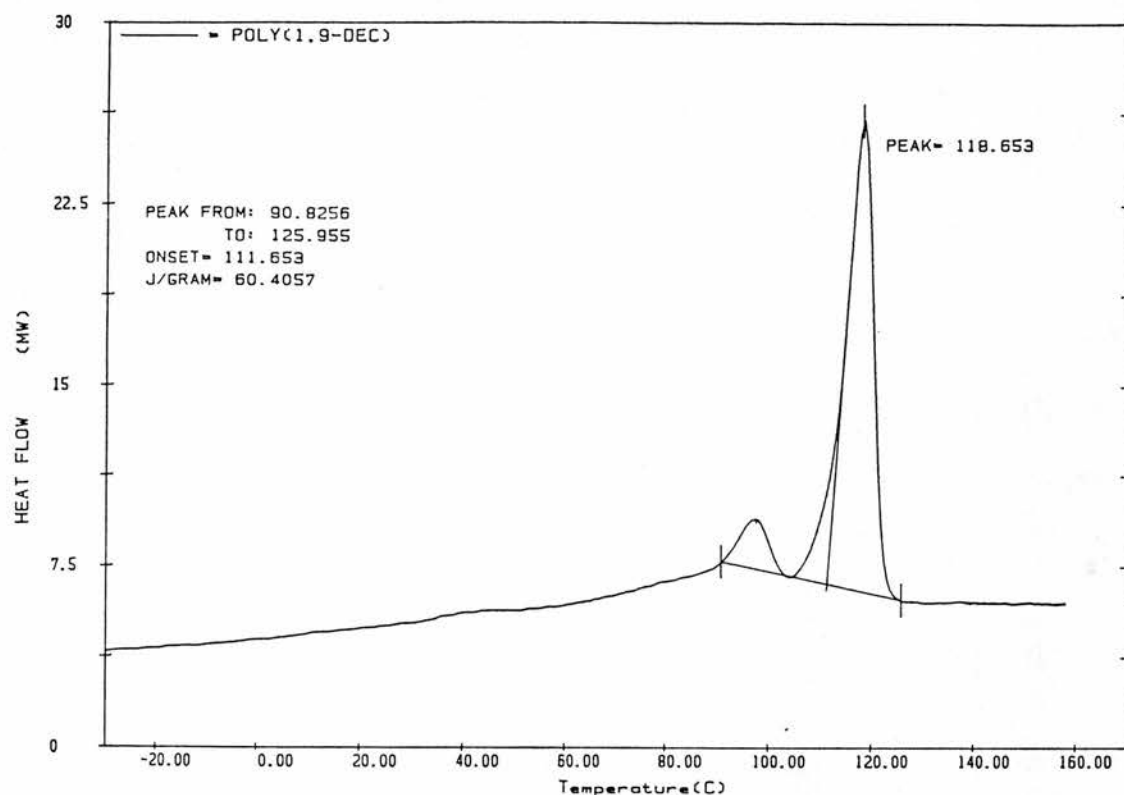


Figure 5.3 DSC thermogram of a solution cast film of P19D from -30°C to 160°C (at $10^{\circ}\text{C}/\text{min}$). Original scan for reference.

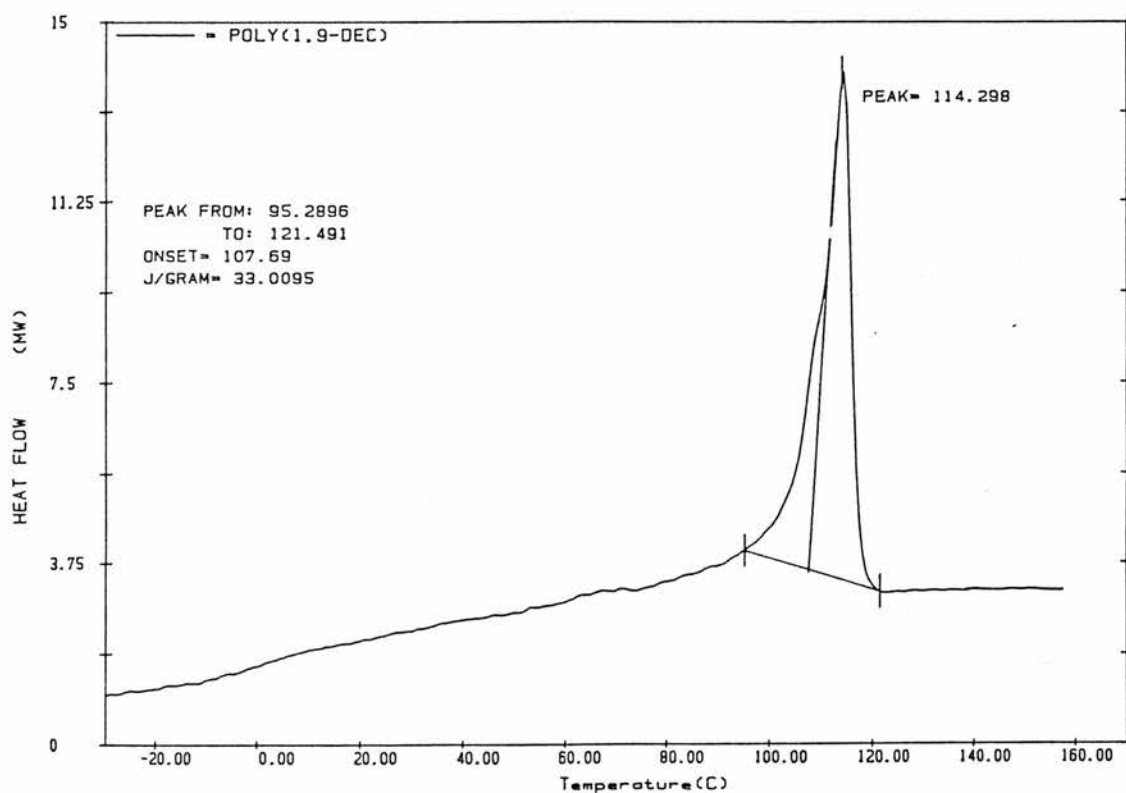


Figure 5.3 scan A - DSC thermogram of a P19D film annealed at 160°C for 0 minutes quenched to -50°C then run from -30°C to 160°C (at $10^{\circ}\text{C}/\text{min}$).

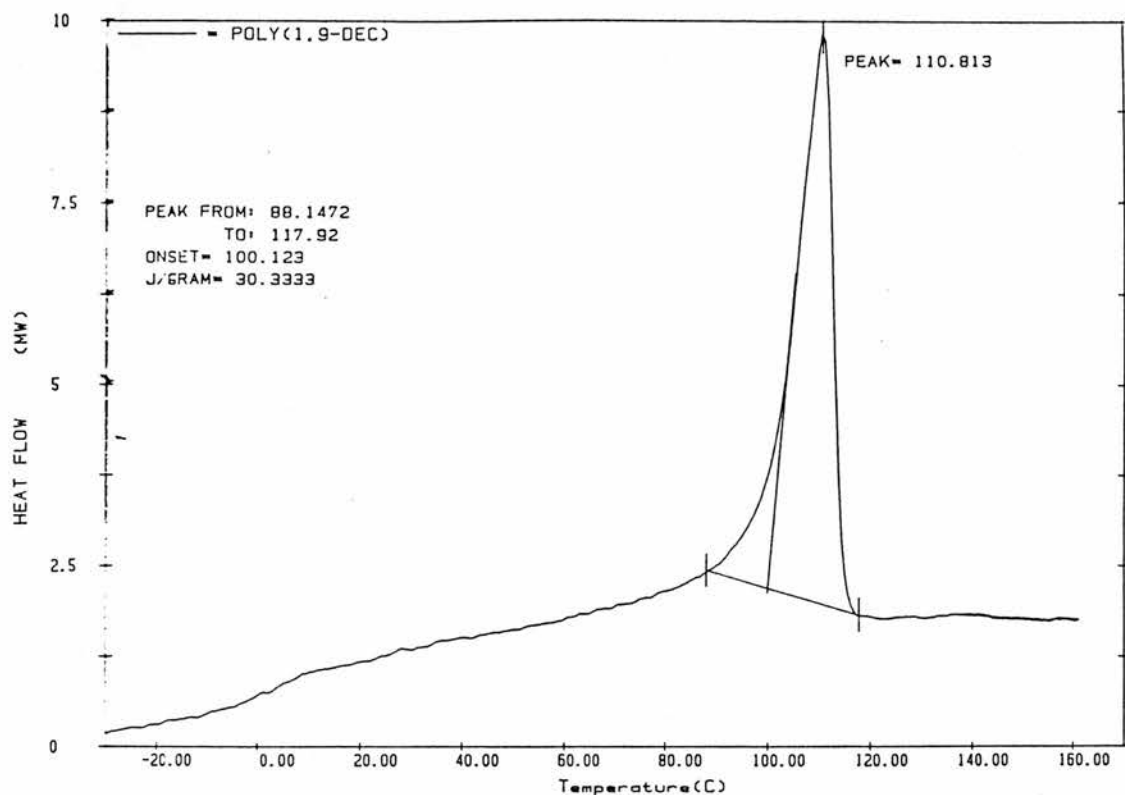


Figure 5.3 scan B - DSC thermogram of a P19D film annealed at 160°C for 10 minutes quenched to -50°C then run from -30°C to 160°C (at 10°C/min).

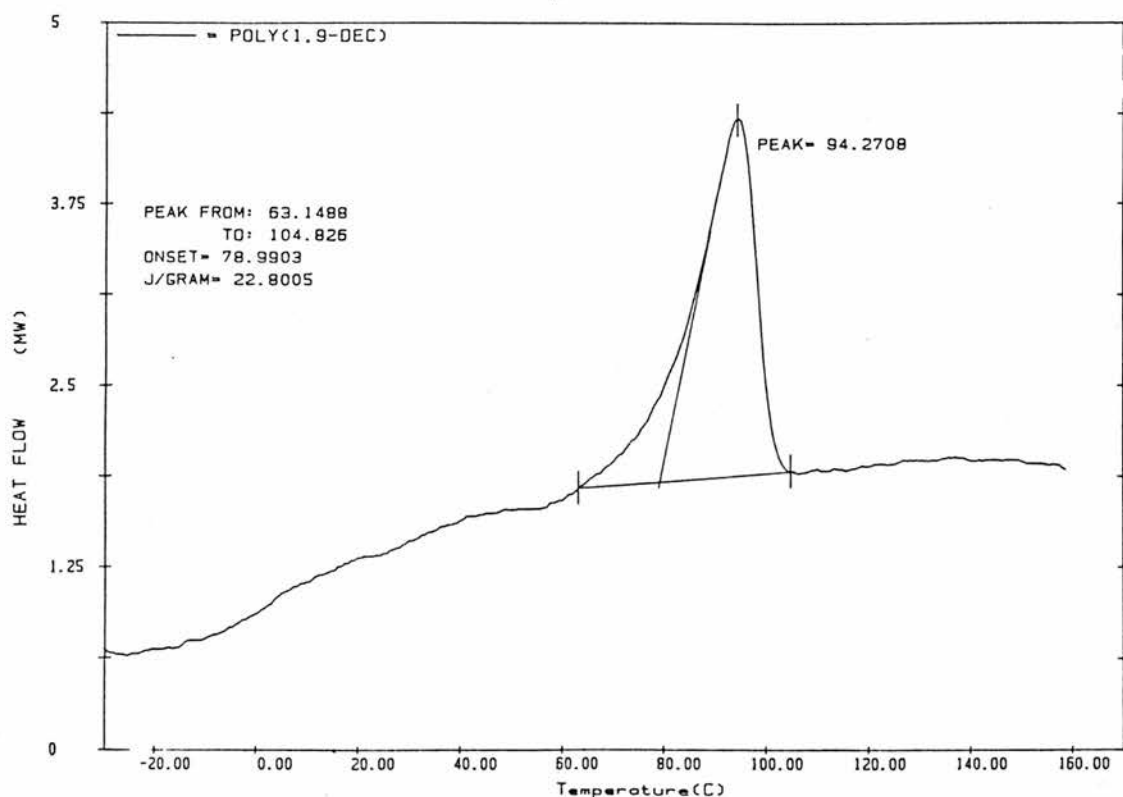


Figure 5.3 scan C - DSC thermogram of a P19D film annealed at 160°C for 20 minutes quenched to -50°C then run from -30°C to 160°C (at 10°C/min).

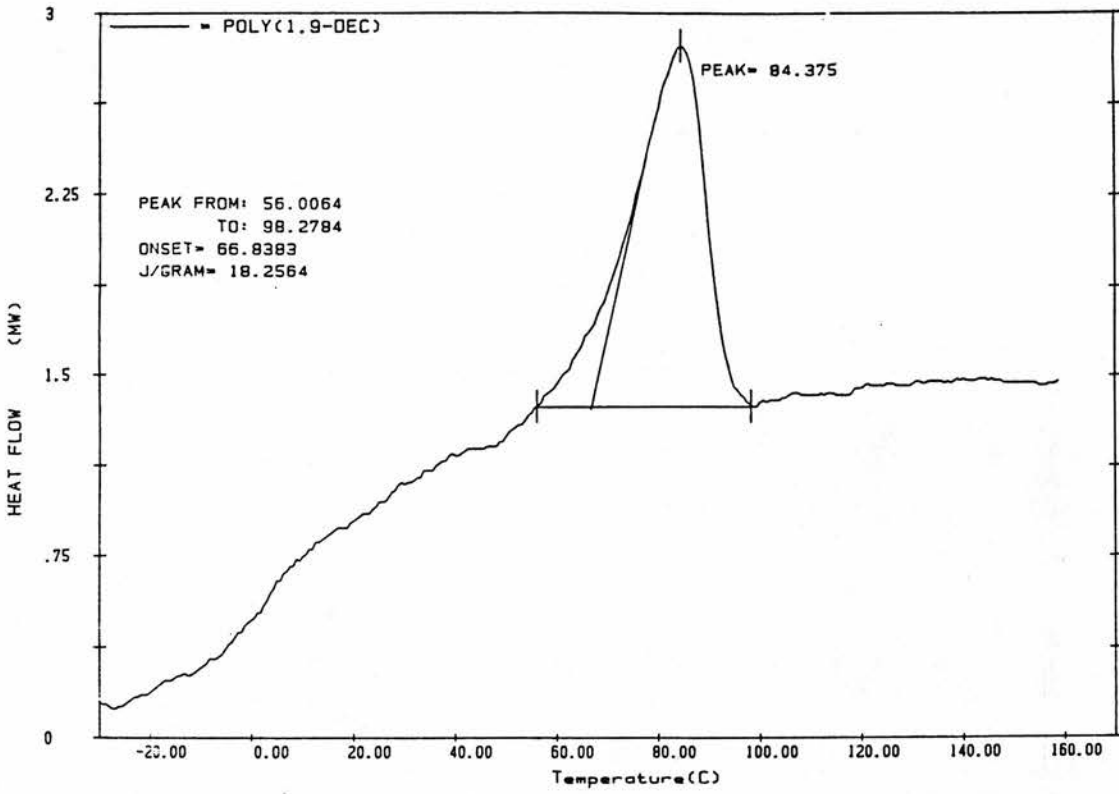


Figure 5.3 scan D - DSC thermogram of a P19D film annealed at 160°C for 30 minutes quenched to -50°C then run from -30°C to 160°C (at 10°C/min).

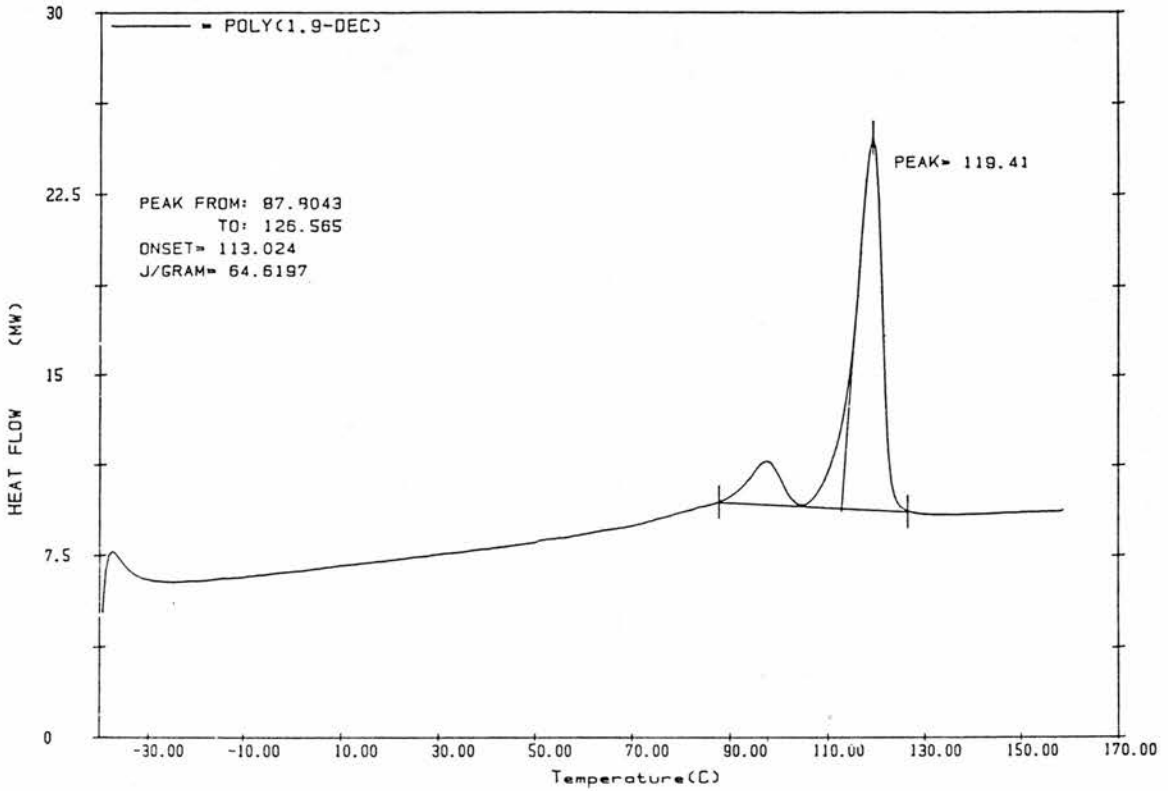


Figure 5.4 DSC thermogram of a solution cast film of P19D from -40°C to 160°C (at $10^{\circ}\text{C}/\text{min}$). Original scan for reference.

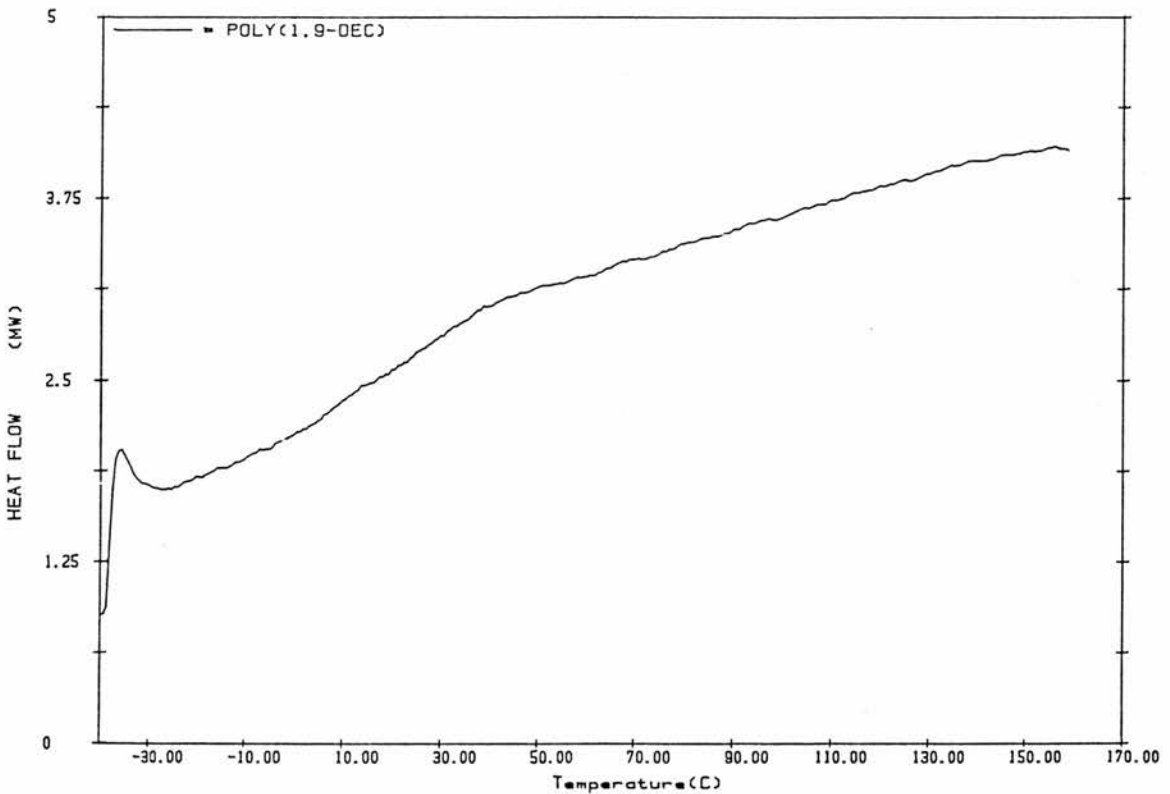


Figure 5.4(a) DSC thermogram of a P19D film annealed at 200°C for 1 hour quenched to -60°C then run from -40°C to 160°C (at $10^{\circ}\text{C}/\text{min}$).

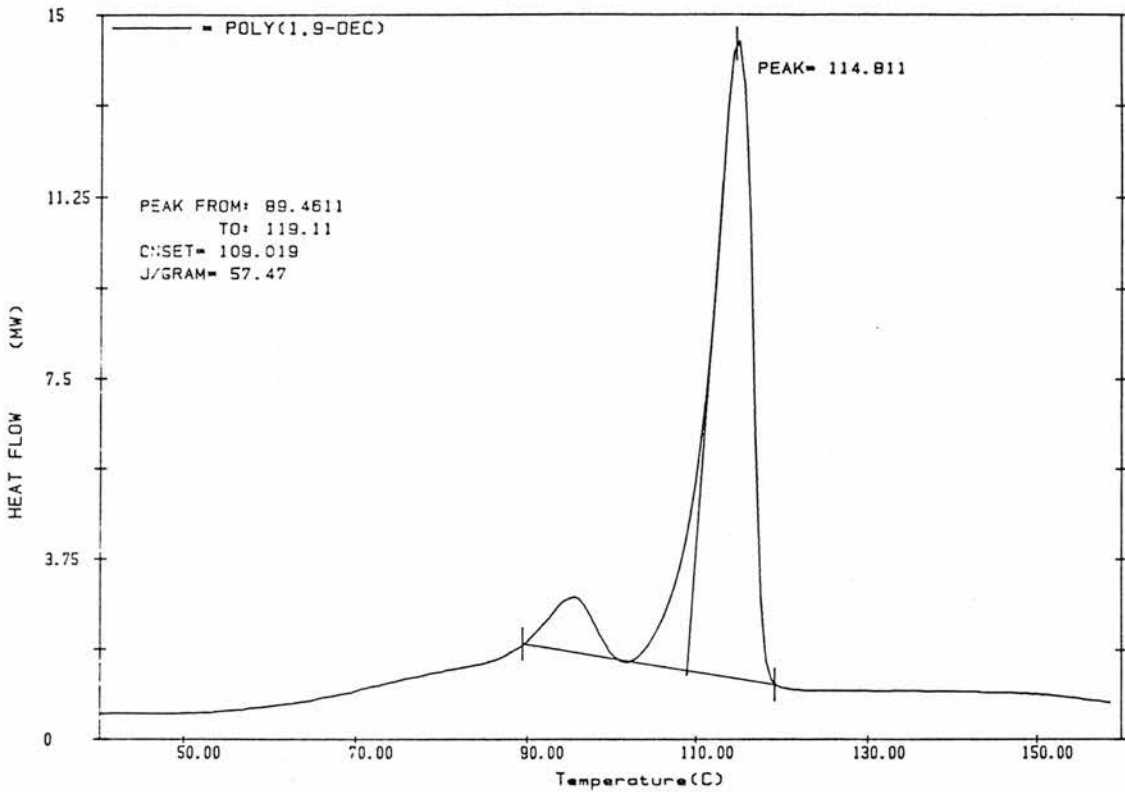


Figure 5.5 DSC thermogram of a solution cast film of P19D from 40°C to 160°C (at 10°C/min). This P19D film had different molar mass characteristics than the previous P19D samples used.

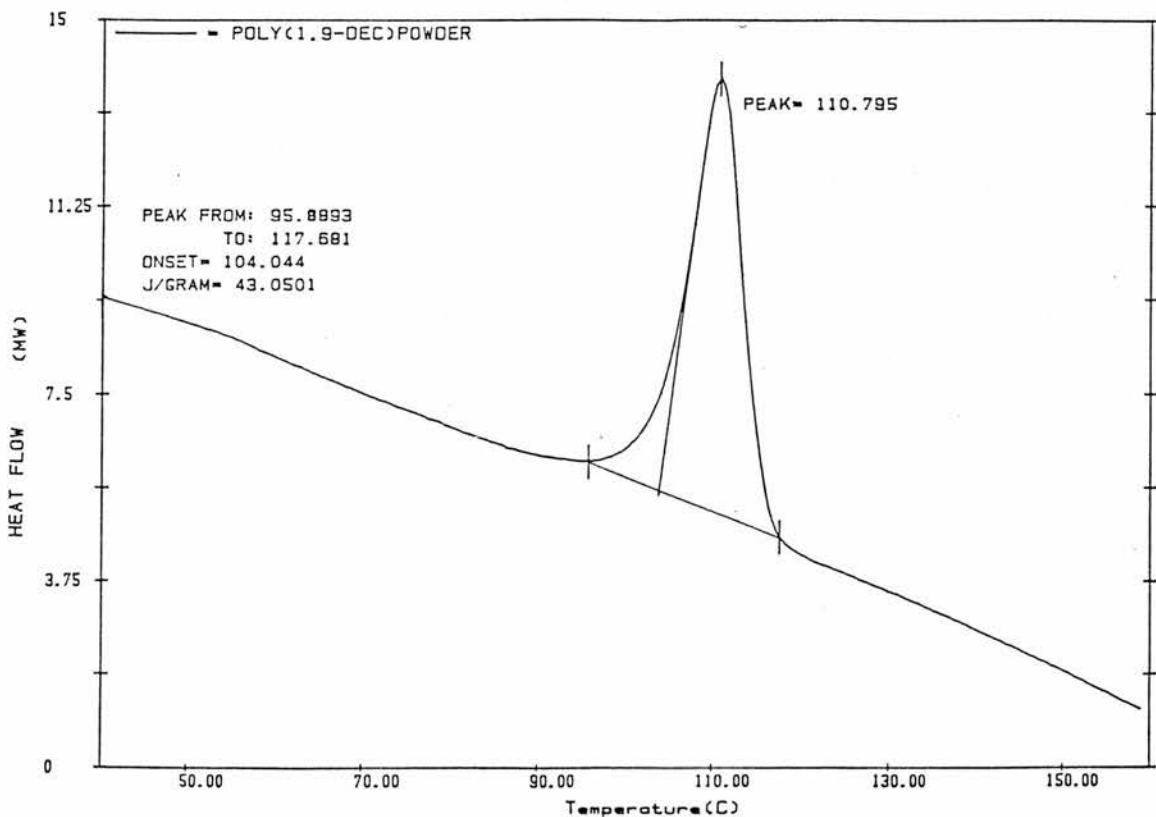


Figure 5.5(a) DSC thermogram of a P19D powder sample of the above polymer from 40°C to 160°C (at 10°C/min).

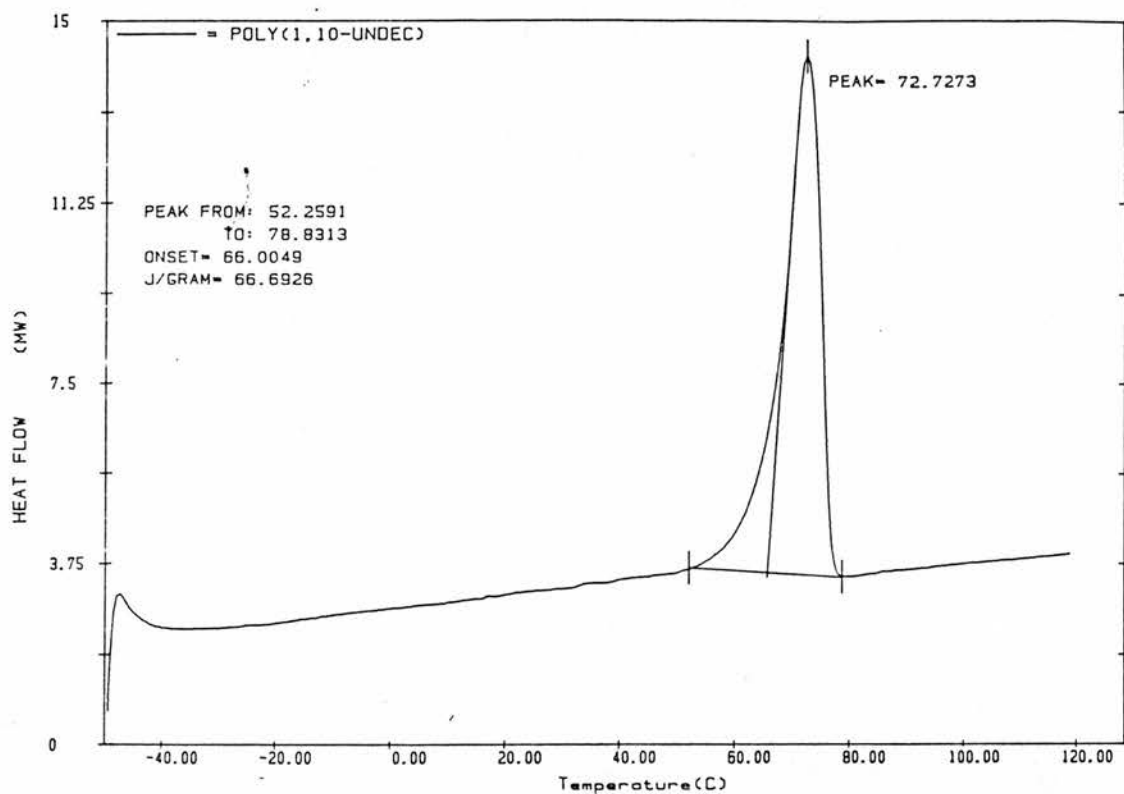


Figure 5.6 DSC thermogram of a solution cast film of P110U from -50°C to 120°C (at 10°C/min). 1st heating cycle. Original scan.

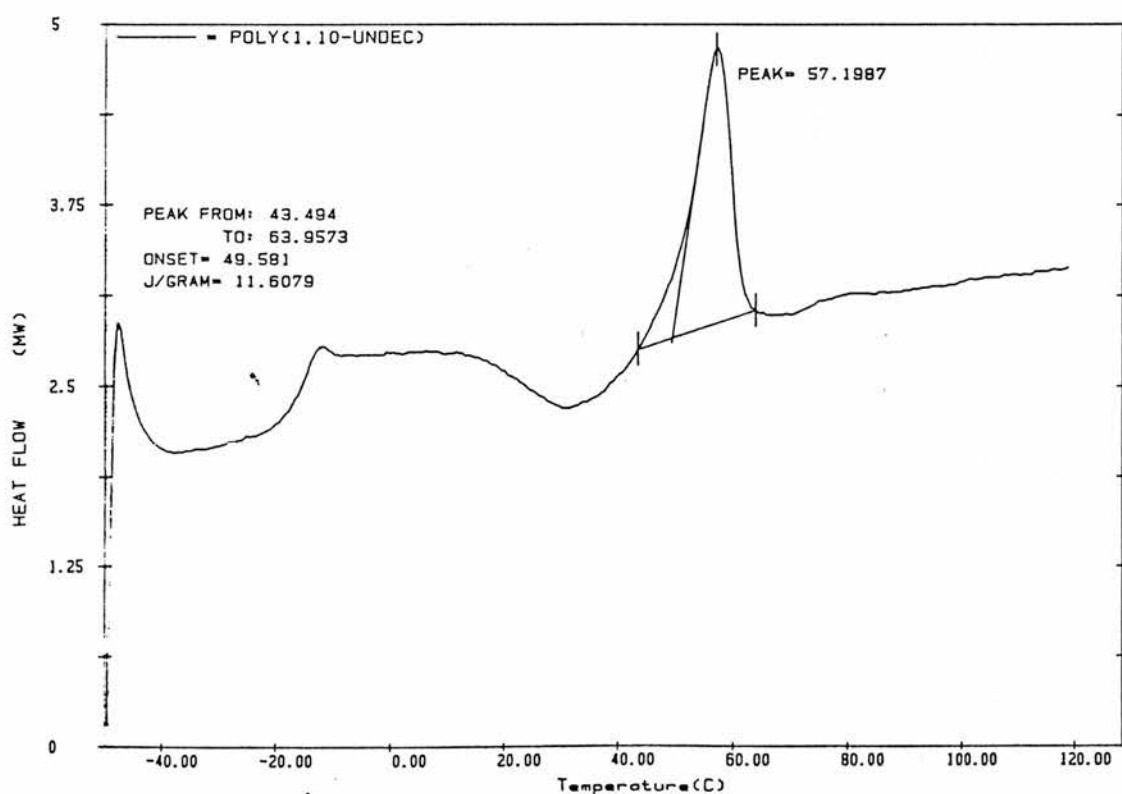


Figure 5.6 scan A DSC thermogram of P110U from -50°C to 120°C (at 10°C/min). 2nd heating cycle. T_m calculation is shown.

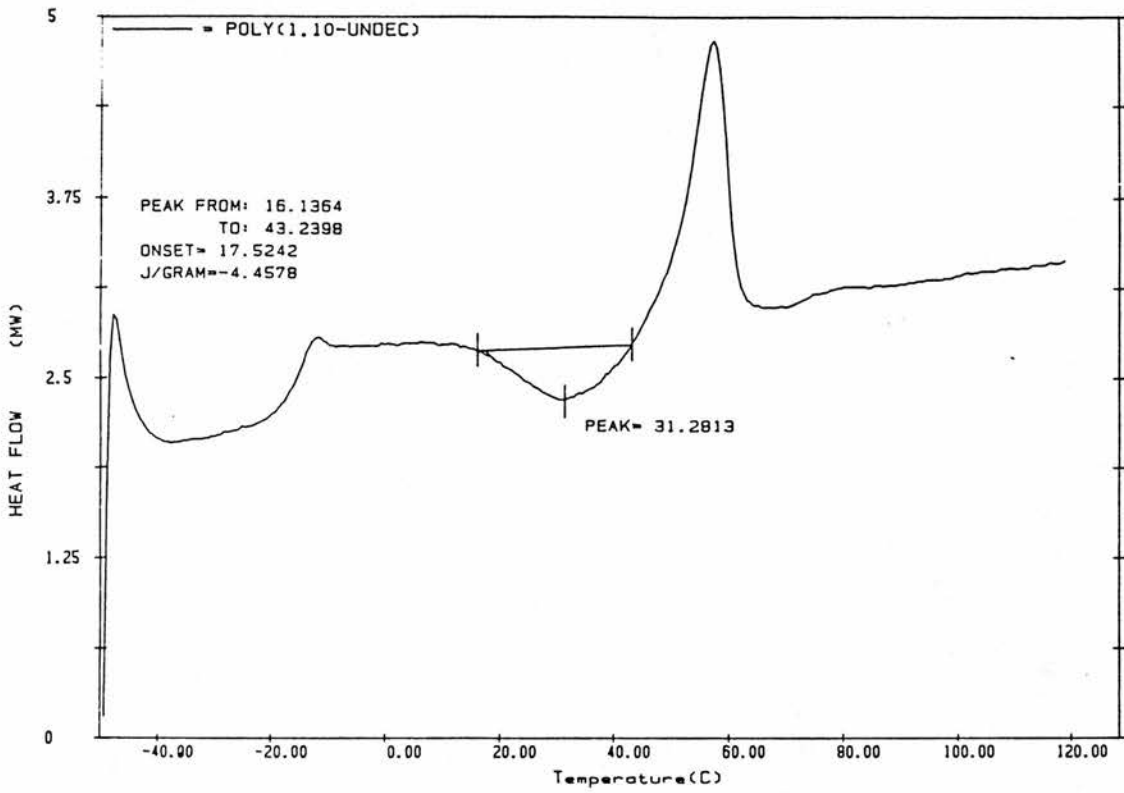


Figure 5.6 scan A T_c calculation.

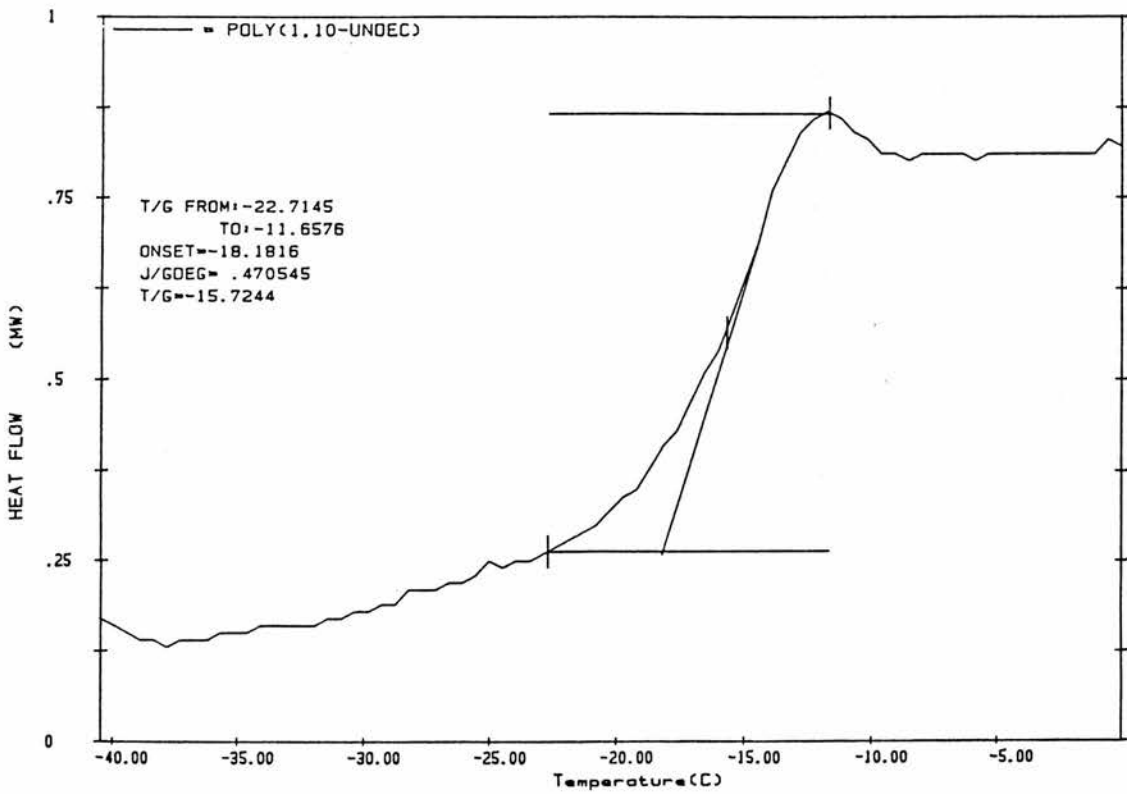


Figure 5.6 scan A T_g calculation.

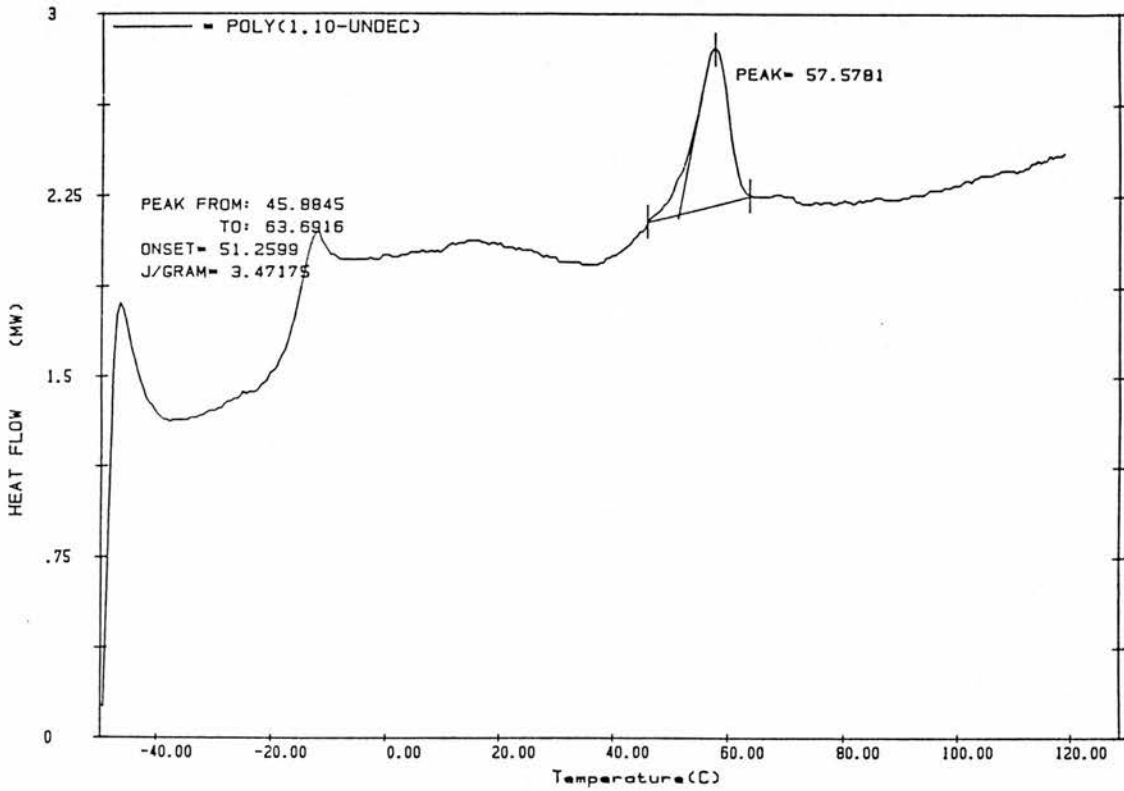


Figure 5.6 scan B DSC thermogram of P110U from -50°C to 120°C (at 10°C/min). 3rd heating cycle. T_m calculation is shown.

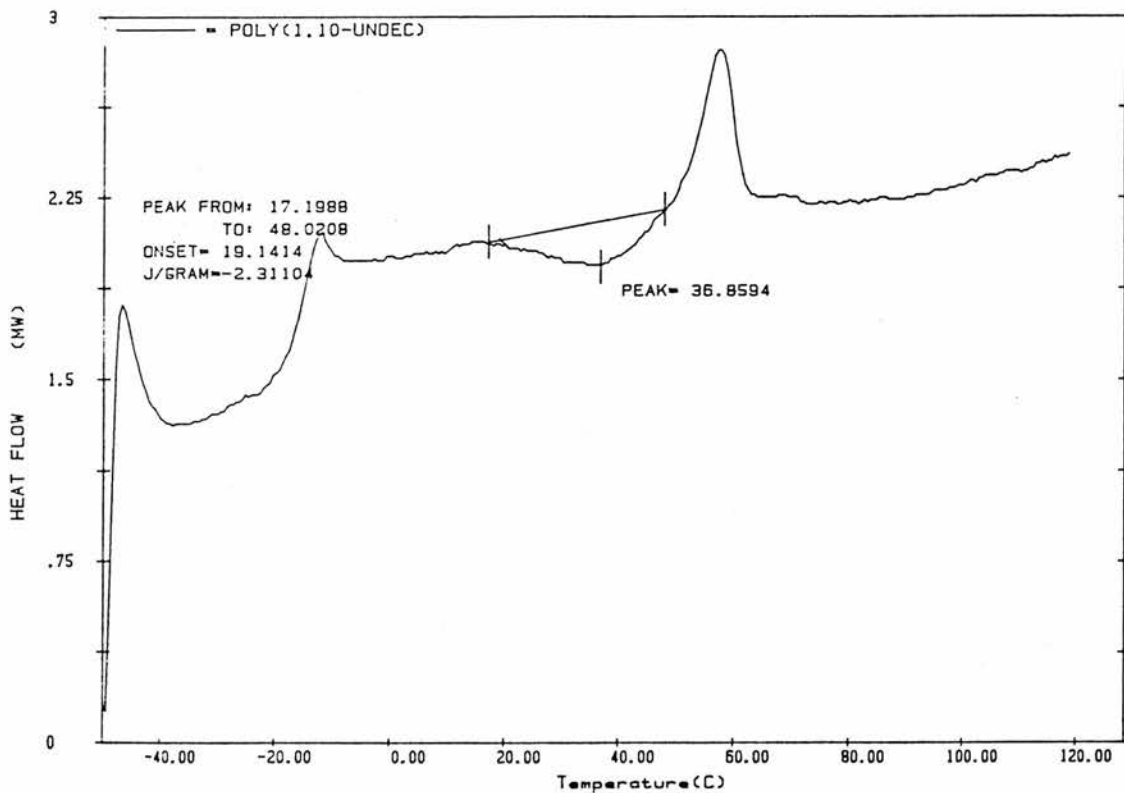


Figure 5.6 scan B T_c calculation.

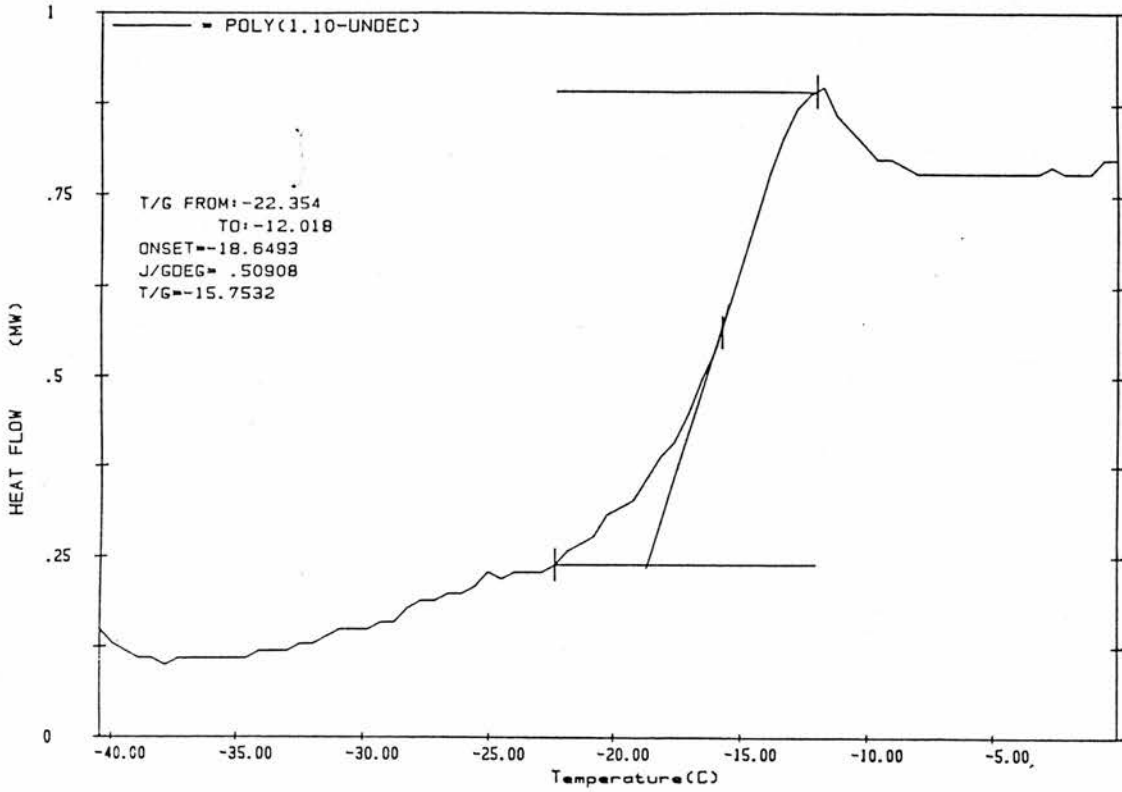


Figure 5.6 scan B Tg calculation.

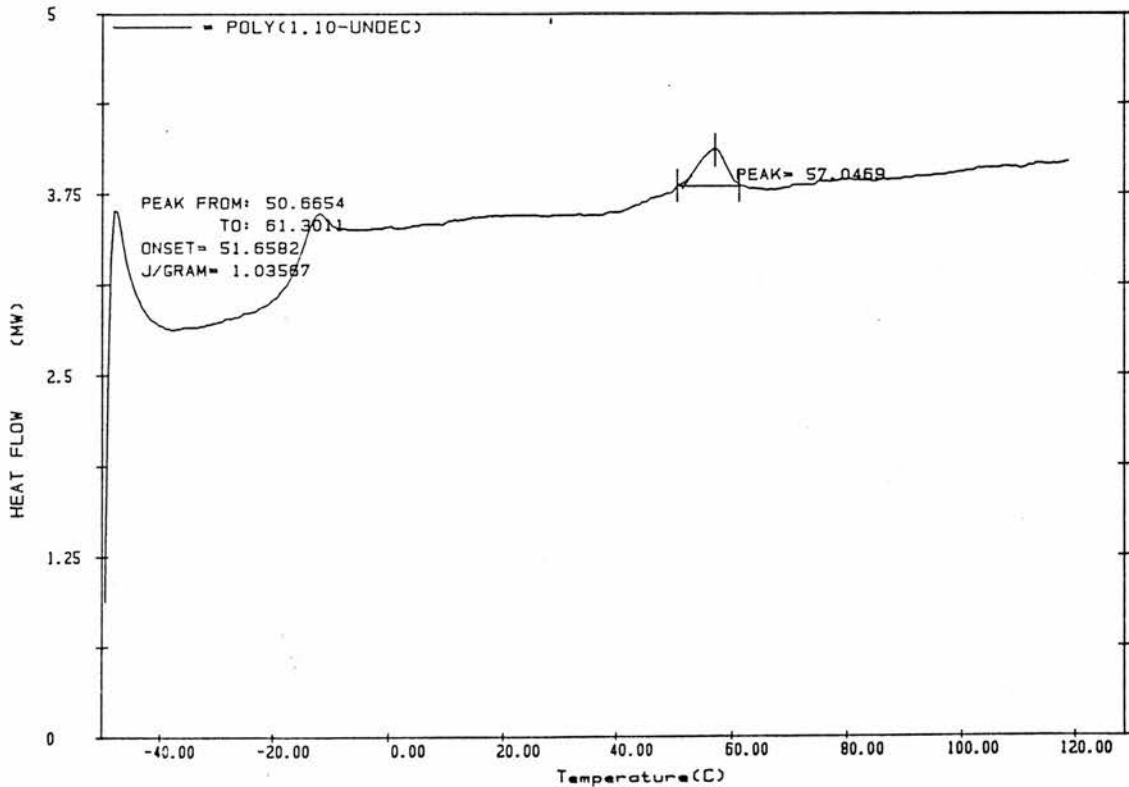


Figure 5.6 scan C DSC thermogram of P110U from -50°C to 120°C (at 10°C/min). 4th heating cycle. Tm calculation is shown.

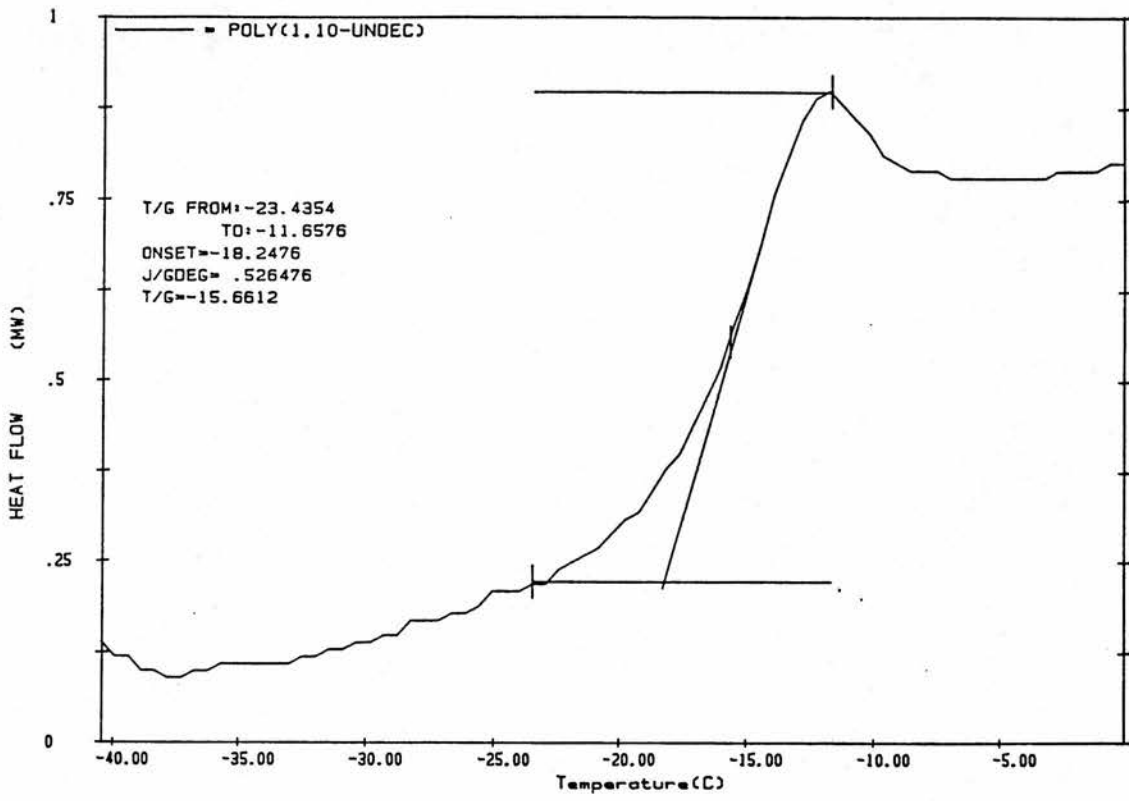


Figure 5.6 scan C Tg calculation.

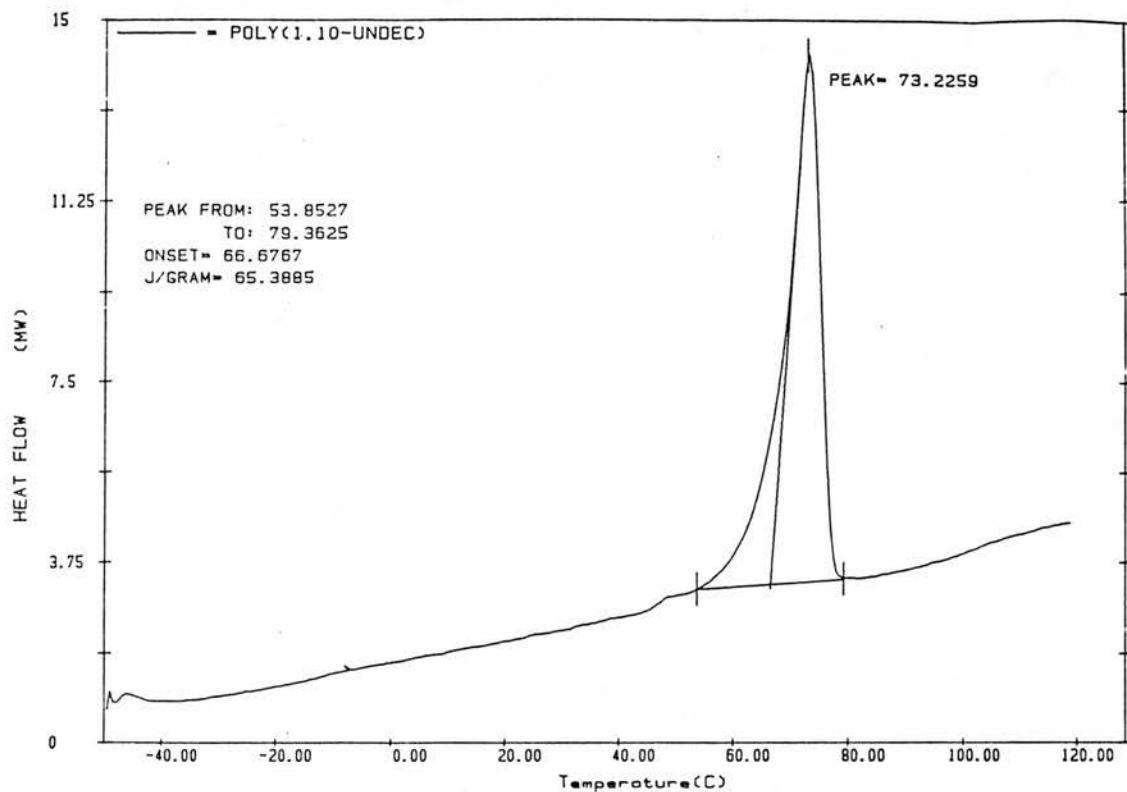


Figure 5.7 DSC thermogram of a solution cast film of P110U from -50°C to 120°C (at 10°C/min). Original scan for reference.

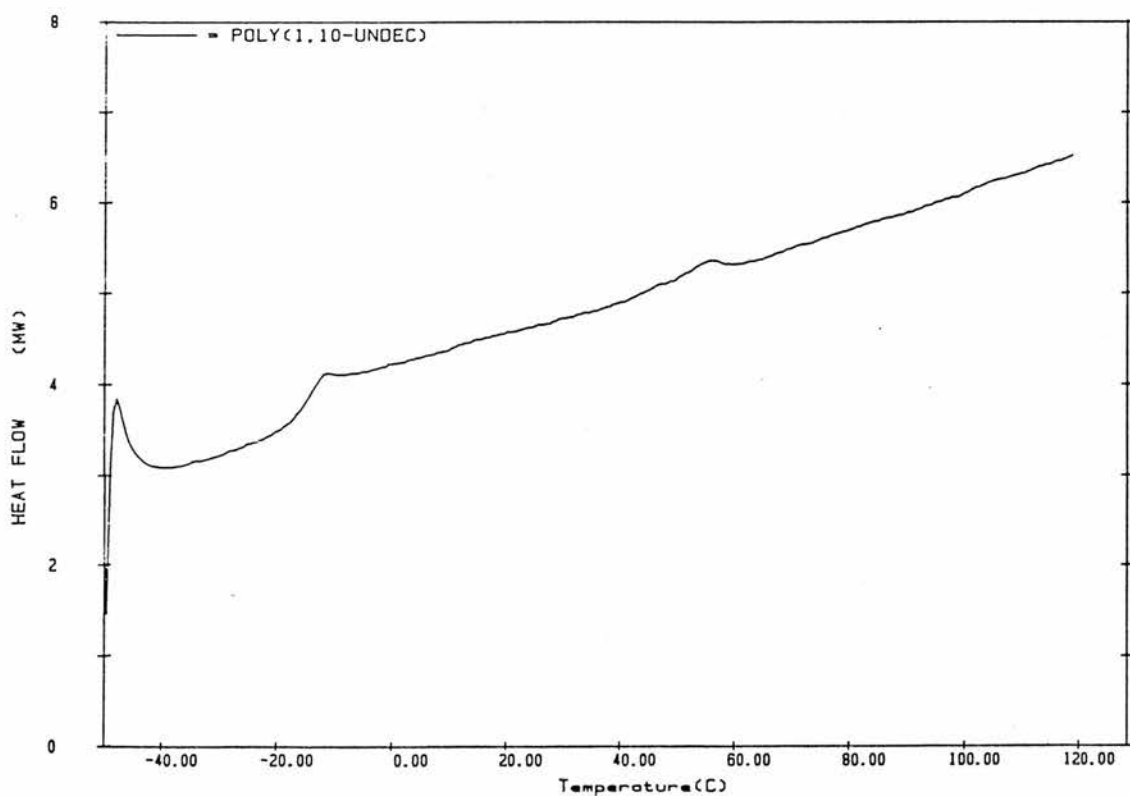


Figure 5.7 scan A DSC thermogram of a P110U film annealed at 120°C for 15 minutes quenched to -70°C then run from -50°C to 120°C (at 10°C/min).

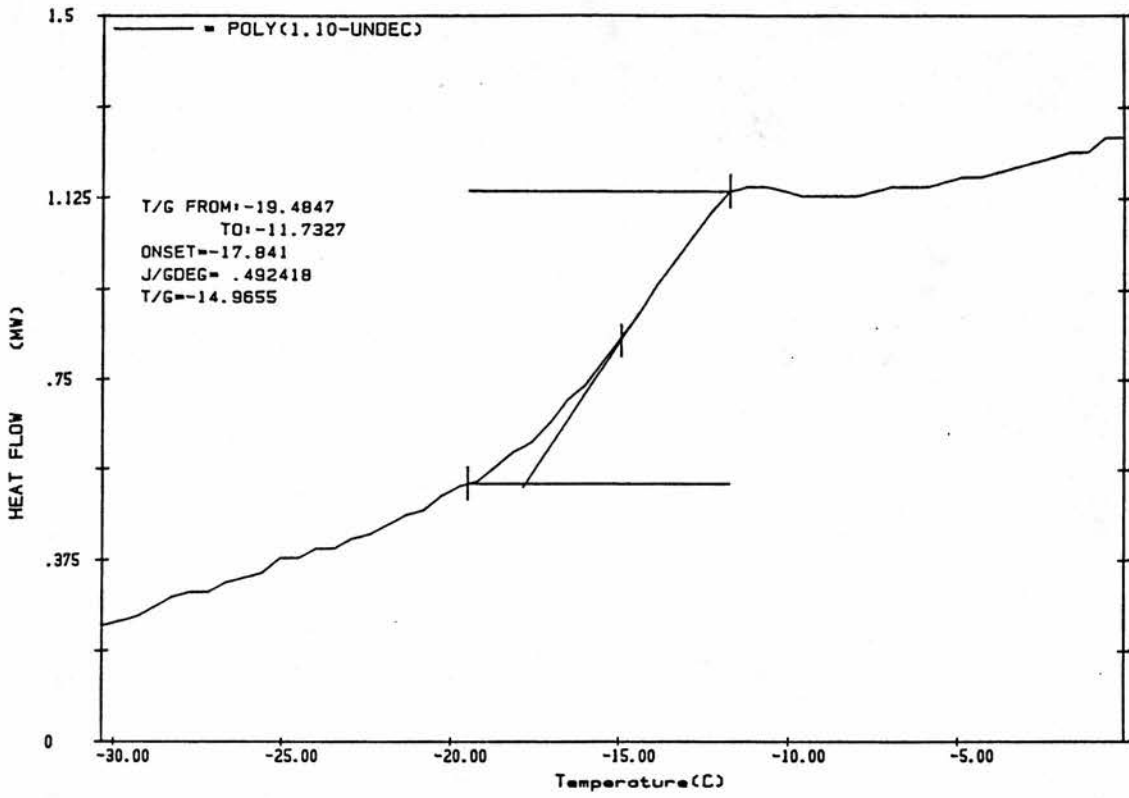
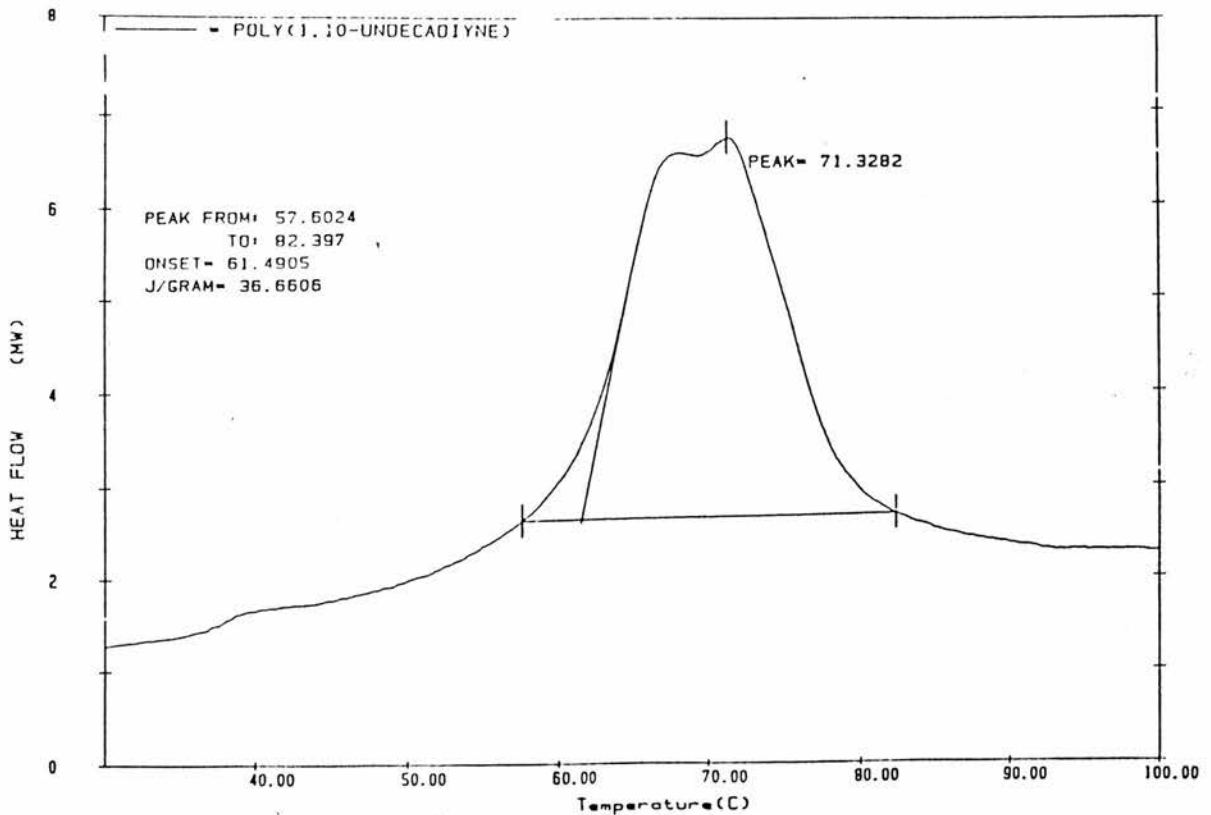
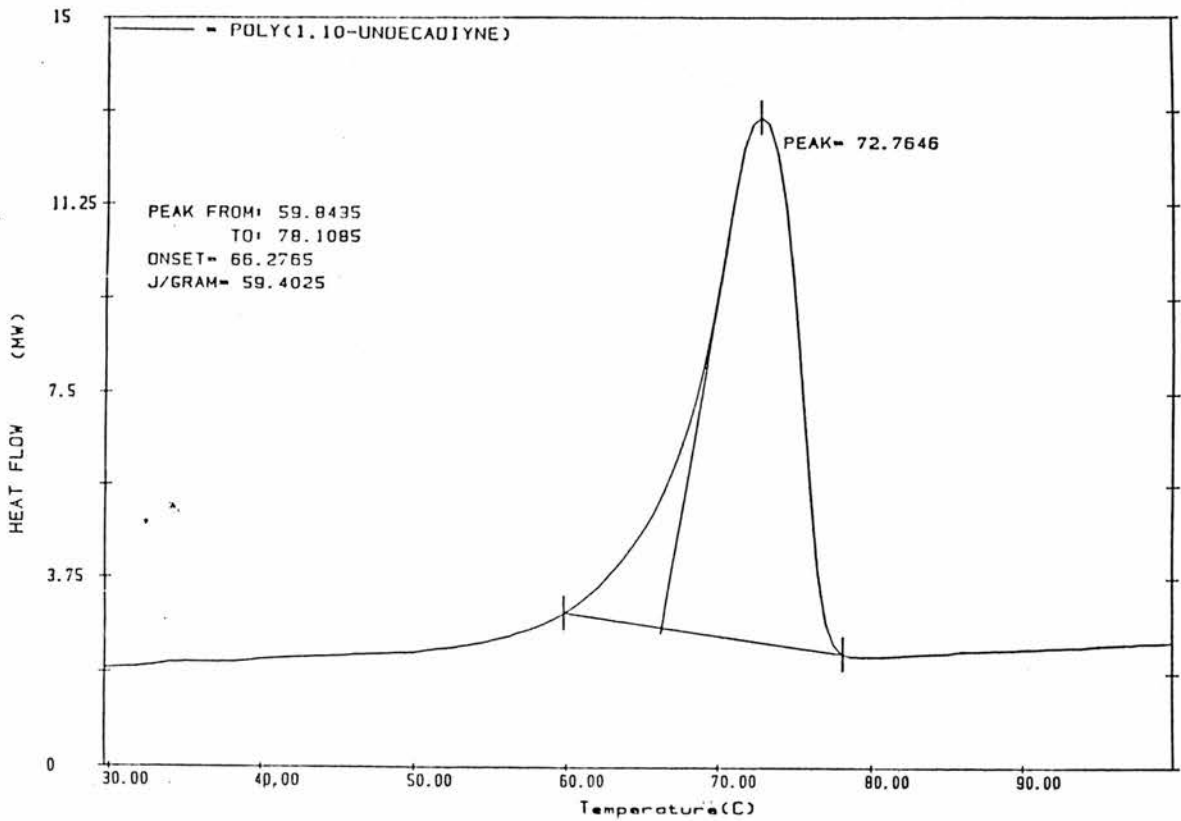


Figure 5.7 scan A Tg calculation from the previous thermogram.



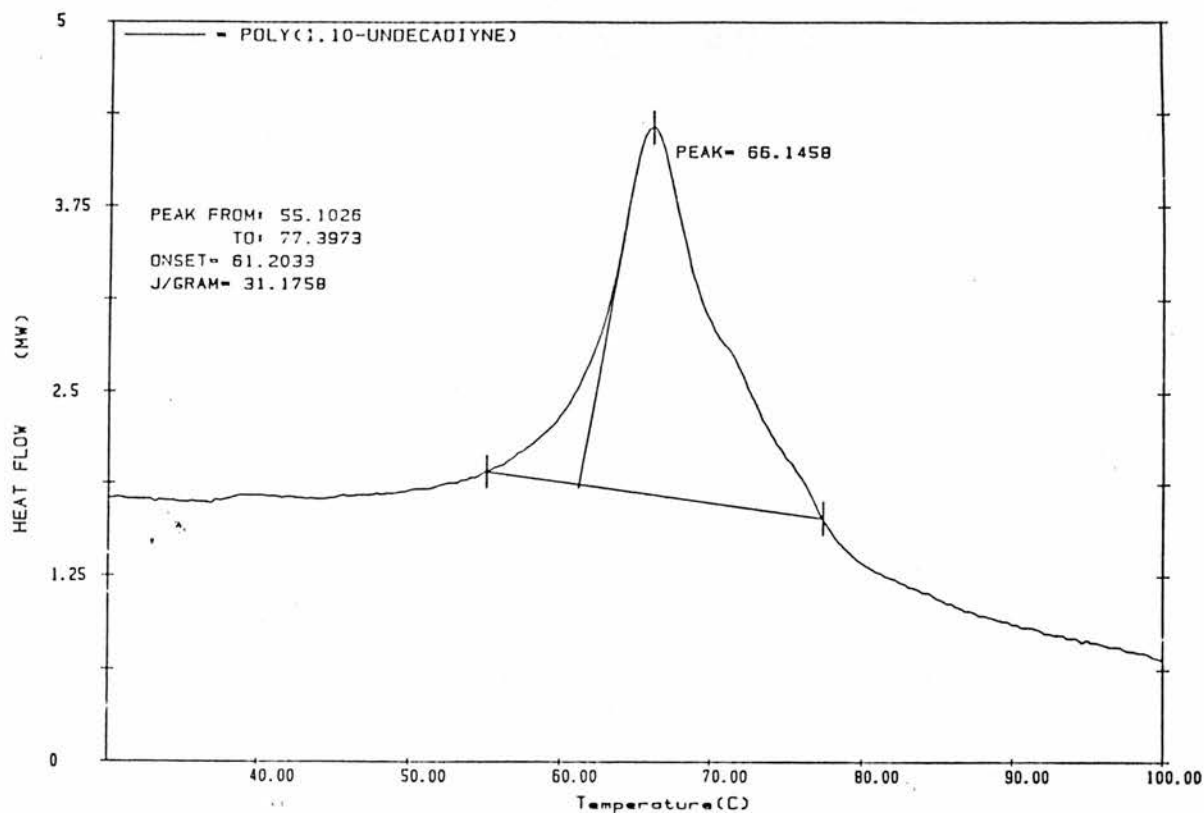


Figure 5.8(c) DSC thermogram of a solution cast film of P110U from 40°C to 120°C (at 10°C/min). UV irradiation time = 2 minutes.

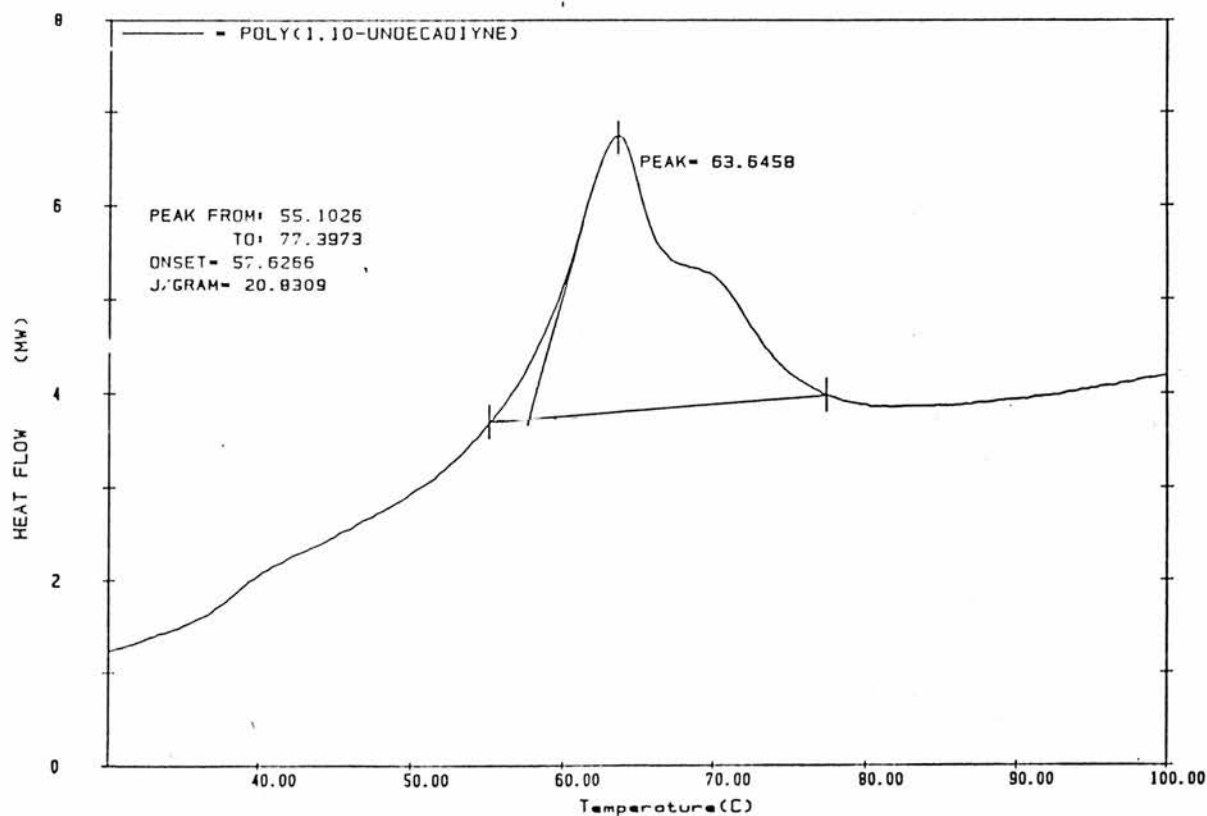


Figure 5.8(d) DSC thermogram of a solution cast film of P110U from 40°C to 120°C (at 10°C/min). UV irradiation time = 5 minutes.

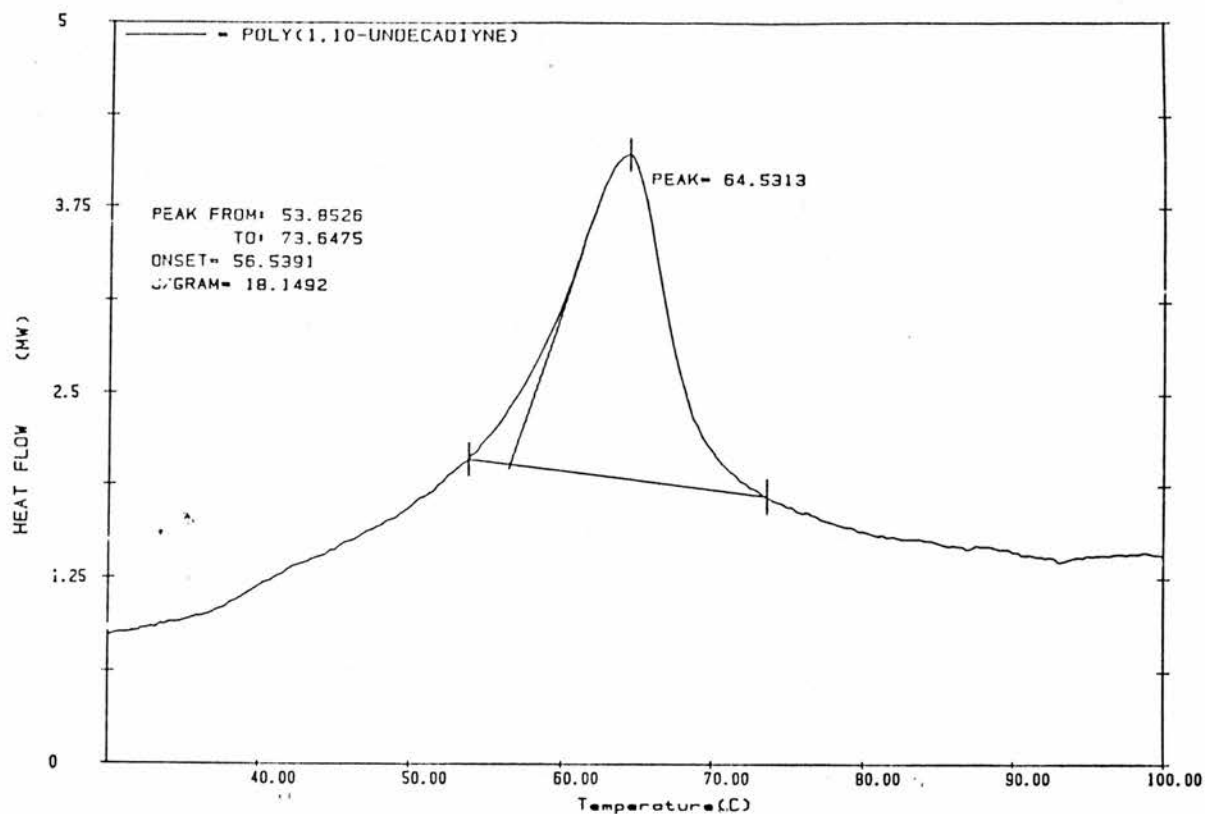


Figure 5.8(e) DSC thermogram of a solution cast film of P110U from 40°C to 120°C (at 10°C/min). UV irradiation time = 10 minutes.

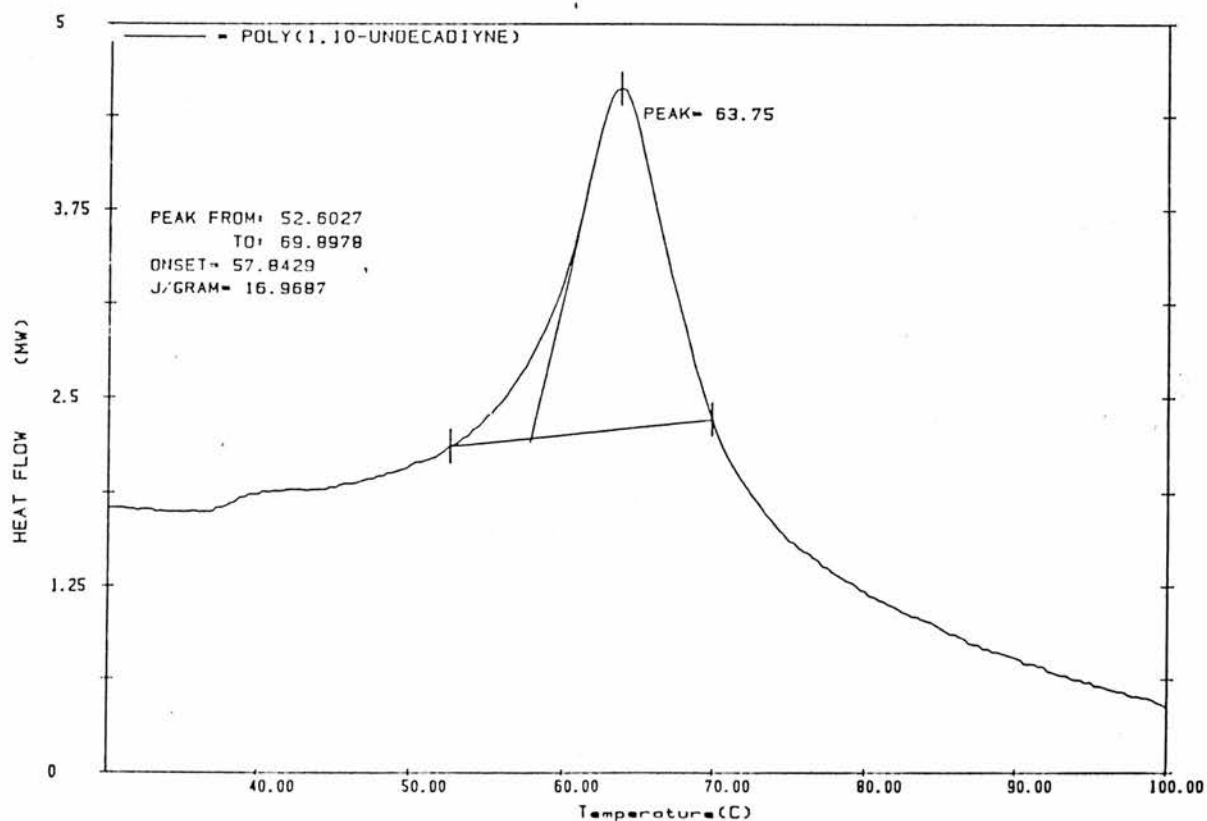


Figure 5.8(f) DSC thermogram of a solution cast film of P110U from 40°C to 120°C (at 10°C/min). UV irradiation time = 15 minutes.

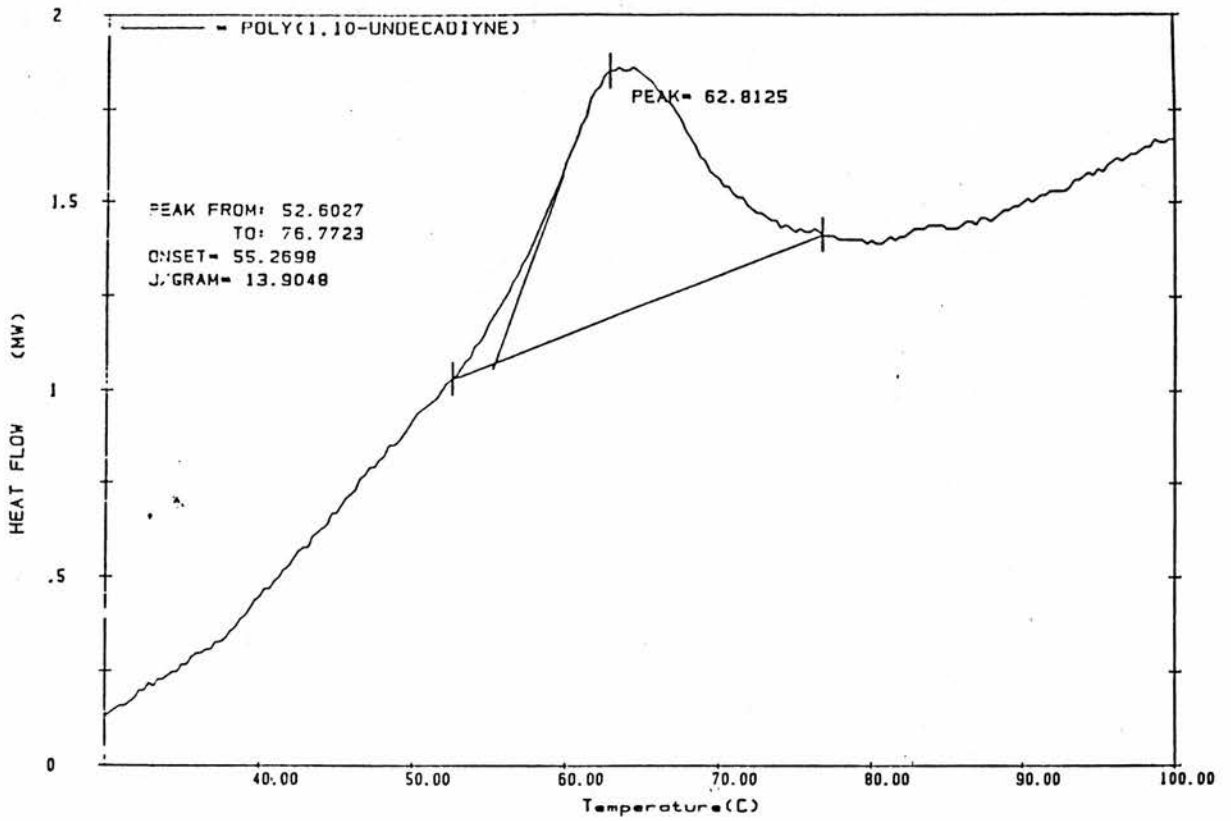


Figure 5.8(g) DSC thermogram of a solution cast film of P110U from 40°C to 120°C (at 10°C/min). UV irradiation time = 20 minutes.

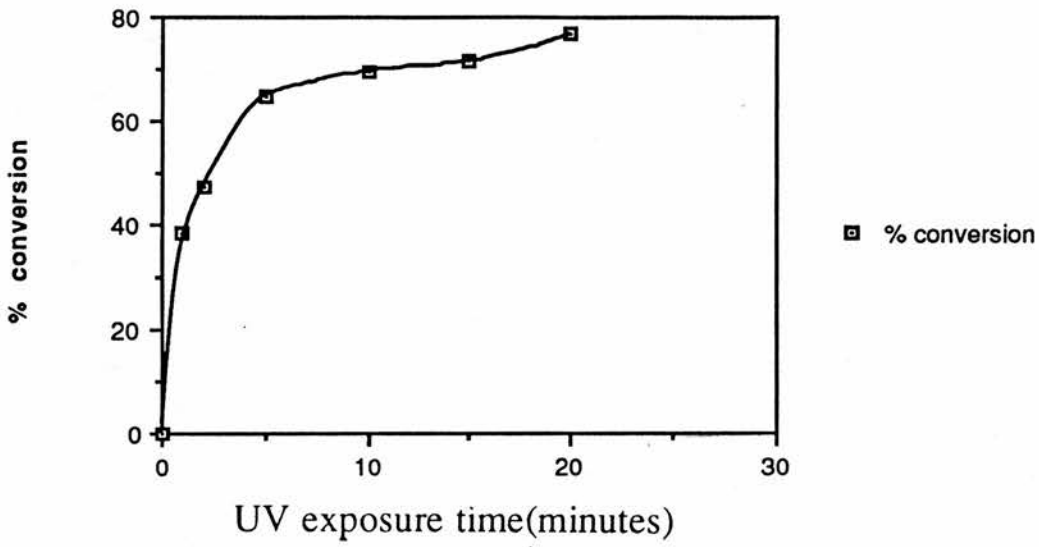


Figure 5.9 Percentage conversion to cross-polymerised form as a function of UV exposure time(minutes) for P110U.

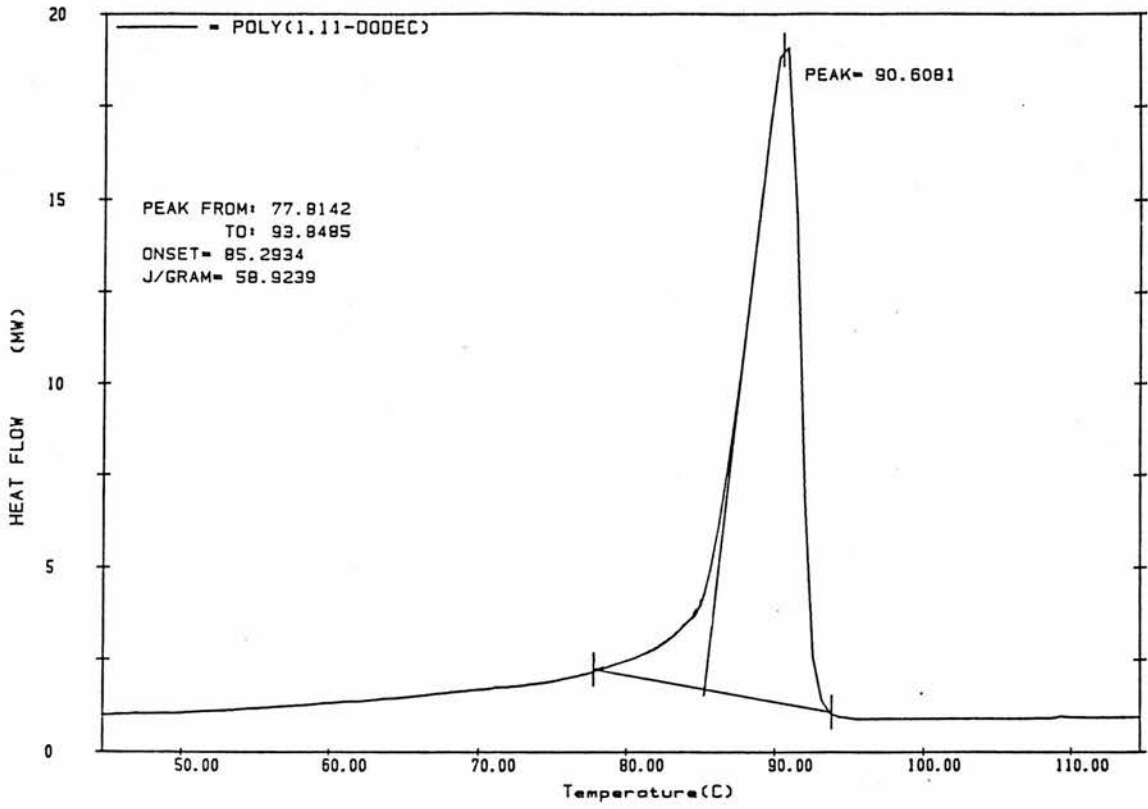


Figure 5.10 DSC thermogram of a solution cast film of P111D from 40°C to 120°C (at 10°C/min).

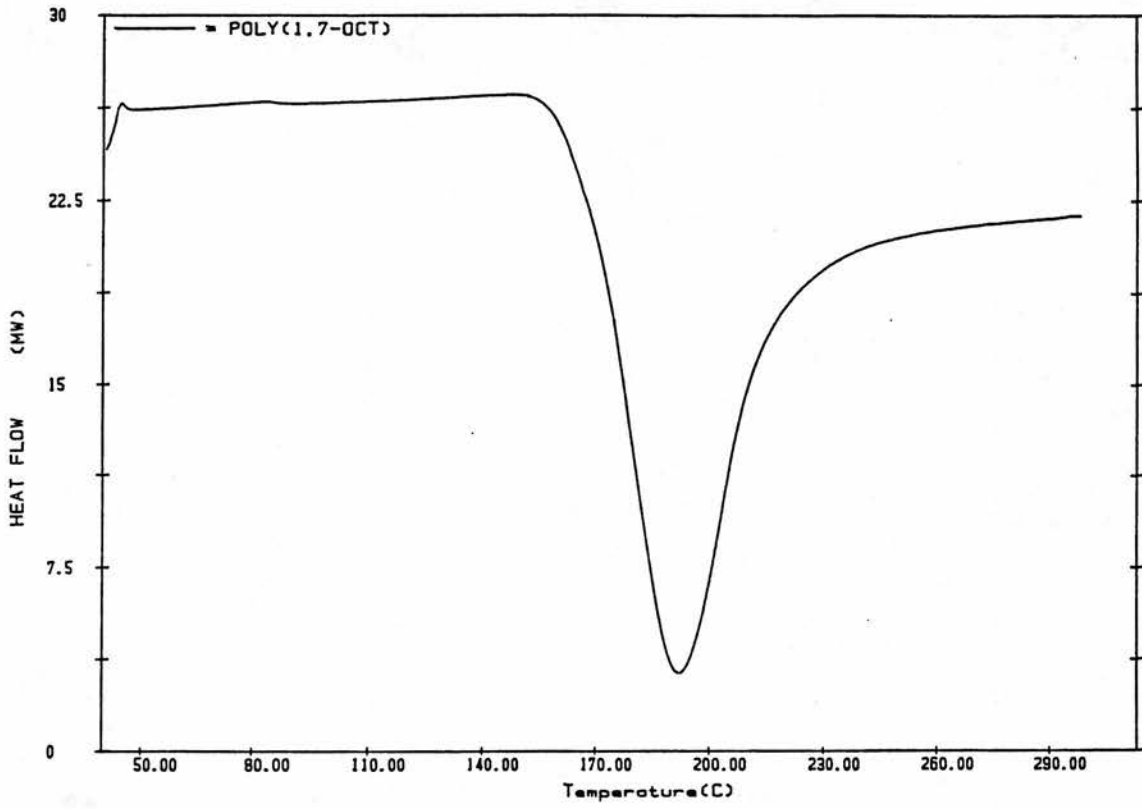


Figure 5.11 DSC thermogram of a P170 powder from 40°C to 300°C (at 10°C/min).

CHAPTER 6

GENERAL BEHAVIOUR OF

POLY(α,ω -ALKYLDIYNES) AND

COPOLY(α,ω -ALKYLDIYNES)

6.1 Introduction

The first section of this chapter deals with the photochemical behaviour of poly(1,9-decadiyne), poly(1,10-undecadiyne) and poly(1,11-dodecadiyne). Visible spectra are recorded for these polymers between 400 nm and 700 nm for increasing exposure to UV light at 254 nm. The kinetics for the photochemical cross-polymerisation reaction are studied for the first five minutes of UV exposure. Plots for Absorbance at 650 nm for the photochemical cross-polymerisation reaction are carried out and the reaction order is determined. The reaction kinetics for the photochemical cross-polymerisation is then discussed.

The next section of work involves UV studies and DSC studies on a 50:50 copolymer powder and copolymer film of poly(1,9-decadiyne) and poly(1,10-undecadiyne). Colour changes upon UV exposure are investigated in both the powder and film of the copolymer. DSC studies on the copolymer powder involve thermal cycling, annealing and quenching studies observing any crystallisation and melting behaviour of the copolymer. DSC studies on the copolymer film are also carried out. Finally the thermal cross-polymerisation at room temperature of the copolymer film and powder is studied.

Conductivity studies are carried out using a 2-point DC measurement system on cross-polymerised films of poly(1,9-decadiyne) and poly(1,11-dodecadiyne). Two methods for the treatment of these polymer films for conductivity measurements are investigated. Resonance Raman spectra are recorded on the cross-polymerised polymers before and after iodine doping observing for any structural

differences. Characterisation of the product from the polymerisation of 1,7-octadiyne (polymerised by route A at 65°C for 5 hours) is carried out using solid state ^{13}C nmr spectroscopy and mass spectroscopy. (This product was found to be insoluble in a range of solvents as shown in 3.4.3).

Finally recommendations for future research α,ω -diyne type polymers is discussed from the work carried out in this thesis.

6.2 Experimental details

Materials: synthesis of poly(1,7-octadiyne), poly(1,9-decadiyne), poly(1,10-undecadiyne), poly(1,11-dodecadiyne) and 50:50 poly(1,9-decadiyne):poly(1,10-undecadiyne).

All the above mentioned polymers were polymerised using the procedure for polymerisation route A outlined in Chapter 3. All were polymerised for 5 hours at 65°C.

Molar mass characteristics: Molar mass characteristics were determined by GPC in Chapter 4 for all polymers excluding poly(1,7-octadiyne).

	Mn	Mw	PDI
poly(1,9-decadiyne)	29,300	180,000	6.14
poly(1,10-undecadiyne)	28,300	59,200	2.09
poly(1,11-dodecadiyne)	14,100	32,100	2.28
50:50 poly(1,9-dec): poly(1,10-undec)	28,300	59,600	2.11

Cross-polymerisation

Cross-polymerisation of poly(1,9-decadiyne), poly(1,10-undecadiyne) and poly(1,11-dodecadiyne) was induced by exposing thin films of the polymers to UV light (1600 $\mu\text{W}/\text{cm}^2$ at 254 nm) under a nitrogen purge. The films were prepared in a similar fashion to those described in Chapter 5 (5.2). The films were formed by casting a 1% weight/volume methylene chloride solution of the chosen polymer onto

a quartz plate* (for use in the visible spectroscopy studies), placed under a petri dish (to control solvent evaporation). The process was carried out on top of a levelled glass plate to ensure film uniformity. Also, the film casting procedure was always carried out in a dark environment. The films were dried in a vacuum oven in the dark for about 30–45 minutes prior to use.

*In chapter 5(5.2) films were solution cast on to a petri-dish.

Visible Spectroscopy

Spectra were recorded on a Perkin-Elmer Lambda-5 spectrometer. Samples used for visible spectroscopy were thin films (0.01–0.05 mm thick) cast directly onto quartz plates.

Differential Scanning Calorimetry (DSC)

DSC work was performed on the 50:50 copoly(α,ω -alkyldiyne) of poly(1,9-decadiyne): poly(1,10-undecadiyne). A powdered sample of the copolymer and a film of the copolymer were investigated.

Experimental details are as described in Chapter 5 (5.2).

Conductivity studies

A two-point DC measurement system was employed.

The probe used for two-point DC resistance measurements is shown in figure 6.1.¹⁰² The probe consisted of a PTFE Block

machined to fit into a glass tube. Within this block was fitted two stainless steel pins (1 mm diam) which had slight indentations in their ends and were sunk just below the surface of the PTFE by two adjusting screws. The probe was contained within a glass vessel which in turn was placed in an oven. The glass vessel was connected by both tubing, to allowing gas to pass through, and electrical connections to the outside of the oven. Electrical connections from the outside of the oven to a Keithly 602 Electrometer were made via BNC connectors and shielded cable. The oven acted as a metal box for the purposes of shielding.

A guard electrode was not used to ease fabrication of the probe. Dried nitrogen gas was passed over the sample before and during measurements hoping that any dirt or surface moisture would be kept to an absolute minimum.

Electrical contacts between the electrodes and the sample were made by 'dag' paint (Acheson Colloids, 915). Nitrogen was dried by a drying column and the solvent (4-methyl-2-pentanone) was allowed to evaporate for ~15–30 minutes to produce a good dry contact. The resistance was then measured using the electrometer on various ranges and from equation 6.1 below¹⁰³, the surface resistivity ρ obtained.

$$R = \frac{\rho}{\pi} \cosh^{-1} \frac{d}{2r_0} \quad \text{Equation 6.1}$$

where d is the separation between the centres of the two terminals (5 mm), $2r_0$ the diameter of the terminals (1 mm) and R the resistance value obtained by the electrometer. The conductivity (σ) in S/cm is the reciprocal of the surface resistivity (ρ).

$$\sigma = \frac{1}{\rho}$$

Equation 6.2

This method can measure samples with conductivities in the region 10^{-6} to 10^{-12} S/cm.

An average value from 5 resistance readings was calculated for each polymer film.

The films used for this study were the respective poly(α,ω -alkyldiyne) cast from a 1% weight/volume methylene chloride solution as described in Chapter 5(5.2).

Doping of the films with iodine vapour was carried out by placing the films in a dessicator with a few crystals of iodine, then placing the dessicator in an air oven at 60°C for $\sim 1-2$ hours until the films went dark.

Films were cross-polymerised for a period of 6 minutes.

Resonance Raman (RR) spectroscopy.

RR spectra were recorded on a Spex 1403 spectrometer interfaced to a DM 1B computer using excitation from a Coherent Radiation Innova 90-6 argon-ion laser and 590 dye-laser with 4-dicyanomethylene-6-p-(dimethylaminostyryl)-2-methyl-4H-pyran as the laser dye. Free standing thin films (0.01–0.05 mm thick) were used for all RR experiments. The films were mounted on a rotating sample

holder to prevent sample heating due to the laser beam. All spectra were obtained with the laser power maintained at <100 mW at the sample, multi-scanned to improve the signal-to-noise ratio, and corrected for the spectral response of the instrument. Wavenumber calibration of the spectrometer was established by reference to the emission spectrum of neon. An incident wavelength (λ_0) of 514.5 nm (5145Å) was used.

Solid-state ^{13}C nmr spectroscopy.

Carbon-13-cross polarisation (CP) magic-angle spinning (MAS) spectra were recorded at 125.758 MHz on a Brüker MSL-500 spectrometer. The polymer sample was placed in a 4 mm rotor with a spinning speed of 8.37 KHz.

Mass spectroscopy

Mass spectra were obtained on a Finnigan Incos 50 mass spectrometer.

6.3 Results and Discussion

6.3.1 Kinetics of photochemical cross-polymerisation by UV irradiation.

Figures 6.2 (a), (b) and (c) show the visible absorption spectra for poly(1,9-decadiyne), poly(1,10-undecadiyne) and poly(1,11-dodecadiyne) films respectively recorded before and after various UV exposure times (as indicated on the spectra by the t values).

None of these spectra were corrected for scattering due to the semi-crystalline nature of the films. (The Lambda-5 spectrometer used for obtaining the visible spectra does not have the facility to subtract the spectra of the polymer film after UV irradiation from the spectra before UV irradiation for the same polymer film). The technique for correcting spectra for scattering and base-line curvature was described by Butera for poly(1,8-nonadiyne) films before and after UV irradiation.³⁰

Therefore in this study, baseline curvature is introduced before the films are exposed to UV irradiation, giving a high initial absorption. As UV exposure time is increased a higher absorption is obtained in the visible spectrum profile. UV exposure times of 5 minutes and 30 minutes (time chosen for infinite absorbance (A_{∞})) show poorly resolved visible spectra profiles.

The Absorbance, A , at a wavelength of 650 nm was monitored for the first five minutes of UV exposure. This high wavelength

absorption at 650 nm is due to the photochemical cross-polymerisation of the poly(α,ω -alkyldiyne) to form long conjugated chains. This has been shown to be a 1,4-addition reaction which takes place in the crystalline regions of the polymer.^{29, 30}

Butera and workers have shown that increasing UV exposure time there is a broadening and blue shifting of the high wavelength absorption at ~ 650 nm to lower wavelengths.³⁰ (This was clearly evident after five minutes of UV exposure — see figure 1.12(a), (b) and (c) page 39 for poly(1,6-heptadiyne), poly(1,8-nonadiyne) and poly(1,11-dodecadiyne) films respectively). Butera and workers postulated that this was a consequence of UV induced degradation of the polydiacetylene chains, which has already been observed in polydiacetylene solutions^{33–35} and could also reasonably be expected to occur, in solid polydiacetylenes.³⁶ Therefore the kinetics of the cross-polymerisation reaction were only evaluated for the first five minutes of UV exposure.

Shown in figures 6.3(a), (b) and (c) are plots of A at 650 nm against UV exposure time(minutes) for poly(1,9-decadiyne), poly(1,10-undecadiyne) and poly(1,11-dodecadiyne) films respectively.

The absorbance, A, value at time $t = 0$ minutes is adjusted in each plot so that it is equal to 0, i.e. if the authentic value for A at time $t = 0$ is 1.6, then $A = 1.6 - 1.6 = 0$ at time $t = 0$. Therefore, 1.6 will be subtracted from all subsequent values for A in that visible spectrum (values for A are shown in Tables 6.1 to 6.3).

In figures 6.3(a) to (c) it is shown that the absorbance at 650 nm increases rapidly for the first five minutes of UV exposure. After this five minutes the absorbance starts to level off until an infinite time for absorbance is reached shortly after 5 minutes of UV exposure.

The following section of work calculates the rate constants for the photochemical cross-polymerisation reaction.

The course of the reaction at $\lambda = 650$ nm may be followed by measuring Absorbance, A , which varies with time according to equation 1.

$$A_{\infty} - A_t = (A_{\infty} - A_0) \exp(-kt) \quad \text{equation 1}$$

A_{∞} = final absorbance reading (taken at $t = 30$ minutes).

A_0 = initial absorbance reading (taken at $t = 0$ minutes).

A_t = absorbance reading measured at time t .

k = rate constant(mins^{-1}) for a simple first order reaction.

t = UV exposure time (minutes).

Equation 1 can be rewritten in the form below for a first-order reaction;

$$\ln(A_{\infty} - A_t) = \ln(A_{\infty} - A_0) - kt \quad \text{equation 2}$$

or for a second-order reaction the rate dependence can be written as;

$$\frac{1}{(A_{\infty} - A_t)} = \frac{1}{(A_{\infty} - A_0)} + k_2 t \quad \text{equation 3}$$

k_2 = rate constant (mins^{-1}) for a second-order reaction.

For a simple first order reaction a plot of $\ln (A_\infty - A_t)$ against UV exposure time (minutes) will give a straight line with the gradient of the line = $-k$ (mins^{-1}). To convert the value into s^{-1} the value of $-k$ must be divided by 60.

For a second-order reaction a plot of $\frac{1}{A_\infty - A_t}$ against UV exposure time (minutes) will give a straight line with the gradient of the line = k_2 (mins^{-1}). Again, to convert the value into s^{-1} the value of k_2 must be divided by 60.

Plots of $\ln (A_\infty - A_t)$ against UV exposure time (minutes) using a least squares programme for a simple line fit gave correlation coefficients (r) in range 0.95 to 0.98 for all first-order plots at 650 nm.

However, plots of $\frac{1}{A_\infty - A_t}$ against UV exposure time (minutes) using the same programme gave a scattered range of correlation coefficients (r) i.e. 0.75 to 0.98 for all second-order plots at 650 nm.

Very good correlation coefficients for straight line plots of $\ln (A_\infty - A_t)$ against UV exposure time (minutes) at 650 nm indicate that the photochemical cross-polymerisation reaction is a first order reaction for the first five minutes of UV exposure (see Table 6.1 to 6.3 for A , $A_\infty - A_t$ and $\ln (A_\infty - A_t)$ values). The rate constants (k) in s^{-1} are shown in Table 6.4 for the photochemical cross-polymerisation reaction at 650 nm.

The reaction rates for the poly(α,ω -alkyldiynes) reveal that; poly(1,11-dodecadiyne) > poly(1,9-decadiyne) > poly(1,10-undecadiyne).

Solubility studies in methylene chloride after increased UV exposure of these films revealed that the polymers were only sparingly soluble.

6.3.1.1 Reaction kinetics involved in the photochemical cross-polymerisation reaction at $\lambda = 650$ nm for the poly(α,ω -alkyldiynes)

Introduction

Diacetylenes are known to polymerise via a 1,4-addition polymerisation reaction.^{4, 5, 95}

Poly(α,ω -alkyldiynes) also cross-polymerise via a 1,4-addition polymerisation to give a 2D cross-polymerised network.^{22, 23, 24, 28-31} The most critical parameter for the cross-polymerisation to take place in the poly(α,ω -alkyldiyne) is the packing of the crystalline segments in these molecules (i.e. the distance between carbon 1 of one chain and carbon 4 of the adjacent chain in the crystalline segments). For a reactive diacetylene this distance $D < 4\text{\AA}$.³

The reaction kinetics for the solid state photochemical cross-polymerisation reaction is now discussed;

The reaction is characterised by three different steps which are explained in the following.

Initiation 104

The initiation results from the reaction of two poly(α,ω -alkyldiyne) crystalline segments forming a diradical dimer.

A crystalline segment in the poly(α,ω -alkyldiyne) P is excited to the singlet state P^* by UV irradiation. The state relaxes (a) to the triplet state P^T by intersystem crossing (ISC), (b) to the singlet state P^S by internal conversion (IC), and (c) to the ground state P by fluorescence. As reaction partners for the diradical dimer (DR_2) formation the triplet state P^T and the singlet state P^S are required. The kinetics of the initiation process is described in ref 104. Summarising, the following reaction scheme is obtained.



Addition

A singlet state is necessary according to the reaction scheme;



Addition reactions can also be observed for dicarbenes (DC) and asymmetric carbenes (AC).

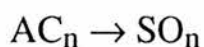
Termination

The radical electrons of a reaction chain end can be saturated by an intramolecular hydrogen transfer reaction.⁷

In a first termination step asymmetric carbenes (AC) are created according to the reaction scheme



The remaining reactive chain end can be saturated in a second termination step



The stable oligomeric structure of the conjugated cross-polymerised poly(α,ω -alkyldiynes) are not reactive any more.

6.3.2 Studies involving a 50:50 copolymer of poly(1,9-decadiyne): poly(1,10-undecadiyne)

6.3.2.1 UV and solubility studies

Clear films and white powdered samples of the copolymer were used. A series of experiments involving exposing the samples to UV light at 254 nm were performed. After exposure to UV light for several hours it was evident that there was no colour change in the clear films by visual examination. However there was a purple tinge to the powdered sample suggesting that cross-polymerisation had taken place, indicating there is some crystalline order in the copolymer powder for the 1,4-addition reaction to take place.

The copolymer film and powder remain soluble in methylene chloride after UV exposure. This is unlike the homopolymer film and powder which are sparingly soluble in methylene chloride.

6.3.2.2 Thermal analysis of the copolymer

This consisted of thermally cycling the copolymer powder three times between the temperatures of -40°C and 140°C at heating and cooling rates of $10^{\circ}\text{C}/\text{min}$, observing any melting or crystallisation behaviour. After the last heating cycle the copolymer sample was annealed at 140°C for thirty minutes, then quenched to -60°C and finally reheated at $10^{\circ}\text{C}/\text{min}$ from -40°C to 140°C in an attempt to destroy the copolymer's crystallinity.

Figure 6.5 shows a DSC heating scan from -40°C to 140°C of the copolymer powder. The scan reveals a T_g at -1°C and a T_m at 41°C . The single T_g denotes that the copolymer is a random copolymer.¹⁰⁵ The T_g value of -1°C lies between the value of -16°C for poly(1,10-undecadiyne) and 36°C for poly(1,9-decadiyne). The T_m has a heat of fusion (ΔH_f) value of 18.26 J/gram which is approximately 42% of the value obtained for a powdered polymer sample of poly(1,9-decadiyne) i.e. 43.05 J/gram see chapter 5 figure 5.5(a). This indicates that the homopolymer, poly(1,9-decadiyne) is ~2.4 times more crystalline than the 50:50 copolymer of poly(1,9-decadiyne): poly(1,10-undecadiyne).

This sample was then cooled to -40°C and subsequently reheated to 140°C to produce figure 6.5. scan A. Compared to the first scan, scan A shows a decrease in endothermic area, a slight increase in the peak value for T_m from 41°C to 42°C and a decrease in the T_g value from -1°C to -4°C . There is also an exothermic peak at 16°C , due to the crystallisation of the copolymer. This is the most significant difference as this exotherm is not present in the original scan.

After two more cycles to produce figure 6.5 scan B and figure 6.5 scan C it can be seen that there is very little difference between these two scans and figure 6.5 scan A. There is only a small decrease in endothermic area and exothermic area. T_m , T_c and T_g value are almost unaffected with values of $41\text{--}42^{\circ}\text{C}$, $16\text{--}17^{\circ}\text{C}$ and -4°C respectively obtained.

As explained in Chapter 5 (5.3.1) page 184 if the melt treatment of a polymer is not too severe, residual local order can remain in the melt and act as primary nucleation sites for crystallisation. Also,

crystallisation temperature (T_c) is critical for further crystallisation influencing the melt history.^{92, 94} If $T_m - T_c$ is small (i.e. for the copolymer $T_m - T_c$ is $\sim 25^\circ\text{C}$ which is small) the primary nucleation rate can be greatly influenced by the amount of residual order carried from the melt. Since thermal cycling treatment on the copolymer is not too severe and $T_m - T_c$ is small it is conceivable that crystallisation will occur on the heating up scans.

Figure 6.6 shows the DSC scan produced after annealing the sample at a temperature of 140°C for thirty minutes, then quenching to -60°C , followed by reheating the sample from -40°C to 140°C . This was performed in an attempt to prevent subsequent crystallisation of the copolymer. However, conditions were not severe enough as figure 6.6 shows that crystallisation followed by crystalline melting still occurs in the copolymer sample. Small broad peaks for T_c at 17°C and T_m at 37°C were obtained. The ΔH_f values both being very small at ~ 1 J/gram. A T_g is also present at -4°C .

Table 6.5 lists the heats of fusion (ΔH_f in J/gram), heats of crystallisation in (ΔH_c in J/gram) for endothermic and exothermic peaks respectively for figures 6.5 and 6.6.

Note: There was no evidence of crystallisation in the cooling down scans for the copolymer as no exotherms were recorded for the copolymer.

Visual observation of the copolymer after the DSC scans showed no evidence of a colour change indicating no thermal cross-polymerisation had occurred during thermal cycling.

From the results obtained by DSC on the copolymer powder it would appear that there is a small percentage of crystal order present which is significant to allow cross-polymerisation of this copolymer. However from UV studies it would appear that this cross-polymerisation reaction is much slower than the cross-polymerisation reaction for the homopolymer.

Note: DSC scans were also performed on a solution cast film of the 50:50 copolymer of poly(1,9-decadiyne): poly(1,10-undecadiyne). However the copolymer films showed no evidence of crystallisation or melting suggesting there is no or very little crystal order in the copolymer film. A T_g was observed on the heating up scans at ~2°C.

A clear film and white powdered sample of the copolymer were left at 20°C under vacuum in the dark for several weeks. No notable colour change had occurred in the film, but the white powdered sample had turned purple indicating thermal cross-polymerisation of the copolymer powder had occurred.

In this copolymer the cross-polymerisation reaction takes place in the crystalline regions as in the poly(α,ω -alkyldiynes).

6.3.3 Conductivity and Resonance Raman spectroscopic studies on cross-polymerised samples of poly(1,9-decadiyne) and poly(1,11-dodecadiyne)

Introduction

Previous conductivity studies have been performed on cross-polymerised poly(1,11-dodecadiyne) by Day and Lando²² and cross-polymerised poly(1,8-nonadiyne) by Knol and co-workers.²⁶ Day and Lando found that the conductivity of the cross-polymerised poly(1,11-dodecadiyne) subsequently doped with iodine increased by 2.5 orders of magnitude. However after iodine was removed the current reverted back to its original value suggesting that the cross-polymerised poly(1,11-dodecadiyne) crystalline matrix was too perfect to allow penetration of the dopant into the interior. Knol and co-workers claimed that the specific conductivity of the cross-polymerised poly(1,8-nonadiyne) subsequently doped with iodine changed from 10^{-12} S/cm to 10^{-6} S/cm. However, this conductivity of poly(1,8-nonadiyne) doped with iodine is many orders of magnitude smaller than that of other doped polymers having a conjugated backbone. Knol eliminated the possibility that the cross-polymerised poly(1,8-nonadiyne) crystalline matrix was too perfect to allow penetration of the dopant into the interior as he claimed large amounts of iodine were incorporated into these films. Knol suggested that the reaction of the cross-polymerised poly(1,8-nonadiyne) with iodine is not merely a charge-transfer process, but partly a chemical bond formation to the polydiacetylene chain causing disruption at the sites of the bonded iodine. This would explain both the small and voltage-dependant conductivity and its independence of the degree of crosslinking.

In this present study it was proposed that there would be a significant increase in the conductivity of the poly(α,ω -alkyldiynes) (poly(1,9-decadiyne) and poly(1,11-dodecadiyne)) by reversing the doping procedure of these polymers i.e. instead of doping with iodine after the cross-polymerisation reaction doping would be carried out before the cross-polymerisation reaction. It was anticipated that the Iodine would be incorporated into the amorphous regions of the uncrosslinked poly(α,ω -alkyldiynes) with greater ease possibly forming chemical bonds with the uncrosslinked polymer. After cross-polymerisation this iodine would be 'trapped' in the polyconjugated matrix making the material a good conductor.

Conductivity measurements were made on thin films of the polymers which were doped by iodine then cross-polymerised by the procedure described in 6.2. Conductivity measurements were also made on films which were cross-polymerised and then doped by iodine as a means of comparison.

Results are shown in Table 6.6.

Resonance Raman spectra were also recorded on the films which were (a) cross-polymerised for six minutes.

(b) doped with iodine and then cross-polymerised for six minutes.

Resonance Raman spectra are shown in figures 6.7 and 6.8.

Resonance Raman spectra data for cross-polymerised poly(1,9-decadiyne) and cross-polymerised poly(1,11-dodecadiyne) are shown in Table 6.7.

The results from the conductivity readings in Table 6.6 show that the cross-polymerised poly(1,9-decadiyne) has an overall better conductivity than the cross-polymerised poly(1,11-dodecadiyne). This would make sense as the methylene spacer group is smaller in the poly(1,9-decadiyne). The method of reversing the doping does not change the conductivity of the polymer films to any great extent, values obtained are comparable with values obtained by the conventional doping procedure.

The resonance Raman spectra shown in figures 6.7 and 6.8 reveal that doping the polymer with iodine has very little effect on the spectrum, indicating that there are no significant structural changes on iodination.

In Table 6.7 it can be shown that the XP19D and XP111D frequencies are similar to XP18N frequencies obtained by Butera.³⁰ Lower frequencies where bands are not assigned are due to side group motions.

From the conductivity results and resonance Raman spectra it is evident that there is no obvious route to exploit the potential conductivity of these poly(α,ω -alkyldiynes).

6.3.4 Characterisation of the product from the polymerisation of 1,7-octadiyne

1,7-octadiyne was polymerised by route A at 65°C for 5 hours and its product was found to be insoluble in a range of solvents as described in 3.4.3. Therefore the product's molar mass could not be characterised by $^1\text{Hnmr}$ (EGA) or by GPC.

Figure 6.9 (a) and (b) are solid state $^{13}\text{Cnmr}$ cross polymerisation (CP) magic angle spinning (MAS) spectra of this product. Peaks denoted by X are spinning side bands.

Figure 6.9 (a) reveals four peaks at 21 ppm, 32 ppm, 66 ppm and 79 ppm. The peaks at 21 ppm and 32 ppm are due to methylene carbons and the peaks at 66 ppm and 79 ppm are due to quaternary alkyne carbons. The peak at 21 ppm is due to the methylene carbons attached to the quaternary alkyne carbons and the peak at 79 ppm is due to the quaternary alkyne carbons attached to the methylene carbons.

Figure 6.9 (b) shows the non quaternary suppression (NQS) spectrum of the product (i.e. only quaternary carbons are shown). The two peaks revealed at 66 ppm and 79 ppm correspond to the quaternary alkyne carbons as described above.

A 1,7-octadiyne polymer structure is shown overleaf with the corresponding chemical shifts labelled.



(c) (d) (a) (b) (a) (d) (c)

(a) = 21 ppm

(b) = 32 ppm

(c) = 66 ppm

(d) = 79 ppm

Figure 6.10 shows the mass spectrum of the compound. The absence of the molecular ion (M^+) peak at 208 for the cyclic dimer and the presence of a small peak at 257 suggests fragmentation of a high molar mass polymer.

Note: The product did not colour on UV exposure at 254 nm suggesting an unfavourable packing in the polymer molecule matrix.

6.4 Conclusions and Recommendations.

From the results obtained in this chapter it can be seen that the packing of the crystalline segments in the poly and copoly(α,ω -alkyldiynes) is the most critical parameter for the cross-polymerisation reaction to take place. Since the 50:50 copolymer powder of poly(1,9-dec):poly(1,10-undec) has less crystal order than the homopolymer powder of poly(1,9-decadiyne), the cross-polymerisation reaction occurs at a much slower rate.

Conductivity studies on cross-polymerised poly(α,ω -alkyldiynes) with methylene spacer groups in between the conjugated chain reveal that that the polymers are insulators and that there is no obvious route to exploit their potential conductivity.

In chapter 4 it was shown that polymerisation route A was a success for synthesising high molar mass poly and copoly(α,ω -alkyldiynes). These polymers could be fabricated into films. However it was not possible to achieve high tensile modulus films as a result of the flexible methylene group sandwiched in between the rigid alkyne groups.

For future research on α,ω -diyne type polymers the following properties of the polymer must be taken into consideration;

- (1) A polymer which can be processed to give a high tensile modulus film.
- (2) A polymer which is thermally and oxidatively stable.
- (3) A semi-crystalline polymer which has good packing properties promoting the 1,4-addition cross-polymerisation reaction.
- (4) A cross-polymerised highly conjugated network which will have potential use in conductivity studies.

An α,ω -diyne type polymer which meets the above criteria must have rigidity built in by the incorporation of aromatic groups in the polymer chain. The aromatic groups will also provide thermal stability (high T_g and T_m). Commercial antioxidants e.g hindered phenols may have to be incorporated into the polymer during processing to give the polymer oxidative stability over a long period of time. The polymer must also have flexibility present in the chain to facilitate processing i.e. a T_m must be present. This can be achieved by methylene spacer groups, ether linkages, etc. It is anticipated that an α,ω -diyne type polymer of this type will be of a semi-crystalline nature with good packing properties in the crystalline segments. This will promote the 1,4-addition cross-polymerisation reaction to give a highly ordered 2D network.

Also unsaturated segments e.g. $\text{CH}_2\text{CH}=\text{CHCH}_2$ segments in the polymer chain will improve the conjugation of the polymer and on cross-polymerisation this α,ω -diyne type polymer will be very highly conjugated and its potential conductivity could be exploited.

If more success had been achieved in the synthesis of the novel α,ω -aromatic diyne monomers in chapter 2 then compounds that fitted into the above criteria i.e. points (1) to (4) could have been successfully polymerised.

A	$A_{\infty} - A_t$	$\ln(A_{\infty} - A_t)$	UV exposure time (mins)
$A_0 = 0$	1.70	0.53	0
$A_1 = 0.9$	0.8	-0.22	1
$A_2 = 1.02$	0.68	-0.39	2
$A_3 = 1.21$	0.49	-0.71	3
$A_4 = 1.43$	0.27	-1.31	4
$A_5 = 1.64$	0.06	-2.81	5
$A_{\infty} = 1.70$	0	-	30

Table 6.1. Absorbance readings for poly(1,9-decadiyne) at $\lambda = 650\text{nm}$ for increasing UV exposure times.

A	$A_{\infty} - A_t$	$\ln(A_{\infty} - A_t)$	UV exposure time (mins)
$A_0 = 0$	2.18	0.78	0
$A_1 = 0.9$	1.18	0.17	1
$A_2 = 1.22$	0.96	-0.04	2
$A_3 = 1.36$	0.82	-0.20	3
$A_4 = 1.69$	0.49	-0.71	4
$A_5 = 1.83$	0.35	-1.05	5
$A_{\infty} = 2.18$	0	-	30

Table 6.2 Absorbance readings for poly(1,10-undecadiyne) at $\lambda = 650\text{nm}$ for increasing UV exposure times.

A	$A_{\infty} - A_t$	$\ln(A_{\infty} - A_t)$	UV exposure time (mins)
$A_0 = 0$	1.70	0.53	0
$A_1 = 0.77$	0.93	-0.07	1
$A_2 = 0.92$	0.78	-0.25	2
$A_3 = 1.25$	0.45	-0.80	3
$A_4 = 1.48$	0.22	-1.51	4
$A_5 = 1.66$	0.04	-3.22	5
$A_{\infty} = 1.70$	0	-	30

Table 6.3 Absorbance readings for poly(1,11-dodecadiyne) at $\lambda = 650\text{nm}$ for increasing UV exposure times.

poly(α,ω -alkyldiyne)	$k(\text{mins}^{-1})$	$k(\text{s}^{-1})$
poly(1,9-decadiyne)	0.58	9.67×10^{-3}
poly(1,10-undecadiyne)	0.34	5.69×10^{-3}
poly(1,11-dodecadiyne)	0.67	0.011

Table 6.4 Rate constants for the photochemical cross-polymerisation reaction at $\lambda = 650\text{nm}$.

Scan no	ΔH_f (J/gram)	T_m ($^{\circ}$ C)	ΔH_c (J/gram)	T_c ($^{\circ}$ C)
1st run	18.26	41	-	-
A	6.72	42	5.90	16
B	5.41	41	5.04	16
C	4.20	41	4.06	17
Annealed at 140 $^{\circ}$ C for 30 mins, quenched to -60 $^{\circ}$ C, then re-run	1.03	37	1.03	17

Table 6.5. Data for Thermal Cycling runs of 50:50 poly(1,9-dec):poly(1,10-undec).

poly(α,ω -alkyldiyne)	Treatment	Conductivity reading(S/cm)
poly(1,9-decadiyne)	Cross-polymerised for 6 minutes.	3.7×10^{-11}
poly(1,9-decadiyne)	Doped with Iodine then cross-polymerised for 6 minutes.	3.1×10^{-11}
poly(1,9-decadiyne)	Cross-polymerised for 6 minutes then doped with Iodine.	3.3×10^{-11}
poly(1,11-dodecadiyne)	Cross-polymerised for 6 minutes.	6.8×10^{-12}
poly(1,11-dodecadiyne)	Doped with Iodine then cross-polymerised for 6 minutes.	7.5×10^{-11}
poly(1,11-dodecadiyne)	Cross-polymerised for 6 minutes then doped with Iodine.	7.7×10^{-11}

Table 6.6. Conductivity readings for poly(1,9-decadiyne) and poly(1,11-dodecadiyne).

Observed Frequencies(cm^{-1})			
XP18N(a)	XP19D	XP111D	Band Assignments
2111	2099	2090	$\nu(\text{C}\equiv\text{C})$
1483	1496	1488	$\nu(\text{C}=\text{C})$
1374	1340	1337 1314	
1281	1239	1252	
1238	1200	1222 1189	
1104	1072	1086	
741	700	700	

Table 6.7. Comparison of Observed Resonance Raman frequencies using Incident Wavelengths of 5145\AA for cross-polymerised poly(1,8-nonadiyne)(XP18N) , for cross-polymerised poly(1,9-decadiyne)(XP19N) and for cross-polymerised poly(1,11-dodecadiyne)(XP111D). All films were exposed to UV light for 6 minutes.

(a) XP18N frequencies taken from ref 30.

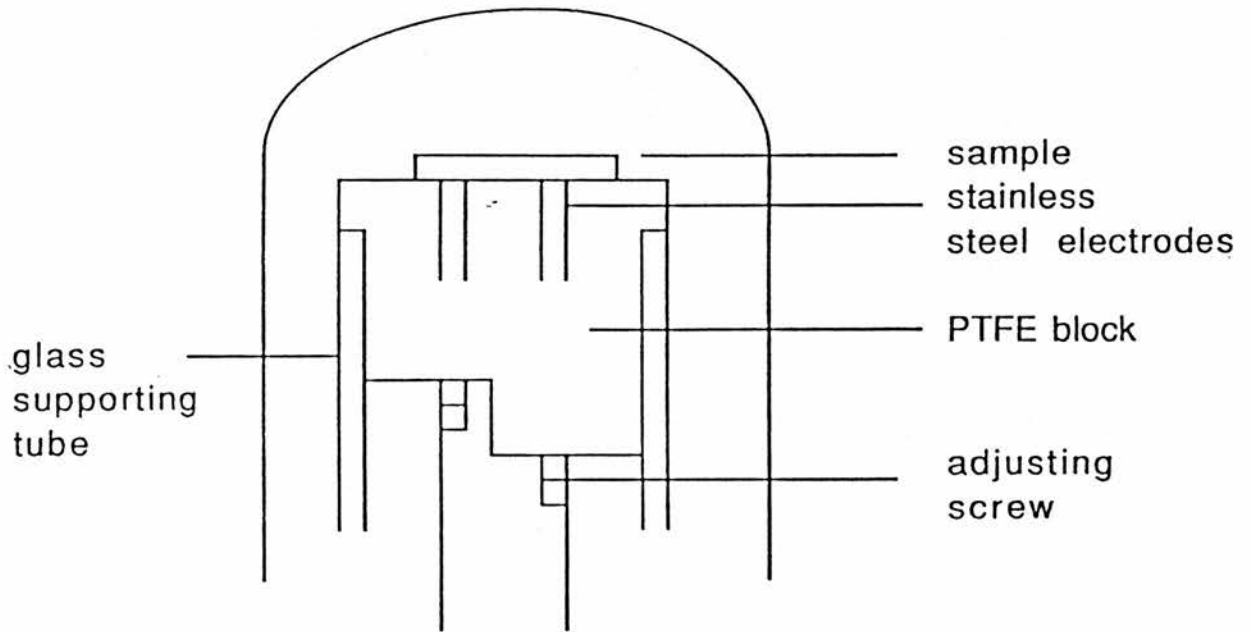


Figure 6.1 Two point DC resistance measurement system (from ref 102).

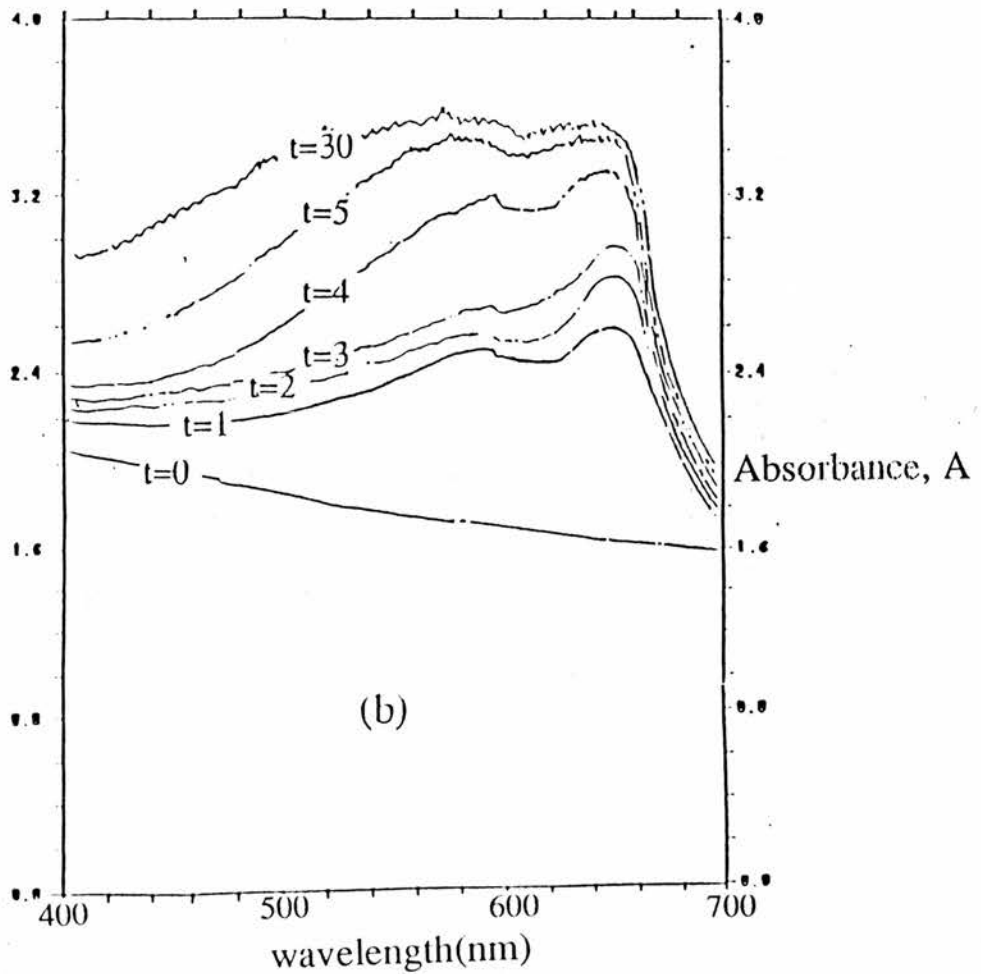
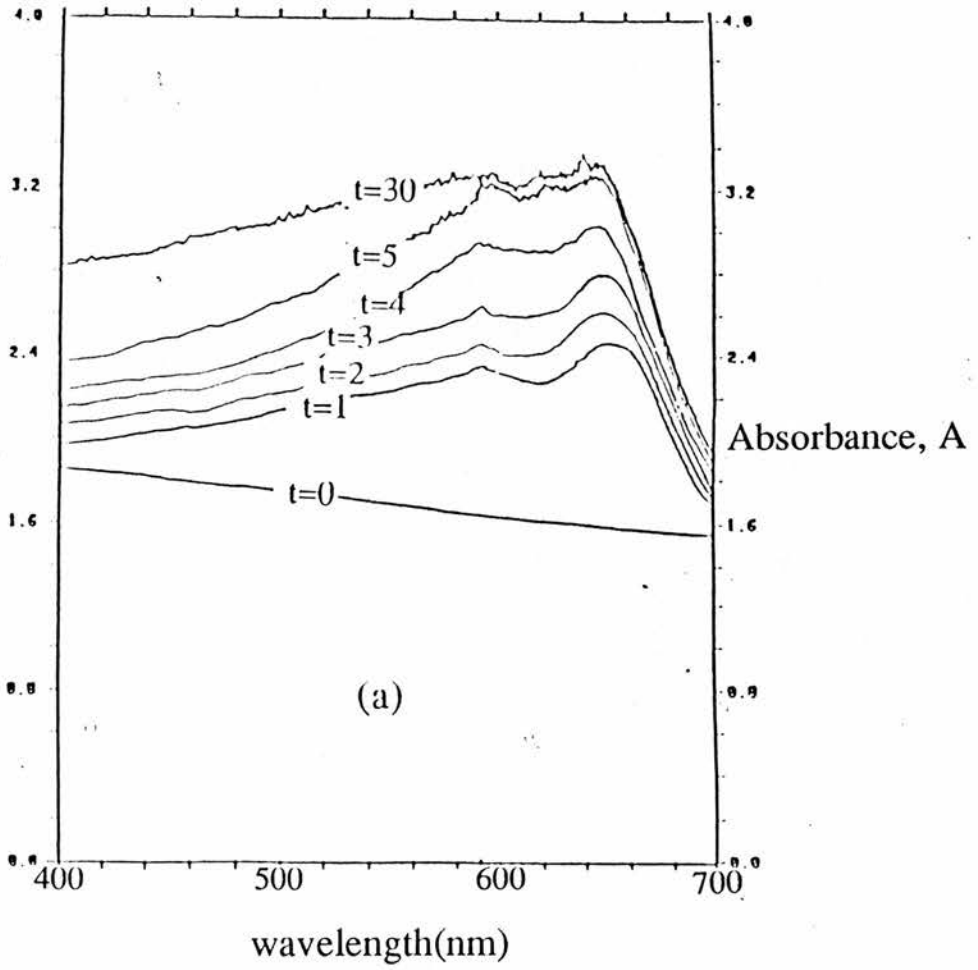


Figure 6.2 see over.

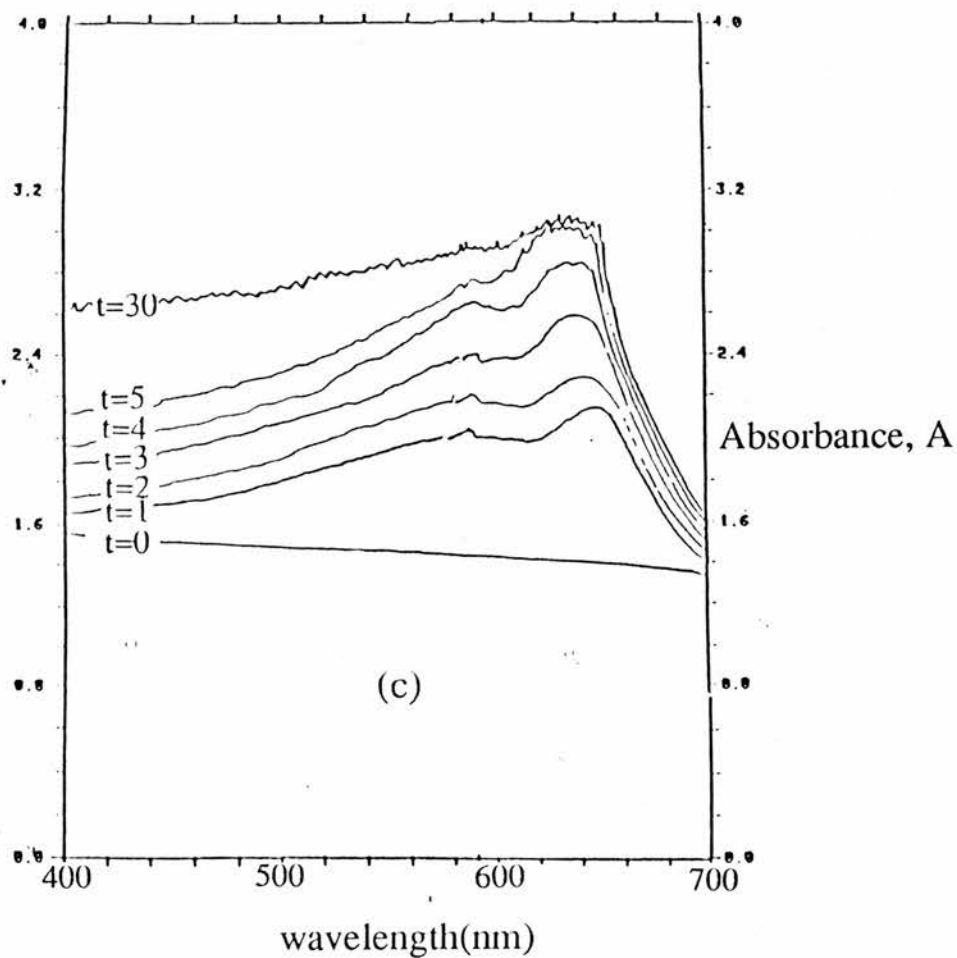


Figure 6.2 Visible absorption spectra of solution cast films of (a) poly(1,9-decadiyne) (b) poly(1,10-undecadiyne) and (c) poly(1,11-dodecadiyne) before and after various UV exposure times (minutes) (as indicated on the spectra by t). Spectra were not corrected for scattering (see 6.3.1).

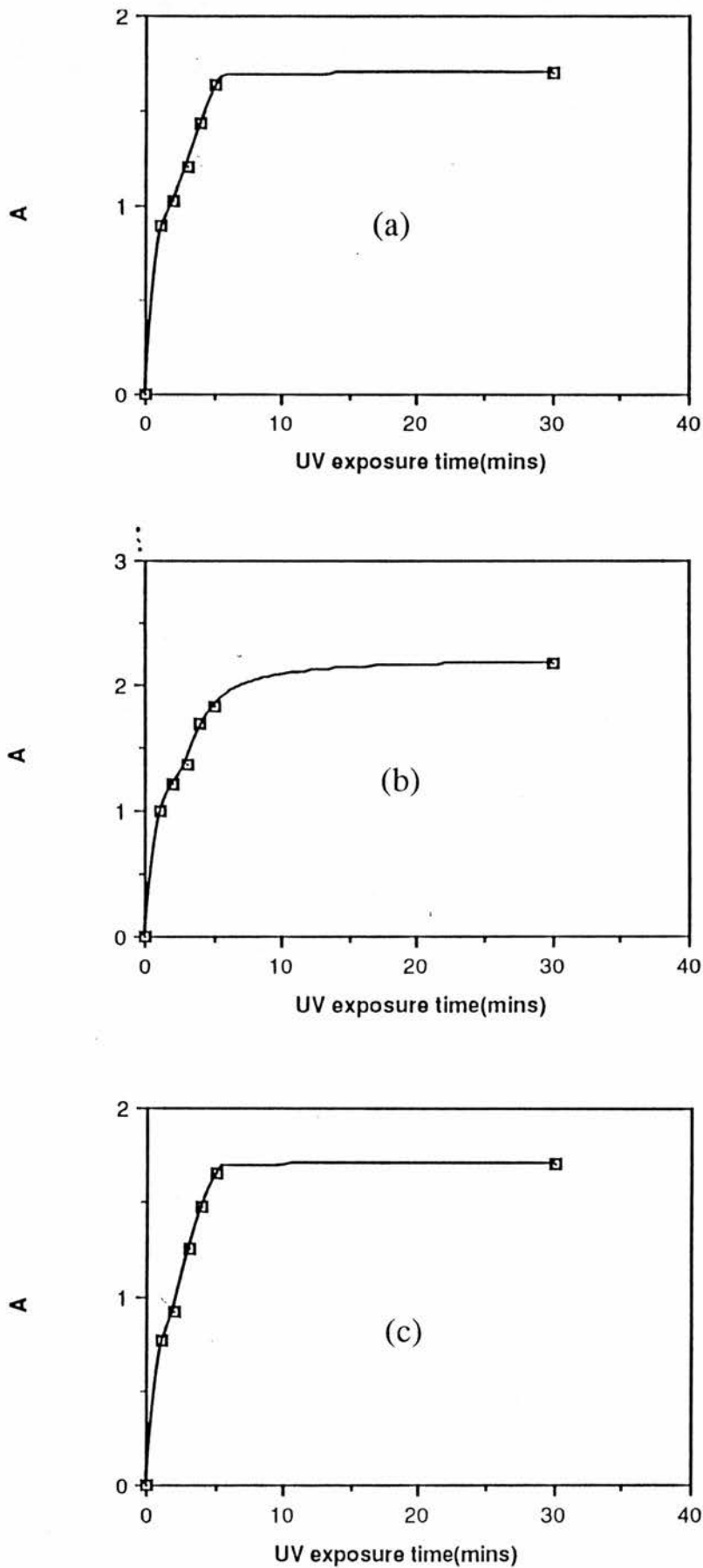


Figure 6.3 Absorbance at 650nm as a function of UV exposure time for (a) poly(1,9-decadiyne) (b) poly(1,10-undecadiyne) and poly(1,11-dodecadiyne).

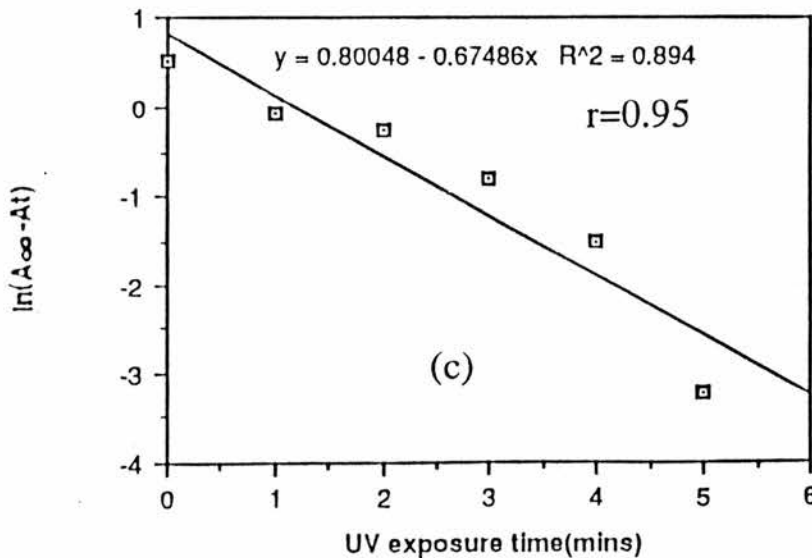
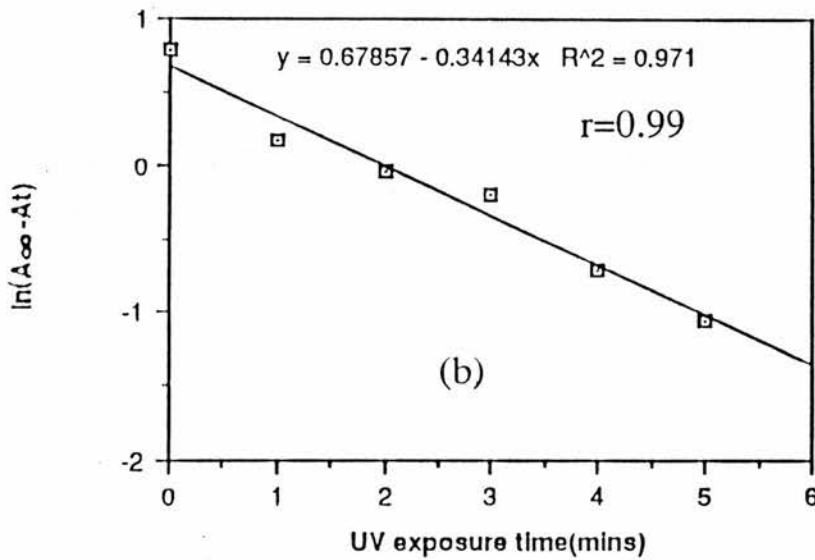
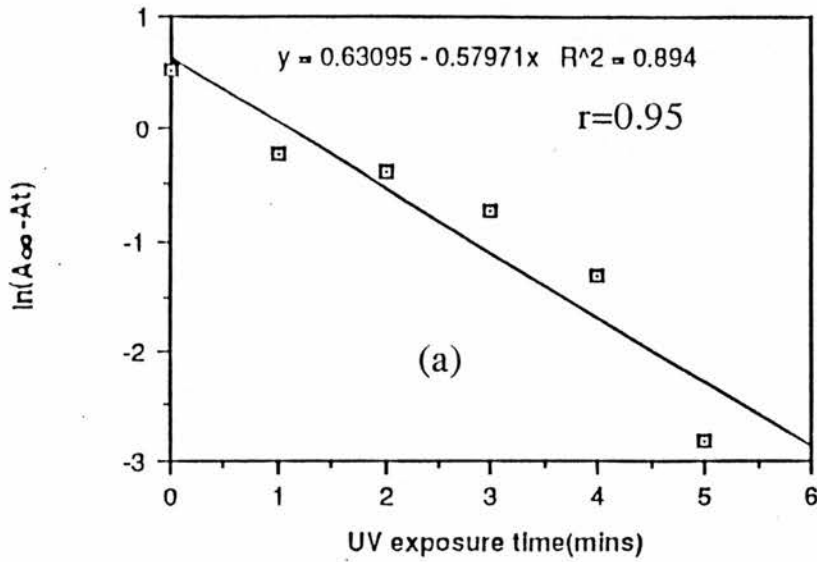


Figure 6.4 First order kinetic plots of $\ln(A_{\infty} - A_t)$ as a function of UV exposure time for (a) poly(1,9-decadiyne) (b) poly(1,10-undecadiyne) and poly(1,11-dodecadiyne).

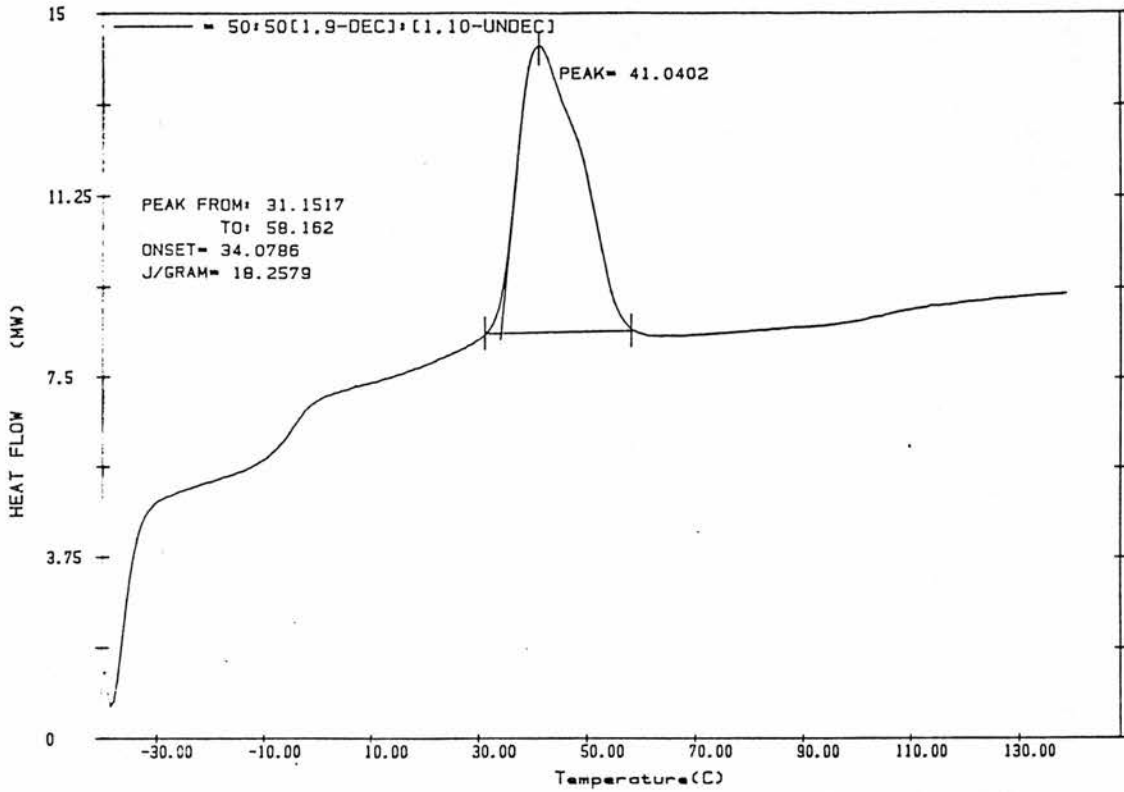


Figure 6.5 DSC thermogram of a 50:50 copolymer powder of poly(1,9-dec):poly(1,10-undec) from -40°C to 140°C (at $10^{\circ}\text{C}/\text{min}$). 1st heating cycle. Original scan.

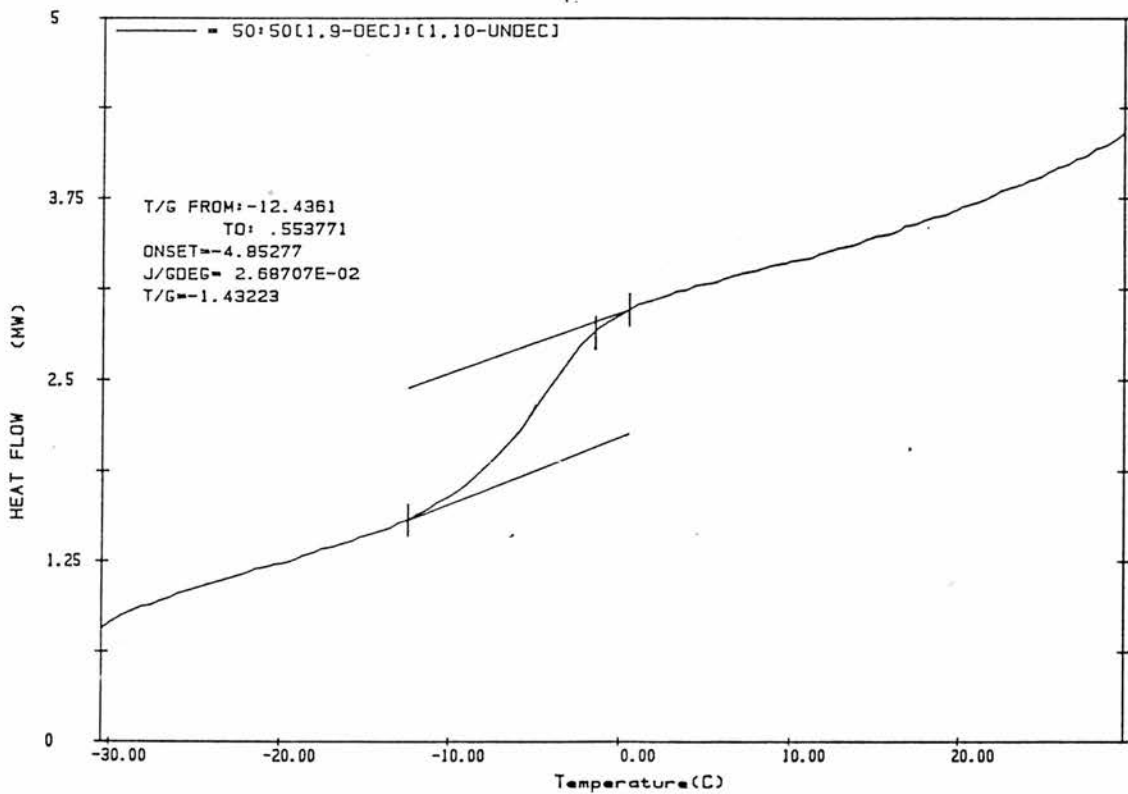


Figure 6.5 T_g calculation from the above thermogram.

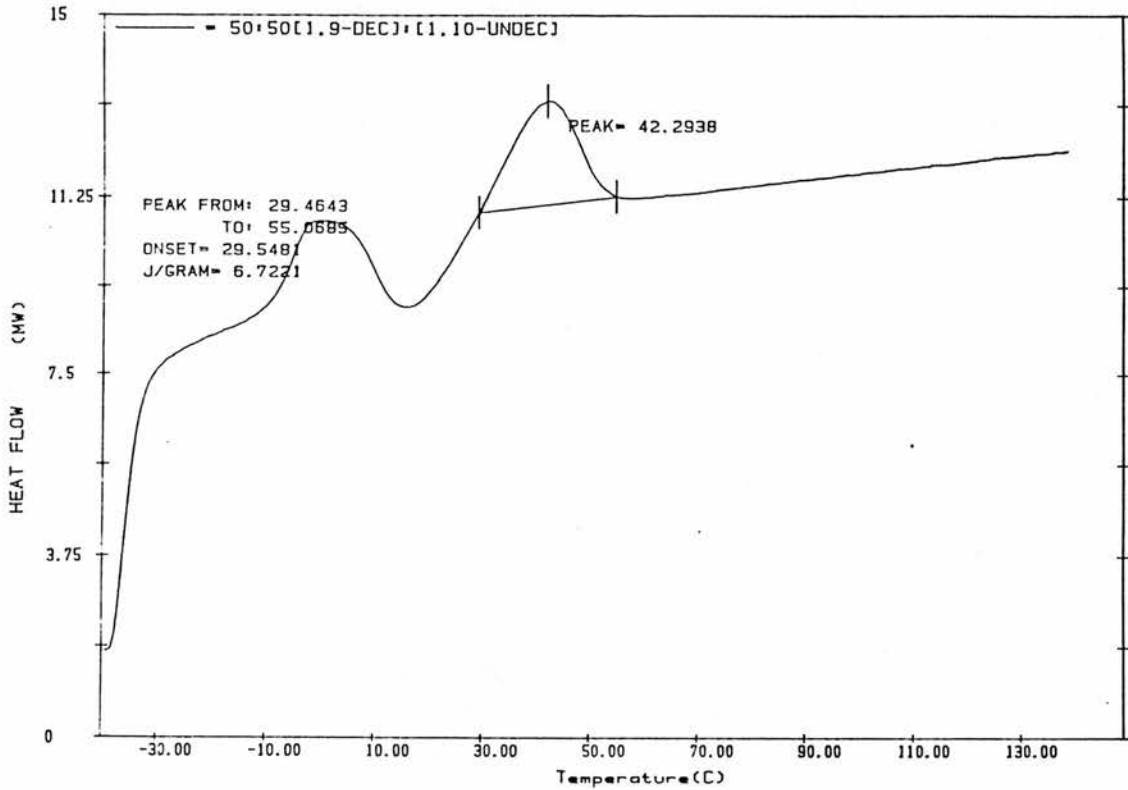


Figure 6.5 scan A DSC thermogram of 50:50 poly(1,9-dec):poly(1,10-undec) from -40°C to 140°C (at 10°C/min). 2nd heating cycle. T_m calculation is shown.

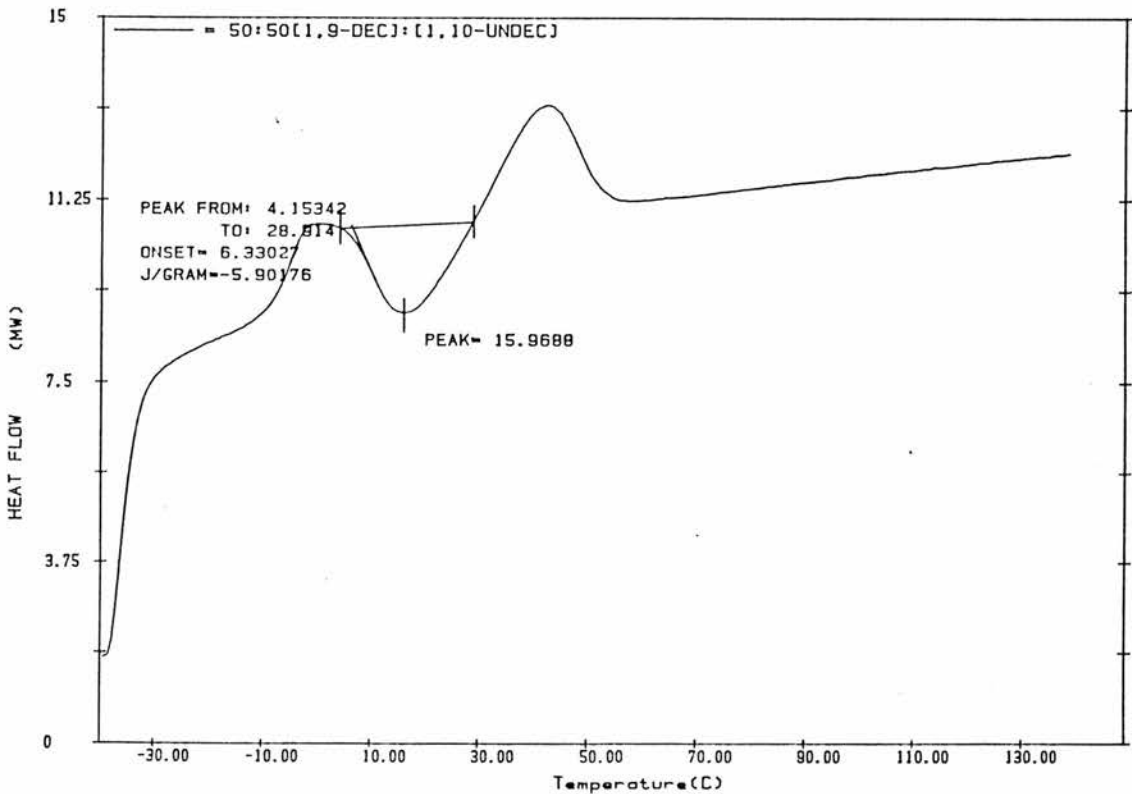


Figure 6.5 scan A T_c calculation.

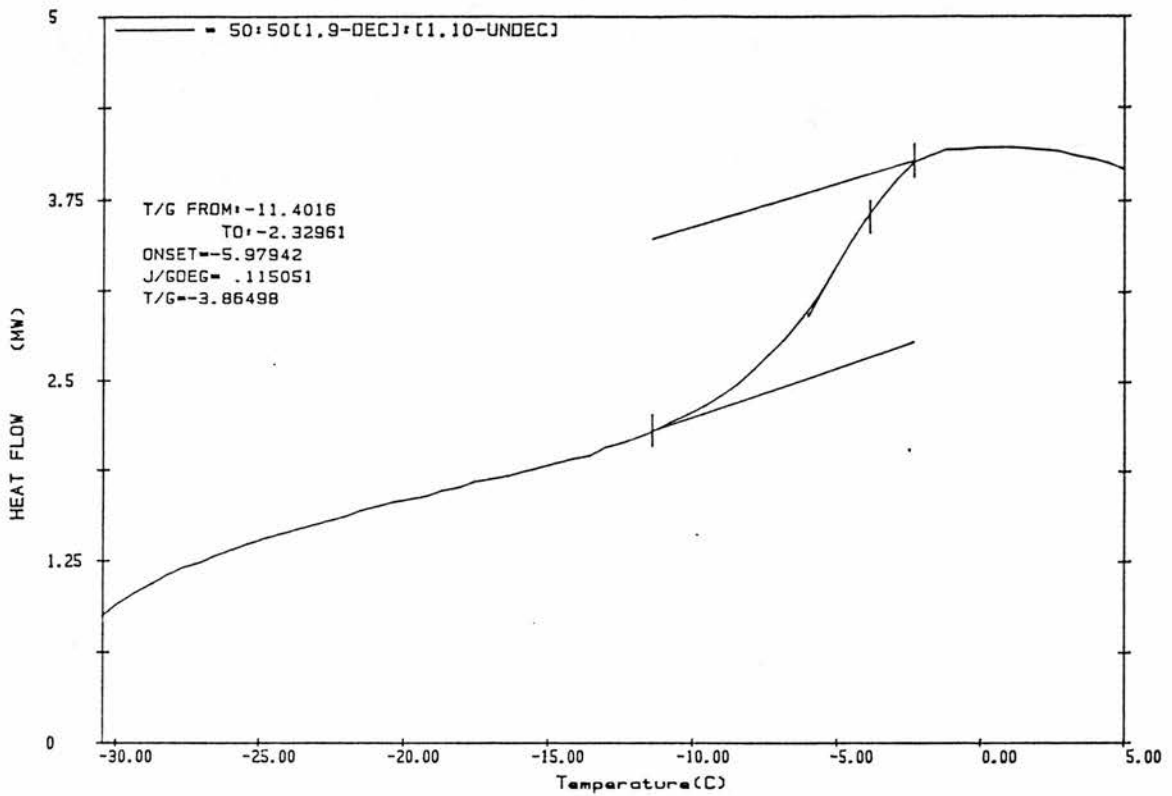


Figure 6.5 scan A Tg calculation.

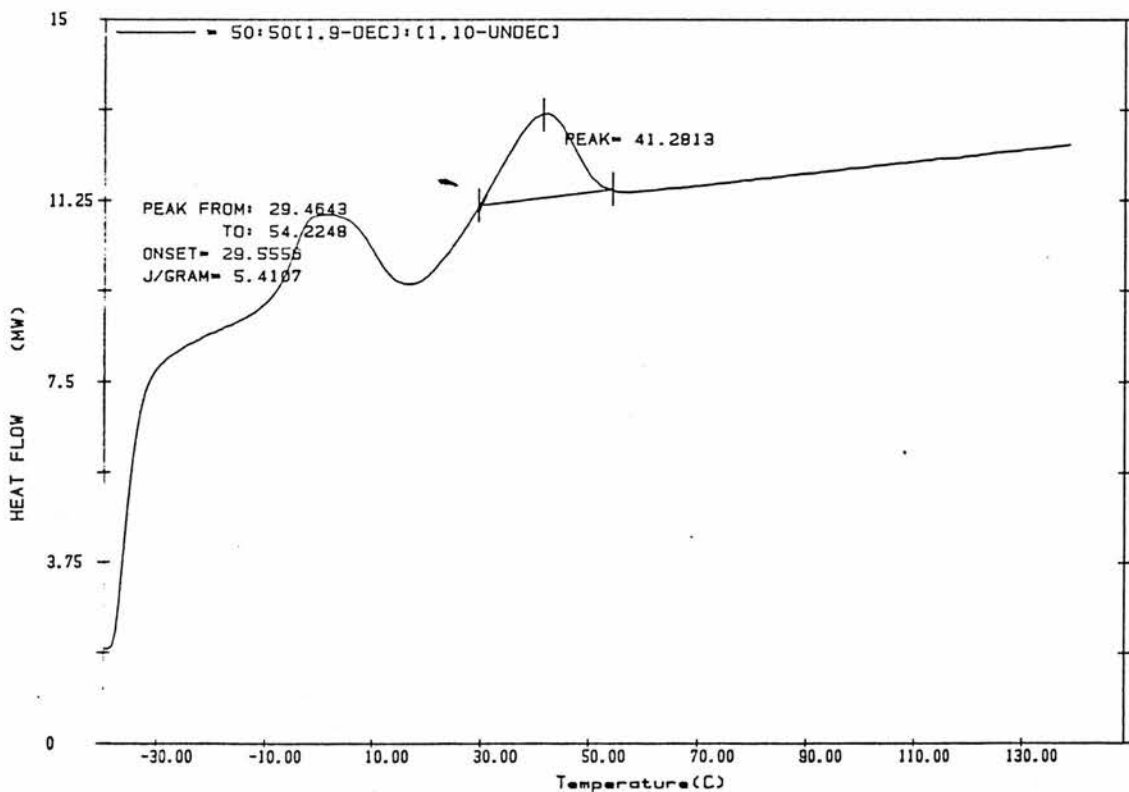
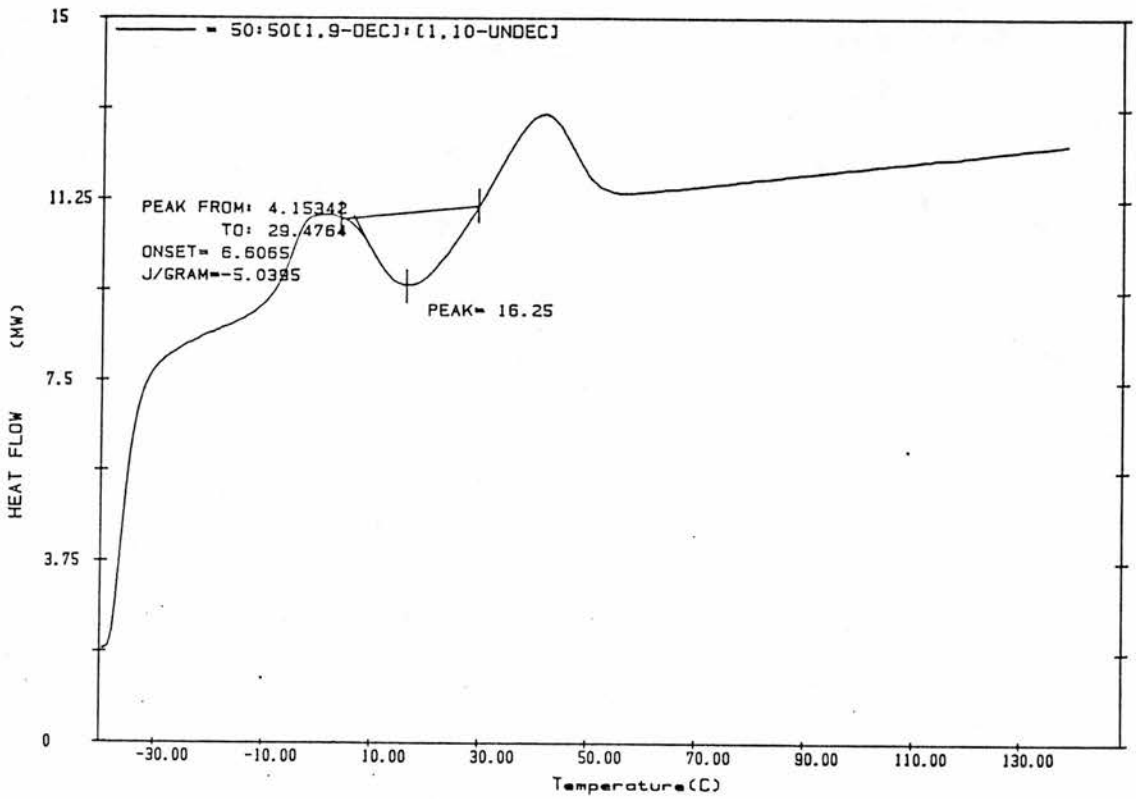
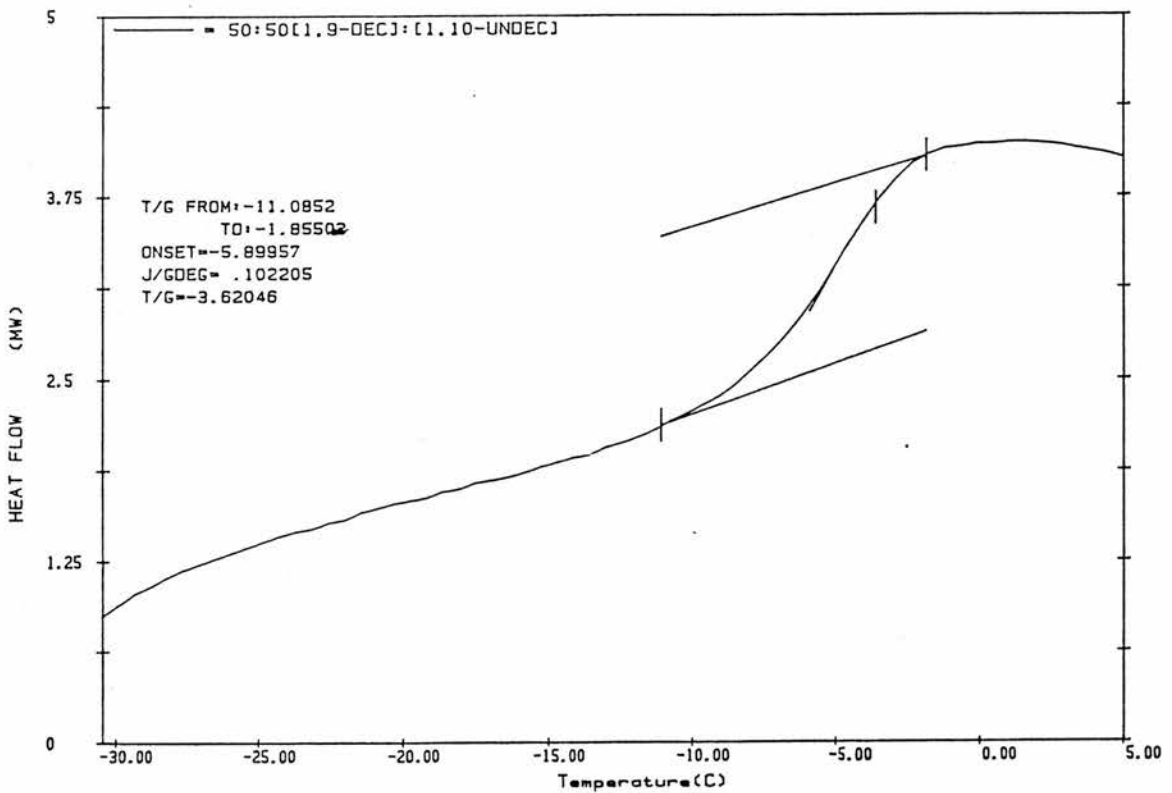


Figure 6.5 scan B DSC thermogram of 50:50 poly(1,9-dec):poly(1,10-undec) from -40°C to 140°C (at 10°C/min). 3rd heating cycle. Tm calculation is shown.

Figure 6.5 scan B T_c calculation.Figure 6.5 scan B T_g calculation.

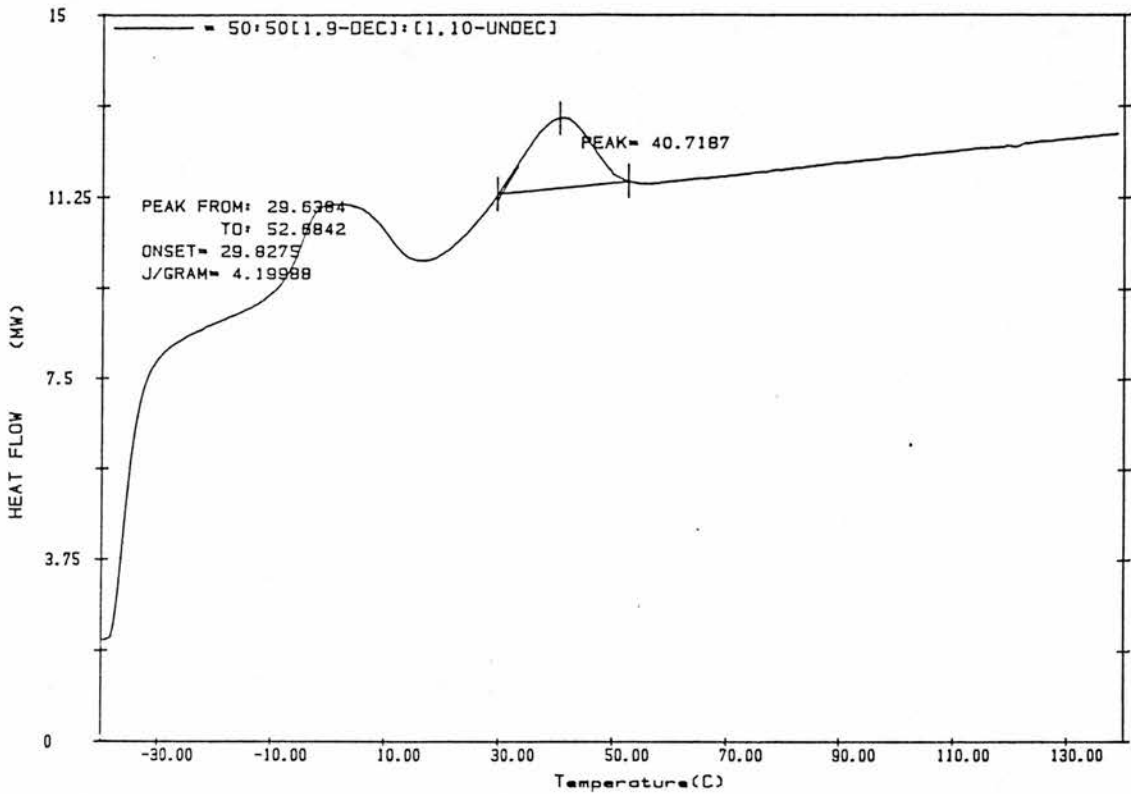


Figure 6.5 scan C DSC thermogram of 50:50 poly(1,9-dec):poly(1,10-undec) from -40°C to 140°C (at $10^{\circ}\text{C}/\text{min}$). 4th heating cycle. T_m calculation is shown.

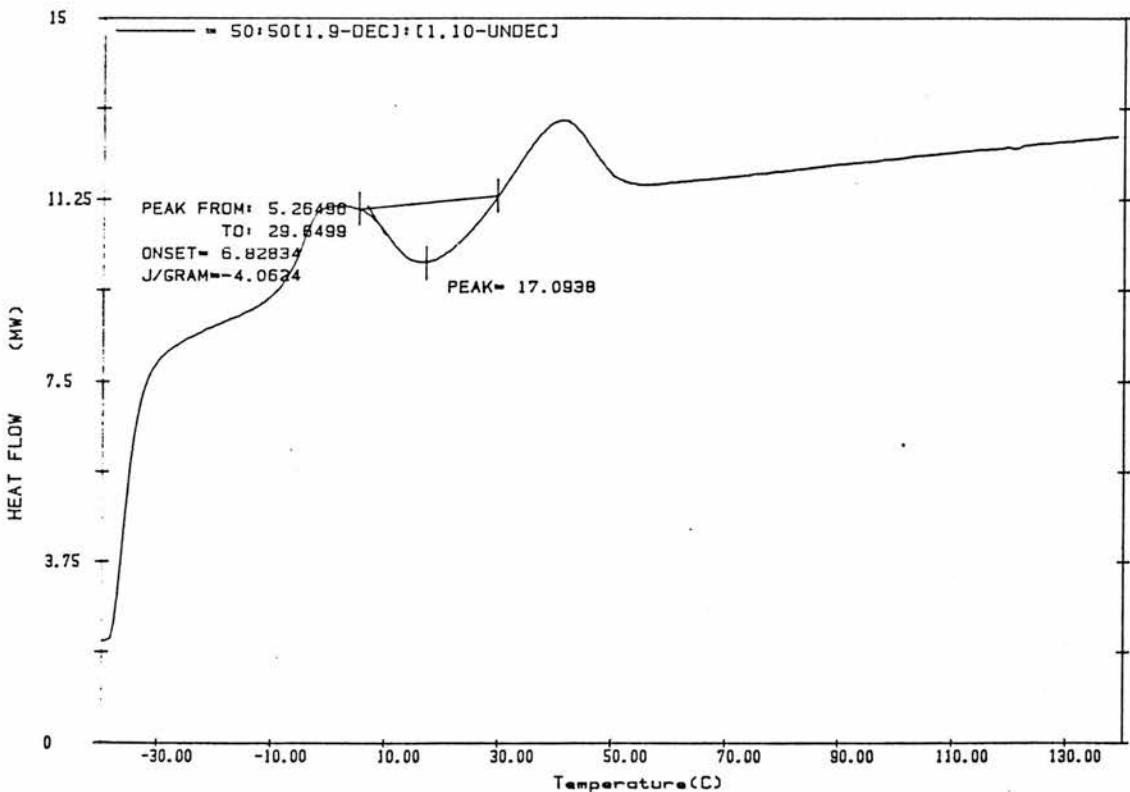


Figure 6.5 scan C T_c calculation.

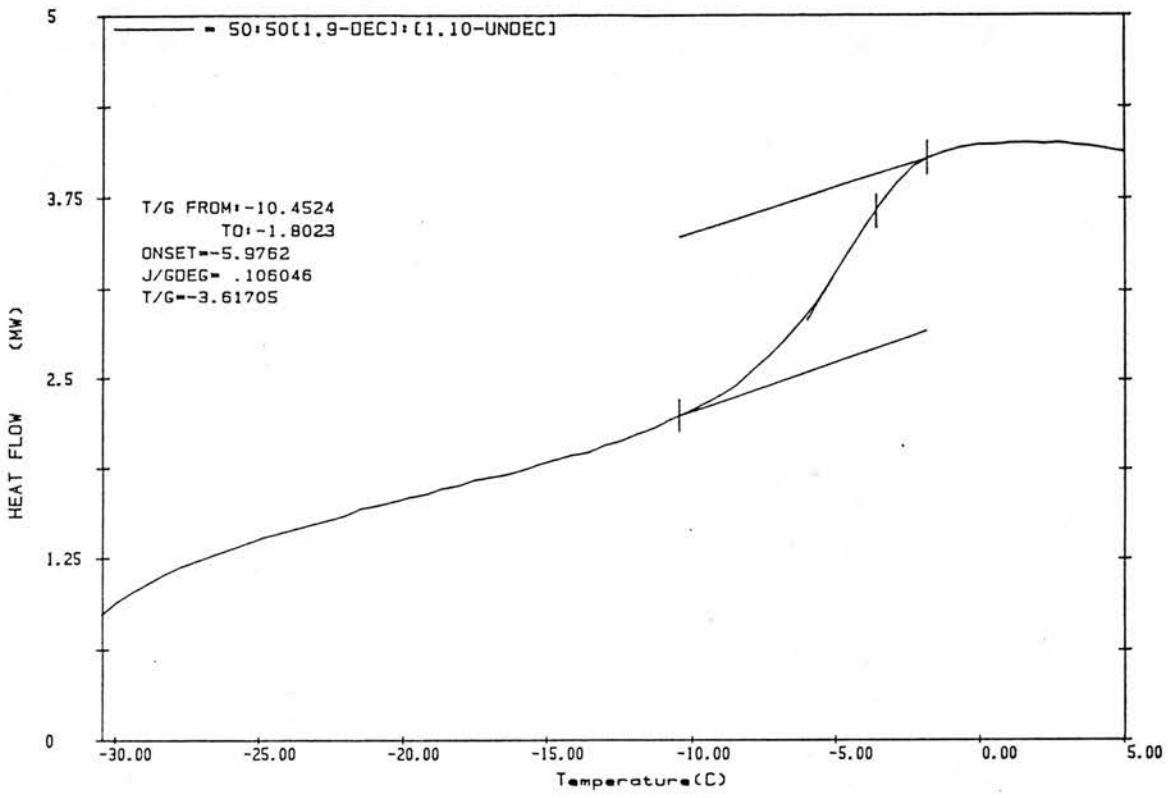


Figure 6.5 scan C Tg calculation.

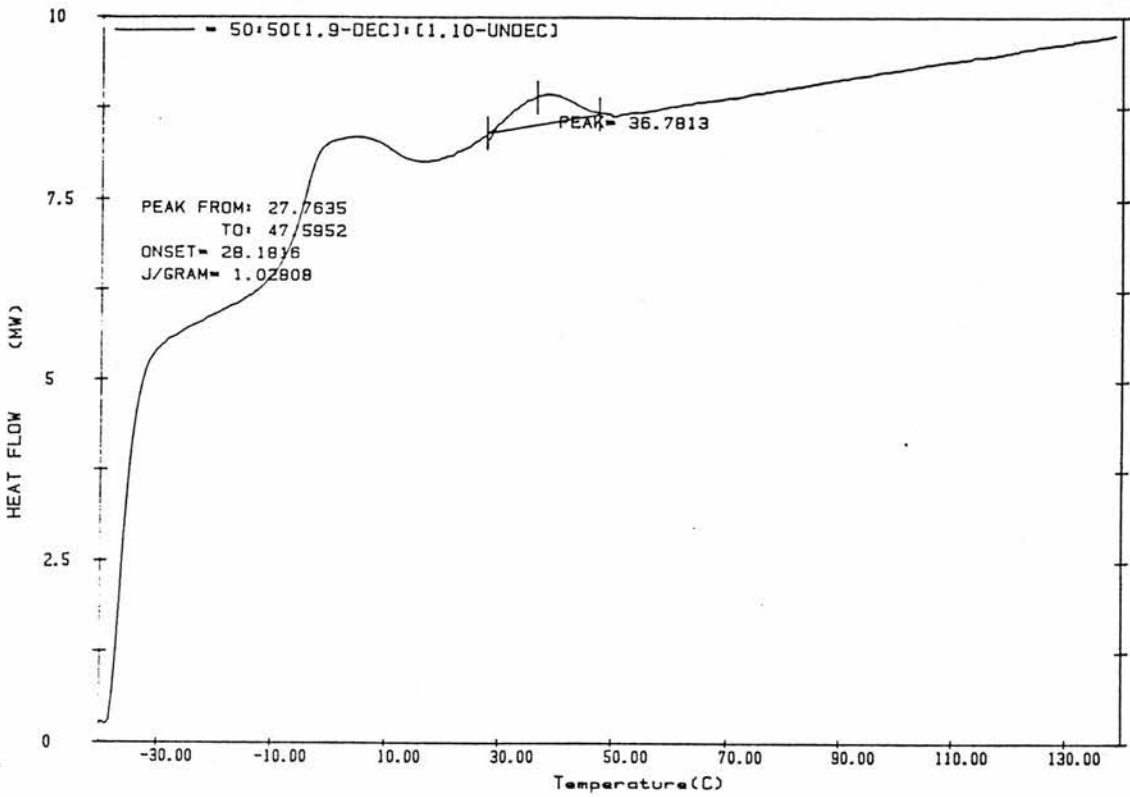


Figure 6.6 DSC thermogram of 50:50 poly(1,9-dec):poly(1,10-undec) annealed at 140°C for 30minutes quenched to -60°C then run from -40°C to 140°C(at 10°C/min). T_m calculation is shown.

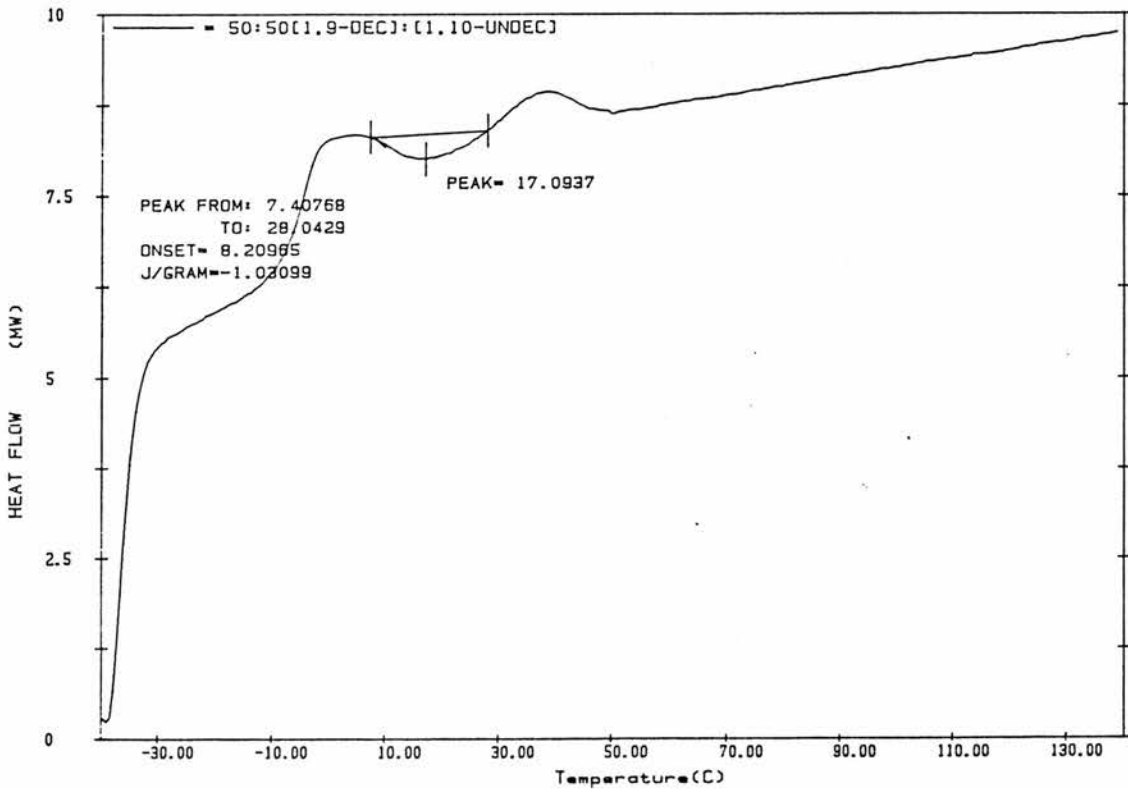


Figure 6.6 T_c calculation.

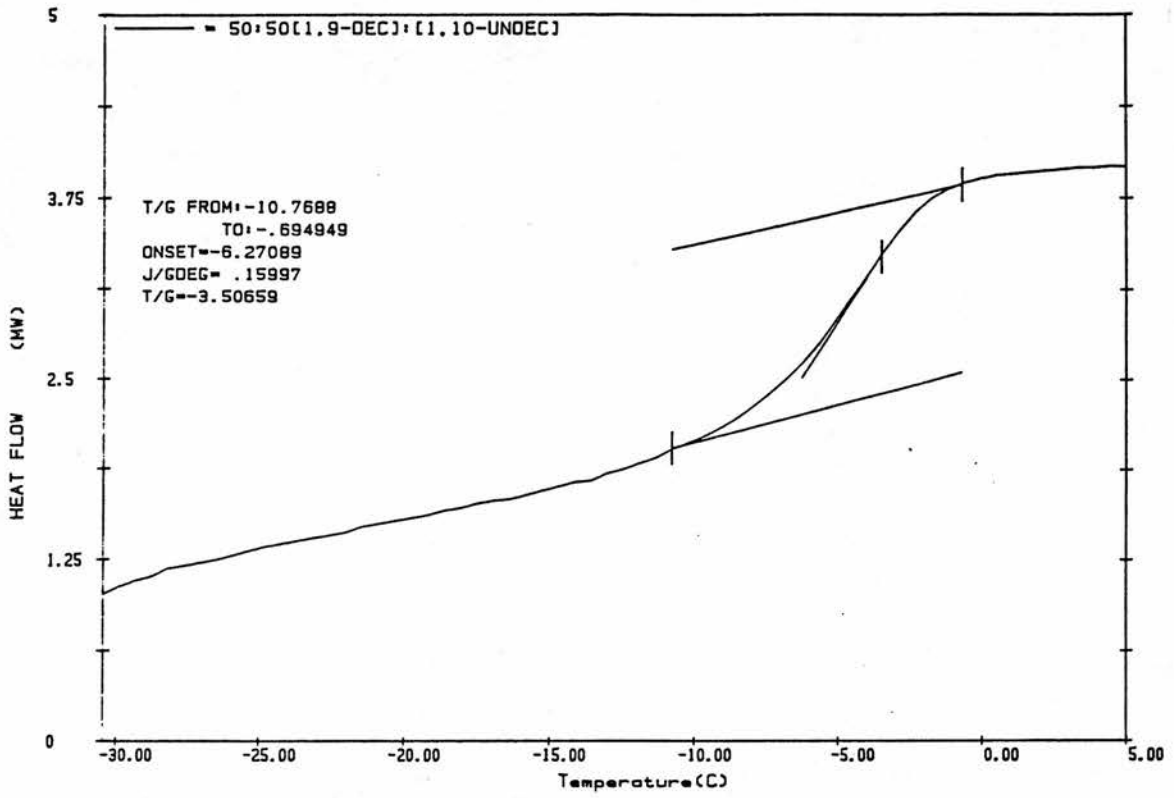
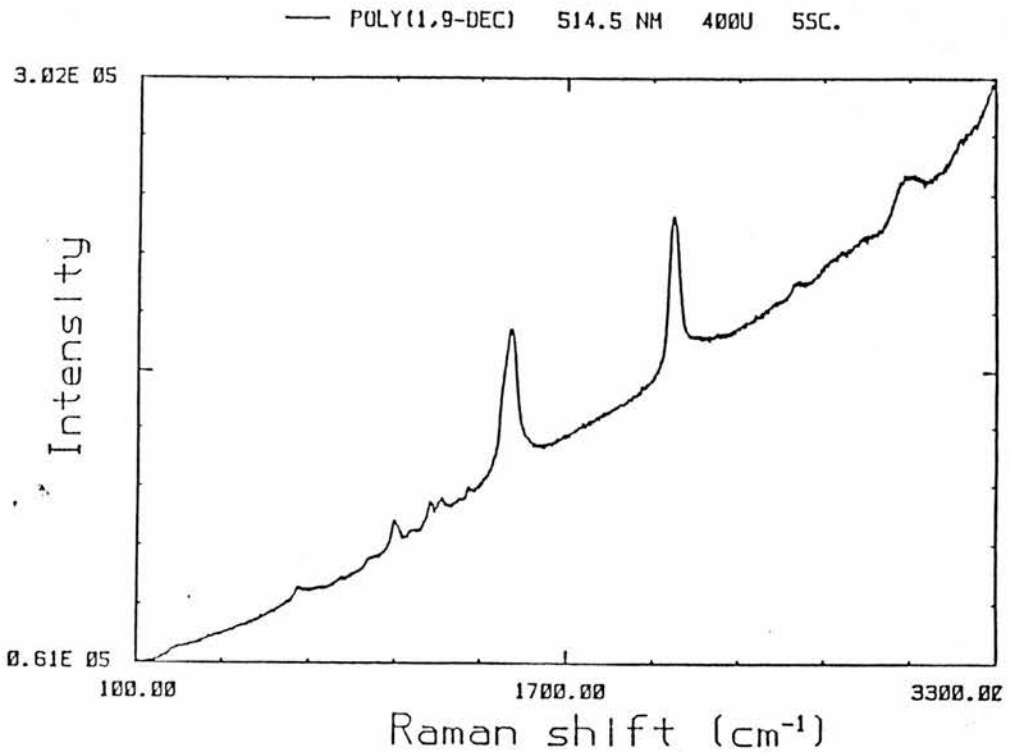
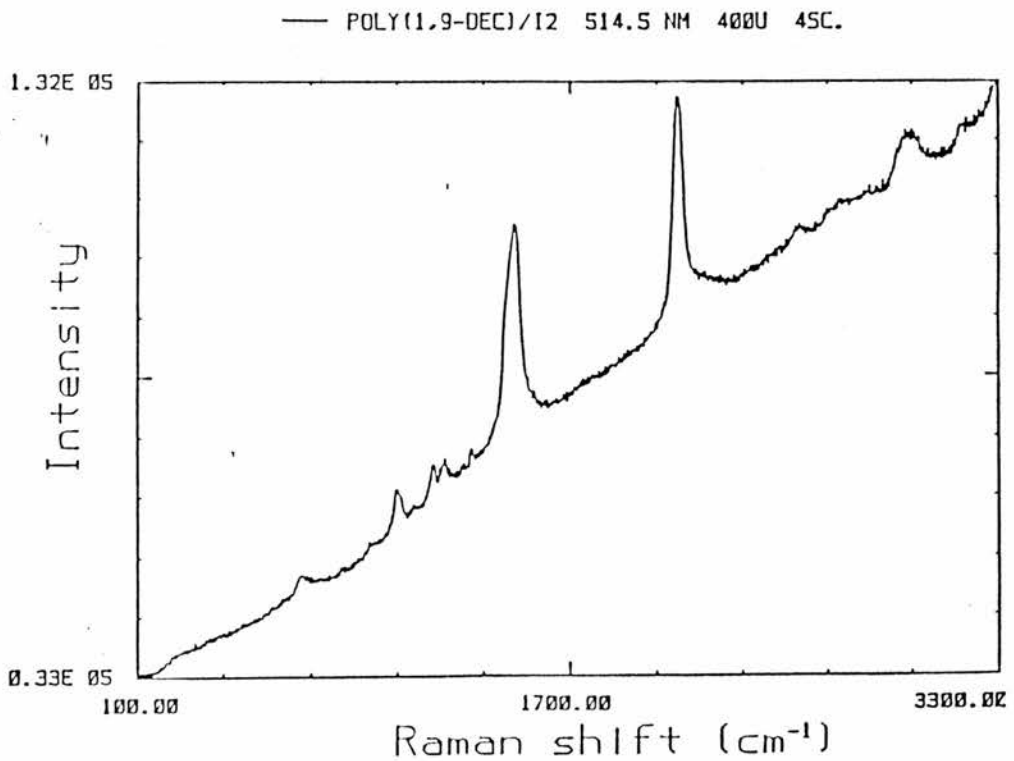


Figure 6.6 T_g calculation.

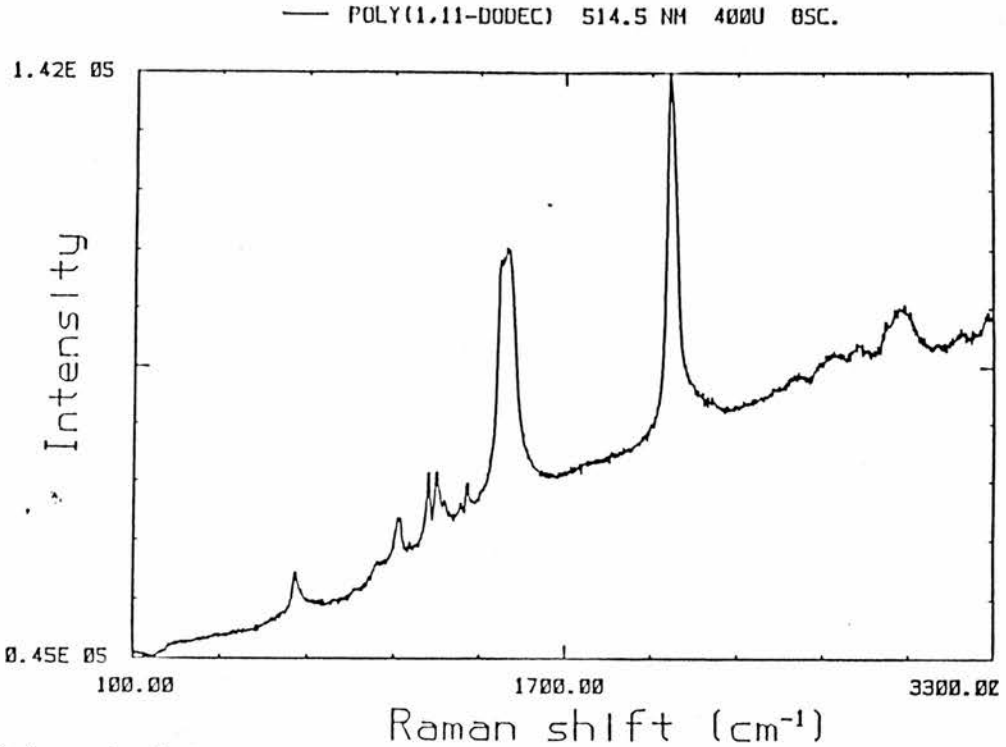


(a) poly(1,9-decadiyne) exposed to UV irradiation for 6 minutes.

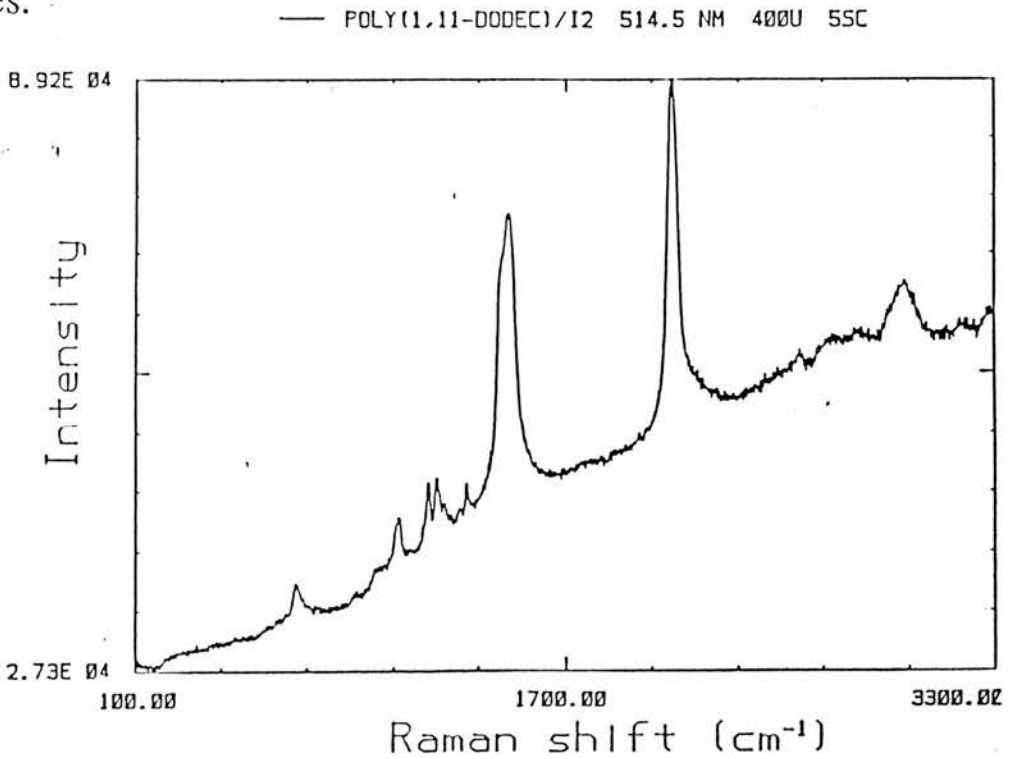


(b) Iodine doped poly(1,9-decadiyne) followed by exposure to UV irradiation for 6 minutes.

Figure 6.7 Resonance Raman spectra recorded at an Incident Wavelength of 5145\AA .



(a) poly(1,11-dodecadiyne) exposed to UV irradiation for 6 minutes.



(b) Iodine doped poly(1,11-dodecadiyne) followed by exposure to UV irradiation for 6 minutes.

Figure 6.8 Resonance Raman spectra recorded at an Incident Wavelength of 5145Å.

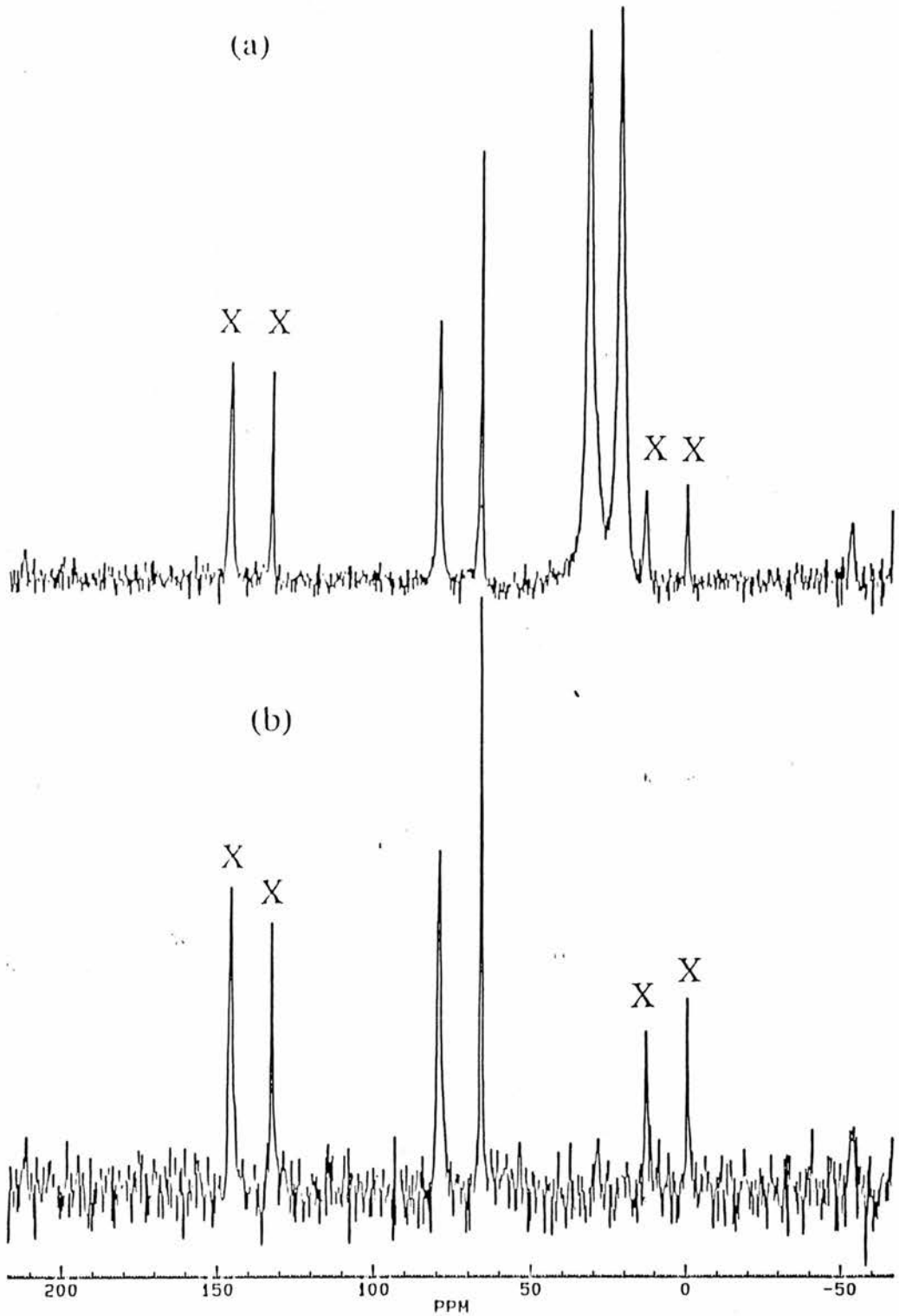


Figure 6.9 Solid state ^{13}C nmr cross polarisation (CP) magic angle spinning spectra of polymer A1 - 1,7-octadiyne polymerised by route A @ 65°C for 5hours.

(a) Spectrum recorded at 125.758 MHz.

(b) NQS(non quaternary suppression) spectrum recorded at 125.758 MHz.

X = a spinning side band

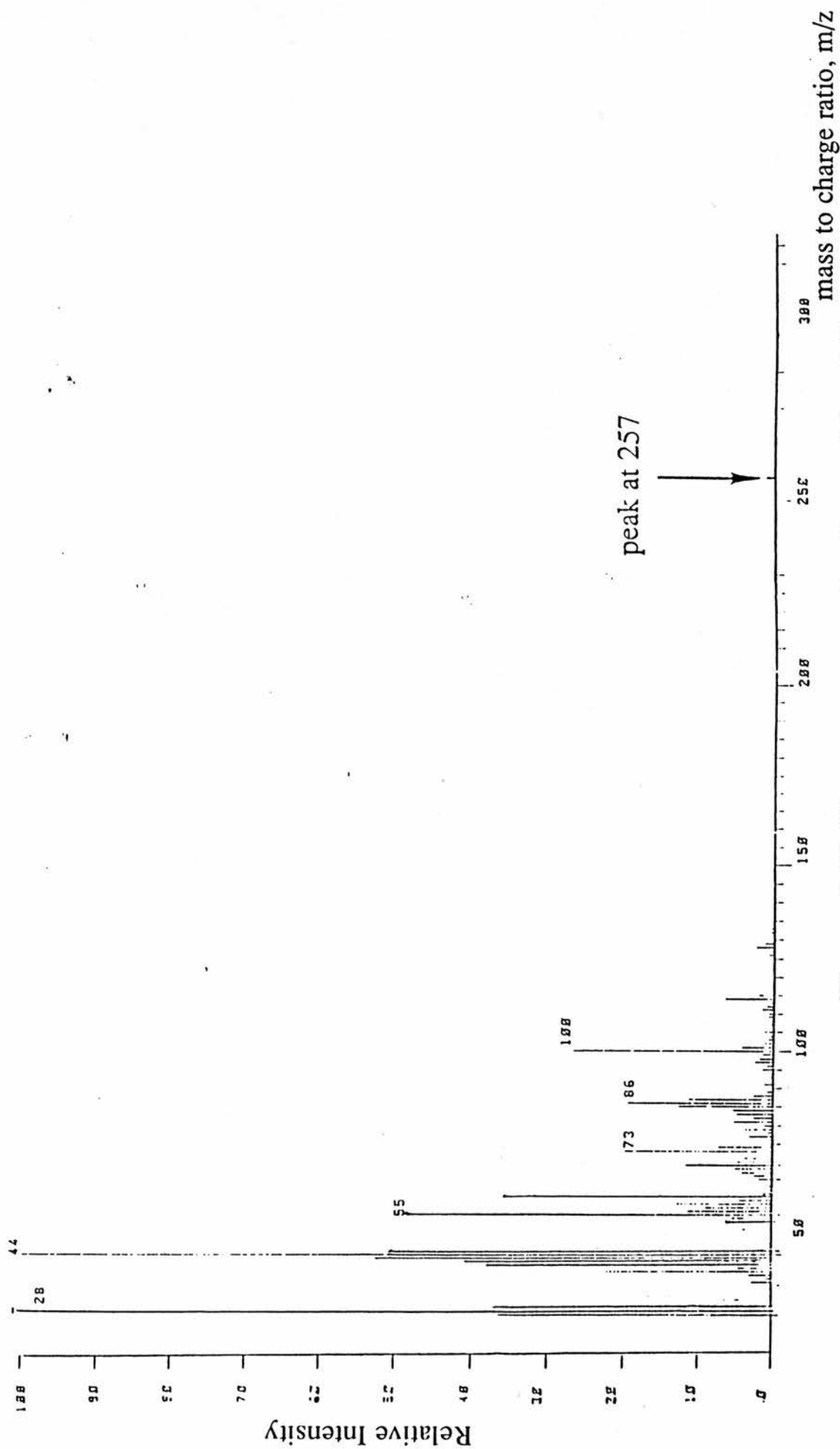


Figure 6.10 Mass spectrum of polymer A1 - 1,7-octadiyne

polymerised by route A @ 65°C for 5 hours.

BIBLIOGRAPHY

Bibliography.

1. C.Glaser , *Chem.Ber.* , 2,422(1869); *Ann.* , 137,154(1870).
2. G.Wegner, *Z Naturforsch.* , 24B,824(1969).
3. D.Bloor in Developments in Crystalline Polymers - 1 , D.C.Bassett , ed., Applied Science Publishers , London , p.151(1982).
4. R.H.Baughman , *J.Poly.Sci. : Poly.Phys.Ed.* , 12,1511(1974).
5. G.Wegner , *Pure and Appl Chem.* , 49,443(1977).
6. H.Bässler , *Adv.Poly.Sci.* , 63,1(1984).
7. H.Sixl , *Adv.Poly.Sci.* , 63,49(1984).
8. V.Enkelmann , *Adv.Poly.Sci.* , 63,91(1984).
9. M.Schott and G.Wegner in Nonlinear Optical Properties of Organic Molecules and Crystals , Vol.2 , D.S.Chemla and J.Zyss , eds ., Academic Press , New York p.3(1987).
10. J.Hine , *J.Org.Chem.* , 31,1236(1966).
11. J.Kaiser , G.Wegner and E.W.Fischer , *Israel J.Chem.* , 10,157(1972).
12. R.H.Baughman , *J.Chem.Phys.* , 68,3110(1978).
13. R.H.Baughman , *J.Appl.Phys.* , 43,4362(1978).
14. C.Kollmar and H.Sixl , *J.Chem.Phys.* , 87,5541(1987).
15. R.R.Chance , G.N.Patel , E.A.Turi and Y.P.Khanna , *J.Amer.Chem.Soc.* , 100,1307(1978).
16. R.R.Chance , G.N.Patel , E.A.Turi and Y.P.Khanna , *J.Amer.Chem.Soc.* , 100,6644(1978).
17. R.R.Chance and G.N.Patel , *J.Poly.Sci. : Poly.Phys.Ed.* , 16,859(1978).
18. A.Prock , M.L.Shand and R.R.Chance , *Macromolecules.* , 15,238(1982).

19. H.Eckhardt , T.Prusik and R.R.Chance , *Macromolecules* , 16,732(1983).
20. C.Bubeck , H.Sixl and W.Neumann , *Chem.Phys* . , 48,269(1980).
21. H.J.Kevelam , K.P.de Jong , H.C.Meinders and G.Challa , *Makromol.Chem.* , 176,1369(1975).
22. D.Day and J.B.Lando , *J.Poly.Sci. : Poly.Lett.Ed* . , 19,227(1981).
23. M.Thakur and J.B.Lando , *Macromolecules* . , 16,143(1983).
24. M.Thakur and J.B.Lando , *J.Appl.Phys* . , 54,5554(1983).
25. J.R.Havens , M.Thakur , J.B.Lando and J.L.Koenig , *Macromolecules.*, 17,1071(1984).
26. K.Knol , L.W.van.Horssen , G.Challa and E.E.Havinga , *Polymer Communications* . , 26,71(1985).
27. R.J.Butera , R.P.Grasso , M.Thakur and J.B.Lando , in *Crystallographically Ordered Polymers* , D.J.Sandman , Ed ., American Chemical Society , Washington , D.C ., ACS Symposium Series No 337,25(1987).
28. R.J Butera , B.Simic-Glavaski and J.B.Lando , *Macromolecules* . , 20,1722(1987).
29. R.J.Butera and J.B.Lando , *J.Poly.Sci. : Polym.Phys Ed.* , 27,2451(1989).
30. R.J Butera , B.Simic-Glavaski and J.B.Lando , *Macromolecules* . , 23,199(1990).
31. R.J Butera , B.Simic-Glavaski and J.B.Lando , *Macromolecules* . , 23,211(1990).
32. D.M.White , *Polym.Prepr.* , (*Amer.Chem.Soc.* , *Div.Polym.-Chem.*) . , 12(1),155(1971).
33. G.Wenz and G.Wegner , *Makromol.Chem.Rapid.Commun.* , 3 ,231(1982).

34. G.Wenz , M.A.Müller , M.Schmidt and G.Wegner , *Macromolecules* , 17,837(1984).
35. S.Yamao and T.Kotaka , *Synth.Met.* , 18,447(1987).
36. K.Se , H.Ohnuma and T.Kotaka , *Polym.J.* , 14,895(1982).
37. H.Eckhardt , D.S.Bourdreaux and R.R.Chance , *J.Chem.Phys.* , 85,4116(1986).
38. M.L.Shand , R.R.Chance , M.LePostellec and M.Schott , *Phys.Rev.B.* , 25,4431(1982).
39. W.F.Lewis and C.N.Batchelder , *Chem.Phys.Lett.* , 60,232(1979).
40. G.N.Patel , R.R.Chance and J.D.Witt , *J.Poly.Sci. : Poly.Lett.Ed.* , 16,607(1978).
41. G.N.Patel , R.R.Chance and J.D.Witt , *J.Chem.Phys.* , 70,4387(1979).
42. R.R.Chance , *Macromolecules* , 13,396(1980).
43. G.J.Exarhos , W.M.Risen and R.H.Baughman , *J.Amer.Chem.Soc.* , 98,481(1976).
44. G.N.Patel , *Polym.Prepr.* , (Amer.Chem.Soc. , Div.Polym.Chem.) 20(2),452(1979).
45. R.R.Chance , G.N.Patel and J.D.Witt , *J.Chem.Phys.* , 71,206(1979).
46. M.F.Rubner , D.J.Sandman and C.Velaquez , *Macromolecules* , 20,1296(1987).
47. M.F.Rubner , *Macromolecules* , 19,2129(1986).
48. G.N.Patel , J.D.Witt and Y.P.Khanna , *J.Poly.Sci. : Polym.Phys Ed.* , 18,1383(1980).
49. G.N.Patel , *Polym.Prepr.* , (Amer.Chem.Soc. , Div.Polym.Chem.) 19(2),154(1978).
50. G.Eglinton and A.R.Galbraith , *J.Chem.Soc.* , 889(1959).
51. Lespieau and Journand , *Compt Rend.* , 188,1410(1929).

52. A.L.Henne and K.W.Greenlee , *J.Amer.Chem.Soc.* , 67,484(1945).
53. J.Dale , A.J.Hubert and G.S.D.King , *J.Chem.Soc.* , 73(1963).
54. L.Brandsma ; Preparative Acetylenic Chemistry. , Elsevier Publishing Company 19-20,22-50(1971).
55. W.Novis.Smith and O.F.Beumel , *Synthesis* . , 441(1974)
56. Y.Gaoni , C.C.Leznoff and F.Sondheimer , *J.Amer.Chem.Soc.* , 90,4940(1968).
57. Ronald.A.Henry , *J.Chem.and.Eng.Data.* , 21,4(1976).
58. G.Markl , *Chem Ber.* , 94,3005(1961).
S.T.D.Gough and S.Trippett , *J.Chem.Soc.* , 2333(1962).
59. R.A.Aitken and S.Seth , *Synlett.* , 211(1990).
60. R.A.Aitken and S.Seth , *Synlett.* , 212(1990).
61. C.Dufraisse and A.Dequesnes , *Bull.Soc.Chim.* , 49,1880(1931).
62. C.Eaborn , A.R.Thompson and D.R.M.Walton , *J.Chem.Soc.* , 1364(1967).
63. C.Eaborn and D.R.M.Walton , *J.Organometallic.Chem.* , 2,95(1964).
64. E.F.Kenny and K.D.Meier , *Angew.Chem.* , 71,245(1964).
65. M.Kracht , German Patent 944311 , June 14 1956 , *Badische Anilin and Soda Fabrik.* , CA 52,16194(1958).
66. W.Beckmann , *Synthesis.* , 7,423(1975).
67. C.M.Bowes , D.F.Montecalvo and F.D.Sondheimer , *Tetrahedron Letters.* , 34,3181(1973) and C.M.Bowes , University College , London PhD thesis pages 74-75 and 114-115(1974).
68. Finkelstein , *Chem.Ber.* , 43,1528(1910).
69. H.Saikachi , Y.Taniguchi and H.Ogawa , *Yakugaku Zasshi.* , 82,1262(1962).
70. O.Issler , H.Gutmann , M.Montavon , R.Rüegg , G.Ryser and P.Zeller , *Helv.Chim.Acta.* , 40,1242(1957).

71. W.C.Huntsman in The Chemistry of the Carbon-Carbon Triple Bond; S Patai , Ed ; John Wiley and Sons : New York.1978 ; pp554-620.
72. W.G.Nigh in Oxidation in Organic Chemistry , Part B; W.S.Trahanovsky , Ed; Academic Press:New York , 1973; pp1-31.
73. T.F.Rutledge , Acetylenic Compounds; Reinhold: NewYork , 1968 , Chapter 6.
74. A.S.Hay , *J.Org.Chem.* , 27,3320(1962).
75. G.Eglinton and W.McCrae , *Adv.Org.Chem.* , 4,225(1963).
76. I.D.Campbell and G.Eglinton , *Organic Syntheses.* , 45,39.
77. F.Sondheimer and Y.Amiel , *J .Amer.Chem.Soc.* , 79,5817(1957).
78. A.S.Hay , *J.Org.Chem.* , 25,1275(1960).
79. A.S.Hay U.S.Patent 3300456(1967).
80. A.S.Hay , D.A.Bolon , K.R.Leimer and R.F.Clark , *Polymer Letters.* , 8,97(1970).
81. H.C.Meinders , R.van.Bolhuis and G.Challa , *J.Mol.Catal.* , 5,225(1979).
82. J.M.G.Cowie , *Polymers: Chemistry and Physics of Modern Materials.* , Intertext Books , London , p7(1973).
83. F.Sondheimer , Y.Amiel and R.Wolovsky , *J.Amer.Chem.Soc.* , 81,4600(1959).
84. F.Sondheimer and Y.Amiel , *J.Amer.Chem.Soc.* , 78,4178(1956).
85. Y.Amiel , F.Sondheimer and R.Wolovsky , *Proc.Chem.Soc.* , 22(1957).
86. F.Sondheimer , Y.Amiel and R.Wolovsky , *J.Amer.Chem.Soc.* , 79,6263(1957).
87. W.Baker , J.F.W.McOmie and W.D.Ollis , *J.Chem.Soc.* , 200(1951).

88. K.Dodgson , D.Sympson and J.A.Semlyen. , *Polymer.* , 19,1285(1978).
89. R.C.Weast , " Handbook of Chemistry and Physics " , 64th ed., The Chemical Rubber Co., Ohio p. D165(1983-84).
90. T.E.Mead , *J.Phys.Chem.* , 66,2149(1962).
91. A.Keller , G.R.Lester and L.B.Morgan , *Phil.Trans. A.* , 247,1(1954).
92. F.D.Hartley , F.W.Lord and L.B.Morgan , *Phil.Trans. A.* , 247,23(1954).
93. F.J.Limbert and E.Baer , *J.Polym.Sci. : A* 1,3317(1963).
94. J.R.Collier and L.M.Neal , *Polym.Eng.Sci.* , 9,182(1969).
95. J.Majer , *Kunststoffe* , 50,565(1960).
96. P.J.Lemstra , T.Kooistra and G.Challa , *J.Poly.Sci. : Polym.Phys Ed.* , 11,2153(1973).
97. G.Wegner , *Makromol.Chem.* , 145,85(1971).
98. E.M.Barrall , T.C.Clarke and A.R.Gregges , *J.Poly.Sci. : Polym.Phys Ed.* , 16,1355(1978).
99. B.Wunderlich , *Macromolecular Physics.Vol 3*.Academic Press (New York) p133(1980).
100. R.Liang , W.F.Lai and A.Reiser , *Macromolecules.* , 19,1685(1986).
101. M.F.Rubner , *Macromolecules.* , 19,2114(1986).
102. L.B.Forsyth , Ph.D. Thesis , University of St Andrews , p143(1989).
103. A.R.Blythe ; *Electrical Properties of Polymers*, Cambridge Univ.Press(1979).
104. H.Gross , W.Neumann and H.Sixl , *Chem.Phys.Lett.* , 95,584(1983).

105. Jan.F.Rabek , " Experimental Methods in Polymer Chemistry " ,
John Wiley and Sons : New York, Chapter 32, p532(1980).